



**Hybrid Combustion-Gasification Chemical  
Looping  
Coal Power Technology Development  
PHASE III - FINAL REPORT**

**Report Issued on September 30, 2008  
Report # PPL-08-CT-25**

**Principal Authors:  
Herbert E. Andrus  
Gregory Burns  
John H. Chiu  
Gregory N. Liljedahl  
Peter T. Stromberg  
Paul R. Thibeault**

**Prepared for**

**U.S. Department of Energy  
National Energy Technology Laboratory  
Pittsburgh, Pennsylvania  
(Under Contract DE-FC26-03NT41866)**

**Prepared by  
US Power Plant Laboratories  
ALSTOM Power Inc.  
2000 Day Hill Road  
Windsor, Connecticut 06095**

**ALSTOM Project Manager  
Herb Andrus**

**DOE Project Manager  
Dr. Ronald W. Breault**



### **Disclaimer Notice**

“This report was prepared as an account of work sponsored by an agency of the United States Government. Neither the United States Government nor any agency thereof, nor any of their employees, makes any warranty, express or implied, or assumes any legal liability or responsibility for the accuracy, completeness, or usefulness of any information, apparatus, product, or process disclosed, or represents that its use would not infringe privately owned rights. Reference herein to any specific commercial product, process, or service by trade name, trademark, manufacturer, or otherwise does not necessarily constitute or imply its endorsement, recommendation, or favoring by the United States Government or any agency thereof. The views and opinions of authors expressed herein do not necessarily state or reflect those of the United States Government or any agency thereof.”



<b>TABLE OF CONTENTS</b>	<b>PAGE</b>
Contents	i
Figures	ii
Tables	vi
Acronyms and Special terms	vii
Summary and Conclusions	ix
1. Introduction	1
1.1 Chemical Looping Overall Objectives	1
2. Chemical Looping Options	3
3. Chemical Looping History	5
3.1 Alstom's Background In Gasification Technology	5
3.2 Green House Gas Economic Study	7
3.3 Phase I and II Accomplishments	11
4. The PDU Project	15
4.1 Objectives	15
4.2 Phase III Task Description	16
4.3 PDU Test Chronology	18
5. PDU Pilot Plant Description	23
5.1 PDU Modifications	24
5.2 Control System Modifications	28
5.3 The PDU Gas Sampling and Analysis System	30
5.4 P&IDs	35
5.5 PDU Process Equipment	36
6. Cold Flow Modeling	57
6.1. Cold Flow Model Goals	57
6.2. Plexiglas Cold Flow Model Tests	58
6.3 Test Summary and Analysis	82
6.4 Scale-Up	104
7. PDU Testing	107
7.1 Chemical Looping Phase III Automatic Controls Feasibility Study	107
8. Prototype Engineering	122
8.1 Prototype Performance Estimate	124
8.2 Heat Exchangers	128
8.3 Calcination Tests	130
8.4 Materials	133
8.5 Refractory Heat Up	143
8.6 Chemical Looping Applications	150
8.7 Prototype Preliminary Design	158
8.8 CFD Modeling	161
9. Technical Reviews	191
9.1 ASME Peer Review	191
9.2 TCGR	204
10. Lessons Learned	207
11. Economics Update	231
11.1 Chemical Looping Retrofit for PC or CFB	231
11.2 Economics Update	234
11.3 COE for H <sub>2</sub> Production	239
11.4 Prototype Cost	244
12. Future Developments	245
References	247

List of Figures	Page
Figure 1-1 High Temperature Chemical and Thermal Looping	2
Figure 2-1 Indirect Combustion With CO <sub>2</sub> Capture – Option 1	3
Figure 2-2 Indirect Gasification With Syngas Production And No CO <sub>2</sub> Capture – Option 2	3
Figure 2-3 Indirect Gasification With Hydrogen Production And CO <sub>2</sub> Capture – Option 3	4
Figure 3-1 The Windsor Connecticut Coal Gasification Pilot Plant	5
Figure 3-2 Process Size Comparison Between A PC Fired Boiler And A Hot Solids Gasifier/Combustor System	6
Figure 3-3 Greenhouse Gas Project Results – Efficiency	8
Figure 3-4 Greenhouse Gas Project Results – EPC Costs	9
Figure 3-5 Greenhouse Gas Report - Cost Of Electricity	10
Figure 5-1 Phase III Chemical Looping Test Facility	23
Figure 5-2 New Gas Burner	24
Figure 5-3 Second Vacuum Pump	25
Figure 5-4 Second Scrubber	25
Figure 5-5 Manual Control Of The SPCV	26
Figure 5-6 Automatic Control Of The SPCV	27
Figure 5-7 Chamber Pots	27
Figure 5-8 Chemical Looping Phase III Automatic Controls Schematic Diagram	29
Figure 5-9 Chemical Looping PDU Phase I P&ID	37
Figure 5-10 Chemical Looping PDU Phase II P&ID	38
Figure 5-11 Chemical Looping PDU Phase III P&ID	39
Figure 5-12 Primary and Secondary Cyclones for the Main reactors	40
Figure 5-13 Cyclones for the Auxiliary Loops	41
Figure 5-14 Solids Heat Exchangers and Spray Coolers	42
Figure 5-15 Seal Pot Control Valve (SPCV)	43
Figure 5-16 SA Sealpot	44
Figure 5-17 Solids Pick Up Device	45
Figure 5-18 Product Gas Burner Design	46
Figure 5-19 Bauxite Heater Design	47
Figure 5-20 Bauxite Heater Heating Element Design	48
Figure 5-21 PDU Equipment Layout	49
Figure 5-22 Layout of Main Loops	50
Figure 5-23 Location of Electrical Heaters and Supports	50
Figure 5-24 Gas Venting System	51
Figure 5-25 Sorbent Activation (SA) Loops	52
Figure 5-26 SA Impactor	52
Figure 5-27 Bauxite Loop	52
Figure 5-28 SA Reactor and Rotary Feed Valve	54
Figure 5-29 Heat Exchangers in the Solids Drain Line	54
Figure 5-30 Primary and Secondary Cyclones in Reducer and Oxidizer Loops	55
Figure 5-31 SPCV	56
Figure 6-1 40-Ft CFM Test Facility	58
Figure 6-2 Original Air Supply System	60
Figure 6-3 Hysteresis In Riser Velocity	60
Figure 6-4 Changes In Pressure For The Air Supply System Of The 40 Ft-Loop	61
Figure 6-5 Main Flow Setting Vs. Recorded Value	62
Figure 6-6 Main Flow Instability – Measured Flow Vs. Set Value	63
Figure 6-7 Deviation Between Recorded Riser Flow From Setting Value	63
Figure 6-8 Air Supply System – Modified On OCT 2006	64
Figure 6-9 Main Flow Stability – 31 OCT 2006 (No Grease Air Header)	65
Figure 6-10 Main Flow Stability – 02 NOV 2006 (Tuned PID)	65
Figure 6-11 Main Flow Stability – 07 NOV 2006 (with Grease Air Header)	66
Figure 6-12 Main Flow Stability – 13 NOV 2006 (GTF Accumulator + G Header)	66
Figure 6-13 Main Flow Stability for the Modified Air Supply System	67

Figure 6-14	Rotometer vs. Orifice Measurement (New Air Supply System)	68
Figure 6-15	Rotometer vs. Orifice Measurement (New Air Supply System, Auto Tuned PID)	68
Figure 6-16	Rotometer vs. Orifice Measurement (New Air Supply System, Auto Tuned PID)	69
Figure 6-17	Rotometer vs. Orifice Measurement (with GTF Accumulator)	69
Figure 6-18	Rotometer vs. Orifice Flow (No GA Header)	70
Figure 6-19	Rotometer vs. Orifice Flow (New Main Control Valve, Positioner, Regulator)	70
Figure 6-20	Rotometer vs. Orifice Flow (Add GA Header)	71
Figure 6-21	Rotometer vs. Orifice Flow (Add GTF accumulator)	71
Figure 6-22	Rotometer vs. Orifice Flow for Grease Air	72
Figure 6-23	Rotometer with GTF vs. Orifice Flow for Grease Air	73
Figure 6-24	Original Sugar-Scoop Design	73
Figure 6-25	Pitot-Tube Traverse – Horizontal (at 3" from SSO)	74
Figure 6-26	Pitot-Tube Traverse – Vertical (at 3" from SSO)	75
Figure 6-27	Pitot-Tube Traverse – 45° (at 3" from SSO)	75
Figure 6-28	Pitot-Tube Traverse – Horizontal (at 34" from SSO)	75
Figure 6-29	Pitot-Tube Traverse – Vertical (at 34" from SSO)	76
Figure 6-30	Pitot-Tube Traverse – 45° (at 34" from SSO)	76
Figure 6-31	Constant Diameter Sugar-Scoop Design	77
Figure 6-32	Erosion at Pickup Exit	77
Figure 6-33	Erosion at Lower Elbow Exit	77
Figure 6-34	Laser Diode Solids Flow Measurement for the 15-ft-loop	78
Figure 6-35	Example of Frequency Analysis for Flow Detection	79
Figure 6-36	Solids Flow by Laser Diode vs. Load Cell Measurement for the 15 Ft-loop	80
Figure 6-37	Laser Diode Solids Flow Measurement for the 40-Ft-loop	81
Figure 6-38	Flow Measurement and Pressure Taps for the 15-Ft-loop	82
Figure 6-39	Solids Level Drop vs. Solids Velocity in the Dipleg	83
Figure 6-40	Solids Velocity in the Dipleg vs. Froude Number	84
Figure 6-41	Effect of Fluidizing Velocity on Discharged Solids Flux	84
Figure 6-42	Grease Air Effect on Pressure for the 40-ft-loop Test	85
Figure 6-43	Grease Air Effect on Pressure at the Entrance and Exit of SPCV	86
Figure 6-44	Grease Air Effect on Frictional Pressure Drop along the Dipleg	87
Figure 6-45	Friction Factor vs. Reynolds Number for Particles w/ moving Solids in the Dipleg	89
Figure 6-46	Friction Factor ( $D_p$ based) vs. Reynolds Number for Particles with Moving Solids in Dipleg	89
Figure 6-47	Typical Superficial Velocity of Grease Air along Dipleg for the 40-Ft-loop	90
Figure 6-48	Pressure Drop across the SPCV Transport Bed vs. Riser Inlet Pressure	91
Figure 6-49	Average Pressure of the SPCV Transport Bed vs. Riser Inlet Pressure	91
Figure 6-50	Pressure Drop across SPCV Transport Bed vs. Froude Number	92
Figure 6-51	Sugar Scoop Pressure Drop vs. Froude Number	92
Figure 6-52	Solids/gas Transport Phase Diagram for Vertical Co-current Flow	93
Figure 6-53	Pressure Drop at the Lower Leg and Lower Elbow vs. Froude Number	95
Figure 6-54	Pressure Drop at the Lower Leg and Lower Elbow vs. Volume Solids Loading	95
Figure 6-55	Pressure Drop at the Lower Leg and Lower Elbow vs. Pressure at the Sugar-Scoop Exit	96
Figure 6-56	Pressure Drop for the Horizontal Leg and Elbow vs. Pressure at the Sugar-Scoop Exit for the 40-ft-loop	97
Figure 6-57	Pressure Drop of the Horizontal Leg and Elbow vs. Pressure at the Sugar-Scoop Exit for the 15-ft-loop	97
Figure 6-58	PSD of Ash Samples for the Chemical Looping CFM – 9 Oct 07	98
Figure 6-59	PSD of Ash Samples for the Chemical Looping CFM – Jun/Jul 07	99
Figure 6-60	Cyclone Fractional Efficiency for the 40-ft-loop -19 SEP 07	99
Figure 6-61	Solids Slip Velocity in the 4" Riser	100
Figure 6-62	Drifting of Fluidizing Air for the SPCV During the 6-Hour Stability Test at the 15-ft-loop	101
Figure 6-63	CFM 6-Hour Stability Test for the 15-ft-loop	102
Figure 6-64	Pressure Drop of the Dipleg and Cross leg for Dual Loop Test	103

Figure 6-65	Solids Flow for Dual Loop Operation at 15-ft-loop - 24 May 07	104
Figure 6-66	Choking Limit for Solids Transport in a Vertical Co-current Flow	105
Figure 7-1	Reducer Pressure Control PID Loop	109
Figure 7-2	PID Controllers for the Reducer and Oxidizer Pressure Control	110
Figure 7-3	Oxidizer And Reducer Loop Pressure During Load Ramp Test	111
Figure 7-4	Long Term Loop Pressure Stability Test	112
Figure 7-5	Loop Pressure during Load following stability test	112
Figure 7-6	Loop Pressure Disturbance Recovery Test	113
Figure 7-7	Shutdown Test Loop Pressures	114
Figure 7-8	Riser Temperature vs Injection Air mass flow rate (SLPM) Trim	115
Figure 7-9	Reducer to Oxidizer Crossover Rate Control Screen	117
Figure 7-10	Oxidizer Solids Crossover Rate Control screen	117
Figure 7-11	Oxidizer Solids Flow Rate PID controller logic	118
Figure 7-12	Solids Flow Rate Testing Pressure and Flow Rate	119
Figure 7-13	Solids Flow Rate Testing Riser Pressure and dP Ratio	119
Figure 7-14	Solids Flow Rate Testing Injection Air	120
Figure 8-1	Chemical looping Prototype Simplified Process Flow Diagram	125
Figure 8-2	Calcining Test Setup	131
Figure 8-3	Refractory Properties	138
Figure 8-4	Typical Refractory Expansion Joint	139
Figure 8-5	Y Anchor	140
Figure 8-6	MS / YF Anchor Combination	140
Figure 8-7	lower Reducer Startup Heat Loss	147
Figure 8-8	Upper Reducer Startup heat Loss	147
Figure 8-9	Oxidizer Startup Heat loss	148
Figure 8-10	Calciner Startup heat Loss	148
Figure 8-11	Feed Pipe Startup Heat Loss	149
Figure 8-12	MTF Startup Heat loss	149
Figure 8-13	PC Steam Boiler	152
Figure 8-14	Simplified Schematic of an Integrated Boiler- Chemical Looping Gasification System	156
Figure 8-15	Preliminary Prototype Design Isometric View and Top View	159
Figure 8-16	Preliminary Prototype Design Side Views	160
Figure 8-17	View of the GMV post-processor window showing the surface mesh and flux planes	164
Figure 8-18	Schematic of the Chemical Looping 40ft Flow Model	165
Figure 8-19	Geometry of the modeled section of the cold-flow loop	167
Figure 8-20	Geometry of Lower Section	168
Figure 8-21	Mesh for the lower section of model	169
Figure 8-22	Size Distribution for typical solid material used by Barracuda	170
Figure 8-23	Particle shapes for 120mesh screen sample	171
Figure 8-24	Velocity distribution near the surface of the tube.	173
Figure 8-25	Centerline gas velocity distribution – lower portion	174
Figure 8-26	Centerline gas velocity distribution – lower portion	175
Figure 8-27	Flow Velocities near base of riser vs. time	176
Figure 8-28	Solids colored by particle velocity in the lower section	177
Figure 8-29	Particle Size Distribution near the 45° solids pick-up pipe	178
Figure 8-30	Solids colored by radius in the mixing tee	179
Figure 8-31	Particle Solids colored by volume fraction	180
Figure 8-32	Particle Velocity Distribution colored by velocity magnitude	181
Figure 8-33	Position of relevant pressure taps	182
Figure 8-34	Pressure Distribution over the full height of the flow model	184
Figure 8-35	Pressure distribution near the lower inclined pipe	185
Figure 8-36	Solids concentration in the lower inclined pipe section	186
Figure 8-37	Measured Differential Pressures	187
Figure 8-38	Measured Differential Pressures	188

Figure 9-1	Cost of Electricity for Advanced CO <sub>2</sub> Capture Technologies	196
Figure 11-1	Incremental Cost of Electricity for Chemical Looping Gasifier (PC4-CLG), O <sub>2</sub> /Flue Gas Recirculation System (PC4-O <sub>2</sub> ) and Ammonia Scrubbing System (PC4- NH <sub>3</sub> )	233
Figure 11-2	Cost of Electricity for Different CO <sub>2</sub> Technologies	235
Figure 11-3	CO <sub>2</sub> Allowance Price (\$/Ton CO <sub>2</sub> Emitted)	235
Figure 11-4	CO <sub>2</sub> Emissions for Short-Term CO <sub>2</sub> Technologies	236
Figure 11-5	Investment Costs for Short-Term CO <sub>2</sub> Technologies	236
Figure 11-6	CO <sub>2</sub> Mitigation Costs for Short-Term CO <sub>2</sub> Technologies	237
Figure 11-7	CO <sub>2</sub> Emissions from Long-Term CO <sub>2</sub> Technologies	237
Figure 11-8	Specific Investment Cost for Long-Term CO <sub>2</sub> Technologies	238
Figure 11-9	CO <sub>2</sub> Mitigation Costs for Long-Term CO <sub>2</sub> Technologies	238
Figure 11-10	PC Retrofit Concepts using Alstom's Chemical looping Process	240
Figure 11-11	Comparison with a Conventional Power Plant	242

List of Tables	Page	
Table 5-1	Compositions of Calibration Gases Used to Prove Method 16B System	31
Table 5-2	Calibration Test Results	32
Table 8-1	Chemical Looping PFD Flow Streams (Scaled from Case13)	127
Table 8-2	Analysis of Calcination Product	132
Table 8-3	Summary of Test Results	132
Table 8-4	Heat Loss Summary	146
Table 8-5	Coal Analysis	151
Table 8-6	Performance Comparison between Base Case and Retrofit Case 1	154
Table 8-7	Performance Comparison between Base Case and Retrofit Case 2	155
Table 8-8	Test Conditions for Barracuda Simulation	166
Table 9-1	Potential Show Stoppers	199
Table 11-1	PC Power Plant Chemical Looping Retrofit Economics	241
Table 11-2	Prototype Equipment Costs	244

## Acronyms and Special terms

15-ft	Fifteen foot tall cold flow model
40-ft	Forty foot tall cold flow model
A&E	Architect and Engineers
ABB	Asea Brown Bovari
ABMA	American Boiler Manufacturers Association
Alstom	Astom Pwer inc.
Ata	Atmospheres, absolute
Blue rack	Gas analysis equipment package
Btu	British Thermal Unit
Calciner	The reaction vessel in the process where CO <sub>2</sub> is recovered
CFB	Circulating fluidized bed
CFD	Computational Fluid Dynamics
CFM	Cold flow model
Chiu valve	SPCV Or Medusa (Invented By J. H. Chiu)
Chamber Pots	Knock Out Drums
CL	Chemical looping
CMB	Circulating Moving Bed
COE	Cost Of Electricity
Crossover	Line carrying solids between reactors
CWL&P	City, Water, Power and Light
D50	Diameter of the mean particle size in a particle size distribution
Dipleg	Solids return pipe over the SPCV
DP	Delta pressure, or pressure drop
DTFS	Drop Tube Furnace System
EOR	Enhanced Oil Recovery
EPC	Engineered, Procured And Constructed
FBC	Fluid Bed Combustor
FBHE	Fluid Bed Heat Exchanger
GC	Gas Chromatograph
GHG	Green House Gas
GMV	A post processing program for use in Barracuda's CFD program
GTF	Grease Air, Transport Air and Fluidizing Air
IGCC	Integrated Gasification Combined Cycle
HRSG	Heat Recovery Steam Generator
HHV	Higher Heating Value
IR	Infrared
Medusa	SPCV or Chiu Valve
Method 16B	An experimental method to determine total sulfur in a gas
MBHE	Moving Bed Heat Exchanger
MCR	Maximum Continuous Rating, the maximum load for a boiler.
MTF	Multi-Use Test facility
OTM	Oxygen Transport Membrane
Oxidizer	The reaction vessel where the oxygen carrier solids are oxidized
PC	Pulverized Coal
PDU	Process Development Unit
PID	Proportional-Integral-Derivative, a control device
Pitt 8	Pittsburgh Coal #8
PPL	(Alstom Power's) Power Plant Laboratories
PSD	Particle size distribution
Reducer	The reaction vessel where coal is gasified or combusted
RH	Relative Humidity
SA	Sorbent Activation
SCF	Standard Cubic Feet
Slpm	Standard liters per minute

SPCV	Seal Pot Control Valve (Chiu Valve)
Sugar Scoop	Solid Pickup Device
TCGR	Technical Concept Gate Review
TGA	Thermo-Gravimetric Analyzer
TPD	Tons Per Day
TRS	Total Reduced Sulfur
UBC	University of British Columbia
UFP	Un-mixed Fuel Processor, GE's chemical looping process
WC	Water column
WGS	Water Gas Shift

## Summary and Conclusions

This report documents the accomplishments of the Phase III work under the DOE/NETL Cooperative Agreement No. DE-FC26-03NT41866 toward the development of Alstom Power's Chemical Looping process.

All of the Phase III milestones have been met, on time, and within the budget.

For the past several years Alstom Power Inc. (Alstom), a leading world-wide power system manufacturer and supplier, has been in the initial stages of developing an entirely new, ultra-clean, low cost, high efficiency power plant for the global power market. This new power plant concept is based on a hybrid combustion-gasification process utilizing high temperature chemical and thermal looping technology

The process consists of the oxidation, reduction, carbonation, and calcination of calcium-based compounds, which chemically react with coal, biomass, or opportunity fuels in two chemical loops and one thermal loop.

The chemical and thermal looping technology can be alternatively configured as i) a combustion-based steam power plant with CO<sub>2</sub> capture, ii) a hybrid combustion-gasification process producing a syngas for gas turbines or fuel cells, or iii) an integrated hybrid combustion-gasification process producing hydrogen for gas turbines, fuel cells or other hydrogen based applications while also producing a separate stream of CO<sub>2</sub> for use or sequestration.

In its most advanced configuration, this new concept offers the promise to become the technology link from today's Rankine cycle steam power plants to tomorrow's advanced energy plants.

The objective of this work is to develop and verify the high temperature chemical and thermal looping process concept at a small-scale pilot facility in order to enable AL to design, construct and demonstrate a pre-commercial, prototype version of this advanced system. In support of this objective, Alstom and DOE started a multi-year program, under this contract.

Before the contract started, in a preliminary phase (Phase 0) Alstom funded and built the required small-scale pilot facility (**Process Development Unit**, PDU) at its Power Plant Laboratories in Windsor, Connecticut. Construction was completed in calendar year 2003.

The objective for Phase I was to develop the indirect combustion loop with CO<sub>2</sub> separation, and also syngas production from coal with the calcium sulfide (CaS) / calcium sulfate (CaSO<sub>4</sub>) loop utilizing the PDU facility. The results of Phase I were reported in **Reference 1**, "Hybrid Combustion-Gasification Chemical Looping Coal Power Development Technology Development Phase I Report"

The objective for Phase II was to develop the carbonate loop – lime (CaO) / calcium carbonate (CaCO<sub>3</sub>) loop, integrate it with the gasification loop from Phase I, and ultimately demonstrate the feasibility of hydrogen production from the combined loops. The results of this program were reported in **Reference 3**, “Hybrid Combustion-Gasification Chemical Looping Coal Power Development Technology Development Phase II Report”

The objective of Phase III is to operate the pilot plant to obtain enough engineering information to design a prototype of the commercial Chemical Looping concept. The activities include modifications to the Phase II Chemical Looping PDU, solids transportation studies, control and instrumentation studies and additional cold flow modeling. The deliverable is a report making recommendations for preliminary design guidelines for the prototype plant, results from the pilot plant testing and an update of the commercial plant economic estimates.

A small pilot plant was constructed by modifying the existing Chemical looping PDU. All of the existing capabilities were retained and additional capabilities were added. Automatic controls were added to the seal pot control valve (SPCV) gas feed lines. A second vacuum pump, scrubber and stack were added to simulate the control action required in the commercial concept where separate outlet streams must be controlled independently because they cannot be mixed. In addition, several upgrades and repairs were made to the PDU including a new gas burner, chamber pots (solids knock out cans), spray nozzles in the heat exchangers, gas outlet controls and an upgraded control system computer and software.

The cold flow model designed and built for the Phase I and Phase II tests was used extensively in Phase III to measure the transport characteristics of the solid material used in the tests. The plastic model was also used to visualize the flow characteristics of the transporting solids. The 15-ft cold flow model was modified by adding a second identical loop to conduct dual loop testing.

A forty-foot tall plastic model was constructed for use in Phase III. This model was used to test higher solids flow rates with a taller static solids seal.

Tests were conducted on both cold flow models to characterize solids transport flow and to provide information for developing an automatic control system for the PDU. Results from the cold flow modeling also provided design information for the prototype, and helped analyze scale-up issues.

The solids flow characteristics of each component of the chemical looping reactors and transport piping were investigated to determine pressure drop versus solids mass flow relations, solids flow choking conditions, fluidizing requirements, grease air methods and other important data.

Results from the cold flow testing were used to make design improvements to system components. Testing of the new designs was successful. An improved SPCV was able

to smooth the solids flow pulses. The cyclone demonstrated 99.9954% efficiency and captured all particles above 7 micron.

The PDU was run to test the feasibility of using automatic controls to control two separate outlet streams, automatically control fluidizing air and transport air to the SPCV, control main air flow with temperature changes and load changes and control start-ups, shut-downs and emergency plant shut-downs. These tests were successful and showed that there was a feasible method for automatic control.

Engineering studies were done to develop a design for the Prototype plant to be proposed for a follow-on Phase IV. A preliminary prototype was developed to size equipment. Materials of construction were investigated for areas of the system that had unique issues. For example, the reducer vessel and associated piping will be expected to operate at high temperatures with a high H<sub>2</sub> content. This required specifying special materials and construction techniques. A set of material recommendations and construction recommendations were developed for the entire chemical looping island.

The proposed prototype plant was sized to run without external heating as needed in the PDU. Heat transfer studies were done to determine that the heat loss was small enough to achieve this condition. It was also determined that the prototype could be heated up in a reasonable time.

An independent economic update of the commercial design was conducted and shown to be consistent with previous studies that showed chemical looping has the potential to be the lowest cost option for CO<sub>2</sub> capture.

Several technical reviews were conducted. Among them was an independent third party review conducted by the ASME for the DOE. A list of comments and recommendations were generated. These recommendations were incorporated into the Chemical Looping Program. The consensus from this review was that the program should proceed to the prototype phase. Several other reviews were conducted by the DOE and Alstom conducted a Technology Concept Gate Review (TCGR).

The Chemical Looping Program has made significant progress in the three program phases. The Phase I and Phase II program produced the following accomplishments:

- The program provided the chemical validation of Alstom's chemical looping process. The following processes were demonstrated and significant data was generated for each:
  - CaS – CaSO<sub>4</sub> looping
  - CaO - CaCO<sub>3</sub> looping
  - Water gas shift:  $\text{CO} + \text{H}_2\text{O} \rightleftharpoons \text{H}_2 + \text{CO}_2$
  - Hydrogen production
  - Sorbent reactivation
  - CO<sub>2</sub> removal
  - Char gasification/combustion via CaSO<sub>4</sub>
  - Coal devolatilization

- The PDU was used to show the simultaneous operation of four solids transport loops at elevated temperatures. The temperatures were about 1800 degrees F at a pressure of about 1 ata.
- The PDU was operated with five solids transport loops simultaneously at ambient temperatures.
- Multi-loop control requirements were established.
- The seal pot control valve (SPCV) operation requirements were established and the operation was controlled and steady for most of the testing.
- Startup requirements were established for smooth startup.
- Emergency quick shut-down and quick restart procedures were established.
- Inspection and maintenance procedures were determined.
- A water condenser, water trap and gas reheater system for the vacuum pump inlet was designed, built and successfully operated.
- The PDU successfully transported four very different solids (inert sand, commercial gypsum, coarse CFB bed material and the normal chemical looping sorbent). It was learned that the angle of repose tests for each solid are required for SPCV design and that cold flow model testing for fluidization rates was directly applicable to the hot case.
- The project team successfully passed the 'Product Development Quality Specification Gate Review' and the Technical Peer Review with very few changes required in the development plan.

The Phase III program produced the following accomplishments:

- A feasible automated control system for the chemical looping process was demonstrated using two separate outlet streams, and automatic SPCV flow control.
- Automated startup and shutdown was demonstrated including emergency shutdown.
- The cold flow modeling characterized pressure drop versus solids flow relationships for the 15-ft model, dual-loop 15-ft model and the 40-ft model.
- Scale-up from a 3/4" diameter riser to a 4" diameter riser was shown to be very easy.

- Cyclone performance was demonstrated to be 99.9954% with the 40-ft cyclone system. All particles above 7 micron were captured.
- Controllable and smooth solids flow was demonstrated in all the cold flow models.
- A new SPCV valve was designed and successfully tested.
- A prototype design was created and material specifications were developed.
- Economic studies were done for retrofit applications for Chemical Looping combustion. The COE for producing hydrogen as a boiler fuel were shown to be competitive.
- The project team successfully passed an independent third party review by the ASME, several DOE technical reviews, internal risk reviews and a Technical Concept Gate Review without any major project revisions.

## **Conclusions:**

The main conclusion from Phase I and Phase II is that all of the PDU chemistry required for the chemical looping process has been validated. The main conclusion from Phase III is that a prototype plant is feasible based on flow control studies, automatic control tests, material and heat transfer studies and economic estimates.

Additional conclusions are as follows:

### **From Phase I (Reference 1)**

1. It is practical to build a chemical looping system using the CaS to CaSO<sub>4</sub> reaction without losing sulfur as either SO<sub>2</sub> or H<sub>2</sub>S.
2. High gasification rates can be obtained in a chemical looping system even with low reactivity coals. A carbon conversion rate of 5%/sec ata was used for the commercial plant economic studies, while the minimum rate achieved in the Chemical Looping PDU was twice the required rate with low reactive char.
3. It is possible to operate three interactive solids transport loops (oxidizer, reducer and sorbent activation), at elevated temperatures (1800 degrees F).
4. It is possible to start up and heat up the solids transport loops interactively.
5. The Chemical Looping PDU design concept is validated.

6. Cold flow modeling provides a valuable tool for simulating the hot chemical looping system. The cold flow model is useful for determining fluidization and solids transport control settings for fluidizing and transport gases.
7. The original economic conclusions were still valid after determining the Phase I chemical reaction rates at the PDU. The original costs studies were based on equipment sizes determined from bench-scale reaction rates. Phase I showed these rates to be conservative.

### **From Phase II (Reference 3)**

1. Operation with five parallel loops is becoming routine. The PDU demonstrated five parallel loops cold and four parallel at operating temperatures.
2.  $\text{CaO} + \text{CaCO}_3$  kinetics were demonstrated in the PDU at operating temperatures.
3. Water gas shift reactions occurred rapidly at PDU operating conditions.
4. Cold flow bench test scale-up methods reveal what the hot PDU behavior will be like.
5. Economics assumptions are still valid after detailed peer review and detailed specification review.
6. Important control strategies were tested and validated.
7. The sorbent activation system vent system can accurately measure flow from the sorbent reactivation reactor.
8. The original economic conclusions are still valid after determining the Phase II chemical reaction rates at the PDU. A  $\text{CO}_2$ -Capture rate (i.e. Rate of conversion of  $\text{CaO}$  to  $\text{CaCO}_3$ ) of 5%/sec-ata was used for the commercial plant economic studies.  $\text{CaO}$  conversion rates achieved in the Chemical Looping PDU were an order of magnitude greater than the required rate for normal-sized sorbent material (i.e. 16 mesh).

### **From Phase III**

1. It is feasible to build an approximately 3 Mw Prototype chemical looping plant that is auto-thermal (requiring no external heaters).
2. It is possible to design and operate an automatic control system for the chemical looping system.
3. It is possible to design reactors for the chemical looping system using standard materials of construction and standard design methods.

4. Cyclone performance of 99.9954% can be achieved with the proper design. It is also possible to keep all solids greater than 7 microns in size in the loop.
5. Controllable and smooth solids flow can be maintained.
6. Scale-up of 28 times in flow area and 2.6 times in height is possible for the chemical looping concept. Scale-up from the 4" diameter CFM to the 18" diameter prototype is only 20.25 times in flow area and 1.5 times in height. Scale-up to the prototype should be feasible.
7. The performance of the cold flow models has shown a very good correlation to the performance of the hot PDU.
8. The Chemical Looping concept is ready for the Prototype Phase.



## 1. Introduction

This report documents the accomplishments of the Phase III work under the DOE/NETL Cooperative Agreement No. DE-FC26-03NT41866 toward the development of Alstom Power's Chemical Looping Process.

All of the Phase III Milestones have been met, on-time and within the budget.

### 1.1 Chemical Looping Overall Objectives

For the past several years Alstom Power Inc. (Alstom), a leading world-wide power system manufacturer and supplier, has been in the initial stages of developing an entirely new, ultra-clean, low cost, high efficiency power plant for the global power market. This new power plant concept is based on a hybrid combustion-gasification process utilizing high temperature (1100–2000 degree F) chemical and thermal looping technology. The process should be capable of:

- \$20/ton of CO<sub>2</sub> avoided (base: conventional coal-fired emissions plant)
- Over 90% CO<sub>2</sub> capture
- \$800/kW capital cost, without CO<sub>2</sub> capture (conventional plant at \$1000, 1997\$)

Specific Gasification Objective:

- Competitive with IGCC on a world-wide basis
- Medium Btu gas or Hydrogen without an Oxygen Plant
- H<sub>2</sub> production for future power plant or industrial applications

The capital cost target of \$800/Kw for a chemical looping plant is based on a total plant cost of \$1000/Kw for a conventional PC (Pulverized Coal) plant in 1997 dollars. As plant costs change the objective for chemical looping is to be at least 20% less costly than a comparable conventional coal based plant cost.

The chemical looping process consists of the oxidation, reduction, carbonation, and calcination of calcium-based compounds, which chemically react with coal, biomass, or opportunity fuels in two chemical loops and one thermal loop. In its most advanced configuration (**Figure 1-1**), this new concept offers the promise to become the technology link from today's Rankine cycle steam power plants to tomorrow's high efficiency advanced energy plants.

Based on previously performed in-house engineering and economic studies at Alstom in 2002, such a process has been shown to have the potential to achieve near-zero CO<sub>2</sub> emissions, exceed all current environmental requirements, and cost less than \$800 per kilowatt without CO<sub>2</sub> capture and less than \$1000 per kilowatt including CO<sub>2</sub> capture for the world-wide power generation market (1997 \$).

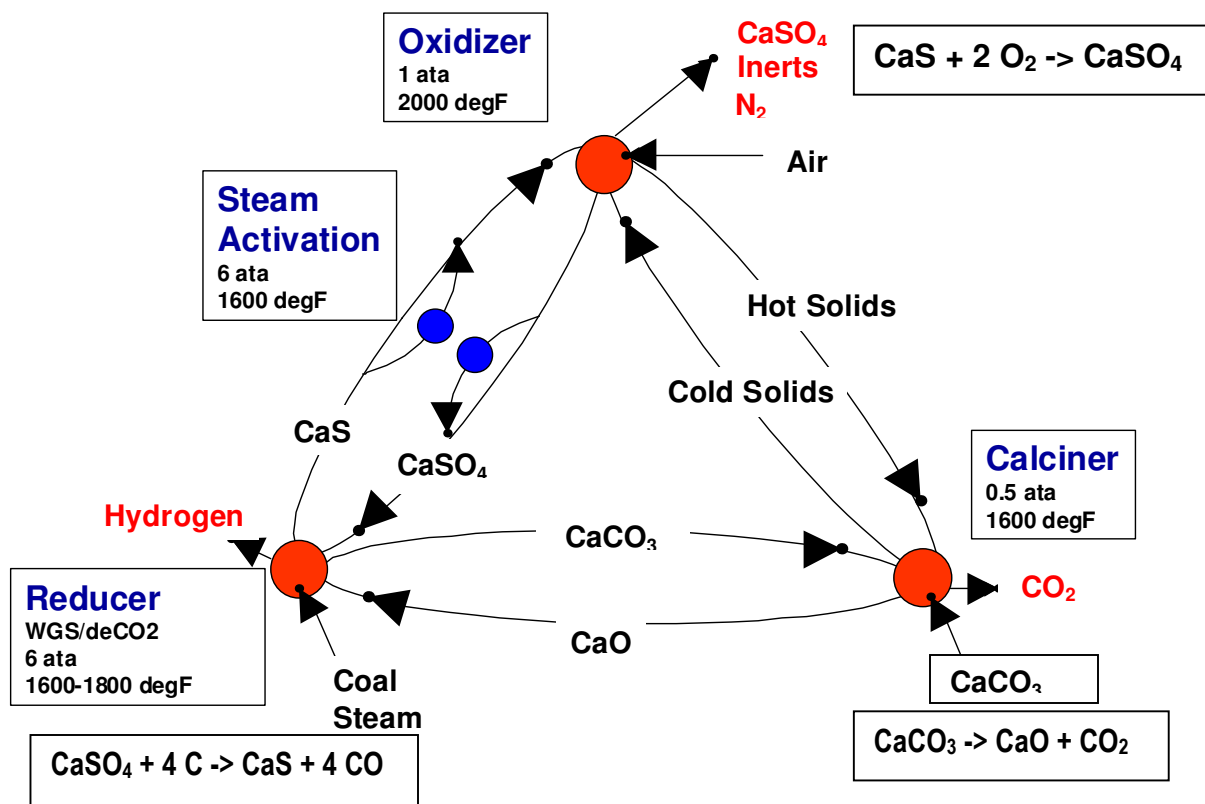
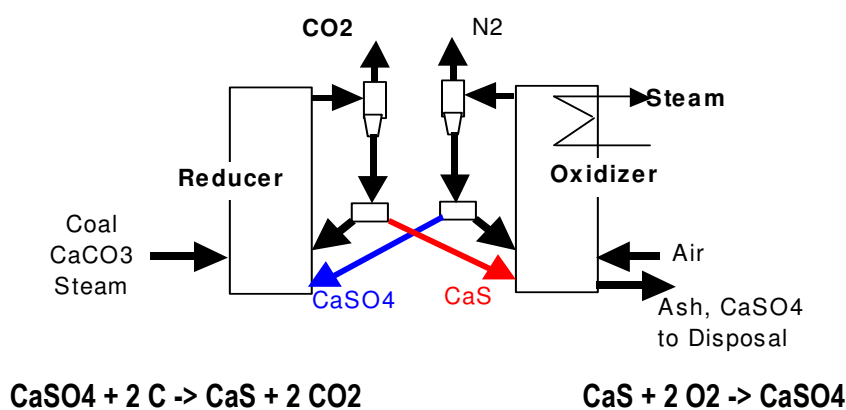


Figure 1-1 High Temperature Chemical and Thermal Looping

## 2. Chemical Looping Options

The Hybrid Combustion-Gasification Chemical Looping Coal Power Technology is an entirely new, ultra-clean, low cost, high efficiency coal power plant technology for the future global power markets. The chemical and thermal looping technology can be alternatively configured as i) a combustion-based steam power plant with CO<sub>2</sub> capture; ii) a hybrid combustion-gasification process producing a syngas for boilers, gas turbines, or fuel cells; or iii) an integrated hybrid combustion-gasification process producing hydrogen for gas turbines, fuel cells or other hydrogen based applications while also producing a separate stream of CO<sub>2</sub> for use or sequestration. These three concepts are schematically illustrated in **Figures 2-1 to 2-3** and are referred to in this report as Options 1, 2, and 3.



**Figure 2-1 - Indirect Combustion with CO<sub>2</sub> Capture – Option 1.**

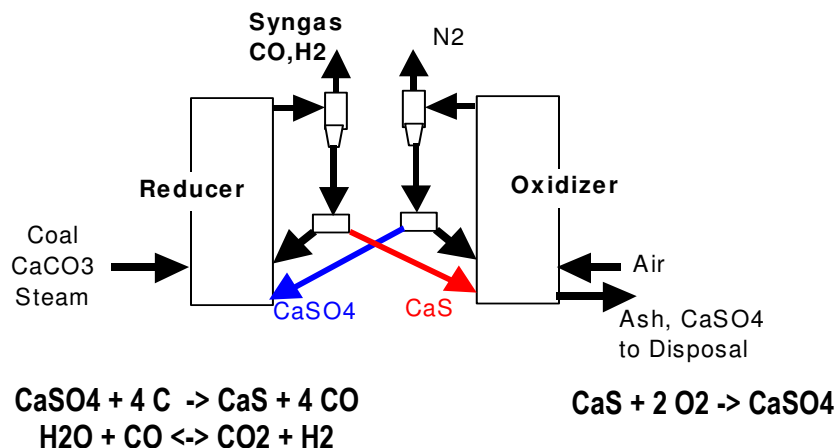


**Figure 2-2 - Indirect Gasification with Syngas Production and No CO<sub>2</sub> Capture – Option 2.**

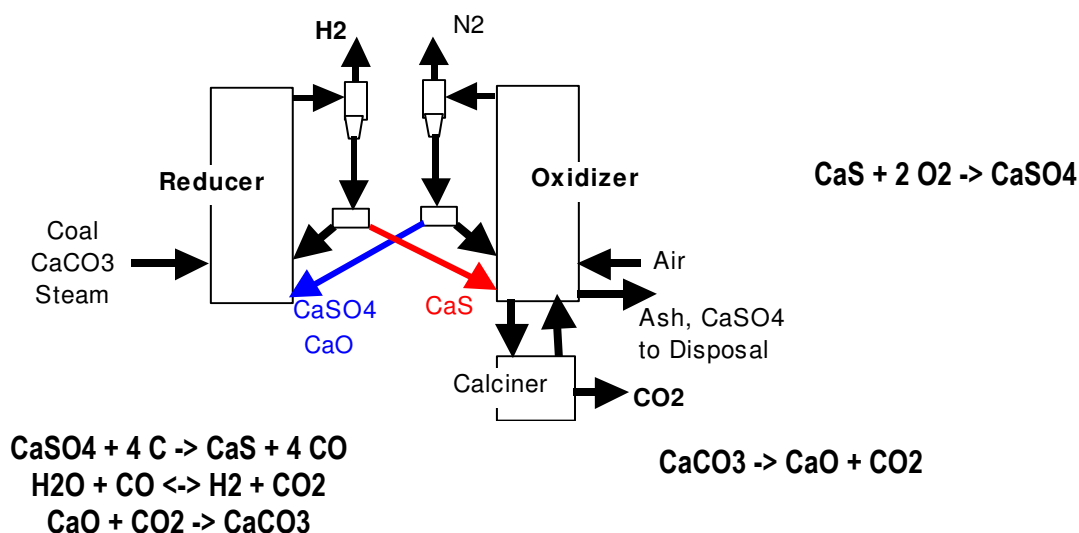


**Figure 2-3 - Indirect Gasification with Hydrogen Production and CO<sub>2</sub> Capture – Option 3.**

By deploying these configurations as independent steps for the evolving future market, this new concept offers the promise to become the technology link from today's Rankine cycle steam power plants to tomorrow's advanced energy plants, being highly efficient and CO<sub>2</sub> capture capable. As these configurations increase in complexity from Option 1 to Option 3, the timing of commercial introduction is likely to proceed from Option 1 to Option 3. In particular, Option 1 represents a "CO<sub>2</sub> capture-ready" coal fired power plant in that CO<sub>2</sub> has been separated from the nitrogen fluegas. In its initial deployment, Option 1 does not require CO<sub>2</sub> clean up and compression. These steps can be added later.

### 3. Chemical Looping History

#### 3.1 Alstom's Background in Gasification Technology

Alstom has significant experience in studying and developing advanced combustion and gasification processes for coal based power generation. In the time period 1974-1981, the company was involved in the development of a coal gasification process aimed at producing a 140 BTU/SCF gas. The process was air blown, but also suited for O<sub>2</sub> blown technique. A 120-ton per day pilot plant (equivalent to 12-15 MW) was built and operated for 3.5 years, **Figure 3-1**.



**Figure 3-1 - The Windsor Connecticut Coal Gasification Pilot Plant.**

The DOE selected this technology for two demonstration projects:

- 150 MW Gulf States Utilities (1980-1982).
- 65 MW IGCC for CWL&P (City Water Power and Light) in Springfield, Illinois (1990-1995).

In addition, the technology was selected as a Japanese National Project to build a 200TPD (equivalent to ~20 MW) pilot plant. The project was initiated in 1985 and successfully completed in 1995. Further plans for commercialization continue in Japan.

In the mid-80's, Alstom pioneered the introduction of CFB (Circulating Fluid Bed) technology in the US. Sizes have increased from 15 MW in the 80s to nearly 400 MW today. Studies are ongoing to apply supercritical steam conditions to the CFB technology. With the aim to advance Alstom's CFB technology further, the company initiated a new effort in the gasification field in 1997. The objective was to develop a process concept that can produce syngas for gas turbines without an O<sub>2</sub> plant. This process, Hot Solids Gasification, would use a solids recycle loop to transfer the necessary O<sub>2</sub> to the system. The solids could be oxidized using air in an oxidizer step and separately the oxygen from this oxidized material would be used to oxidize the fuel - chemical looping. The chemical reactions of FeO to Fe<sub>2</sub>O<sub>3</sub> and CaS to CaSO<sub>4</sub> were studied in laboratory TGA (Thermo Gravimetric Analyzer) and drop tube tests. The measured kinetic reaction rates for the CaS/CaSO<sub>4</sub> loop were used in a design study in 1998. Calcium was used because it can carry more O<sub>2</sub> per pound than metal oxides and it is more readily available. The study showed that, with this technology, a coal-based power plant can be designed significantly smaller than a state of the art PC fired boiler, illustrated in **Figure 3-2**.

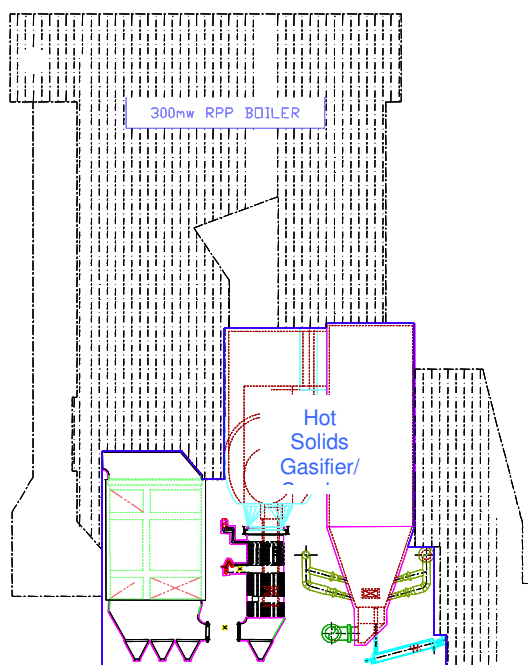


**Figure 3-2 - Process Size Comparison between a PC Fired Boiler and a Hot Solids Gasifier/Combustor System.**

## 3.2 Greenhouse Gas Economic Study

Under the U.S. DOE NETL Cooperative Agreement No. DE-FC26-01NT41146, Alstom carried out a project entitled “Greenhouse Gas Emissions Control by Oxygen Firing in Circulating Fluidized Bed Boilers” (**Reference 2**). As part of this project, a comprehensive conceptual design study was done comparing the technical feasibility and economics for several alternative process concepts involving control of CO<sub>2</sub> emissions. Plant types included in this study were coal combustion and coal gasification type power plants. Comparisons of plant performance, investment costs, and economics were developed. The complete results of the study are reported in the Phase-1 Topical Report (**Reference 2**). In that study two chemical looping based plants with CO<sub>2</sub> capture were analyzed and were evaluated very favorably as compared to other CO<sub>2</sub> capture options studied. Costs used for all of these studies are accurate to within 25% on an absolute basis, but are more accurate on a relative basis and provide a firm basis for economically comparing power plant alternatives.

A total of thirteen (13) Greenfield case studies, listed below, were analyzed in this evaluation. The thirteen cases were subdivided into three groups. Seven of the cases were grouped as Coal Combustion cases, four were IGCC cases, and two were Chemical Looping gasification cases. One Combustion case, two IGCC cases and one Chemical Looping gasification case were analyzed without CO<sub>2</sub> capture. These cases without CO<sub>2</sub> capture represent Base Cases for comparison with the respective CO<sub>2</sub> capture cases. Inclusion of the Base Cases allows accurate quantification of the impact of CO<sub>2</sub> capture and gas processing on plant efficiency, cost, and cost of electricity. CO<sub>2</sub> mitigation costs (\$/Ton of CO<sub>2</sub> avoided) were also calculated relative to the appropriate Base Case. Within each technology group, the order of the various cases roughly represents increasing levels of technology development complexity (i.e., within the combustion cases with CO<sub>2</sub> capture, Cases-6 & -7 would require the most development and Case-2 the least).

### Coal Combustion Cases:

- Case-1: Built and operating Air Fired Circulating Fluidized Bed (CFB) without CO<sub>2</sub> Capture (Base Case for Comparison to Cases 2-7)
- Case-2: Oxygen Fired CFB with CO<sub>2</sub> Capture (trace O<sub>2</sub> and SO<sub>2</sub> removed for EOR)
- Case-3: Oxygen Fired CFB with CO<sub>2</sub> Capture (sequestration-only, less pure than Case -2)
- Case-4: Oxygen Fired Circulating Moving Bed (CMB) with CO<sub>2</sub> Capture (advanced boiler concept)
- Case-5: Air Fired CMB with CO<sub>2</sub> Capture utilizing Regenerative Carbonate Process
- Case-6: Oxygen Fired CMB with Oxygen Transport Membrane (OTM) and CO<sub>2</sub> Capture
- Case-7: Indirect Combustion of Coal via Chemical Looping and CO<sub>2</sub> Capture

### IGCC Cases:

- Case-8: Built and Operating Present Day IGCC without CO<sub>2</sub> Capture (Base Case for Comparison with Case-9)
- Case-9: Built and Operating Present Day IGCC with shift reaction and CO<sub>2</sub> Capture added
- Case-10: Commercially Offered Future IGCC without CO<sub>2</sub> Capture (Base Case for Comparison with Case-11)
- Case-11: Commercially Offered Future IGCC with shift reaction and CO<sub>2</sub> Capture

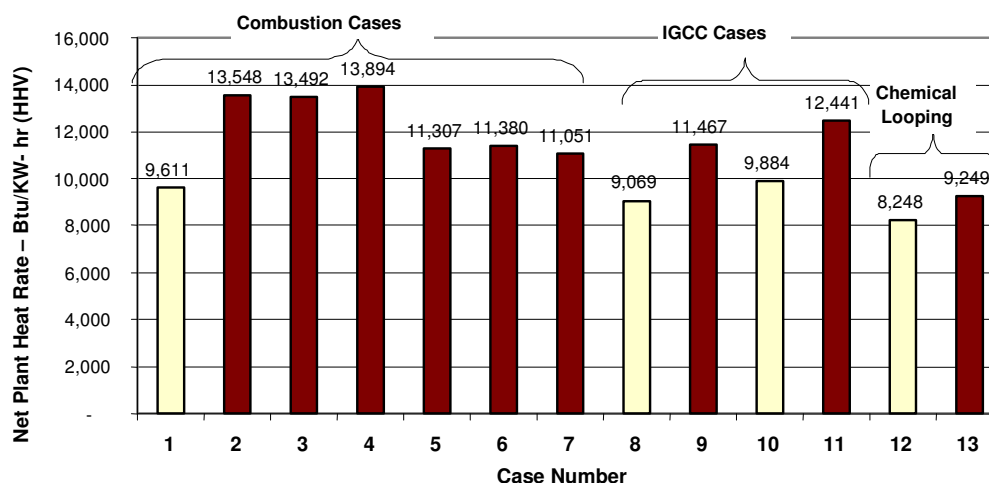
#### Chemical Looping Gasification Cases:

- Case-12: Indirect Gasification of Coal via Chemical Looping (Base Case for comparison to Case-13)
- Case-13: Indirect Gasification of Coal and CO<sub>2</sub> Capture via Chemical Looping

All plants were designed for the identical coal and limestone analyses, ambient conditions, site conditions, etc. such that each case study provided results which are directly comparable, on a common basis, to all other cases analyzed within this work. The ambient conditions used for all material and energy balances were based on the standard American Boiler Manufacturers Association (ABMA) atmospheric conditions (i.e. 80 °F, 14.7 psia, 60 percent relative humidity).

Performance results are shown in **Figure 3-3**. Case 1 is the base case without CO<sub>2</sub> removal. With CO<sub>2</sub> removal all of the combustion cases incur significant heat rate penalties, but Case-7 had the lowest penalty (Chemical Looping Combustion).

**Figure 3-3 - Greenhouse Gas Project Results – Efficiency.**



Case-7, the chemical looping combustion case with CO<sub>2</sub> capture, shows the highest net plant thermal efficiency at about 30.9 percent. For this case, the efficiency reduction is almost entirely due to the power required for the compression and liquefaction of the captured CO<sub>2</sub>. For this case there is essentially no energy penalty associated with the

capture of CO<sub>2</sub> other than the energy required to recirculate the solids between the oxidizer and reducer vessels.

CO<sub>2</sub> capture Cases-9, -11 and -13 all incur significant power output degradation as compared to their Base Case counterparts (Cases-8, -10, and -12), due to the heavy demands of auxiliary power for gas processing which includes CO<sub>2</sub> compression. The efficiency differences among these cases are a reflection of the differences in gasification processes, CO<sub>2</sub> capture processes, and auxiliary power requirements.

The Chemical Looping gasification cases (Cases 12 and 13) were found to be more efficient both with and without CO<sub>2</sub> capture (36.9 and 41.4 percent HHV, respectively) than all other CO<sub>2</sub> control cases including the comparable Texaco based IGCC cases. Case-12 was 10 and 20 percent more efficient than Cases-8 and -10 respectively, while Case-13 was 24 and 34 percent more efficient than Cases-9 and -11 respectively.

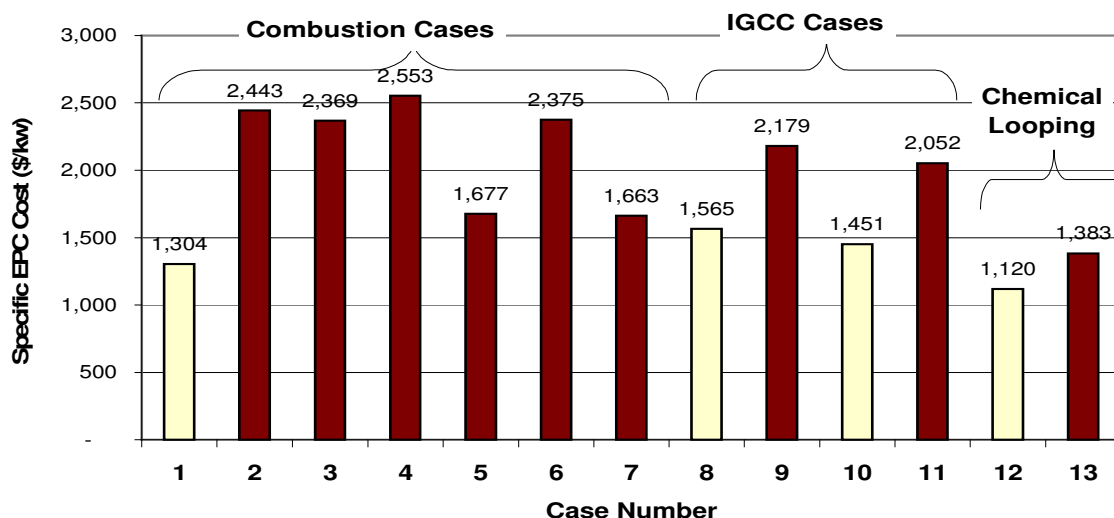


**Figure 3-4 - Greenhouse Gas Project Results – EPC Costs.**

The capital cost for the Base Case without CO<sub>2</sub> capture was 1,304 \$/kW (2003 \$). The plant investment cost range for the remaining combustion cases (Cases-2 thru -7) with CO<sub>2</sub> capture was from about 1,660 to 2,550 \$/kW. Case-7 (Chemical Looping Combustion) was found to be the lowest cost of the combustion based capture cases (1,663 \$/kW) followed closely by Case-5, the Regenerative Carbonate Process, at 1,677 \$/kW. Cases-2, -3, and -4, all variants of the cryogenic based oxygen fired process, were found to have significantly higher EPC (Engineered, Procured and Constructed) costs (2,370 – 2,550 \$/kW). Case-3, which used a simplified Gas Processing System (drying and compression only), showed a savings of about 74 \$/kW or about 3 percent as compared to Case-2. Case-6 (oxygen fired via an advanced OTM system) was slightly less costly than the comparable cryogenic case at about 2,375 \$/kW, a savings of about 7 percent as compared to Case 4.

The plant investment costs (EPC basis) for the Texaco Base Cases (Cases 8 and 10) without CO<sub>2</sub> capture was 1,565 and 1,451 \$/kW. The plant investment costs for the corresponding cases (Cases-9 and -11) with CO<sub>2</sub> capture were 2,179 to 2,052 \$/kW respectively. Case-13 (Chemical Looping gasification) was found to be the lowest cost of the capture cases (1,383 \$/kW) as compared to Case-12 without CO<sub>2</sub> capture at 1,120 \$/kW, a 23.5% differential.

**Figure 3-5** summarizes the economic results for all thirteen cases in this study. It shows levelized cost of electricity for all cases.

For cases with CO<sub>2</sub> capture, Case-13, Chemical Looping gasification, represents the best of the cases studied based on both levelized COE (Cost of Electricity) and CO<sub>2</sub> mitigation cost evaluation criteria. Case-7, Chemical Looping combustion, and Case-5, the regenerative carbonate process, were about 12 and 14 percent higher than Case-13 with respect to levelized COE. These three cases showed significant COE advantages as compared to all other capture cases in this study.

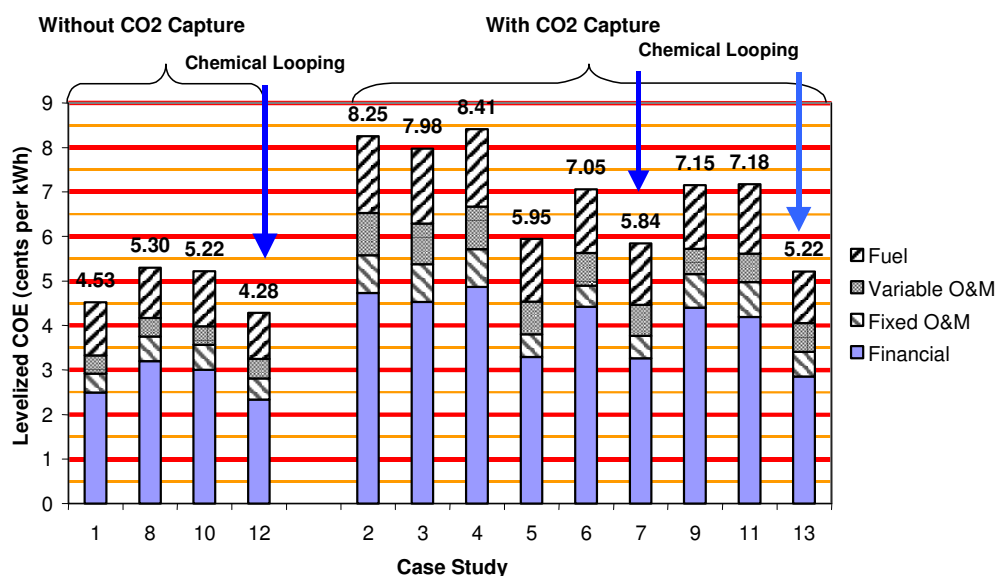


**Figure 3-5 – Greenhouse Gas Report - Cost of Electricity**

### 3.3 Phase I and Phase II Accomplishments

Before the contract started, in a preliminary phase (Phase 0) Alstom funded and built the required small-scale pilot facility (**Process Development Unit**, PDU) at its Power Plant Laboratories in Windsor, Connecticut. Construction was completed in calendar year 2003.

The objective for Phase I was to develop the indirect combustion loop with CO<sub>2</sub> separation and syngas production from coal with the calcium sulfide (CaS) / calcium sulfate (CaSO<sub>4</sub>) loop utilizing the PDU facility. The results of Phase I were reported in **Reference 1**, “Hybrid Combustion-Gasification Chemical Looping Coal Power Development Technology Development Phase I Report”

The objective for Phase II was to develop the carbonate loop – lime (CaO) / calcium carbonate (CaCO<sub>3</sub>) loop, integrate it with the gasification loop from Phase I, and ultimately demonstrate the feasibility of hydrogen production from the combined loops. The results of Phase II were reported in **Reference 3**, “Hybrid Combustion-Gasification Chemical Looping Coal Power Development Technology Development Phase II Report”

The PDU was modified at the start of Phase II to make several changes and repairs to accomplish the Phase II tasks. Modifications included adding a moisture condenser upstream of the vacuum pump, upgrading the steam supply system, developing another solids flow measuring device, upgrading the venting system from several process loops and upgrade the gas analysis system to measure the product gas for the Phase II tests.

The cold flow model designed and built for the Phase I test was used extensively in Phase II to measure the transport characteristics of the solid material used in the Phase II tests. The plastic model was also used to visualize the flow characteristics of the transporting solids. A forty-foot tall plastic model was constructed for use in Phase III. This model has been used later to test higher solids flow rates with a taller static solids seal.

As in Phase I, engineering support was required throughout Phase II to support the test program and analyze the resulting data. As part of this work, all of the required modifications were designed and built, and the design of the new forty-foot tall cold flow model was completed. In-house process and economic models simulating the mass, energy and chemical transport in the looping process using data derived from the PDU were used as tools to aid in the development of commercial plant concepts.

A rigorous technical peer review was accomplished. In addition to the technical peer review, a project review was conducted to show that the Chemical Looping project was being developed with realistic technical and economic specifications and that the project development plan was addressing commercialization needs.

The topics addressed in the reviews were reaction kinetics in the chemical looping reactors, solids transport, economic issues and a number of other minor issues. As a

result of the reviews, the project plan was modified to address any shortcomings in the original plan.

The kinetics rates were questioned from the standpoint that if the rates were not fast enough the reactors might be sized too small and therefore the plant cost estimates might be too low. It was determined that the rates established in Phase I and Phase II tests were faster than the rates assumed when the economic analysis was done. Additionally, even if the rates were slower than the assumptions by a factor of ten, the net effect on the overall plant costs were still small and didn't change the original economic conclusions (**Reference 2**).

The solids transport concerns were that the chemical looping system uses fairly high solids loading. It was shown that while the solids loadings are aggressive there is a considerable amount of experience in industry to show that the loadings used in the chemical looping concept are reasonable.

The economic analysis reviewed the cost of using more transport gas than originally assumed and found that the impact of changes in capital cost of the plant as well as the energy consumed did not significantly affect the overall economics and the efficiency of the chemical looping concept.

The reviews also included comparisons with other limestone-based processes such as the Consol CO<sub>2</sub> Acceptor process, and the Exxon O<sub>2</sub> Donor process. Outside consultants were used to assist in all of the reviews conducted.

Testing was done in the PDU and in the 4-inch diameter Fluid Bed Combustor (FBC). Tests were run primarily to provide data concerning the calcium oxide to calcium carbonate reactions and the water gas shift reactions. Tests were also run at the PDU to show the operation of several loops operating at the same time.

The Phase I and Phase II program produced the following accomplishments:

- The program provided the chemical validation of Alstom's chemical looping process. The following processes were demonstrated and significant data was generated for each:
  - CaS – CaSO<sub>4</sub> looping
  - CaO - CaCO<sub>3</sub> looping
  - Water gas shift:  $\text{CO} + \text{H}_2\text{O} \rightleftharpoons \text{H}_2 + \text{CO}_2$
  - Hydrogen production
  - Sorbent reactivation
  - CO<sub>2</sub> removal
  - Char gasification/combustion via CaSO<sub>4</sub>
  - Coal devolatilization

- The PDU was used to show the simultaneous operation of four solids transport loops at elevated temperatures. The temperatures were about 1800 degrees F at a pressure of about 1 ata.
- The PDU was operated with five solids transport loops simultaneously at ambient temperatures.
- Multi-loop control requirements were established.
- The seal pot control valve (SPCV) operation requirements were established and the operation was controlled and steady for most of the testing.
- Startup requirements were established for smooth startup.
- Emergency quick shut down and quick restart procedures were established.
- Inspection and maintenance procedures were determined.
- A water condenser, water trap and gas reheater system for the vacuum pump inlet was designed, built and successfully operated.
- The PDU successfully transported four very different solids (inert sand, commercial gypsum, coarse CFB bed material and the normal chemical looping sorbent). It was learned that the angle of repose tests for each solid are required for SPCV design and that cold flow model testing for fluidization rates was directly applicable to the hot case.
- The project team successfully passed the 'Product Development Quality Specification Gate Review' and the Technical Peer Review with very few changes required in the development plan.

## **Conclusions:**

The main conclusion from Phase I and Phase II is that all of the PDU chemistry required for the chemical looping process has been validated.

Additional conclusions are as follows:

### **From Phase I (Reference 1)**

1. It is practical to build a chemical looping system using the  $\text{CaS}$  to  $\text{CaSO}_4$  reaction without losing sulfur as either  $\text{SO}_2$  or  $\text{H}_2\text{S}$ .
2. High gasification rates can be obtained in a chemical looping system even with low reactivity coals. A carbon conversion rate of 5%/sec ata was used for the

commercial plant economic studies, while the minimum rate achieved in the Chemical Looping PDU was twice the required rate with low reactive char.

3. It is possible to operate three interactive solids transport loops (oxidizer, reducer and sorbent activation), at elevated temperatures (1800 degrees F).
4. It is possible to start up and heat up the solids transport loops interactively.
5. The Chemical Looping PDU design concept is validated.
6. Cold flow modeling provides a valuable tool for simulating the hot chemical looping system. The cold flow model is useful for determining fluidization and solids transport control settings for fluidizing and transport gases.
7. The original economic conclusions were still valid after determining the Phase I chemical reaction rates at the PDU. The original costs studies were based on equipment sizes determined from bench-scale reaction rates. Phase I showed these rates to be conservative.

#### **From Phase II (Reference 3)**

1. Operation with five parallel loops is becoming routine. The PDU demonstrated five parallel loops cold and four parallel at operating temperatures.
2.  $\text{CaO} + \text{CaCO}_3$  kinetics were demonstrated in the PDU at operating temperatures.
3. Water gas shift reactions occurred rapidly at PDU operating conditions.
4. Cold flow bench test scale-up methods reveal what the hot PDU behavior will be like.
5. Economics assumptions are still valid after detailed peer review and detailed specification review.
6. Important control strategies were tested and validated.
7. The sorbent activation system vent system can accurately measure flow from the sorbent reactivation reactor.
8. The original economic conclusions are still valid after determining the Phase II chemical reaction rates at the PDU. A  $\text{CO}_2$ -Capture rate (i.e. Rate of conversion of  $\text{CaO}$  to  $\text{CaCO}_3$ ) of 5%/sec-ata was used for the commercial plant economic studies.  $\text{CaO}$  conversion rates achieved in the Chemical Looping PDU were an order of magnitude greater the required rate for normal-sized sorbent material (i.e. 16 mesh).

## **4.0 The PDU Project**

### **4.1 Objectives**

The overall objective of the Chemical Looping Project is to develop and verify the high temperature chemical and thermal looping process concept and to design, construct and demonstrate a pre-commercial, demonstration version of this advanced system. In support of this objective, Alstom proposed an extension to the original two-year, two-phase program. The extension was for three additional phases to bring the Chemical Looping concept to commercial status.

The Chemical Looping concept is exceptionally flexible. There are many potential commercial options. However, Alstom determined the chemical looping combustion option to be a more near term option for “capture ready” applications. As such, more emphasis on this approach was looked at in Phase III.

The objective of Phase III is to operate the pilot plant to obtain enough engineering information to design a prototype of the commercial Chemical Looping concept. The activities include modifications to the Phase II Chemical Looping process development unit (PDU), solids transportation studies, control and instrumentation studies and additional cold flow modeling. The deliverable is a report making recommendations for preliminary design guidelines for the prototype plant, results from the pilot plant testing and an update of the commercial plant economic estimates.

The objective of Phase IV is to design, build and operate a prototype unit in the size range of 5 to 10 million BTUs per hour of heat input (i.e. 500 to 1000 lb/hr of coal). This work will include the prototype testing and development. The commercial plant design and economic analysis will be verified based on data generated from testing the chemical looping prototype. Cold flow tests will be done. Engineering studies and commercial planning will also be done. Plans for the demonstration plant will also be done including arranging funding, selecting demonstration sites, finding sponsors, contacting A&E's, and other demonstration plant requirements. A final report will be written describing the results of the prototype construction and testing and will include the updated demonstration and commercialization plans.

The objective of Phase V is to design, build and operate a demonstration plant. This will include developing project management plans, lining up participants, signing agreements, securing funding, doing environmental impact studies, permitting, EPC, startup and commissioning, operations, testing, modifying the unit as required and standards development. A commercial planning update will also be done. A final report will be written documenting all the Phase V activities.

These three phases constitute the remaining work required to bring Alstom's Chemical Looping process to commercial status. There will be a decision- point at the end of each phase, during which Alstom and the DOE will review of the results of the phase and then separately decide whether or not to proceed with the next phase. As part of these

decision points, the work scope, cost and schedule of the following phases will be re-examined by Alstom and changed as required.

## **4.2 Phase III Task Description**

### **Phase III – Pilot Plant Testing**

The primary purpose of Phases I and II was to verify the chemistry for the process and determine the kinetic rates of the important reactions. These objectives have been successfully accomplished. The emphasis during Phase III is on material handling, solids transport, automatic control and scale up. The results from these studies will be used to design, build and test the prototype facility planned for Phase IV.

#### **Task 3.1 – Process Testing**

A small pilot plant was constructed by modifying the existing Chemical Looping PDU. All of the existing capabilities of the PDU were retained for the pilot and additional capabilities were added. Modifications allow carbon burnout testing for the reducer, and included separate stacks for the oxidizer and the reducer and more automatic controls. Repairs of the existing facility were made to improve reliability. The new pilot facility was prepared by shakedown testing of the facility systems (flow controls, data acquisition, reactors, solids transport equipment, feeders, heaters, coolers, etc.). The pilot plant operation included integrated operation of the various loops including the reducer, sorbent activation loop and oxidizer with emphasis on solids transport, material handling and process control and employed both hot and cold operation. Various control strategies were tested to develop practical methods for control for use in the Phase IV prototype facility.

#### **Task 3.2 – Transport Testing**

In support of Task 3.1, cold flow transport test design and testing was done based on commercial and prototype concepts. Testing was done to simulate the pilot plant. Solids transport was modeled for the solids lifting legs and the letdown legs for the reducer to oxidizer and the oxidizer to reducer crossover lines. Modifications were made to the existing 15-foot and 40-foot cold flow facilities for this purpose.

#### **Task 3.3 – Analytical Support**

PPL's Laboratory Services group supported the program by preparing and supplying reactants (e.g., fixed carbon, coal,  $\text{CaSO}_4$ , lime, limestone, etc.) for the pilot facility. Bench-scale testing and sample analysis were performed on a periodic basis to support testing under Tasks 3.1 and 3.2.

#### **Task 3.4 – Engineering Support**

Engineering support of Task 3.1 and 3.2 was required throughout Phase III. As part of this work, the commercial plant concept was reviewed and updated. The reactor was based on Phase I and Phase II results. The specifications were rechecked. The results of the commercial concept were used to develop a prototype concept for Phase IV.

Results to date indicate that a circulating bed (CFB) reactor operating at about 30 feet per second gas velocity with coal and limestone size distributions similar to those of Alstom's CFB boilers meets all performance and economics targets. However, this velocity is about 50% higher than Alstom's current CFB practice. Therefore, the commercial plant study compared the performance and economics of the current Chemical Looping concept with that employing Alstom's traditional CFB design and design conditions.

Engineering studies also considered the following areas:

1. Refractory and metallurgy;
2. Mechanical concepts;
3. Controls;
4. Turndown and load following;
5. Integrated gasification concepts;
6. Plant configuration;
7. High temperature air heater;
8. Solids transport;
9. Plant construction cycle time;
10. Safety;
11. Reliability and maintainability;
12. Startup and shutdown;
13. Backend cleanup;
14. Environmental requirements;
15. Plant specification review;
16. Updated environmental performance and costs;
17. Preliminary equipment specifications;
18. H<sub>2</sub>S removal and
19. Pilot plant and prototype test plan.

#### Task 3.5 – Project Management

The project manager tracked and maintained the overall project scope and budget, prepared required periodic and final reports, and represented Alstom to the DOE. The lead technical investigator, working with the project manager, directed the concept development and process engineering. Upon the completion of Phase III, Alstom completed and submitted this Phase III report and submitted a proposal for the Phase IV work.

### 4.3 Phase III Test Log Summary

Test results are in **bold**.

#### 15 Foot Cold Flow Model

31-Oct-06	Air supply control system check
13-Nov-06	Air supply control system check.
21-Nov-06	<b>Smooth air flow distribution after pickup demonstrated.</b>
01-Dec-06	Shake down and startup test after modifications
05-Dec-06	Air pressure control testing
06-Dec-06	Air Pressure reducer valve test.
08-Dec-06	Solids flow test.
12-Dec-06	New 'sugar scoop' test.
15-Dec-06	<b>Seal pot rebuilt. Test with Seward FBHE ash.</b>
20-Dec-06	Air supply control system check. <b>Controllable air supply system demonstrated</b>
	Cyclones inspected. New 'Chiu Sugar Scoop' tested.
21-Dec-06	Solids flow test. Cyclone plugged.
22-Dec-06	Solids flow test.
27-Dec-06	Tested 3/8" insert installed in seal pot for flow control. Tested Laser velocity probe.
28-Dec-06	Continued Solids flow test. Steady state achieved for 15 min.
01-Jan-07	Continued Solids flow test
03-Jan-07	Continued Solids flow test
04-Jan-07	Alternate video flow meter tested.
05-Jan-07	Laser probe calibration. New 'sugar scoop'.
09-Jan-07	Solids flow test.
10-Jan-07	Solids flow test with .5" orifice in seal pot.
11-Jan-07	Solids flow test with .61" orifice in seal pot.
12-Jan-07	Remove sugar scoop pickup. Solids test. Seal pot failure.
15-Jan-07	Rebuilt seal pot. Reinstalled 'sugar scoop'. Used 3 – 3/8" orifices spaced 3/4" vertically in seal pot.
16-Jan-07	Used 3 – 3/8" orifices spaced 1/2".
17-Jan-07	Used single 1/2" insert.
18-Jan-07	Continue last test. <b>Smooth long duration solids flow demonstrated</b> <b>Accurate laser diode velocity flow meter operation demonstrated.</b>
19-Jan-07	Continue last test.
22-Jan-07	Solids flow test.
23-Jan-07	Bulk density measured. Fluidizing test.
24-Jan-07	Minimum fluidization test. Air leak in supply
25-Jan-07	Repeat fluidization test. Bad air flow control valve.
29-Jan-07	New control valve. Repeat fluidization test.

02-Feb-07	New seal pots fabricated for two loops. ½" orifice for main recirc and 3/8" orifice for crossover. Flow test started.
05-Feb-07	Solids flow test continued.
06-Feb-07	Solids flow test continued.
07-Feb-07	Added 9/16" wide slit orifice to seal pot.
08-Feb-07	Added ¾" orifice to dipleg. Too small - Bored out to 1".
12-Feb-07	Removed dipleg orifice.
13-Feb-06	Added .188" orifice in fluidizing air supply.
15-Feb-07	Test on laser velocity probe.
16-Feb-07	Replaced seal pot grid plate with sintered mesh type.
19-Feb-07	ruptured seal pot due to pressure excursion.
20-Feb-07	Rebuilt A seal pot.
21-Feb-07	Sealed leak in seal pot.
22-Feb-07	Flow test. 'A' loop not stable.
23-Feb-07	Used pickup tee with no scoop in 'B' loop.
26-Feb-07	Flow test
27-Feb-07	Continued flow test.
28-Feb-07	Opened crossover valves from B to A loops.
01-Mar-07	Flow test stopped when PC failed.
02-Mar-07	Switched 'sugar scoops' in A and B loops.
05-Mar-07	Switched 'sugar scoops' back.
06-Mar-07	Modified seal pot fluidizing pad
07-Mar-07	Flow test.
14-Mar-07	Fluidized column and orifice test.
15-Mar-07	'B' seal pot flow test.
16-mar-07	Continue seal pot flow test.
19-Mar-07	Continue seal pot flow test.
20-Mar-07	Continue seal pot flow test. Use ¼" orifice.
21-Mar-07	Install 3/8" orifice.
22-Mar-07	Install ½" orifice. Test then installed 7/16" orifice.
23-Mar-07	Installed .26" orifice.
26-Mar-07	Installed 1/8" orifice. Flow meter test.
27-Mar-07	Bypass Calibration test 1/2" orifice in 'B' discharge, .25" in crossover.
28-Mar-07	Tried different orifice sizes in crossover.
29-Mar-07	Tried different orifice sizes in crossover.
30-Mar-07	Calibration of Flow meters.
02-Apr-07	Two loop test.
03-Apr-07	Continue crossover flow test.
04-Apr-07	<b>Dual loop operation sucessfully demonstrated.</b> Laser probe calibration test.
05-Apr-07	Continue flow test. Changed orifices.
06-Apr-07	Continue flow test. Moved crossover orifice position. Added knife edge to orifice.
09-Apr-07	Continue flow test.
11-Apr-07	reassembled 'A' and 'B' loop

12-Apr-07	Test of crossover flow.
13-Apr-07	DP cell calibration. Crossover test.
17-Apr-07	Crossover test. Tried different orifices.
18-Apr-07	Disassembled Seal pot for revision found leaks.
01-May-07	Installed new seal pot designs. Started crossover test.
02-May-07	Continue crossover tests.
03-May-07	Continue crossover tests. Changed orifices.
04-May-07	Continue crossover tests. Changed orifices.
07-May-07	Continue crossover tests. Changed orifices.
08-May-07	Continue crossover tests. Changed orifices.
09-May-07	Continue crossover tests.
15-May-07	Modified seal pots.
16-May-07	Continue crossover tests. Changed orifices. Both crossovers operating together.
24-May-07	Changed orifices. Continue crossover tests

## 40 Foot Cold Flow Model

11-June-07	<b>Smooth operation demonstrated on initial startup. Successful scale up from 3/4" diameter to 4" diameter demonstrated.</b>
12-June-07	Seal Height Test
13-June-07	Continue Seal Height Test
14-June-07	Grease Air Test
15-June-07	2x Grease Air Effects Test
20-June-08	Install new 'Sugar Scoop'
21-June-07	Test 36 fps in riser
22-June-07	Test 43 fps in riser. Fixed leak in SPCV valve.
25-June-07	New solids pickup designed. Ran 24 foot seal height.
26-June-07	Ran 24 foot seal height.
27-June-07	New 4 inch pickup installed. Saltation limit reached at 45 fps.
28-June-07	Repairing cyclone leak.
29-June-07	Continued cyclone leak repair.
05-July-07	Test of emergency shutdown for slip velocity calculation.
06-July-07	Test of emergency shutdown to observe dipleg change.
09-July-07	Check orifice size on SPCV. Ruptured SPCV exit pipe.
13-July-07	New plenum installed to reduce leakage.
16-July-07	Grease air injection point modified. SPCV cracked.
18-July-07	SPCV fixed. 197 inch seal height tested.
19-July-07	Slip velocity test. Recalibrate Baghouse load cell.
23-July-07	397 inch seal height test.
25-July-07	Repair secondary cyclone cone leak.
26-July-07	Tested 2.7 inch orifice.
27-July-07	Tested 2x1.4 inch and 2x1.9 inch orifices with 296 inch seal.
30-July-07	Tested 2x1.4 inch and 2x1.9 inch orifices with 358 inch seal.
02-Aug-07	Tested 2x1.75 inch and 2x2.0 inch orifices.
13-Aug-07	Bulk density test. Tested 316 inch seal.
30-Aug-07	Tested 2x1.75 inch and 2x2.5 inch orifices. SPCV exit failed
17-Sept-07	Rebuilt SPCV. New startup.
18-Sept-07	35 fps in riser.
19-Sept-07	New software for laser probe. 'Stop Velocity' test.
21-Sept-07	Checked Labview software problems
24-Sept-07	Tested 390 inch seal. Ruptured 4 inch elbow.
26-Sept-07	Erosion damage fixed. Ran 35 fps in riser.
27-Sept-07	Varied SPCV transport air at 35 fps. 'Stop Velocity' test.
28-Sept-07	Ran 394 inch seal with 37 fps in riser.
18-Oct-07	Ran 75 fps in riser with 'Stop Velocity' test.
19-Oct-07	Grease air test with 392 inch seal and 36 fps in riser.
01-Nov-07	Tested variable riser velocity.
02-Nov-07	Tested 35 fps in riser with 359 inch seal height.
05-Nov-07	Video-taped 'Stop Valve' test to calibrate previous calcs.
08-Nov-07	Ran 391 inch seal height.

## Pilot Plant PDU

29-Mar-07	Shakedown Pilot Plant for Phase III configuration.
02-Apr-07	Correct control system programming. Leak check PDU.
17-Sept-07	Start PDU with both Vacuum pumps in automatic control. Operation with automatic flow control to SPCV Determine automatic control methodology.
18-Sept-07	Vacuum pump bypass fixed, Control system modifications
19-Sept-07	Air system checked out
20-Sept-07	Thermocouple problems resolved. Operational issues.
21-Sept-07	Vacuum pump logic test on air only. Riser flow logic test on air only.
24-Sept-07	Control system set point change test heater control system test Vacuum pump air only control test.
25-Sept-07	Clear plugs in process lines and instrument lines. Set vacuum pump control loops. Test load change response.
26-Sept-07	<b>1. Vacuum pump control test, air only with solids in loops.</b> <b>2. Test load change response. One pump on automatic control.</b> <b>3. Long term vacuum pump loop stability control test with 2 pumps in automatic control, no solid recycle but solids in SPCV's</b> <b>4. Solid transport test in one loop with auto control</b> <b>5. Shut down test with auto controls.</b> <b>6. manual reducer solids recycle test.</b> <b>7. SPCV solids transfer test.</b>
27-Sept-07	<b>1.Startup in automatic control mode.</b> <b>2.Automatic warm up flow control.</b> <b>3. Long term load following test.</b> <b>4. Oxidizer solids recycle test with crossover in auto.</b> <b>5. Test of fast automatic shut down (intentional).</b>
28-Sept-07	After test equipment assessment. <b>Oxidizer solids recycle control test.</b>
01-Oct-07	Equipment cleanout and minor repairs and adjustments.
19-Oct-07	Test of gas analyzer rack and Method 16 sulfur measuring system.
23-Oct-07	Continued gas analyzer test.

## 5.0 PDU Pilot Plant Description

The objective of the first two phases of this program was to investigate the chemistry of the Chemical Looping process and to determine how to transport solids in each part of the system. The objective of Phase III was to obtain enough information to design and construct a prototype of the commercial Chemical Looping concept. The emphasis was on material handling, solids transport, automatic control and scale-up.

A small pilot plant was constructed by modifying the existing Chemical looping PDU. All of the existing capabilities were retained and additional capabilities were added. Automatic controls were added to the SPCV gas feed lines. A second vacuum pump, scrubber and stack were added to simulate the control action required in the commercial concept where separate outlet streams must be controlled independently because they cannot be mixed. In addition, several upgrades and repairs were made to the PDU including a new gas burner, chamber pots (aka solids knock out cans), spray nozzles in the heat exchangers, gas outlet controls and an upgraded control system computer and software.

A simplified process flow diagram of the upgraded facility is shown in **Figure 5-1**.

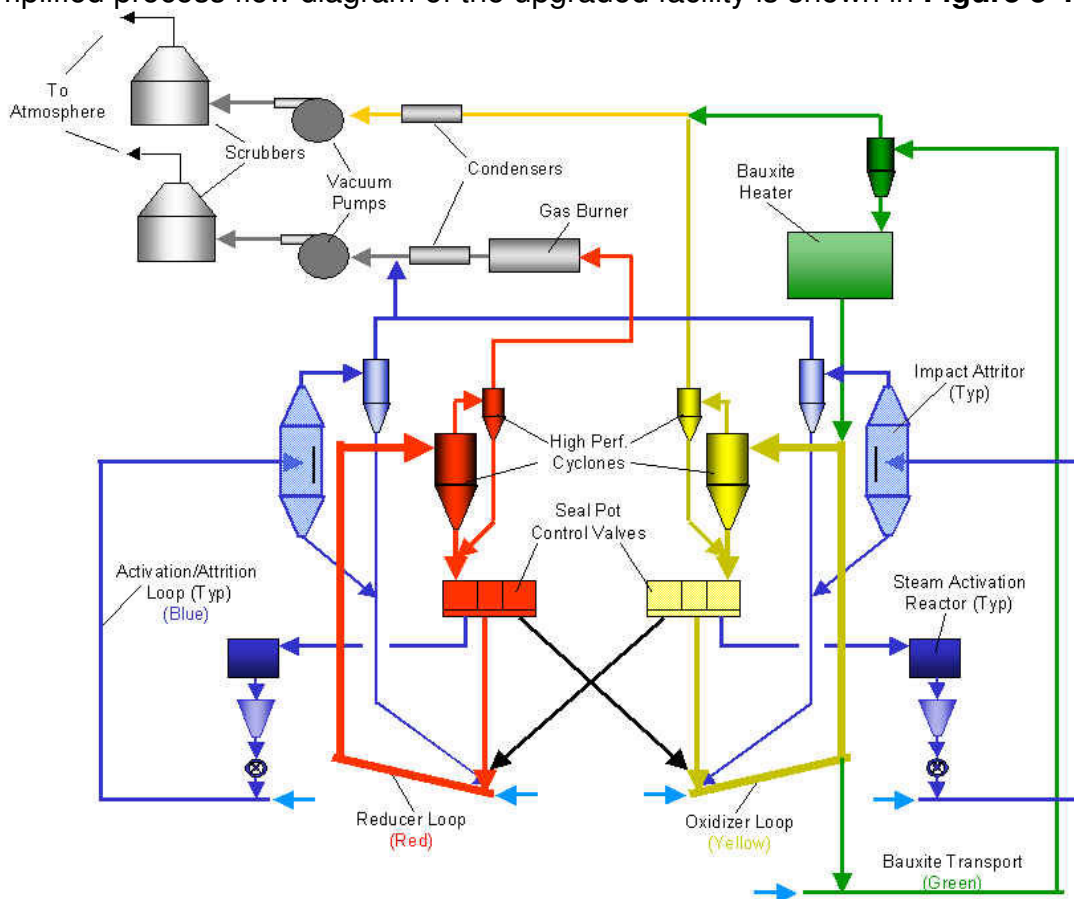


**Figure 5-1 – Phase III Chemical Looping Test Facility**

## 5.1 PDU Modifications

### Burner Can Modifications:

At the end of Phase II, the burner can was found to have several problems. Several small leaks occurred from the water cooling jacket, corrosion was found in the welds, stress cracks were found around the site glass penetration tube and water was found to be pooling on the bottom of the burner can inner vessel.

The burner can was redesigned to eliminate metal fatigue and cracking from thermal expansion and corrosion. The internal chamber was redesigned to eliminate the “step” such that any water or condensation would be moved to the process drain or carried through to the condensers. The cone at the exit was replaced with an offset frustrum. The sight port was relocated from the water-cooled jacket to the front of the burner where it penetrates refractory. These changes seemed to eliminate most of the problems. The modified burner can (before it was reinsulated) is shown in **Figure 5-2**.

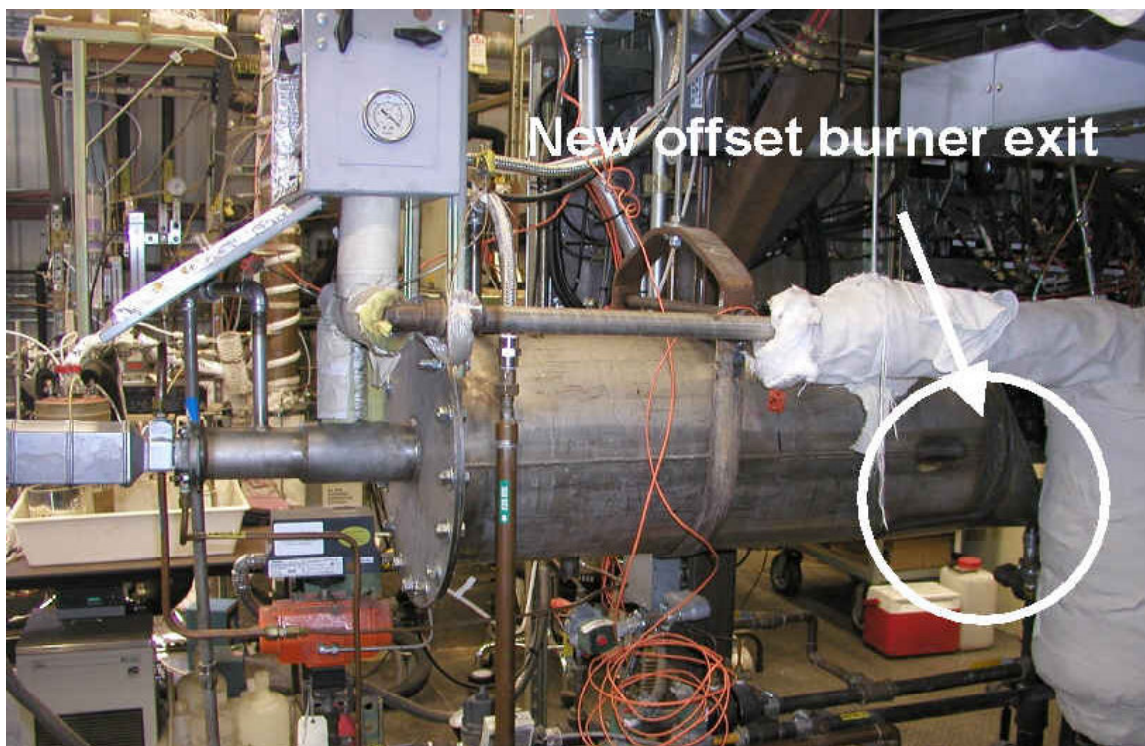


**Figure 5-2 – New Gas Burner**

### Vacuum Pump Installation:

The second vacuum pump was mounted above the existing one. This entailed relocating the original scrubber system and piping. The two vacuum pumps were then plumbed such that both systems (reducer and oxidizer) could run on either pump or as their own independent systems. Additionally, all sensors and safety devices needed to be reconfigured to provide data and safe operation regardless of operating configuration.

Two other system enhancements were pneumatically operated by-pass valves and three way ball valves to allow for post-test maintenance on the pumps. The pneumatic valves allow the operator to control by-pass flows from the control room. The three way valves allow him to operate the vacuum pumps on ambient air for drying and lubrication of the impellers prior to shut down. The vacuum pump installation is shown in **Figure 5-3**.



Figure 5.3 – Second Vacuum Pump

### Scrubbers:

To facilitate the installation of the second scrubber (**Figure 5-4**), the original scrubber and containment system were relocated. This allowed keeping the scrubbers as an “island” and increase hydraulic head to prevent any back flow during shutdown. Additionally, this provided more floor space near the vacuum pumps to allow for plumbing of the process gas streams and exits to the scrubbers and stacks. The extended containment system allowed the location of the auxiliary scrubber equipment (water supply, drain & pH control systems) on the same island. The pH monitoring and level control systems were installed and wired to the Siemens Control System.



Figure 5.4 – Second Scrubber

The exhaust manifold was also dismantled and reassembled such that the two gas streams cannot mix. Additionally, stack instrumentation was relocated and rewired.

### **SPCV Modifications:**

Two main modifications to the SCPV system were the addition of manual pressure balancing valves on the crossover legs and automated control of fluidizing and transport flows.

To help maintain control over the crossover flows, manual ball valves were installed between the crossover leg and SCPV vent header for each system. This allows for improved delta-p control between the two systems.

In an effort to automate the system, Mass Flow controllers were purchased and installed on the fluidizing and transport flows. The challenge was to provide sufficient range of flows to accommodate fluidizing velocities over a broad temperature range. This was accomplished by using multiple flow controllers on each system plumbed in series. The rotameters were left in the system to provide visual verification of actual flows and provide another level of control.

The original method of controlling the fluidizing and transport air flows was with the rotameters as shown in **Figure 5-5**. This method was cumbersome but it was necessary to understand the concept of controlling the SCPV and the three solids streams it controls. A great deal of the work in understanding the function of the SCPV was also carried out in the 15-ft cold flow model (CFM).



**Figure 5.5 – Manual Control of the SCPV**

The automatic flow controllers were programmed into the computer and methods of controlling the SPCV were developed and verified in Phase III (**Figure 5-6**).



#### **Sorbent Activation System Modifications:**

The two modifications for the sorbent activation systems were the fabrication and installation of solids collection cans and a large hot box on the outlet vents.

One solid collection can (Chamber Pot) was installed on each sorbent activation system (Oxidizer, Reducer), **Figure 5-7**. These were installed to absorb solids during system upsets and prevent full pluggage of these systems from condensing water in the vents.

The hot box was installed to maintain higher temperatures on the filters and prevent condensation of the steam, while still allowing for solids removal.



## **Feed Systems:**

One additional feeder was purchased and integrated into the Siemens Control System. This allows the capability to feed two products to the reducer and one to the oxidizer loop simultaneously.

## **Heat Exchanger Air and Water Supply Modifications:**

Supply headers for these two systems were significantly modified to eliminate flow deviations and waterside deposits.

The water supply system was overhauled to prevent spray nozzle plugging. Spray nozzle flow calibrations and heat exchanger temperature control issues indicated large fluctuations in spray nozzle performance. Visual inspection showed up to 70% of the nozzles were partially or completely plugged with an iron deposit. The water system was re-plumbed to remove all iron materials from the system (except stainless steel nozzles) and inlet filters were installed to reduce particulates. Additionally, the header was redesigned so pressures could be better monitored and drops in feed pressure were reduced regardless of water usage.

The air supply system to the heat exchangers was subject to flow instabilities due to varying pressures and flow requirements. A larger header system with better instrumentation and distribution to the flow controllers was installed to eliminate these issues.

## **5.2 Control System Modifications**

The timely delivery of reactants (mass) and energy is vital to the chemical looping process to sustain the desired chemical reactions.

The endothermic reducer (fuel) reactor relies on energy and oxygen from the oxidizer (air) reactor to sustain the fuel combustion and generate the desired combustion byproducts. In order for the CL energy conversion process to be commercialized a reliable automatic control strategy needs to be developed for all modes of CL operation.

During the CL Phase III program, a milestone was established to demonstrate that automated process control of the CL solids transport process was feasible. This automated controls feasibility milestone translated into a short controls testing period at the PDU.

The automated control elements that were added in Phase III were the control valves for the gas supply lines to the SPCVs and the second vacuum pump. In Phases I and II, the gas outlet vents from each loop (oxidizer, reducer and sorbent activation) were controlled with one pump and pressure control valves for each line. The commercial concept will have separate CO<sub>2</sub>, N<sub>2</sub> and product gas streams, which cannot be mixed. These will require separate fans and controls. In Phase III the control system for

separate pumps was investigated and a control concept was designed. Testing was done to prove the concept for the chemical looping application. The over-all objective of the Phase III controls testing was to gain insight relative to the challenges connected with automatic solids control of multi-loop two-phase air-solids flow.

Regardless of which CL reactor loop one considers the primary method of solids transport control will be based on pressure monitoring. This is true for both the intra-reactor solids transport (recycle) and inter-reactor solids transport (crossover). Whether it is actual airflow, static loop pressure or differential pressure, automated controls for CL will be based on a functional relationship between the measured solids transport and the measured pressure control parameters.

For the CL Phase III automated controls testing three control loops were defined and instrumented (**Figure 5-8**) at the CL PDU. This CL configuration was intended to allow the investigation of the basic feedback control concepts for solids transport control without the added complexity of chemical reactions. Automated controls feasibility needs to be established during steady state operation, during heat up and during transient operation. It was also intended to see what load change rates might be possible.

The areas of Automated controls investigated in Phase III are:

1. **Inter-Loop Pressure control**
2. **Process Temperature Trim of Injection Air control**
3. **Solids Transport Rate control**

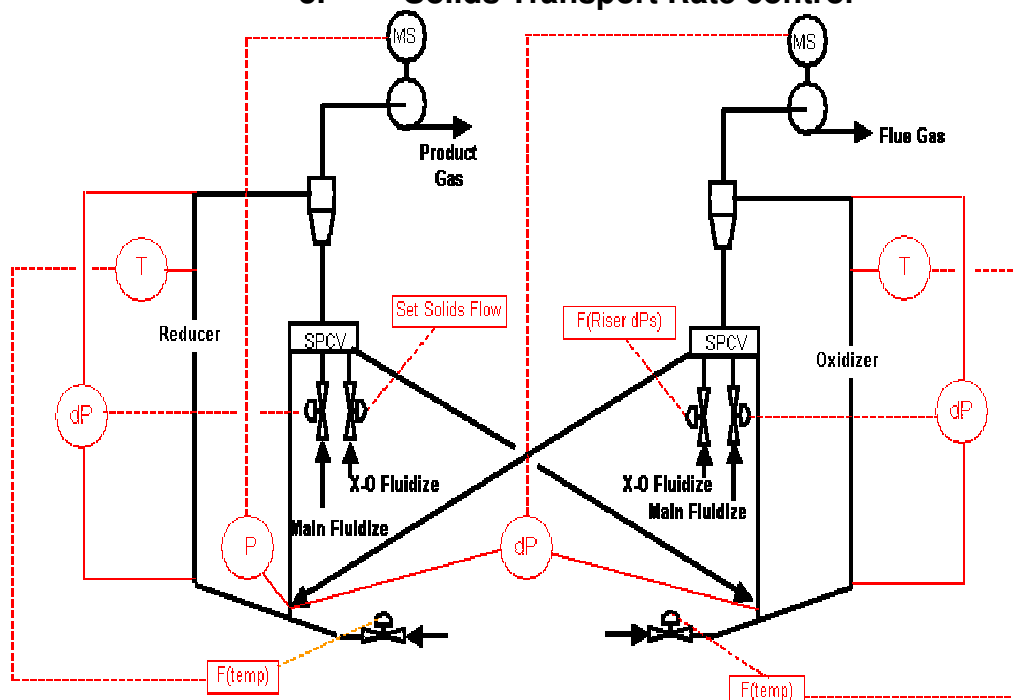


**Figure 5-8 - Chemical Looping Phase III Automatic controls Schematic Diagram**

### **5.3 PDU Gas Sampling and Analysis System**

In Phase III, several modifications were made to the Gas Sampling and Analysis System. This included modifications to the Method 16B Total Sulfur Measurement equipment, physical modifications to the sampling equipment, calibration modifications and adding input data options.

To automate the sample delivery pressure, a Jordan Proportional Control Valve and a pressure transmitter combined with a Siemens control logic program was installed. The intention was to dynamically control sample pump recirculation flow to control sample delivery pressures to gas conditioning and monitoring systems. Validation of Method 16B was necessary to prove the accuracy of the modifications to it. The method was modified to accommodate the combustible nature of the sample.

#### **5.3.1 Method 16B – Usual applicability of the method**

Method 16B is normally used to quantify the emissions to atmosphere of Total Reduced Sulfur (TRS) compounds from stationary sources related to Kraft pulp mills. The emissions sources are typically either products of combustion, as from a lime kiln, or ambient air based, as from a pulping tank vent. Sulfur compounds, including TRS, are oxidized to SO<sub>2</sub> in a tube furnace, by oxidation with the inherent excess O<sub>2</sub> in the sample. The resulting SO<sub>2</sub> is measured directly.

The sample gas normally measured by this method may also contain ppm levels of carbon monoxide (CO) and hydrocarbon gases, both of which will also combust in the tube furnace to CO<sub>2</sub>. This change to the sample matrix is insignificant due to the typically low levels of these components, with the Moles of gas leaving the tube furnace being assumed equal to the Moles of gas entering the tube furnace.

In the Chemical Looping gas analysis system, the goal is the same: quantify the levels of TRS in the sample gas stream. The difference is that the sample stream is a fuel feed stock comprised mainly of H<sub>2</sub> and CO, with percent levels of hydrocarbons, in a balance of CO<sub>2</sub>, with little N<sub>2</sub> and essentially no O<sub>2</sub>. In order for the TRS to be oxidized to SO<sub>2</sub>, the combustible fractions of the sample must also be completely combusted, with some O<sub>2</sub> excess air. This requires addition of combustion air at roughly the volume rate of the sample, and an overall change in the moles of products of combustion, compared to the moles of sample and air.

The tube furnace effluent is then analyzed, per Method 16A, for SO<sub>2</sub>. O<sub>2</sub> is also measured, in order to insure adequate excess air for complete oxidation. The sample gas sulfur content is then calculated indirectly, using a custom made Excel spreadsheet, which accepts the above SO<sub>2</sub> and O<sub>2</sub> data, as well as real time analyses of the sample gas composition.

A series of gases was analyzed in order to test the measurement system's ability to predict sample sulfur levels based on real time measurements. The test gas compositions were specified in order to simulate multiple Chemical Looping process gas scenarios.

The following table, **Table 5-1**, below, shows the components of each cylinder.

<b>Table 5-1</b> <b>Compositions Of Calibration Gases Used To Prove Out Method 16B System</b> Chemical Looping Process Development Unit (Hot) Alstom Power, Inc. Windsor, Ct. November, 2007								
	H <sub>2</sub>	N <sub>2</sub>	O <sub>2</sub>	CO	CO <sub>2</sub>	CH <sub>4</sub>	H <sub>2</sub> S	COS
Air		78.9	21.1					
4500 ppm SO <sub>2</sub> cal gas		99.6						
Scott #1	25.04	59.95		4.99		10.05		
Scott #2	54.5			35	10.02		0.5	
Scott #3	46.45	2		35	10	6	0.5	.05
Scott #4	47.95	2		35	10	5		.05

All values are v/v %

Air was used to check for a system zero level of SO<sub>2</sub>, at varying excess air dilutions, with no combustion present. The SO<sub>2</sub> cal gas was used to establish how accurately the ppm prediction was, at varying excess air dilutions, with no combustion present.

Scott #1 was used to check for a system zero level of SO<sub>2</sub>, at varying excess air dilutions, with combustion occurring.

Scott #2 was used to check the conversion efficiency of H<sub>2</sub>S to SO<sub>2</sub>, at varying excess air dilutions, with combustion occurring.

Scott #3 was used to check the conversion efficiencies of both H<sub>2</sub>S and COS to SO<sub>2</sub>, at varying excess air dilutions, with combustion occurring. The balance gases are a better simulation of process gas than are Scott #1 or #2.

Scott #4 was used to check the conversion efficiency of COS to SO<sub>2</sub>, at varying excess air dilutions, with combustion occurring. The balance gases are a better simulation of process gas than are Scott #1 or #2.

## Results of Validation Tests

Three tests were run on simulated process gas containing sulfur compounds. These tests used the cylinders described above as "Scott #2, Scott #3, and Scott #4". The results are shown below in **Table 5-2**.

**Table 5-2**  
**Calibration Test Results**

Cylinder	Sulfur species	% conversion to SO <sub>2</sub>
Scott #2	H <sub>2</sub> S	96%
Scott #3	H <sub>2</sub> S & COS	84%
Scott #4	COS	88%

Each conversion efficiency number is an average of the conversion efficiencies at multiple tube furnace excess air levels. In general the conversion efficiency is highest at near-stoichiometric O<sub>2</sub> levels and tends to drop off as excess air increases. Tube furnace exit temp was monitored and stayed steady throughout the tests at 1400 degF +/- 30 degF. The efficiency drop off at high excess air rates may reflect increasing extrapolation of the SO<sub>2</sub> values measured, as dilution increases. Overall tube furnace flows remained steady across multiple excess air settings, by reducing sample gas as air increased. This may have reduced conversion efficiencies at high excess air, by decreasing heat output via sample combustion.

Overall, the Method 16B sampling system was seen to operate well for both sulfur species, at multiple operational settings.

### **5.3.2 Physical Modifications**

The sampling system for measuring sulfur compounds employed by the Chemical Looping Process Development Unit (Hot) was based upon the system described in the US EPA Method 16B, found in the Code of Federal Regulations, Title 40, Part 60, Appendix A. As described in **Section 5.1**, above, the Method 16B train was modified to accommodate the requirements of this application. Each of the modifications is described below.

#### **Buffer Solution for SO<sub>2</sub> Scrubbing**

Method 16B specifies the use of a citric acid/sodium citrate buffer solution, located before the tube furnace, to selectively remove SO<sub>2</sub> from the sample stream. In this way, all of the SO<sub>2</sub> measured at the tube furnace exit is due to the conversion of TRS compounds. The Chemical Looping gas analysis system did not employ the citric acid/sodium citrate buffer solution for SO<sub>2</sub> removal, due to the lack of SO<sub>2</sub> in the reducer side process gas stream. This modified Method 16B sample train converts any of the reduced sulfur species (e.g. H<sub>2</sub>S, COS, C<sub>2</sub>S) to SO<sub>2</sub>, thereby measuring total sulfur.

#### **Blending Excess Air**

Combustion air was blended into the process sample gas at the inlet to the tube furnace, in order to provide sufficient combustion air to burn off (oxidize) the fuel

fractions of the sample, as well as to oxidize all sulfur species to  $\text{SO}_2$ . Rather than trying to accurately meter the fuel and air streams separately via mass flow controllers or rotameters, it was decided that a real time oxygen analyzer would be used to indicate the presence of excess air at the tube furnace outlet, in parallel with the  $\text{SO}_2$  analyzer. The total flow rate of sample gas and combustion air was limited to that required to satisfy the two analyzers, which was approximately 2 liters per minute.

In the standard application of Method 16B to paper mill type samples, combustion air is not required, as there is sufficient excess oxygen in the sample to facilitate oxidation of sulfur compounds to  $\text{SO}_2$ .

### **Burner Tip**

A simple burner tip was installed at the tube furnace inlet, to smoothly mix the combustible sample gas with air at the point of combustion. This arrangement avoided the build-up of potentially explosive gases in the section of 5/8 inch diameter quartz tubing, which lined the tube furnace. Operation without this burner tip caused a pulse of flame to periodically propagate up the quartz tube, to the point of gas mixing, causing a pressure pulse throughout the system.

### **H<sub>2</sub>O Conditioning**

The combustion of sample gas in the tube furnace generated  $\text{H}_2\text{O}$  as a product of combustion. This wet gas stream was passed through a Peltier sample dryer (Universal Analyzers, Inc. Model 1090 PV), to provide a dry sample to the  $\text{O}_2$  and  $\text{SO}_2$  analyzers. The sample dryer employed was designed by the manufacturer to be used with  $\text{SO}_2$  samples without introducing a negative system bias due to interaction between  $\text{SO}_2$  and condensate.

### **5.3.3 Calculations Modifications**

The calculation of sulfur compound content in the sample gas was based upon the Method 16B calculations. The above described modifications to the physical arrangement of the sampling system caused additional calculation steps to be required, in order to account for the combustion of the fuel fractions of the sample and to factor in the dilution effect of excess air.

The input data required to achieve these corrections and to ultimately determine the sulfur compound level of the process sample are as follows:

- v/v % composition of  $\text{CO}$ ,  $\text{CO}_2$ ,  $\text{H}_2$ ,  $\text{O}_2$  and  $\text{H}_2\text{O}$  in process sample gas.
- v/v % composition of  $\text{O}_2$  and ppm level of  $\text{SO}_2$  in tube furnace exit gas.

In the simplest terms, the calculations take the following form:

1. Start with one standard liter of process sample,
2. calculate how many standard liters of product gas are formed in the tube furnace, after combustion and dilution,

3. Measure the SO<sub>2</sub> in the product gas,
4. Calculate the process sample sulfur content by multiplying the measured product gas SO<sub>2</sub> by the ratio of product liters vs. sample liters.

The detailed calculations are listed below. The Excel spreadsheet used to calculate the results of tube furnace measurements (tfurnace ver2.xls) shows the calculation steps which lead to the result. Each calculation step listed below follows test 4D of the spreadsheet, renamed 102307tfurnace t4 (version 1).xls, in which compressed gas Scott #2 was used (see Table 5.1 above for more info on Scott #2).

A. Composition of Process sample gas and tube furnace exit gas, v/v:

- a) CO = 38% by reducer rack analyzer
- b) CO<sub>2</sub> = 11.3% by reducer rack analyzer
- c) H<sub>2</sub> = 52.41% by micro gas chromatograph
- d) N<sub>2</sub> = 0% by micro gas chromatograph
- e) CH<sub>4</sub> = 0% by micro gas chromatograph
- f) O<sub>2</sub> = 0% by reducer rack analyzer
- g) H<sub>2</sub>O = 0% by Vaisala probe on process
- h) H<sub>2</sub>S = 0.5% rough approx. by 2x tube furnace exit SO<sub>2</sub>
- i) SO<sub>2</sub> at Tube furnace exit = 1940 ppm by SO<sub>2</sub> analyzer
- j) O<sub>2</sub> at tube furnace exit = 2.48% by O<sub>2</sub> analyzer

B. Moles of each above component in one standard liter of process sample gas:

- a) CO = (38/100) \* (1mol/24.04liters) = 0.015807
- b) CO<sub>2</sub> = (11.3/100) \* (1mol/24.04liters) = 0.004700
- c) H<sub>2</sub> = (52.41/100) \* (1mol/24.04liters) = 0.021801
- d) N<sub>2</sub> = 0
- e) CH<sub>4</sub> = 0
- f) O<sub>2</sub> = 0
- g) H<sub>2</sub>O = 0
- h) H<sub>2</sub>S = (0.5/100) \* (1mol/24.04liters) = 0.000161

C. Moles of combustion products from oxidizing each component:

- a) CO<sub>2</sub> from CO and CH<sub>4</sub> combustion = 0.015807 + 0 = 0.015807
- b) H<sub>2</sub>O from H<sub>2</sub> and CH<sub>4</sub> combustion = 0.021801 + (2 \* 0) = 0.021801
- c) Inert CO<sub>2</sub> and N<sub>2</sub> in product gas, from sample = 0.004700 + 0 = 0.004700

D. Moles of O<sub>2</sub> consumed by combustion of each component:

- a) O<sub>2</sub> consumed by CO = 0.5 \* 0.015807 = 0.007903
- b) O<sub>2</sub> consumed by H<sub>2</sub> = 0.5 \* 0.021801 = 0.010901
- c) O<sub>2</sub> consumed by CH<sub>4</sub> = 0.5 \* 0.0 = 0.0
- d) O<sub>2</sub> consumed by H<sub>2</sub>S and COS = 1.5 \* 0.000161 = 0.000242

E. O<sub>2</sub> required for stoichiometric combustion

- a) Stoichiometric O<sub>2</sub> = [ D.a) + D.b) + D.c) + D.d) ] – B.f) = 0.019046 moles

- F.  $N_2$  added from stoichiometric combustion air and excess air:  
a) Stoichiometric  $N_2$  =  $0.019046 * (79.1/20.9) = 0.072084$  moles  
b) Excess air  $N_2$  =  $A.j) * [79.1/20.9] =$
- G. Stoichiometric liters of product gas per liter of fuel:  
a) Std. liters =  $[C.a) + C.c) + B.d) + F.a)] * 24.04 = 2.225896$
- H. Excess air  $O_2$  and  $N_2$   
a)  $O_2$  from excess air =  $[1/24.04] * [A.j) / 100] * [20.9 / [20.9 - A.j)]] * G.a) = 0.002554$  moles  
b)  $N_2$  from Excess air =  $H.a) * [79.1 / 20.9] = 0.009665$  moles
- I. Dry Actual Liters of product gas per liter of fuel:  
a) Dry Act. Liters =  $G.a) + [(H.a) + H.b)] * 24.04 = 2.519633$  liters
- J.  $H_2O$  % at tube furnace exit:  
a)  $H_2O$  % =  $[(C.b) * 24.04] / [(C.b) + I.a)] * 24.04] * 100 = 0.857829\%$   
b) Wet liters/liter fuel =  $I.a) + [(J.a) / 100] * I.a)] = 2.541247$
- K. Process Sample Gas  $H_2S$  and/or  $COS$  ppm concentration  
a) Dry ppm =  $A.i) * I.a) = 4888$  ppm  
b) Wet ppm =  $A.i) * J.b) = 4888$  ppm

### 5.3.4 Input Data Options

The composition of the gas sample being withdrawn from the reducer is measured by the analyzers in the Reducer Rack. These volume percent concentrations of gases are used, among other things, in the calculations shown above.  $H_2$  content is measured indirectly, in real time, by an on-line thermal conductivity monitor manufactured by ABB.  $H_2$  as well as  $N_2$  are measured directly, every two minutes by a micro gas chromatograph manufactured by Agilent Technologies.

The real time ABB  $H_2$  data is useful for monitoring process trends, but is not as accurate as the micro GC direct measurement.  $N_2$  can be calculated from the reducer rack data, by subtraction, yielding a real time trendable  $N_2$  value. Similarly to  $H_2$ , this  $N_2$  value is useful for monitoring process trends, but is not as accurate as the micro GC direct measurement. Therefore, the above calculations use the  $H_2$  and  $N_2$  data from the micro GC preferentially over the real time  $H_2$  and calculated  $N_2$  data. The spreadsheets referred to in the calculations section above, show results using both data sources. The better accuracy using micro GC data can be seen in these spreadsheets.

### 5.4 P&IDs

Process flow and Instrument Diagrams (P&ID) were updated from the Phase I and Phase II P&IDs, to incorporate the changes discussed in Section 5. As described above the primary differences were: 1) the addition of the second vacuum pump and controls

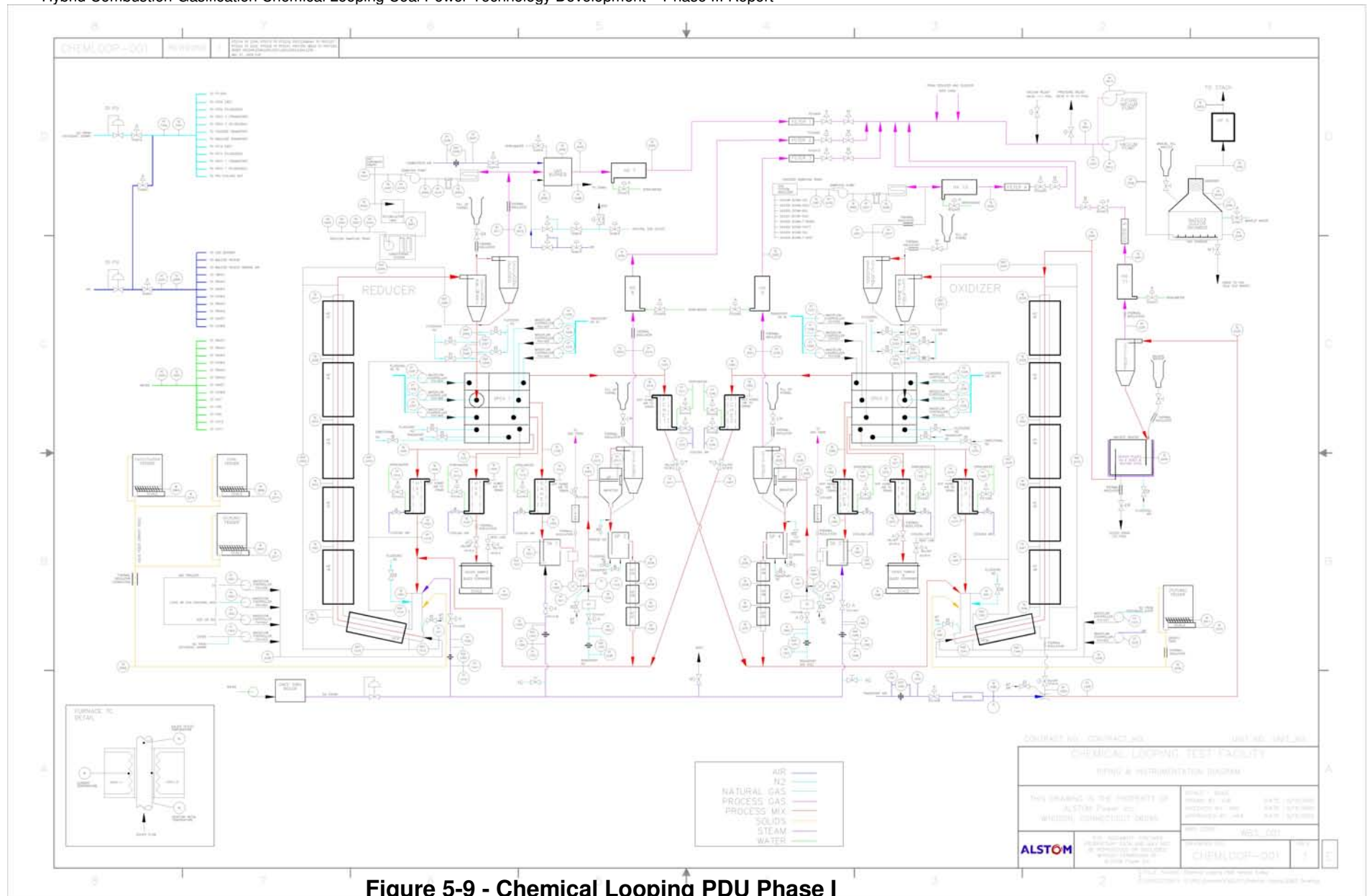
to test control of two main outlet gas streams; 2) the addition of automatic controls on the SPCV fluidizing gas to test control of the solids transport loops under load following, temperature control, and warm-up; and 3) the addition of new gas sampling instruments. The P&IDs from Phase I and Phase II are shown in **Figures 5-9 and 5-10** and the updated Phase III P&ID is shown in **Figure 5-11**.

## **5.5 PDU Process Equipment**

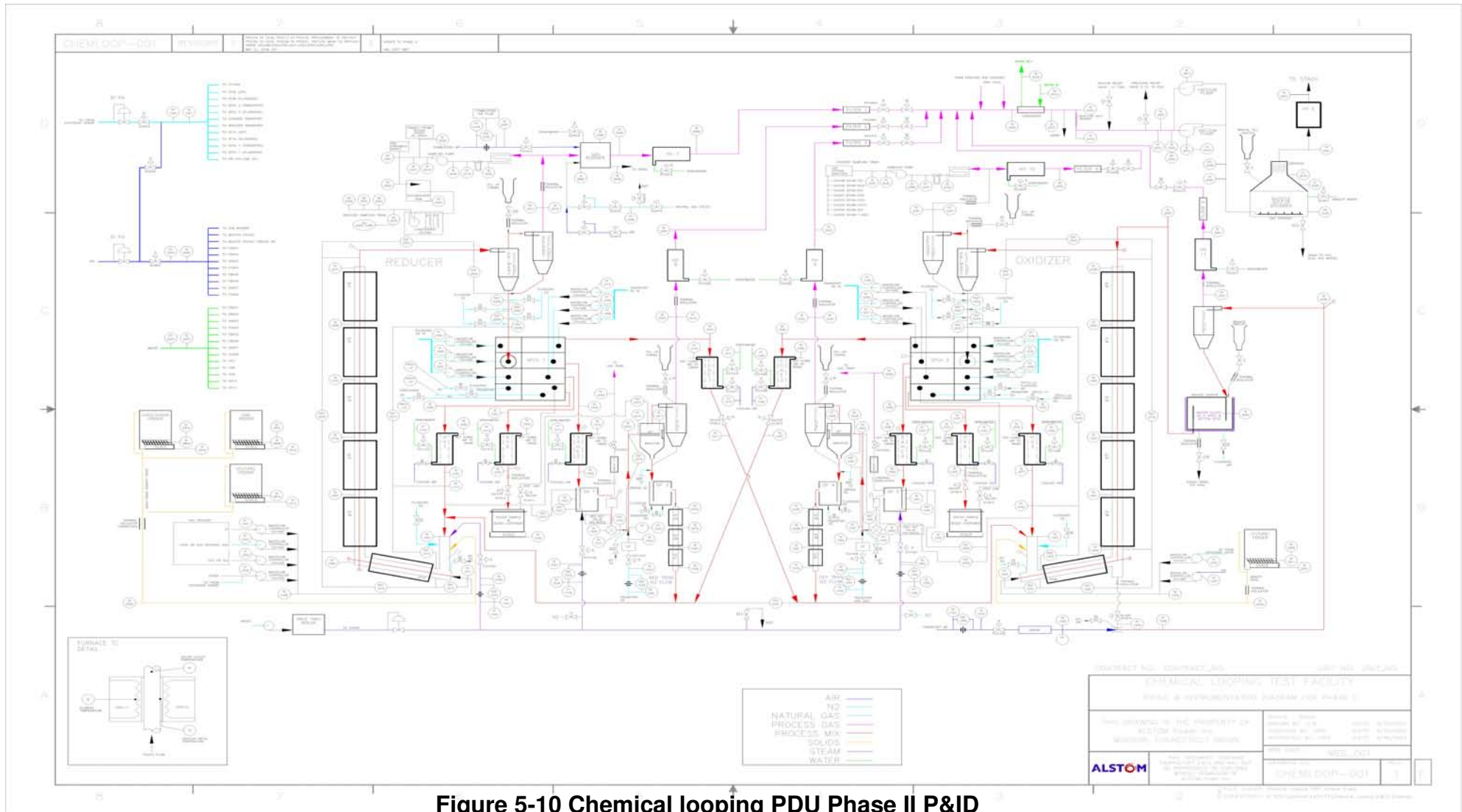
Equipment used in the PDU for Phase I testing is shown in **Figure 5-12** through **Figure 5-20** and the layout of this equipment is shown in isometric views in **Figure 5-21** through **Figure 5-31**.

The PDU was modified for the Phase II testing as described in **Reference 3**. For Phase III the PDU was again modified as described in **Section 5.1** of this report.

**Figure 5-12** and **Figure 5-13** show the design of the cyclones used for the main process loops and the gas vents from the SA and Bauxite Loops. **Figure 5-14** shows the design of the water-cooled heat exchangers used for cooling the solids and the spray coolers used for cooling the gas vents from each process loop. The solids heat exchangers shown were also used for measuring solids flow by calculating a heat balance around the heat exchangers. **Figure 5-15** shows the original Seal Pot Control Valve (SPCV) and **Figure 5-16** shows the seal pot used in the SA loops. **Figure 5-17** shows the solids original pick-up device. **Figure 5-18** shows the product gas burner design. **Figure 5-19** and **Figure 5-20** show the bauxite heater design.



**Figure 5-9 - Chemical Looping PDU Phase I P&ID**



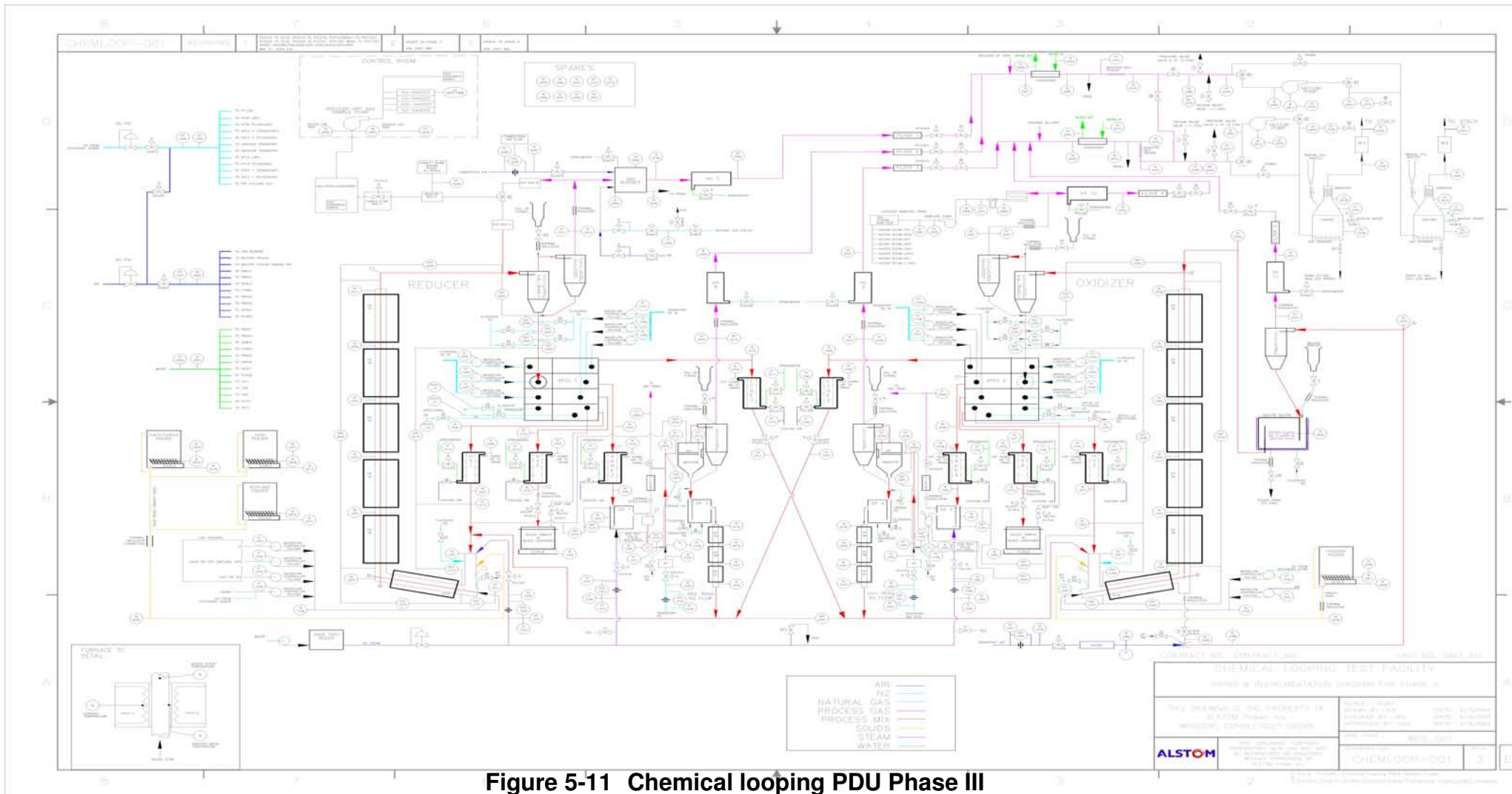
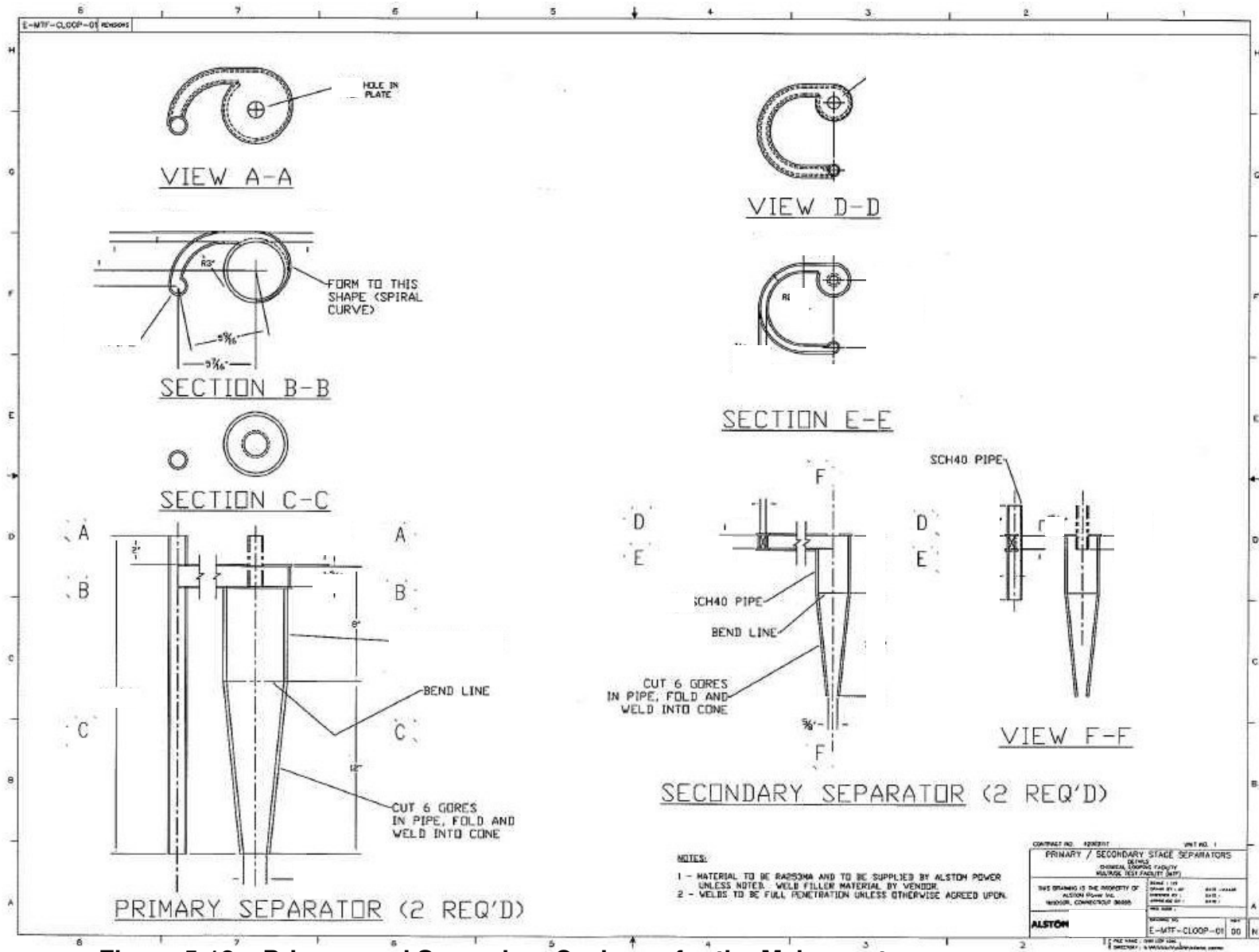


Figure 5-11 Chemical looping PDU Phase III



**Figure 5-12 – Primary and Secondary Cyclones for the Main reactors**



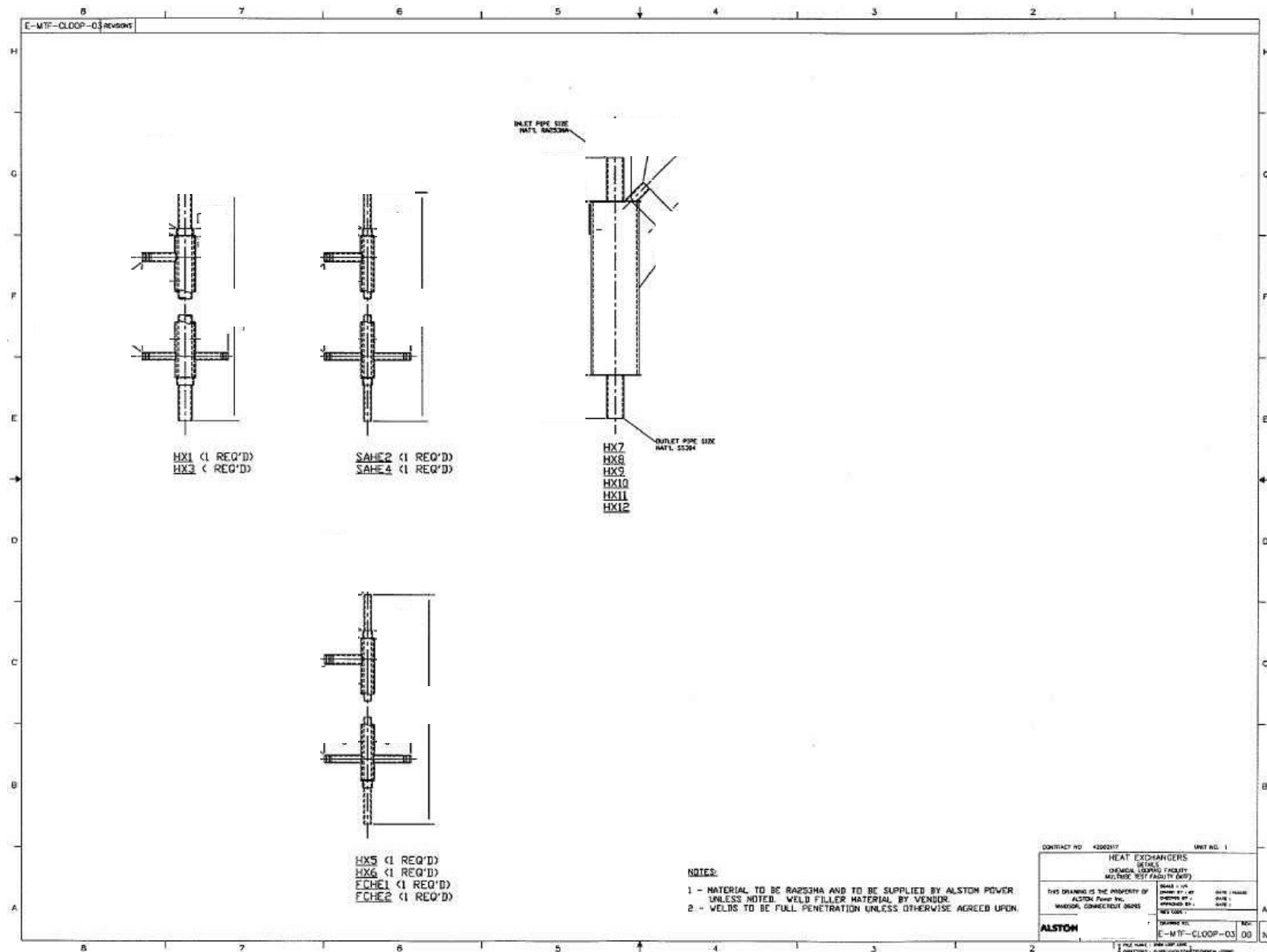
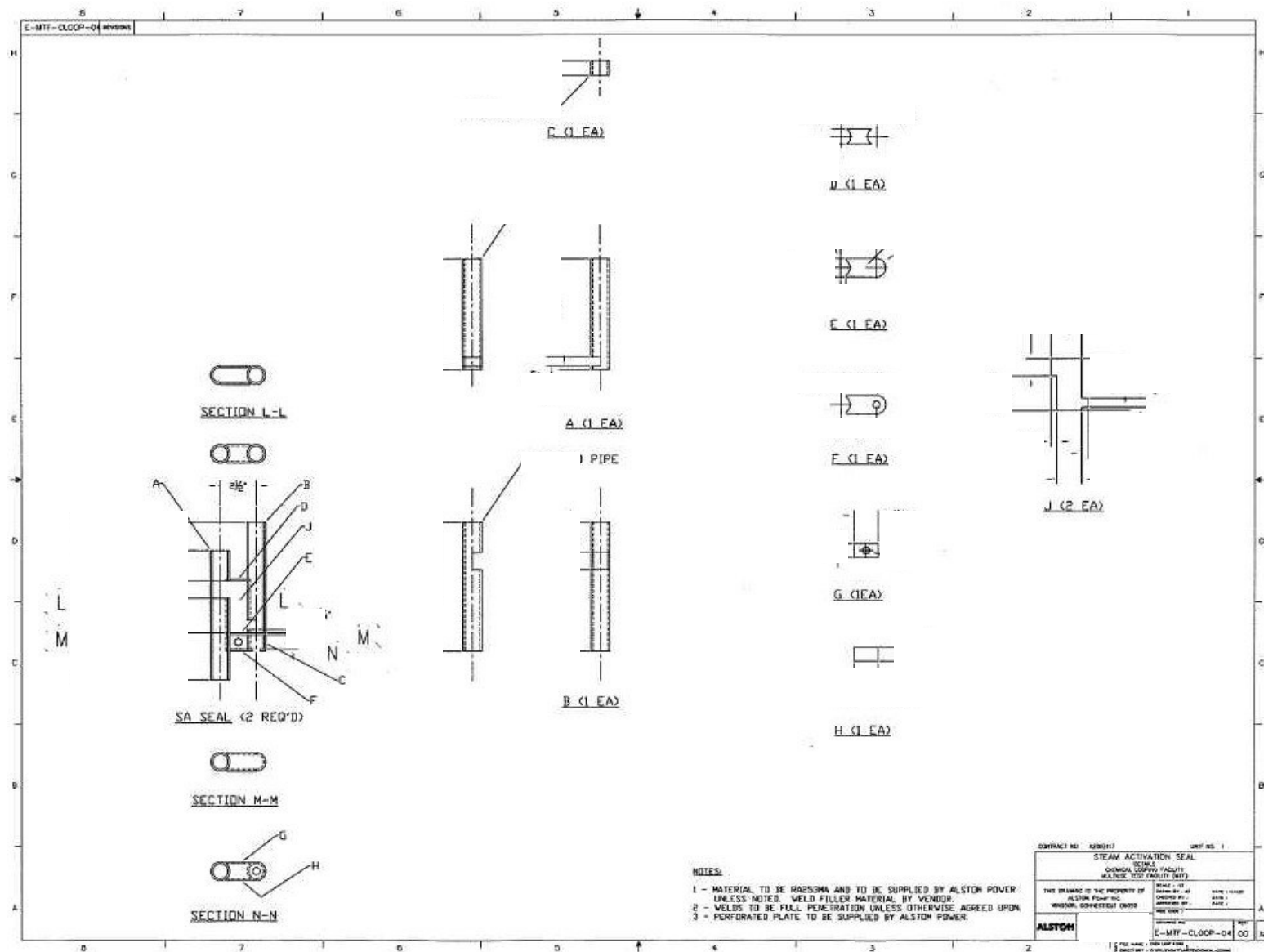


Figure 5-14 – Solids Heat Exchangers and Spray Coolers





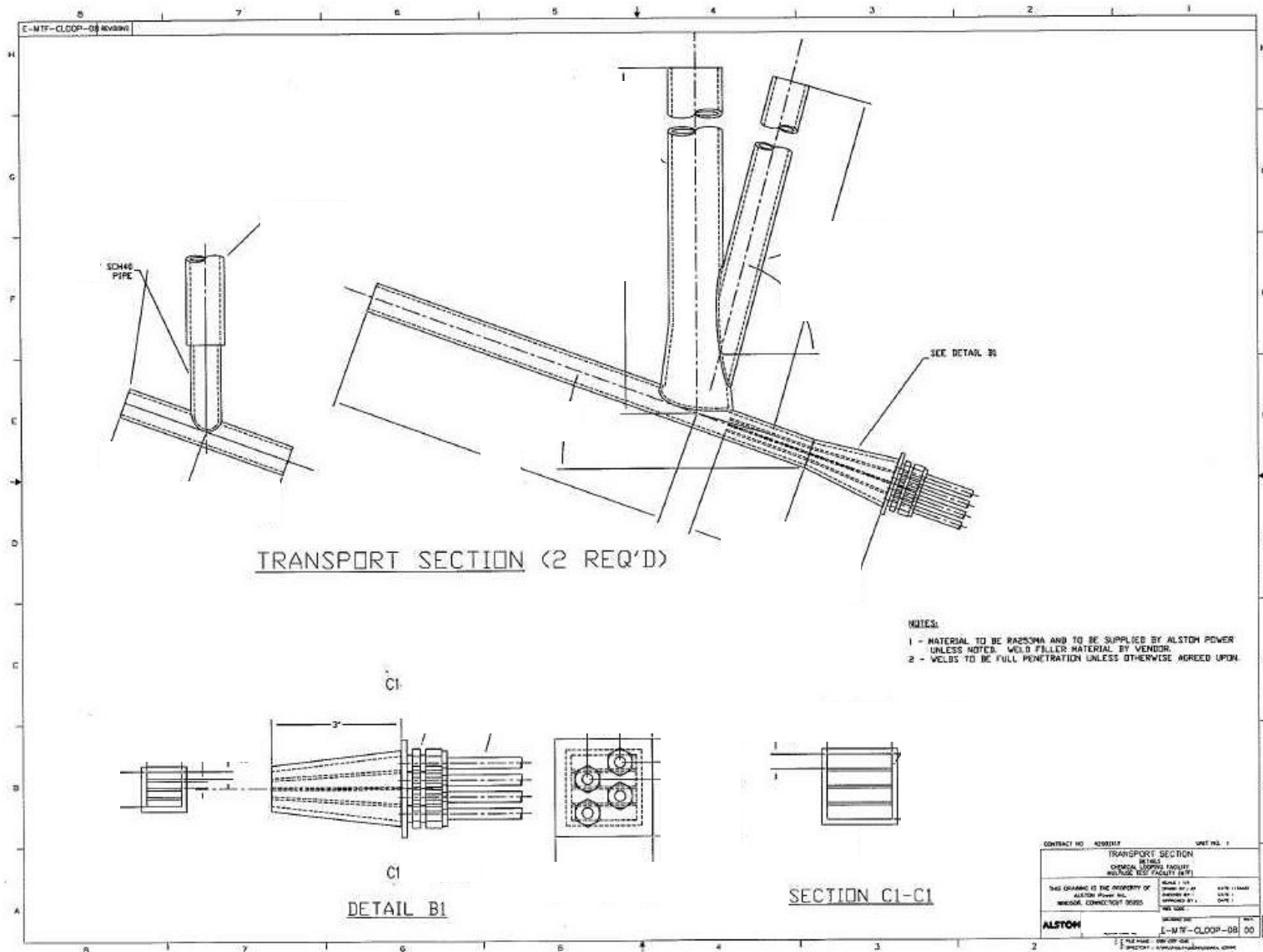


Figure 5-17 – Solids Pick Up Device

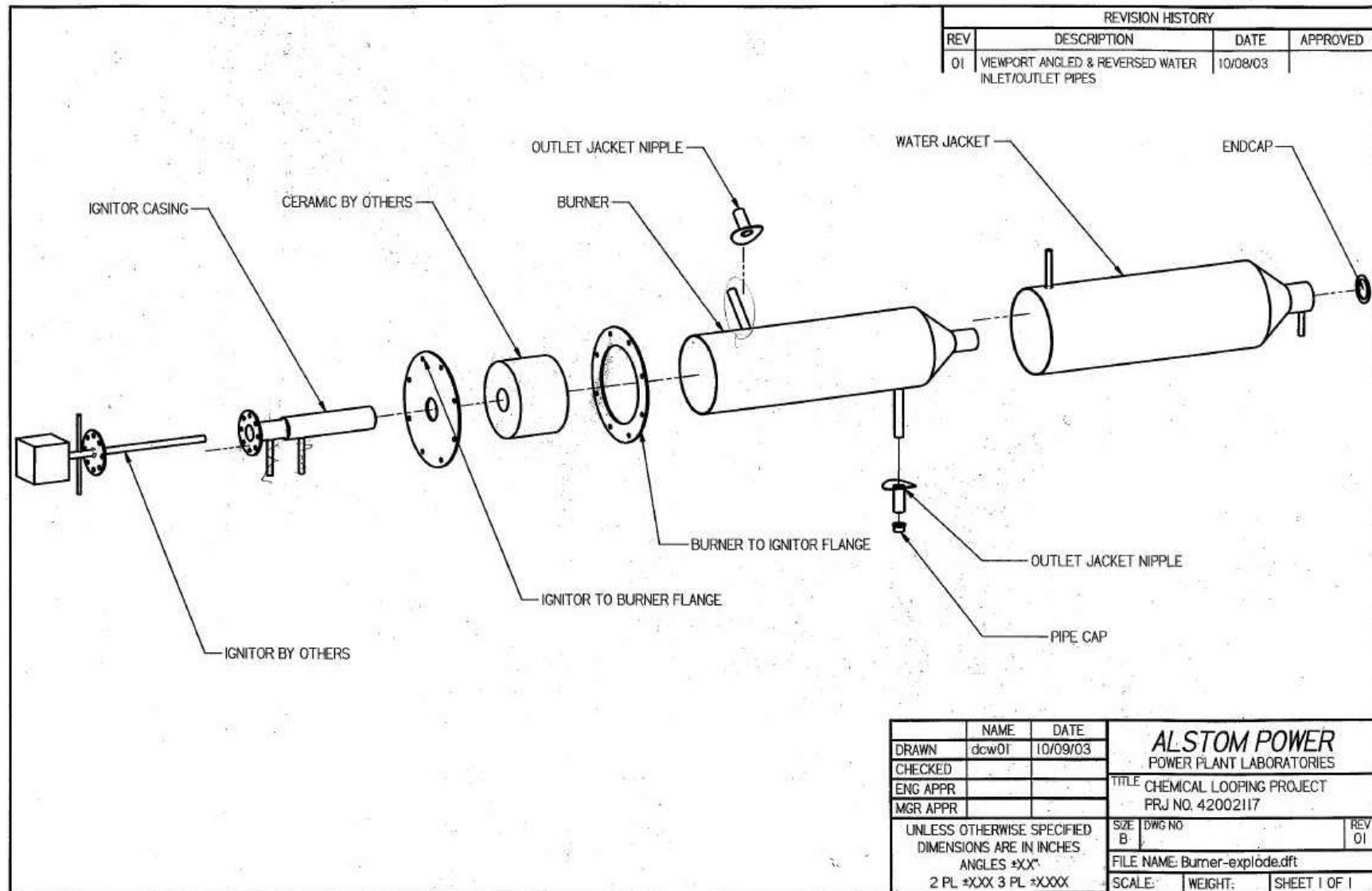


Figure 5-18 – Product Gas Burner Design

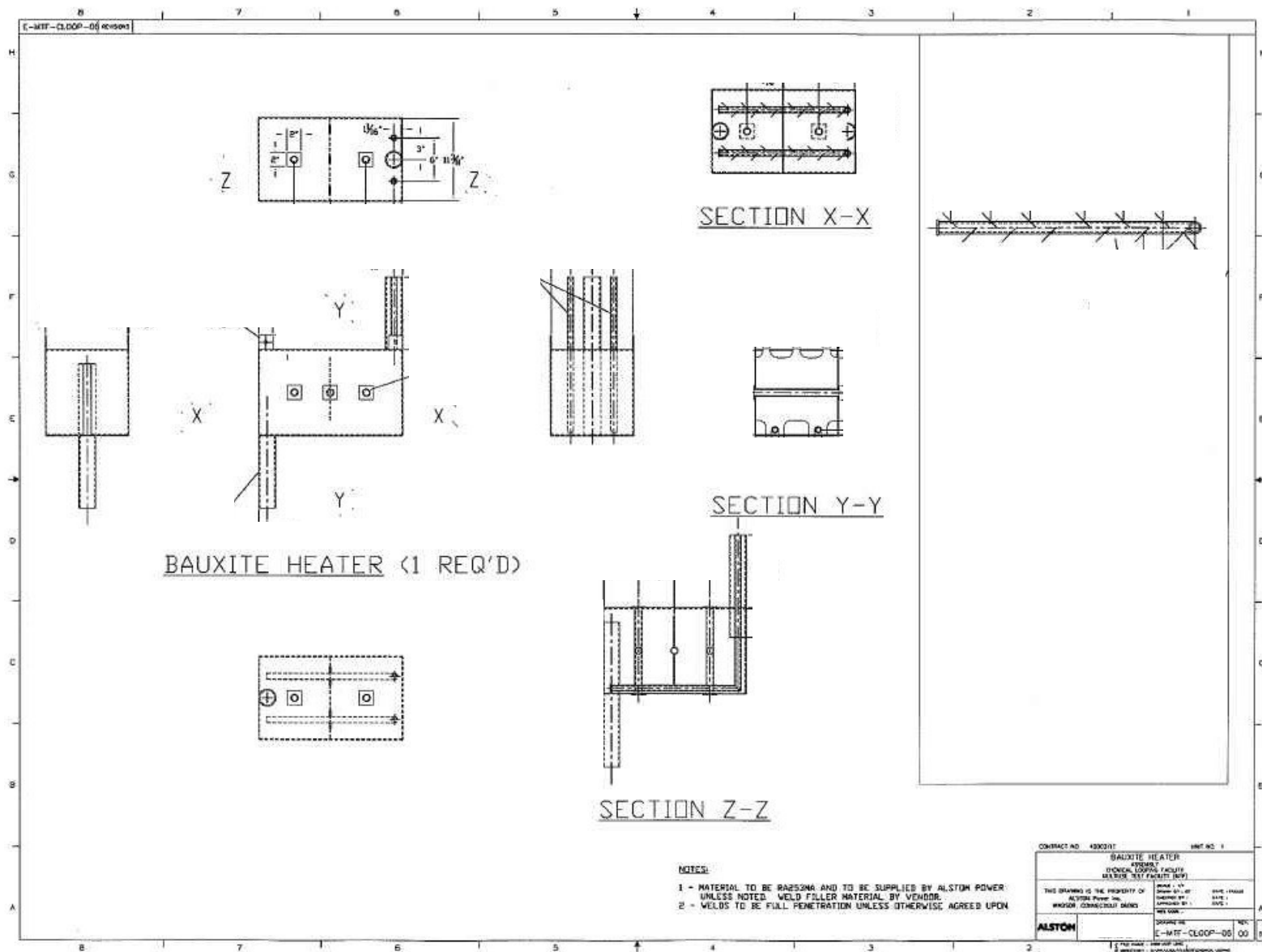


Figure 5-19 – Bauxite Heater Design

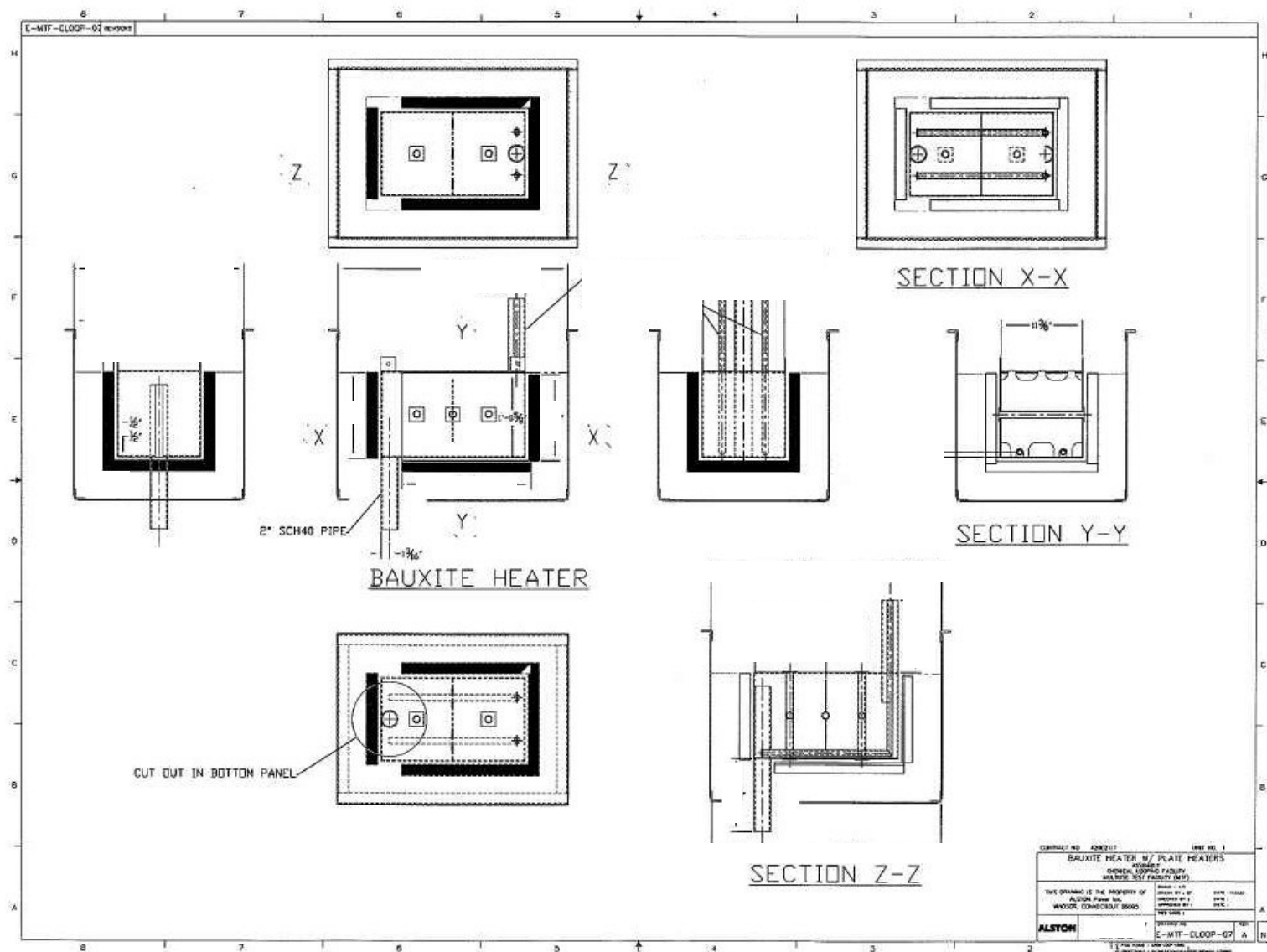
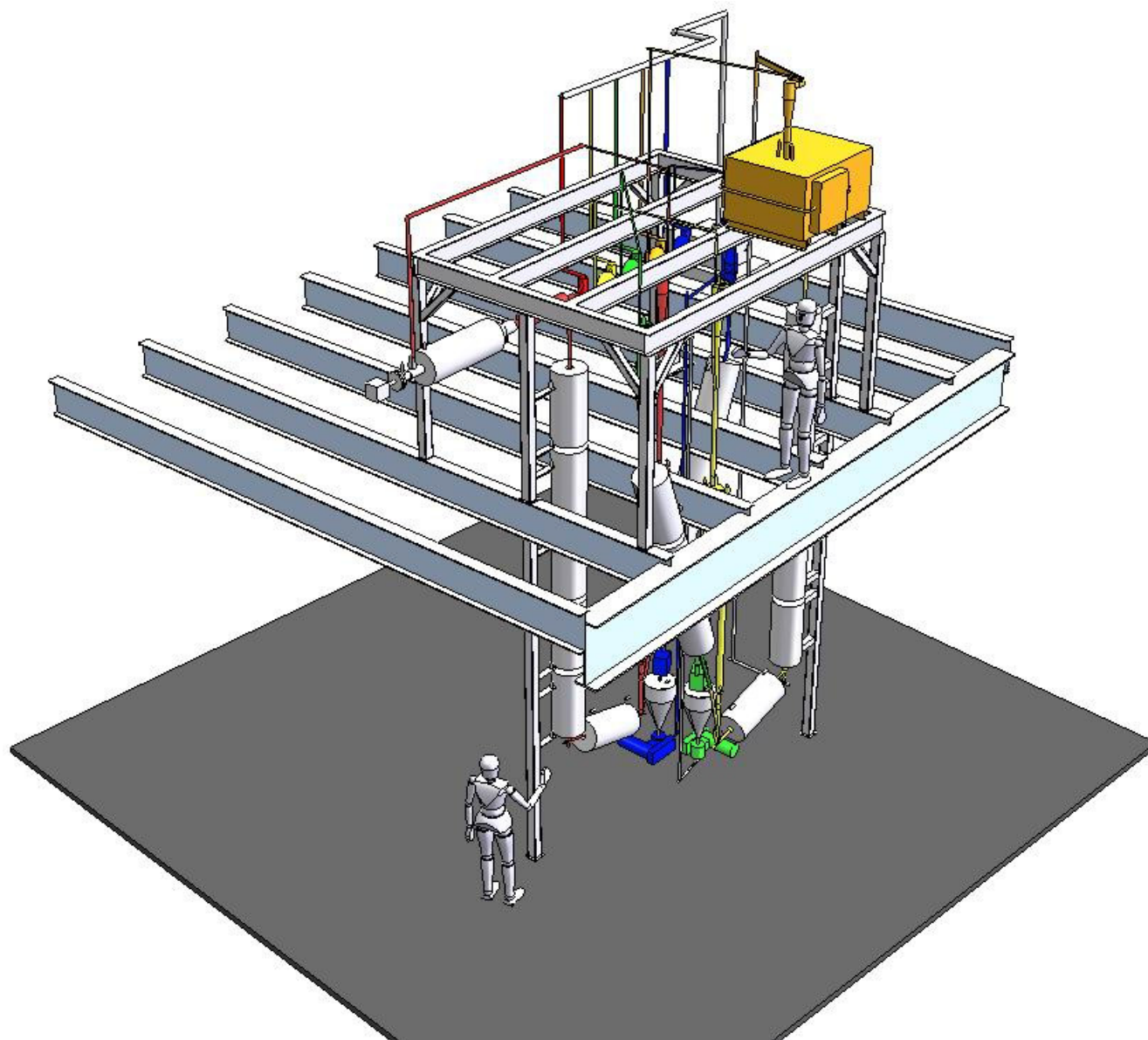
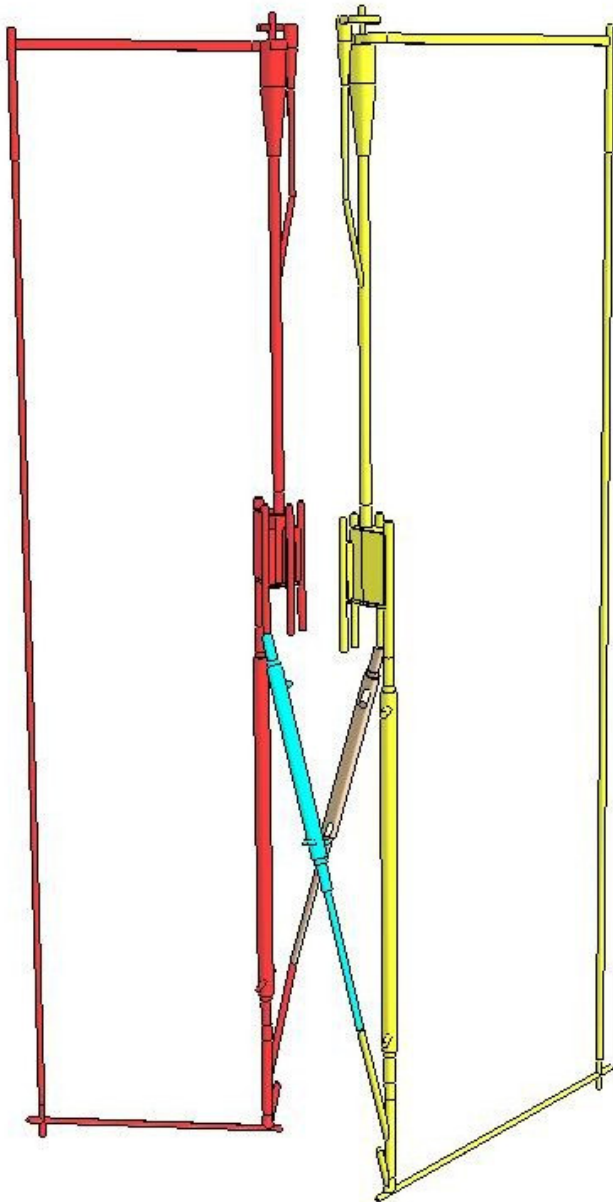


Figure 5-20 – Bauxite Heater Heating Element Design



**Figure 5-21 – PDU Equipment Layout**



**Figure 5-22 – Layout of Main Loops**

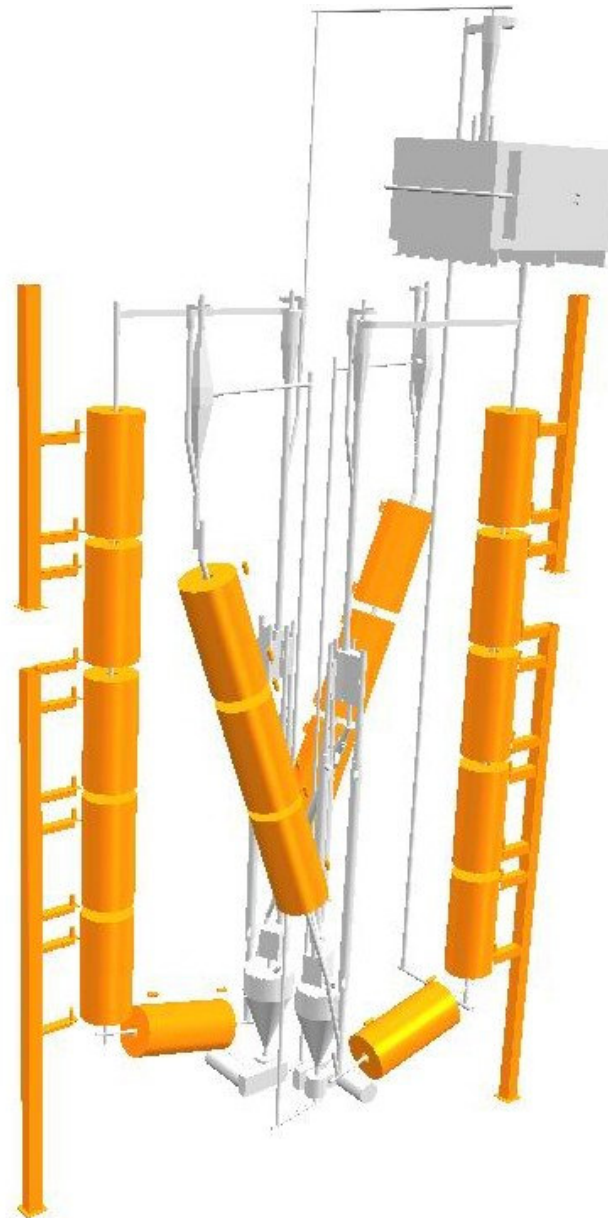


**Figure 5-23 – Location of  
Electrical Heaters and Supports**

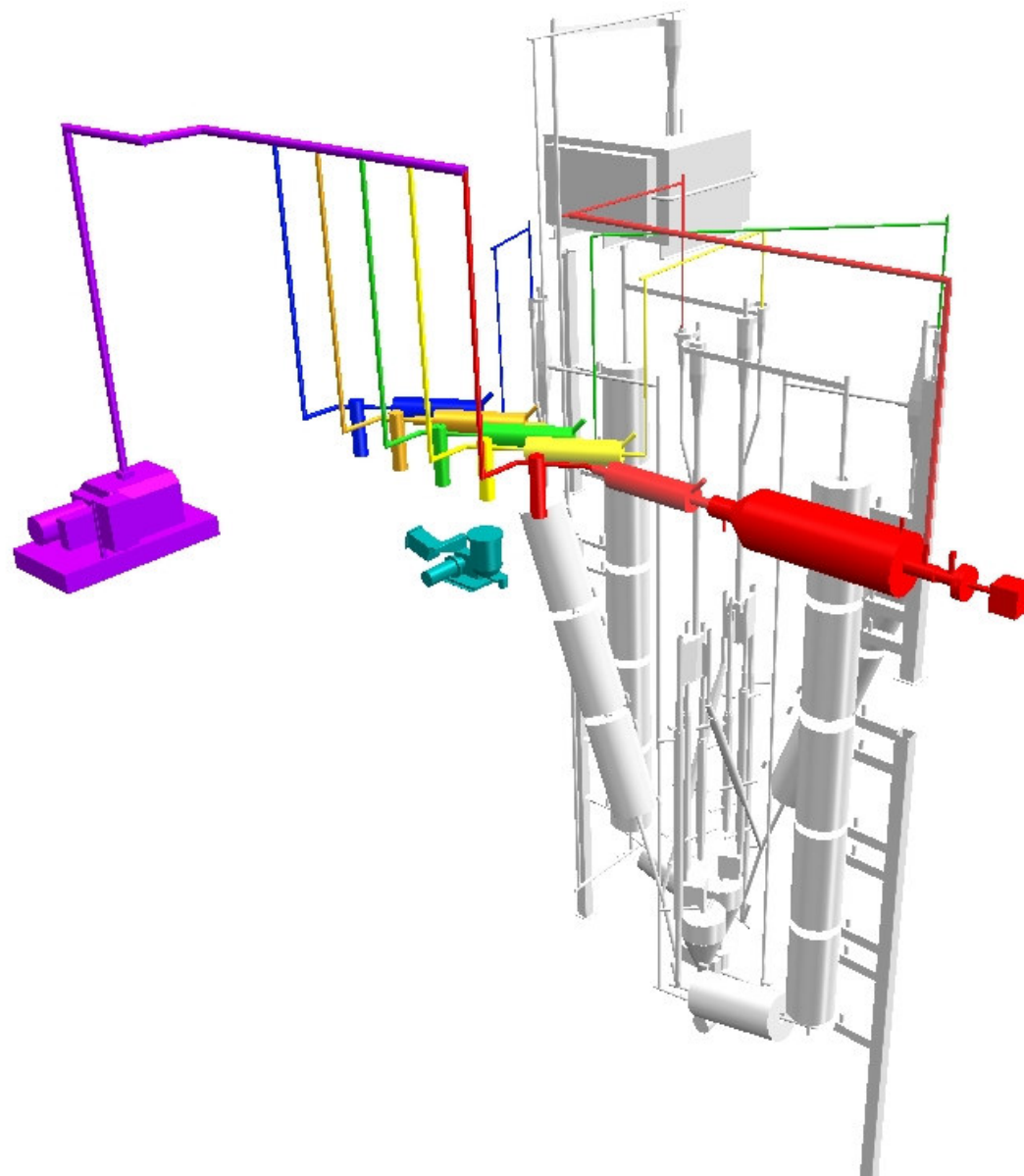


**Figure 5-24 – Gas Venting System**

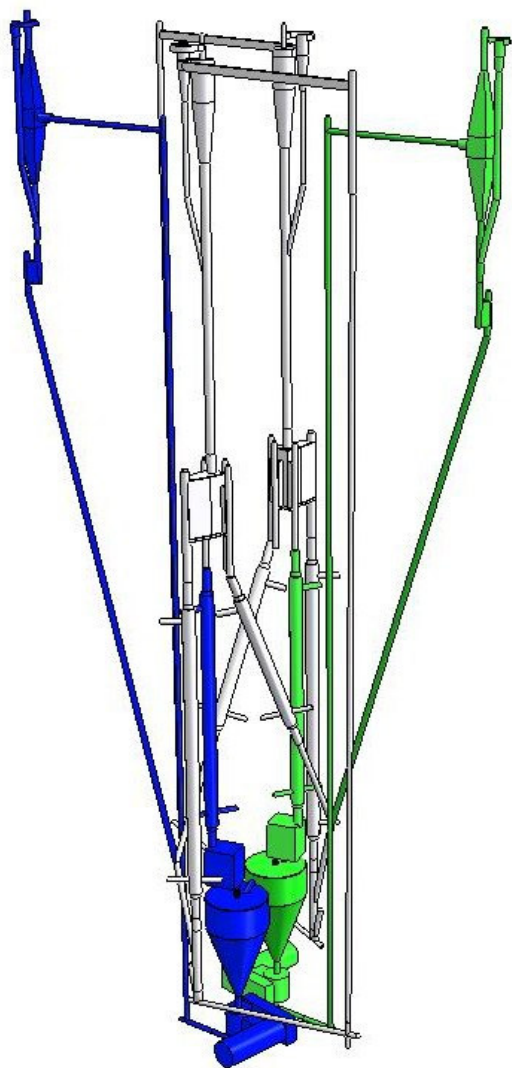


**Figure 5-25 – Sorbent Activation (SA)  
Loops**

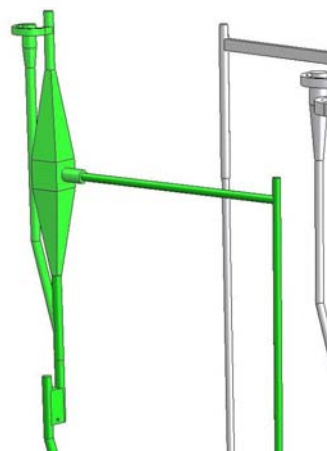


**Figure 5-26 – SA Impactor**

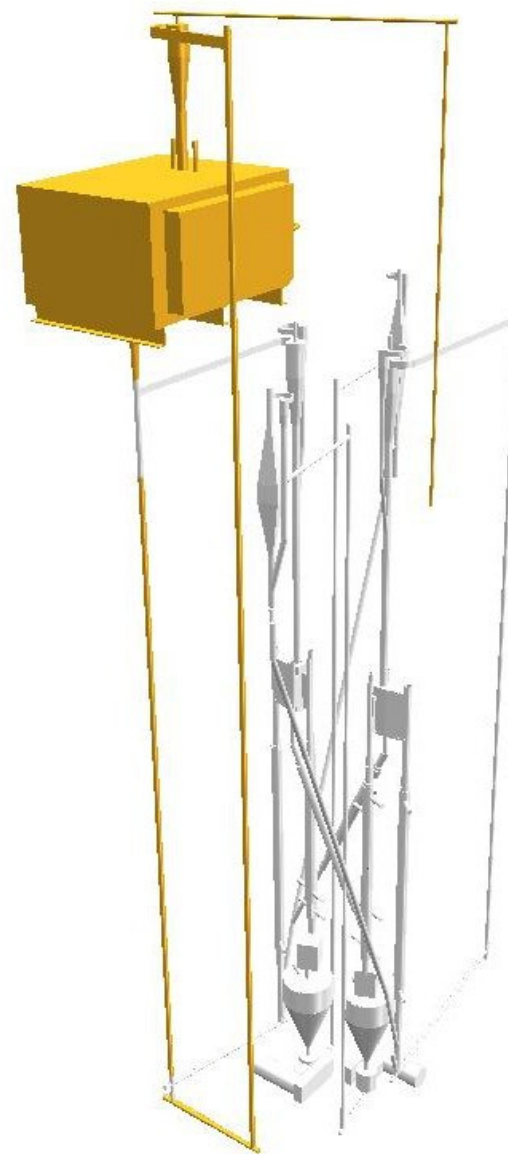


**Figure 5-27 – Bauxite Loop**

The overall equipment layout is shown in **Figure 5-21**. The PDU is assembled on three levels for good access to all of the process equipment. The main reactors (the oxidizer and the reducer) are both 15 feet tall, with additional height needed for drains and solids loading equipment.

**Figure 5-22** shows the two main process loops, the reducer and the oxidizer. The reducer is shown in red and the oxidizer is shown in yellow. The reducer reaction vessel is the long vertical pipe at the left of the figure. Similarly, the oxidizer is the long pipe on the right of the figure. In the center of the figure at the top are primary and secondary cyclones for each loop. Underneath the cyclones are diplegs feeding into the SPCVs. Underneath each dipleg there are two heat exchangers shown. One is for solids returning the solids pick up device at the bottom of the loop, and the other is for solids in the crossover to the other loop.

**Figure 5-23** shows the installation of the electrical process heaters. Both the reducer and the oxidizer have six electrical process heaters, five in the vertical reactor and one in the supply pipe that is angled 20 degrees from the horizontal after the solids pick up device. The return lines from the sorbent activation loops also have three electrical heaters each.

**Figure 5-24** shows the venting system for the PDU up to the vacuum pump. Gas vents from each of the loops, including two SA loops, the oxidizer and the bauxite loop, go through a spray cooler and a filter. The reducer vent first goes through the product gas burner before a spray cooler and filter. After the filters there are gas control valves and the vents are combined before the vacuum pump. Not shown in this figure is the scrubber and the stack.

**Figure 5-25** shows the sorbent activation loops. There is an identical SA loop for both the oxidizer and the reducer. Underneath each SPCV there is a pipe with a solids cooler that goes to the SA reactor. Below the reactor, there is an expansion chamber for solids drop out and to control pressure pulses. Then there is a rotary valve to inject the solids into a transport line to the SA impactor. A larger view of the solids impactor is shown in **Figure 5-26**. Solids falling from the impactor go through a seal pot and then are recycled back to the pick up devices. The vent gases go through smaller cyclones (shown in **Figure 5-13**) and then to the vent system.

The bauxite system is shown in **Figure 5-27**. This system is simply a solids heater that discharges into the oxidizer riser. A pickup device at the bottom of the oxidizer injects the solids into a vertical transport line back to the heater. A cyclone is located above the heater to separate solids from the transport line and the transport gas is discharged through the vent system.

The SA reactors, rotary feeders and expansion chamber are shown in **Figure 5-28**. **Figure 5-29** shows the solids coolers located in the drain lines below the SPCV valves. **Figure 5-30** shows a larger view of the primary and secondary cyclones for both the reducer and oxidizer loops. **Figure 5-31** shows a larger view of the reducer SPCV.

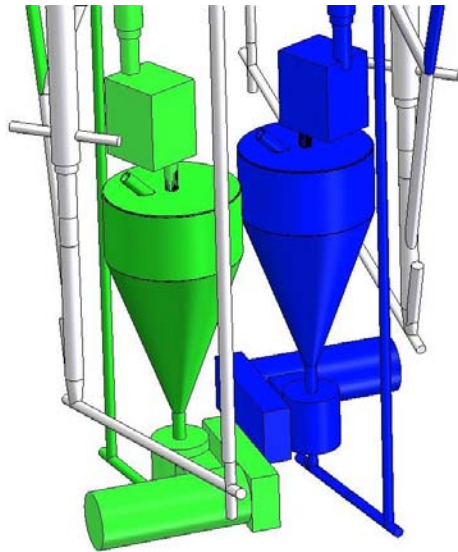


**Figure 5-28 – SA Reactor and Rotary Feed Valve**

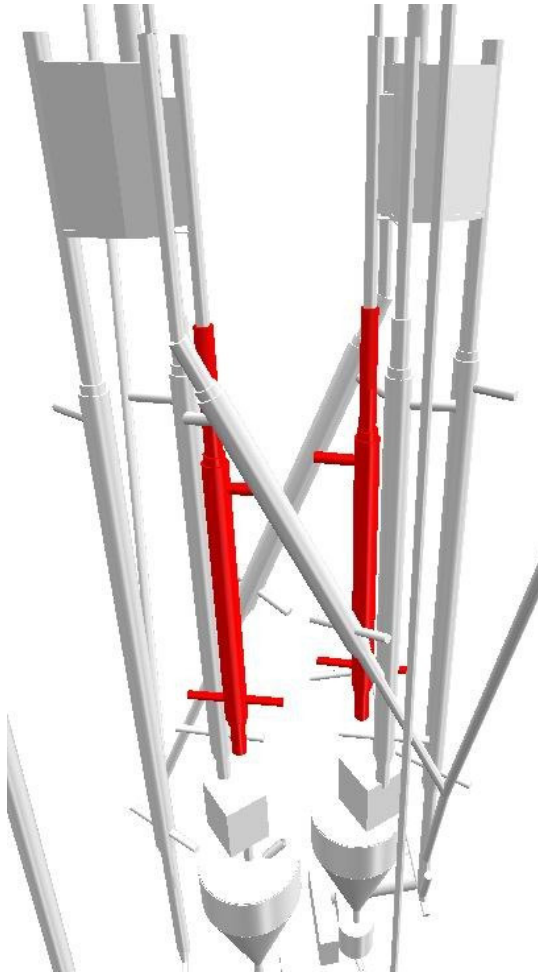


**Figure 5-29 – Heat Exchangers in the Solids Drain Line**

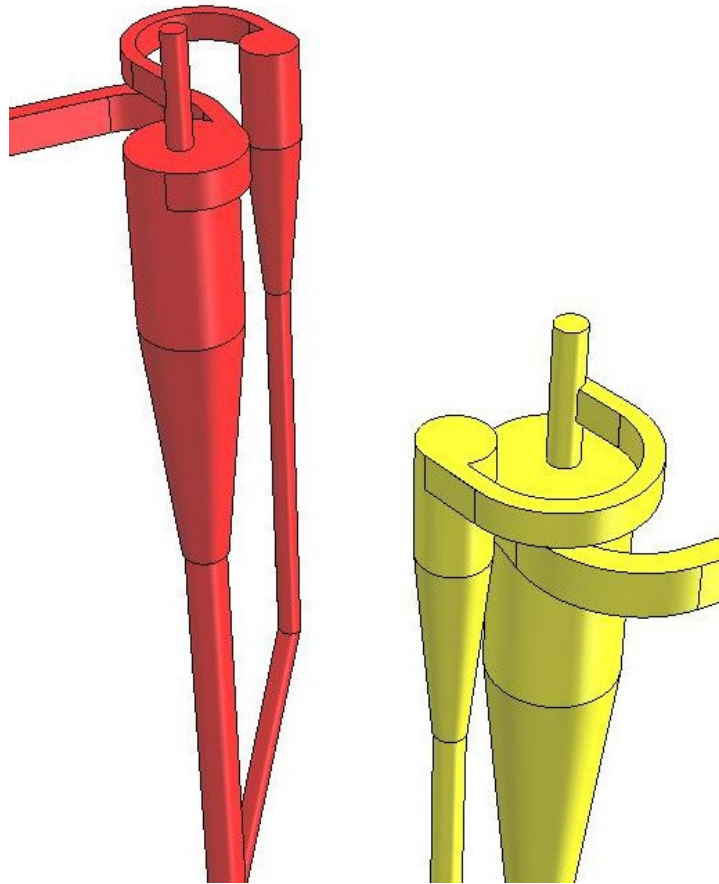


**Figure 5-30 – Primary and Secondary Cyclones in Reducer and Oxidizer Loops**

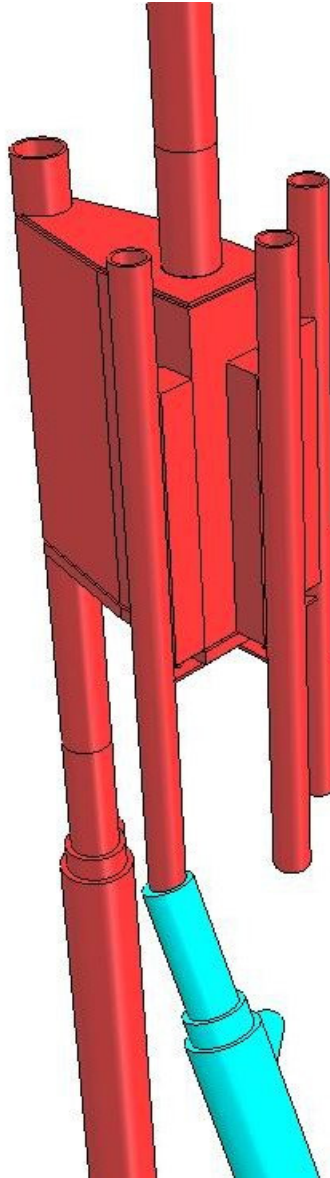


**Figure 5-31 - SPCV**

## **6.0 Cold Flow Modeling**

### **6.1 Cold Flow Model Goals**

The goals of the Cold Flow Modeling (CFM) are to analyze and visualize solids transport in Alstom's chemical looping process, and to develop methods to transport, distribute and control solids flow for the operating loops. The specific needs are to establish a controllable and stable performance in the operating range, maximize solids flow for the given pressure system and minimize pressure drop for each looping system.

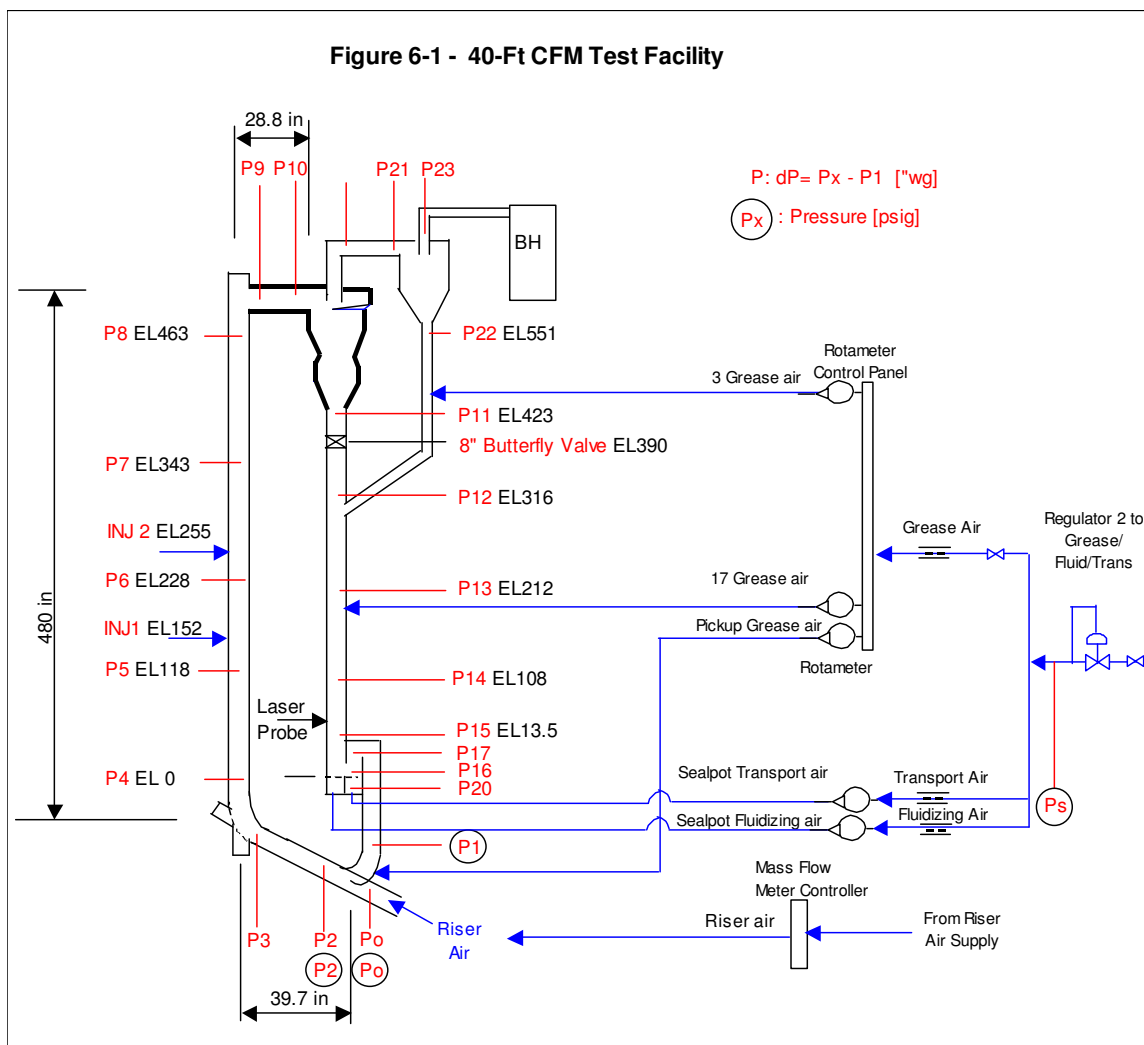
The cold flow models are developed to serve as tools for:

- Establishing operating guidelines for the hot loop (PDU) operation as a training tool and as a trouble-shooting device,
- Determining scale up rules for four scaling steps:
  - 0.75" ID and 15 ft CFM to 0.75" ID and 15 ft hot PDU
  - 0.75" ID and 15 ft CFM to 4" ID 40-ft CFM
  - 4" ID and 15 ft CFM to 18" ID prototype plant
  - 18" ID prototype to demonstration plant size,
- Creating process control methodologies that are effective, reliable and robust in the process control design,
- Establishing performance prediction for the gas/solids system.

## 6.2 Plexiglas Cold Flow Model (CFM) Tests

### 6.2.1 40-ft CFM Test Facility

The 40-foot CFM test model was built in 2006 during the Phase II project as shown in **Figure 6-1**. The riser leg has a 4-inch inside diameter and is 40 feet high. The dipleg under the primary cyclone has a 6.6875-inch inside diameter and is about 35 feet high.



There are 17 grease air injection elevations along the primary dipleg and 3 grease air injection ports along the secondary cyclone dipleg, spaced about 2 feet apart. The bottom grease air injection ports (number 2 to number 6) were later modified to two ports per elevation, which reduces the solids counter-flow effect and provides better solids aeration. The bottom grease air port (number 1) was increased to three ports and showed better solids aeration. A specially designed SPCV was installed at the bottom of the primary dipleg. The main riser air is introduced through a 'sugar-scoop' device, which is also used to pickup solids from the seal pot down-comer.

Pressure taps are used to measure the pressure drop and local pressure as shown in **Figure 6-1**. All pressure drops are measured relative to the pressure at the P1 point, which is located at the down-comer pipe above the sugar-scoop device. Each pressure tap has a respirator mesh pad behind the 0.25 inch diameter sampling hole to prevent pluggage by solid particles.

There are two additional air injection ports at an elevation of 152 inches and at an elevation 255 inches along the vertical section of the riser to simulate gas generation. Air is injected through the circumference of a 12 inch long perforated sintered mesh screen. The sintered mesh has an opening size of 5 microns.

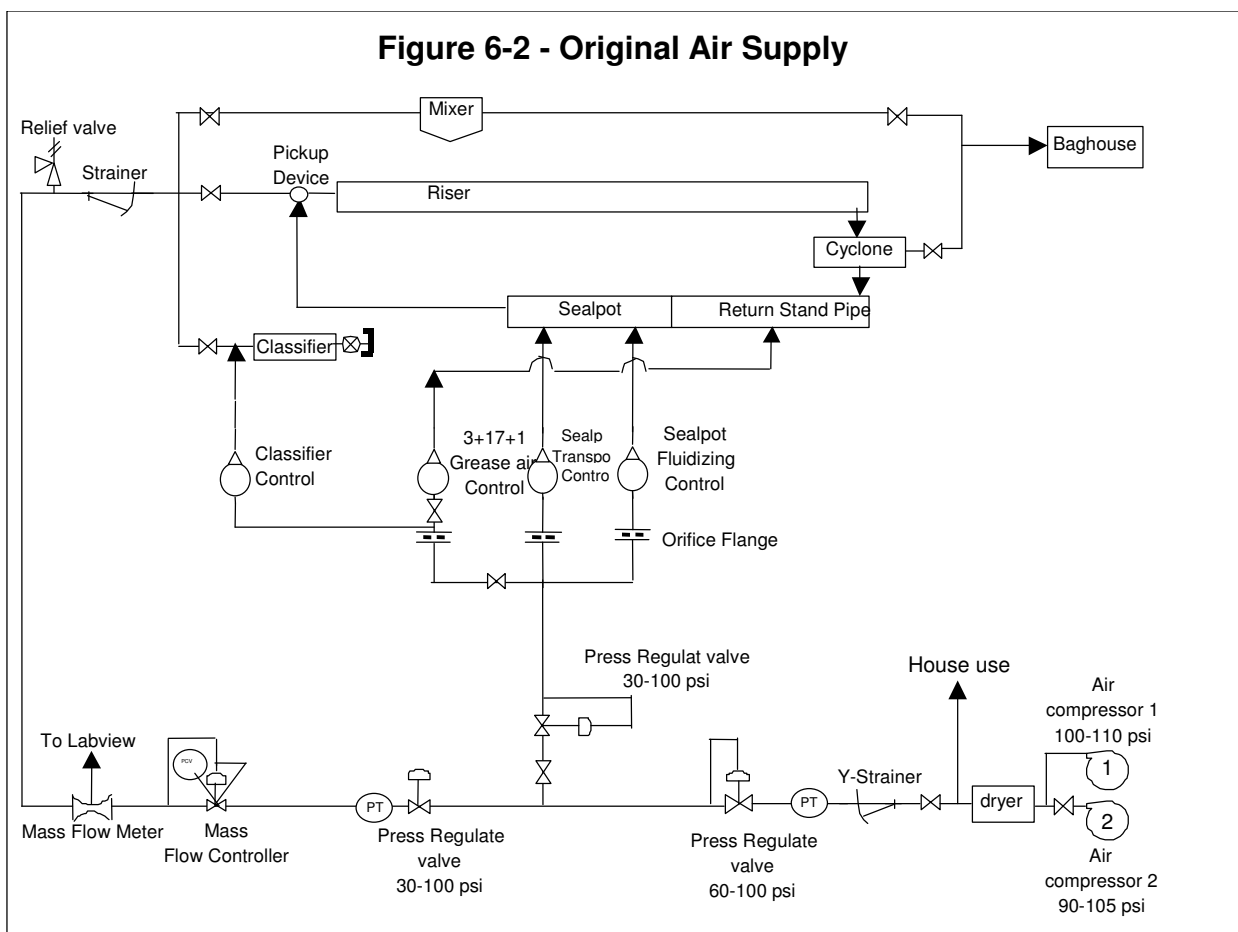
A laser-diode based probe is installed at the top of the SPCV to measure solids flow velocity along the dipleg. An 8-inch butterfly valve is installed at an elevation of 390 inches from the bottom of the seal pot grid plane. This butterfly valve is used to calibrate the solids circulation flow rate, with the assistance of a video recorder, to compare to the laser-diode based solids flow measurement probe.

Airflow in the riser, including air injected from the two injection ports, is controlled by mass flow meters. Air flow for the seal pot transport zone, seal pot fluidized zone, and grease air are measured and controlled by rotameters, and are independently measured by orifice flow methods described in **Reference 20** “Fluid Meters Their Theory and Application”, report of ASME Committee on Fluid Meters, Sixth Edition, 1971, edited by Howard S. Beam. Flow to each individual grease air port is pro-rated according to the rotameter setting and an orifice flow calculation. Rotameter readings are set and recorded in the logbook. Orifice pressure drop is automatically recorded through the facility data acquisition system.

### **Original Air Supply System**

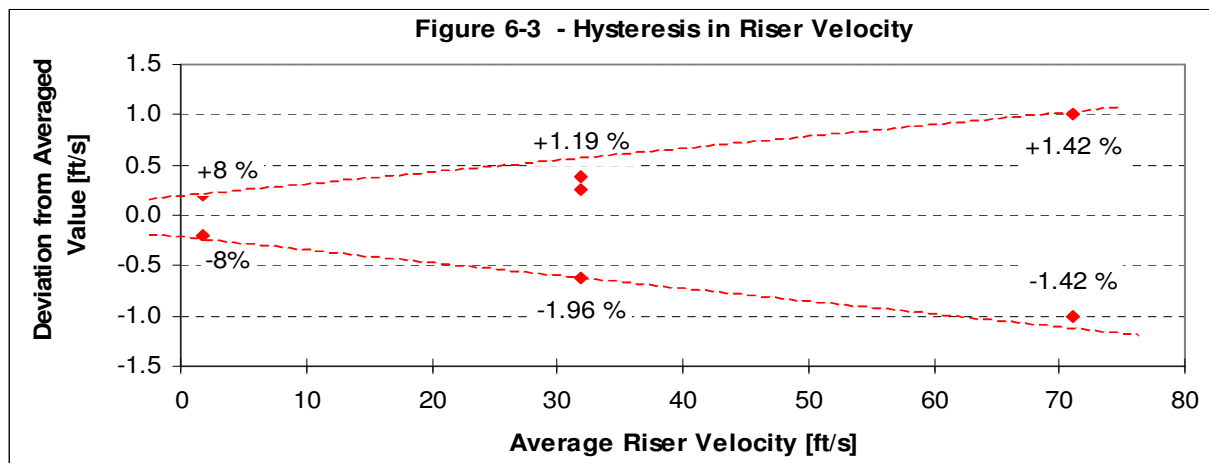
The air supply system was set up originally as shown in **Figure 6-2**. The opening of the main flow valve was controlled by feed back from the pressure down stream of the mass flow meter. Several issues were identified and needed further modification during the startup of the system:

- There was a hysteresis effect in the pressure response of the control valve that induced instability on the riser main flow.
- The riser velocity was affected by the upstream compressor pressure variance.
- The flow meter needed calibration.



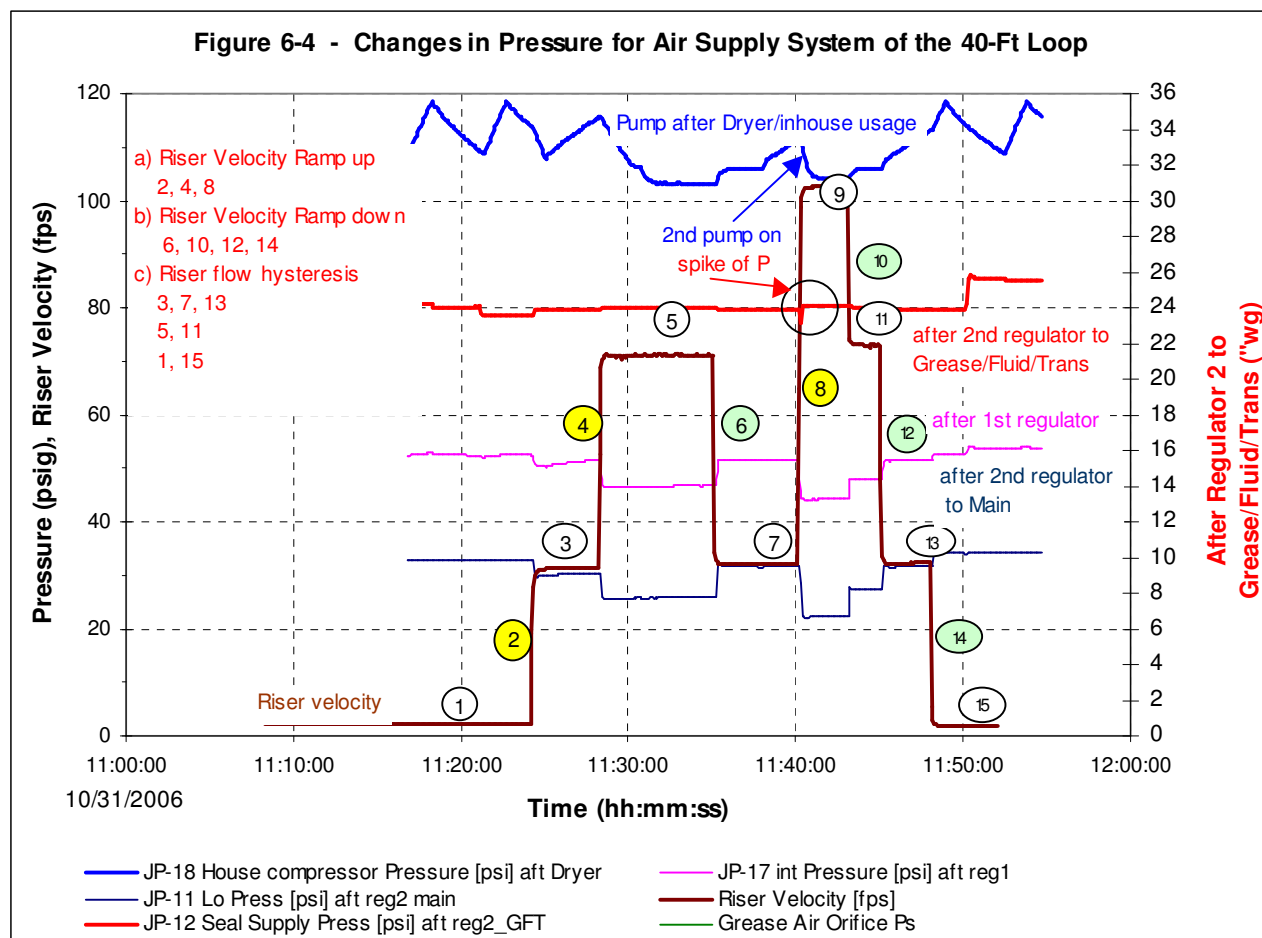
## Hysteresis Effect on Riser Velocity

With the original air supply system, a hysteresis effect on riser velocity occurred during the mass flow meter ramp up and ramp down with a maximum deviation of  $\pm 1.19\%$  at about 70 ft/s to  $\pm 8\%$  at about 2 ft/s velocity as shown in **Figure 6-3**. This hysteresis may be induced from the orifice effect of the opening of valve positions and actuator response time.



## Effect on Riser Velocity Caused by Compressor Pressure Variation

The source of the instability of the riser flow was traced to the compressor pressure cycling. The compressor pressure was cycling even with the installation of regulators. **Figure 6-4** shows several pressure changes at different locations during the ramp up and ramp down testing. These pressure locations are at the compressor outlet after the compressor dryer, after the 1<sup>st</sup> regulator, after the 2<sup>nd</sup> regulator to the grease and sealpot air lines and after the 2<sup>nd</sup> regulator on the main line.

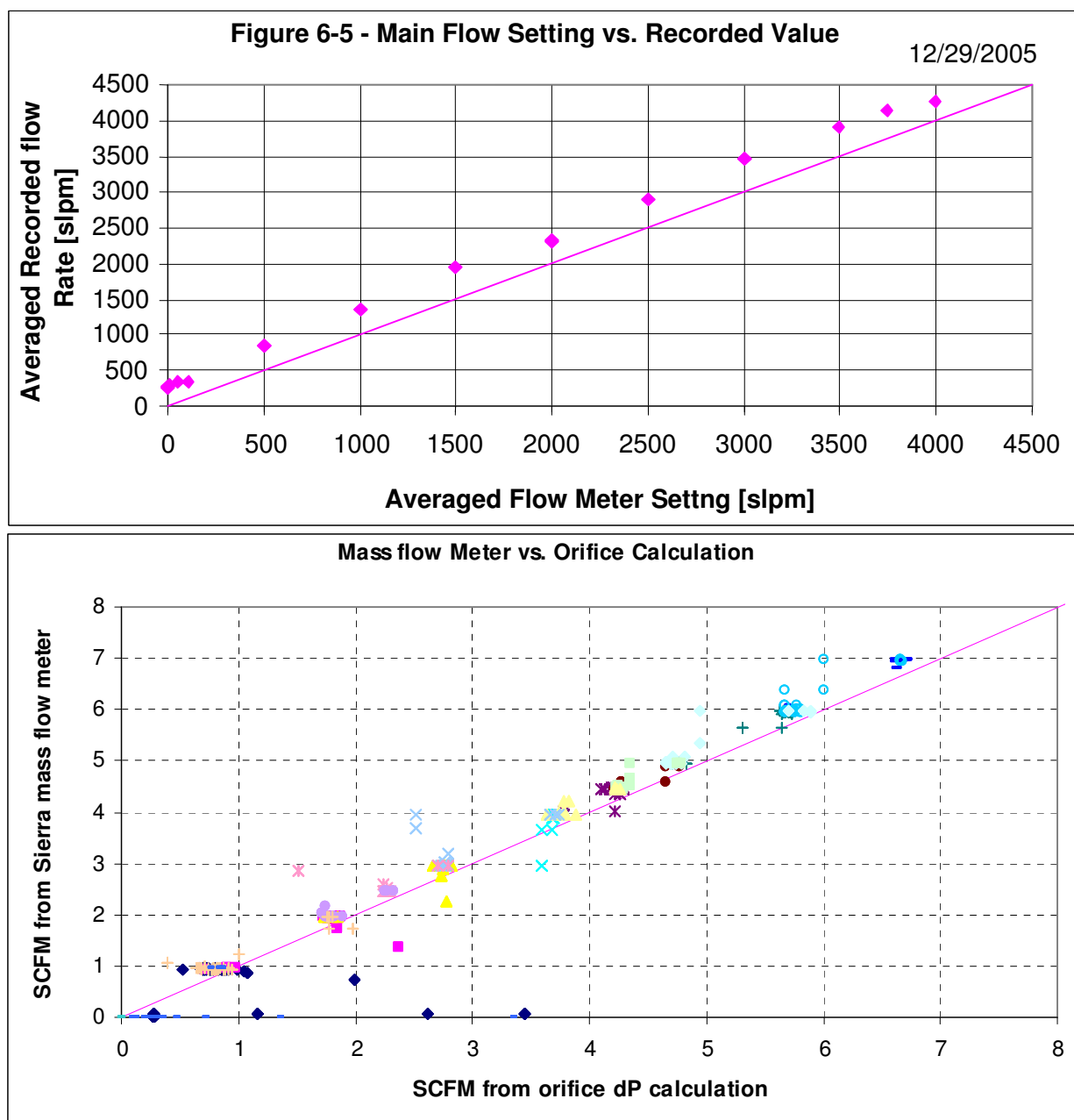


The compressor pressure between the dryer exit and the test loop was cycling about  $\pm 10$  psi. This cycling value was reduced to  $\pm 5$  psi after the first regulator. The pressure after the second regulator, feeding to grease air and fluidizing air, was reasonably stable (less than 1% change), even though the riser flow velocity was varied from 0 to 102 ft/s. The smoothness of the pressure supply to the sealpot was critical in the control of the sealpot solids flow, especially in a small-scale facility like the 15-ft CFM. The 1<sup>st</sup> regulator range was 150 psi to 50 psi and the 2<sup>nd</sup> regulator range was 50 to 30 psi. The second regulator was effective in keeping the pressure smooth. However, a spike in pressure change did occur when the second compressor air source started. It started when the velocity ramped from 30 ft/s to 120 ft/s over the supply range of the main

compressor. The main pump supplied up to 80 ft/s of riser air velocity, without the interference of the other in-house usage. This covered most of the planned tests.

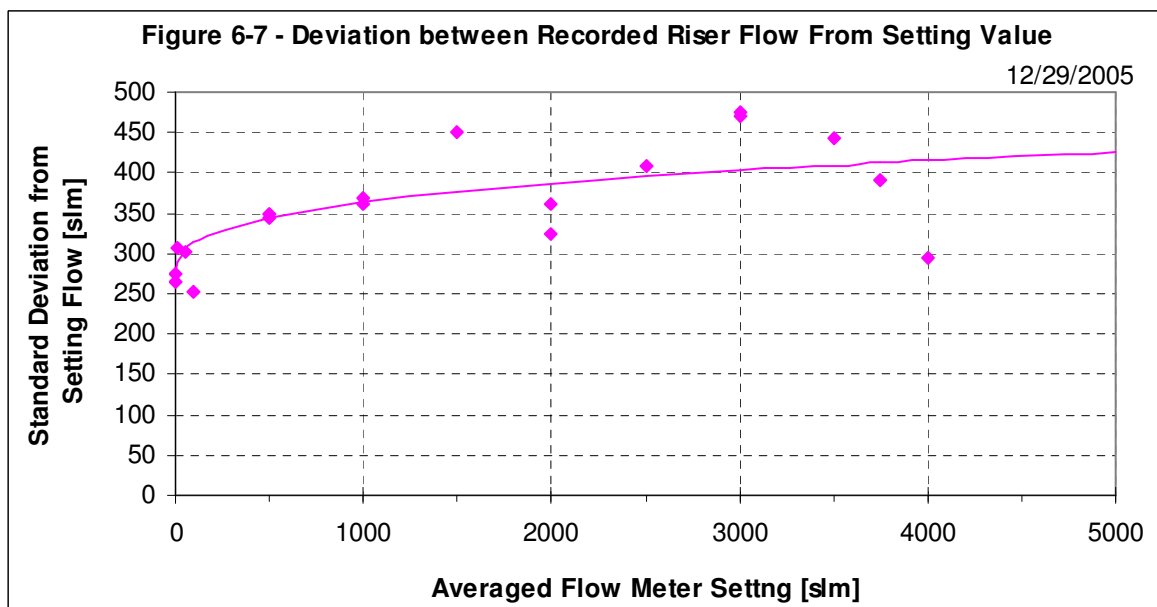
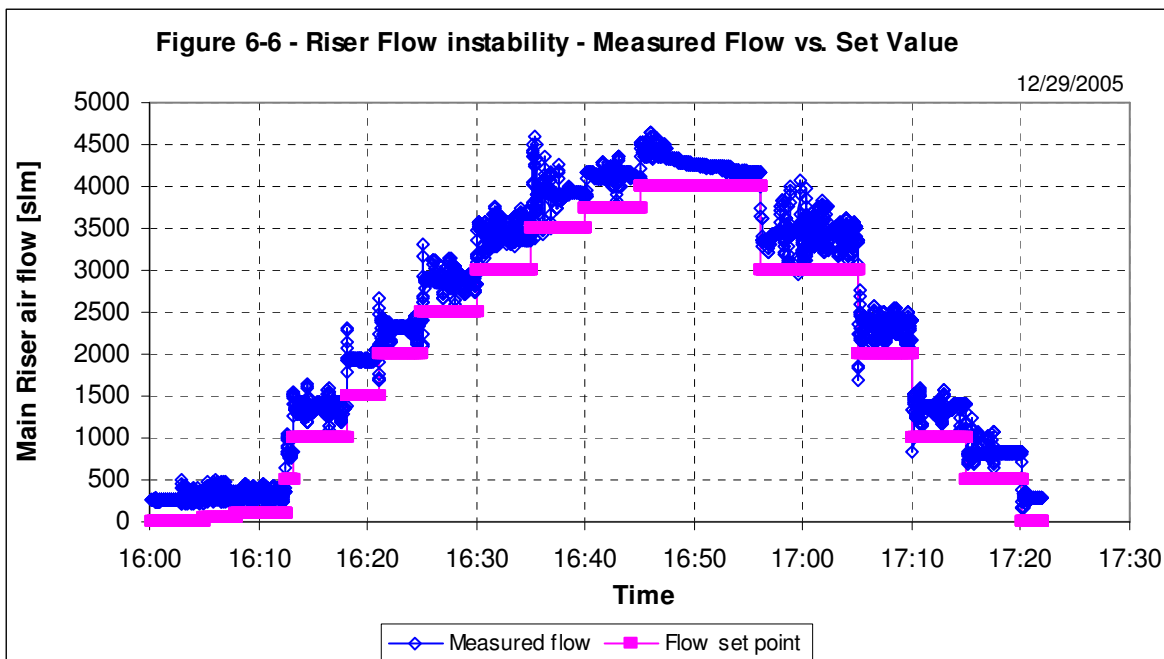
### Calibration of the Mass Flow Meter

In calibrating the mass flow meter, the actual flow rate recorded by the mass flow meter was almost linearly proportional to the setting value, as shown in **Figure 6-5**. The calibration of zero was shifted about 265 slpm to 400 slpm higher than the setting value. The calibration was performed at the by-pass line with the main flow off. The deviation between the set value and the recorded value could be improved by calibrating the mass flow meter with the main flow on. The mass flow meter was also checked with the calculated orifice value with reasonable agreement.



## Instability of the Riser Main Flow

The main flow rate in the riser was originally controlled by feedback from the pressure downstream of the valve. **Figure 6-6** shows the mass flow rate recorded during the testing period compared to the corresponding control setting. Under this control method, the main flow rate fluctuated and was unstable, especially at lower flow rates. The deviation on the flow rate varied from 263.9 slpm to 463.7 slpm, for the corresponding setting values of 0 and 3000 slpm, when the riser velocity was under 19.6 ft/s. This is shown in **Figure 6-7**. This fluctuation was too high for the application.

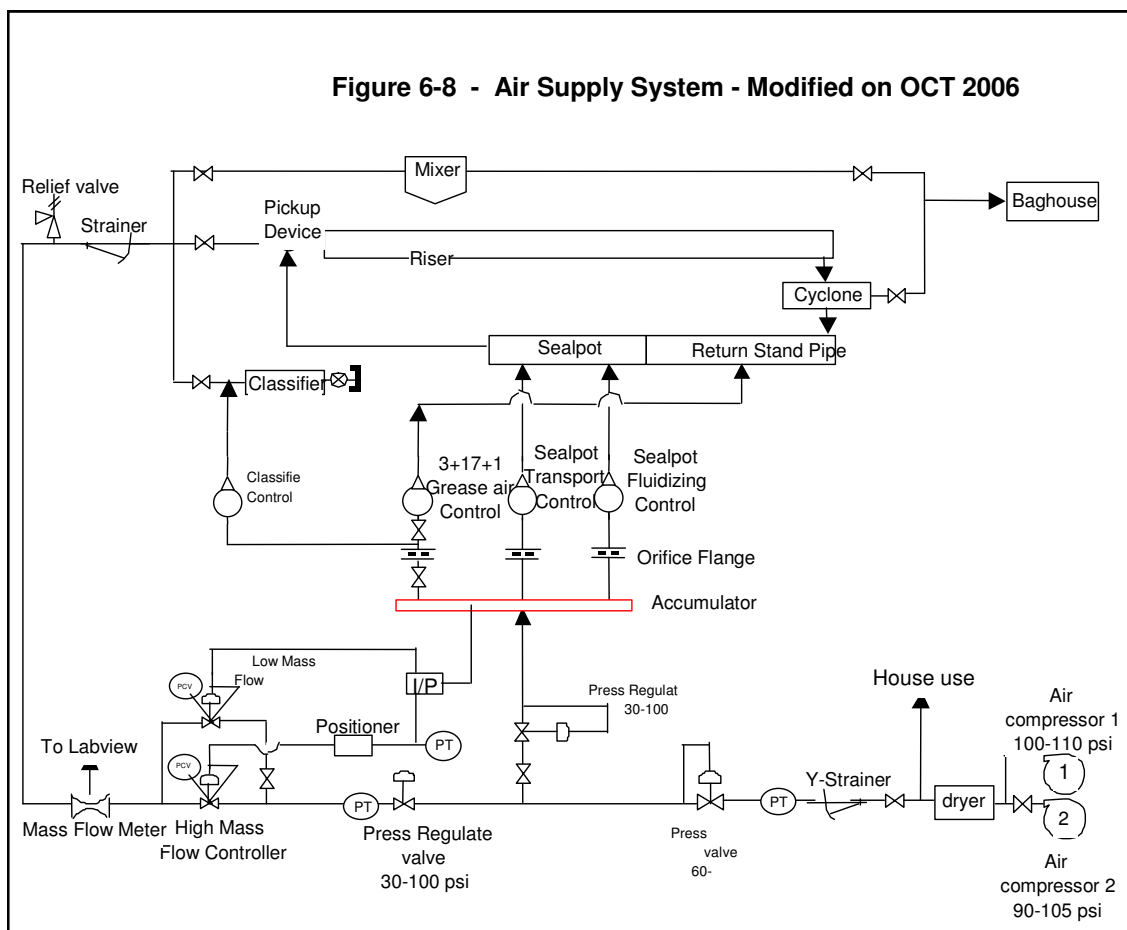


## Modified Air Supply System on the 40-Foot Model

Because of the large fluctuation in the main gas flow rate, a modification of the air supply system was necessary. These modifications included:

1. Regulate both compressor operating ranges (90-105 psi and 100 to 110 psi);
2. Add a new pressure regulator at the inlet of the air supply system to the CFM (60 to 100 psi) and set it to 52 psi;
3. Re-size the second pressure regulator in the main line (set to 35psi, 400 psi, max 3", inlet range 50-110 psi, Cash ACME serial #8595B, Type EE56);
4. Add a second regulator to the feed line for grease air and sealpot air (GTF) (30 to 100 psi and set to 30 psi);
5. Add a pneumatic valve (WB Anderson Control Valve serial # 2005VA32.233, 2" Linear Trim) and positioner (WB Anderson, model 165EL, 4-20mA input valve positional) to control the opening of the mass flow meter using pressure after the second regulator valve actuation;
6. Add a new valve (WB Anderson serial # 000DA32.230, 1.5" Liner Trim) in parallel with the large valve;
7. Install a new auto tune PID control for main air flow control.

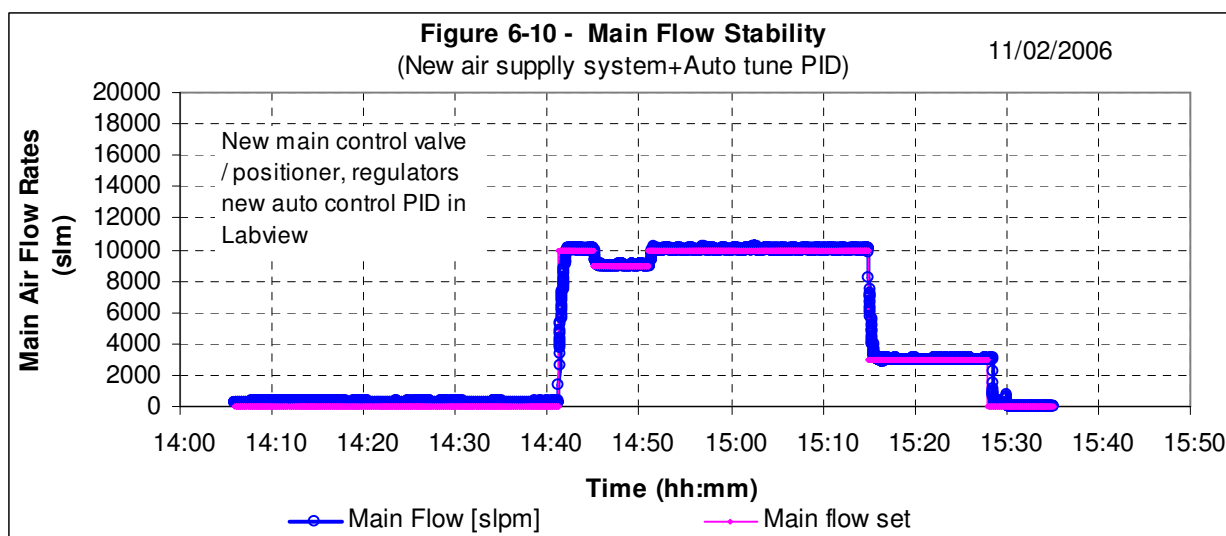
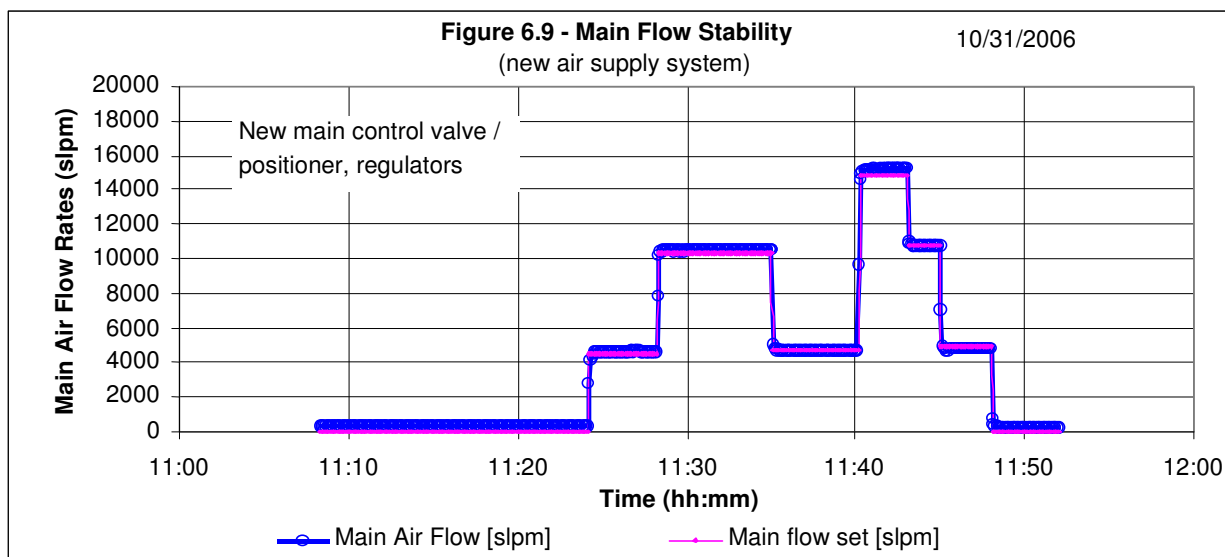
**Figure 6-8** shows the modified air supply system, which now operates well.

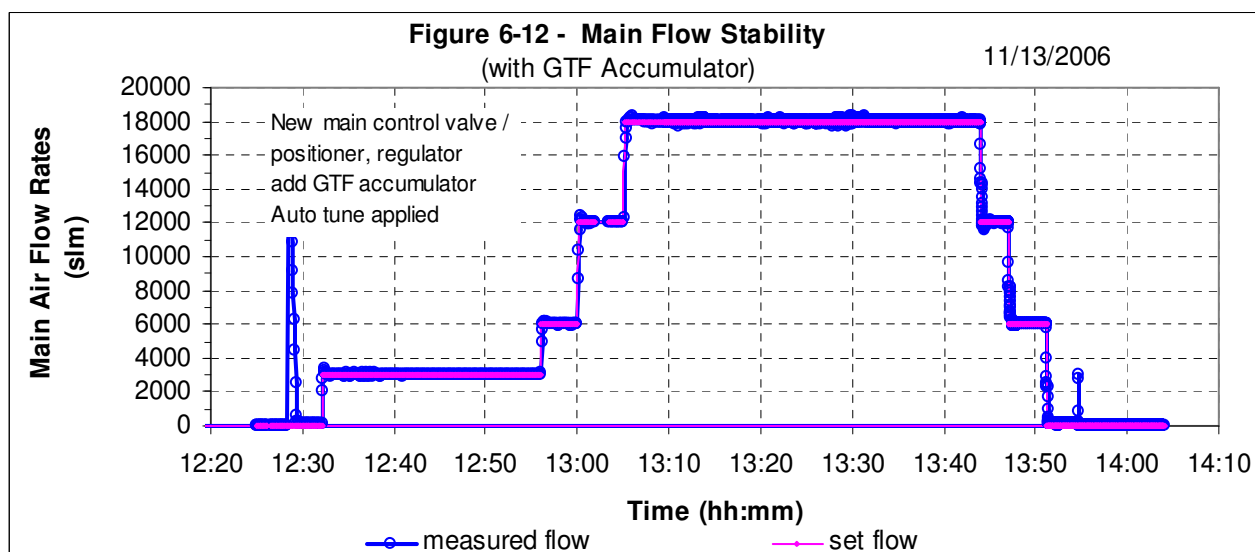
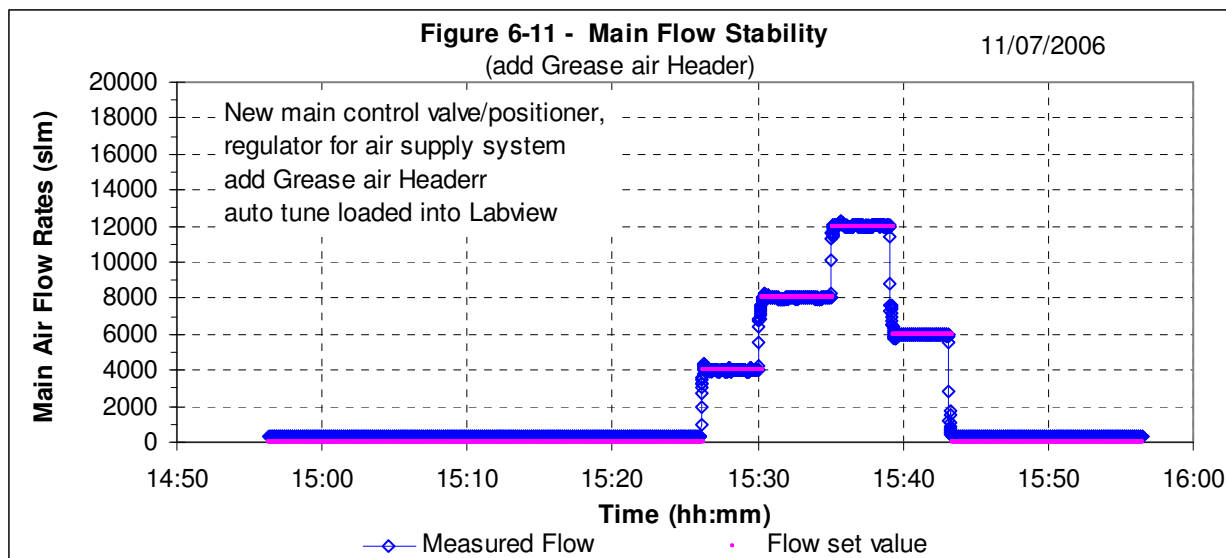


## Riser Flow Stability with New Air Supply System

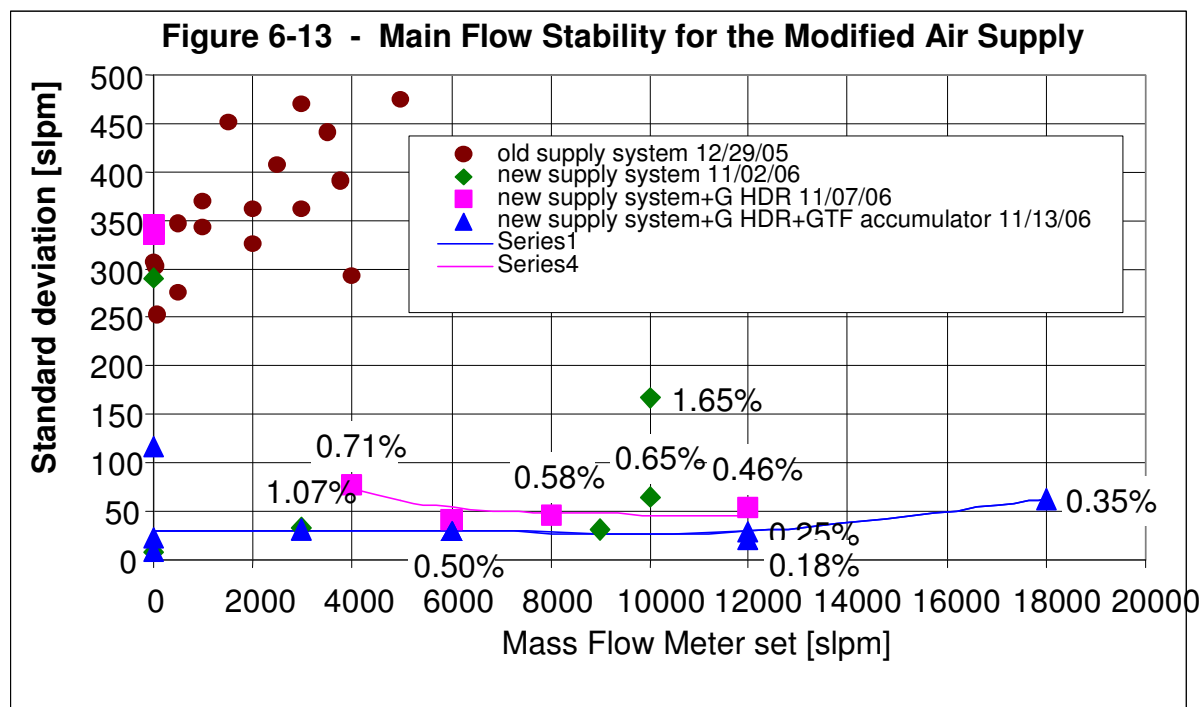
With the added pressure regulator and the use of more steady pressure at the Grease air/Sealpot Transport air /Sealpot-Fluidization air (GTF) supply line (after the second regulator) to control the valve opening, the stability of the main flow rate made a dramatic improvement. **Figures 6-9 to 6-12** show the main flow stability compared to the set value at various settings during testing. There were four stages in modifying the air supply system:

- With the new air supply system (**Figure 6-9**)
- With the new air supply system and the new auto control PID (**Figure 6-10**)
- With the new air supply system, new auto control PID and new grease air header between the orifice and rotometer panel (**Figure 6-11**)
- With the new air supply system, new auto control PID, new grease air header between the orifice and rotometer panel and the GTF accumulator (**Figure 6-12**)





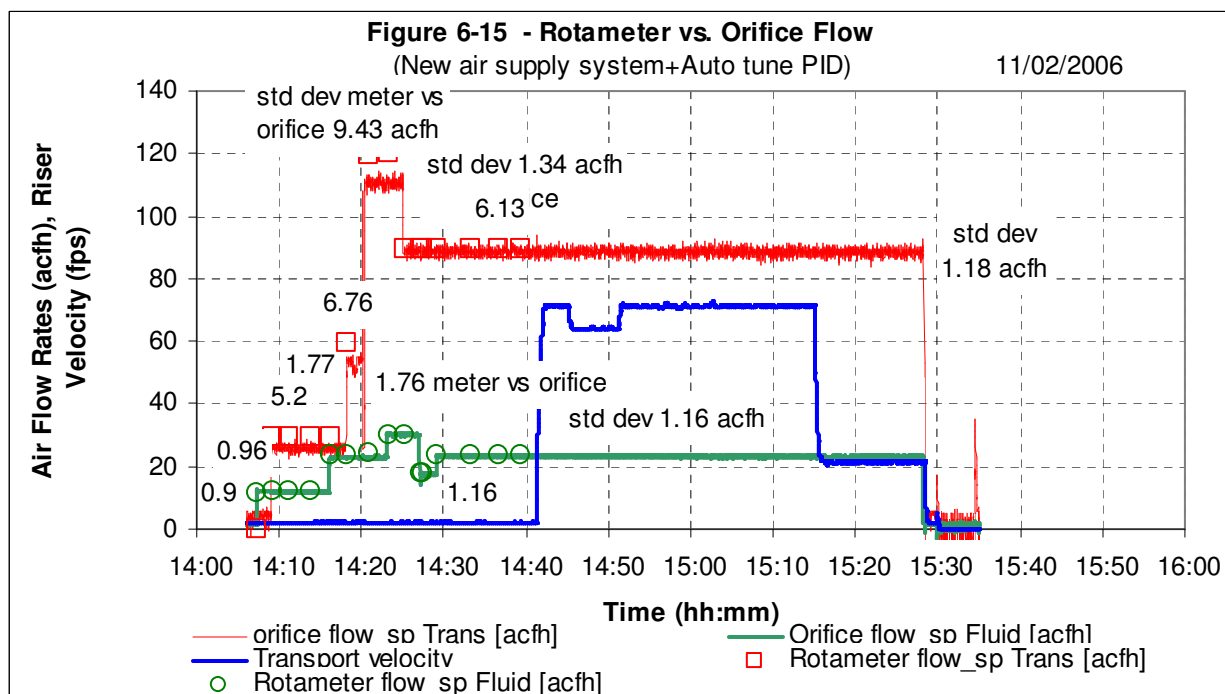
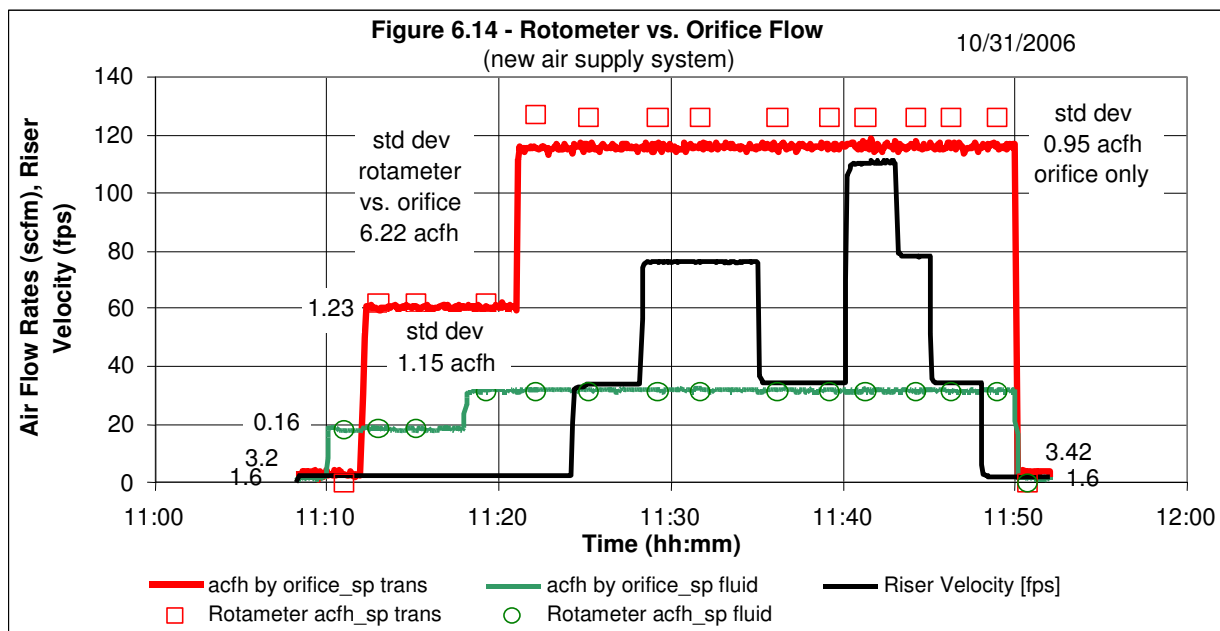
The calculated standard deviation from the setting value is shown in **Figure 6-13** for the new air supply system. After modification of the air supply system, the standard deviation improved from about 450 slm (11.3% of 4000 slm) to about 50 slm (1.3%). Allocating more volume in the air supply system lines improved the deviation slightly but not by much. For example, adding the grease air header alone improved the deviation from 0.65% to about 0.5% at 1000 slm. The addition of a GTF accumulator, further improved the deviation from 0.5% to 0.25%. The setting value and the measured value of the main airflow agreed consistently over a wide range. This air supply line arrangement was acceptable for the chemical looping application.

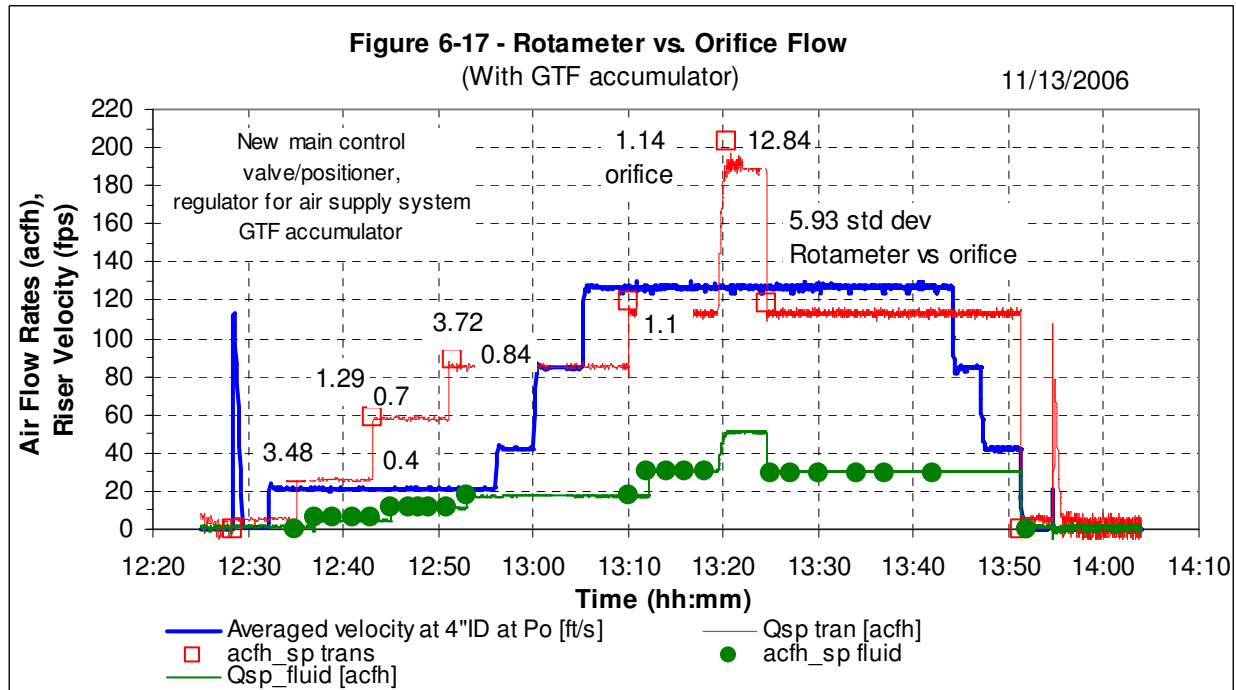
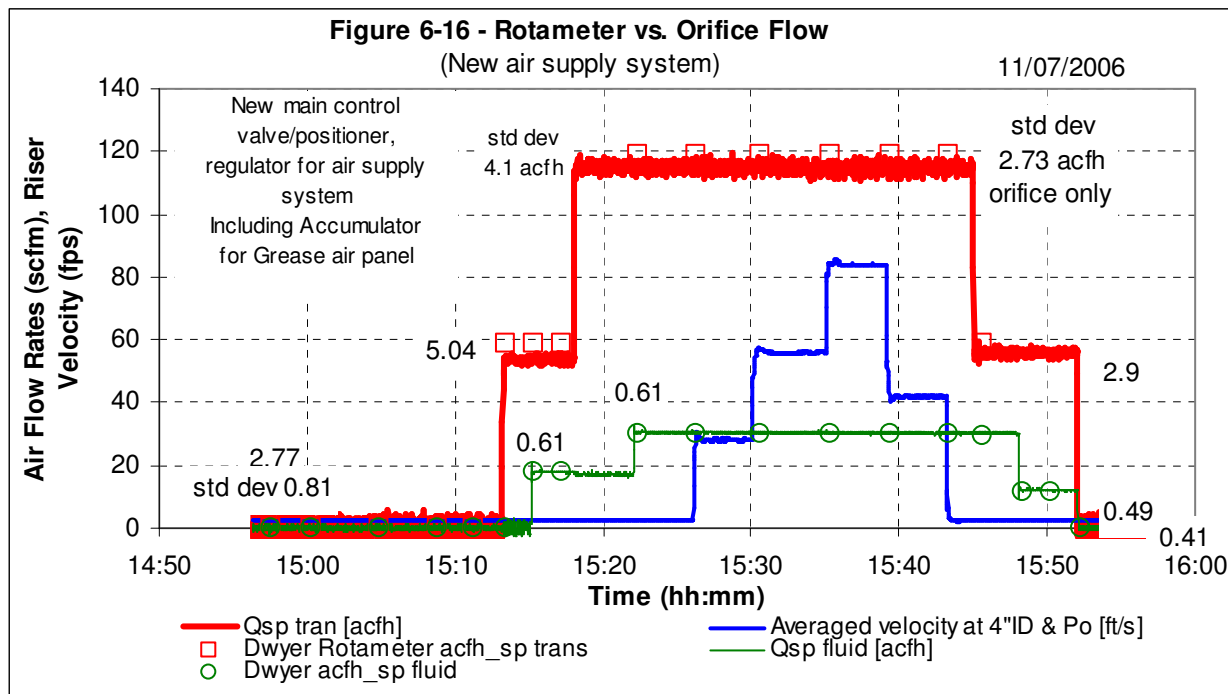


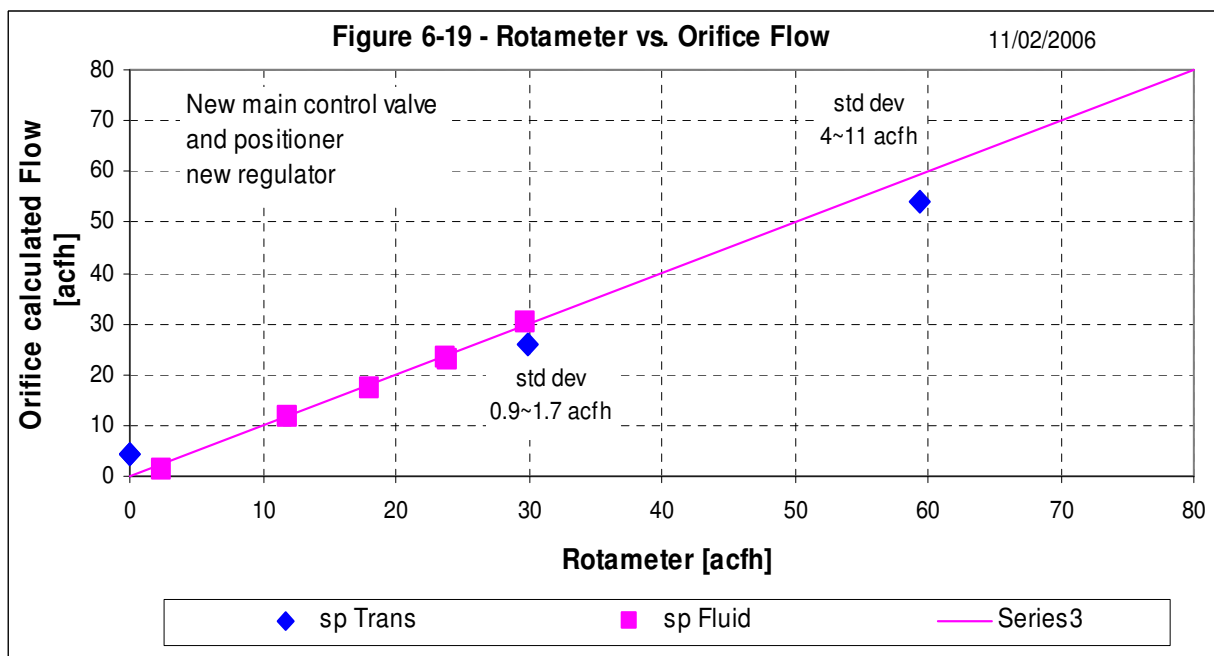
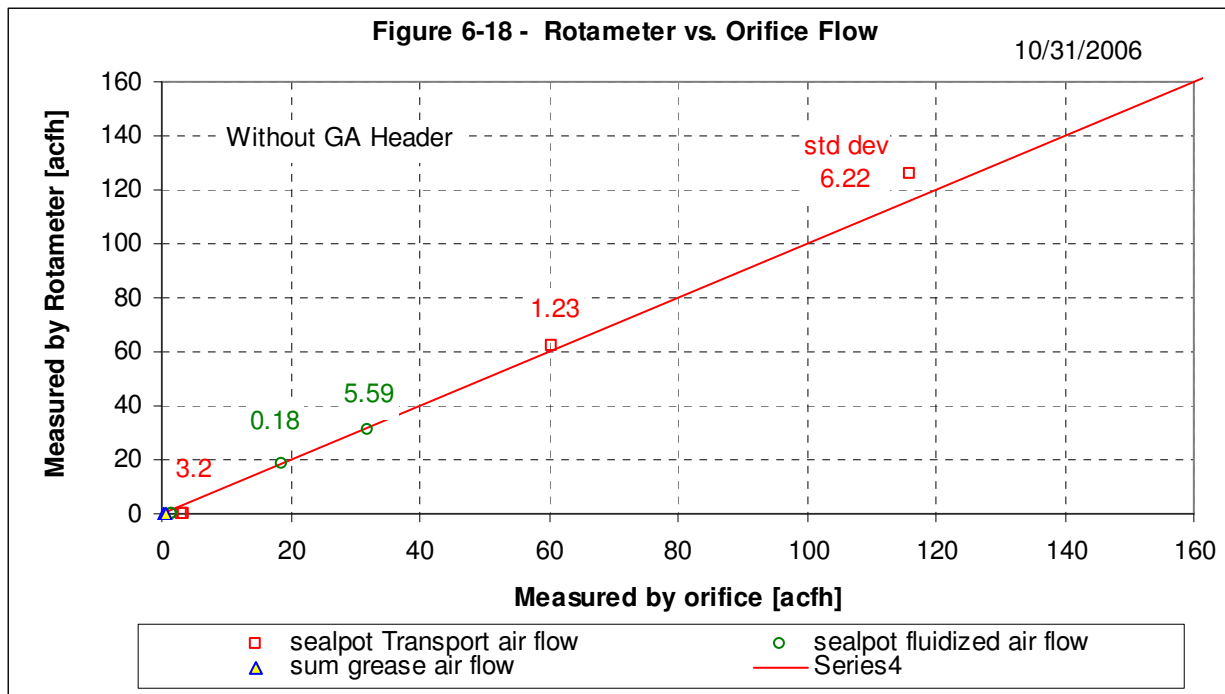
### Sealpot Flow Measurement: Rotameter vs. Orifice Calculation

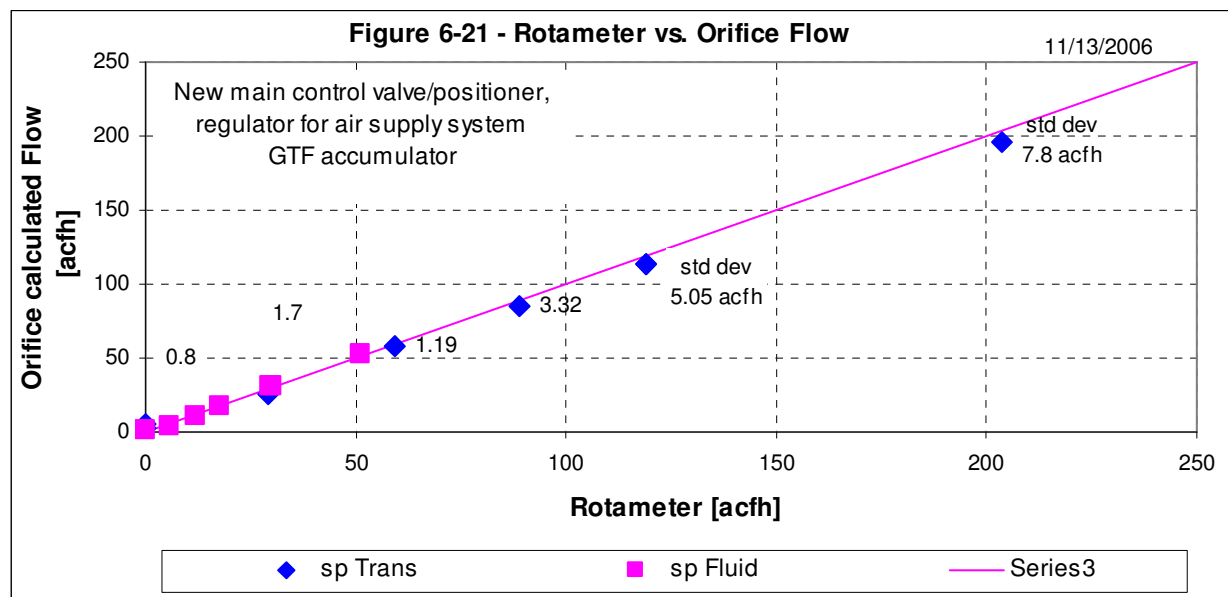
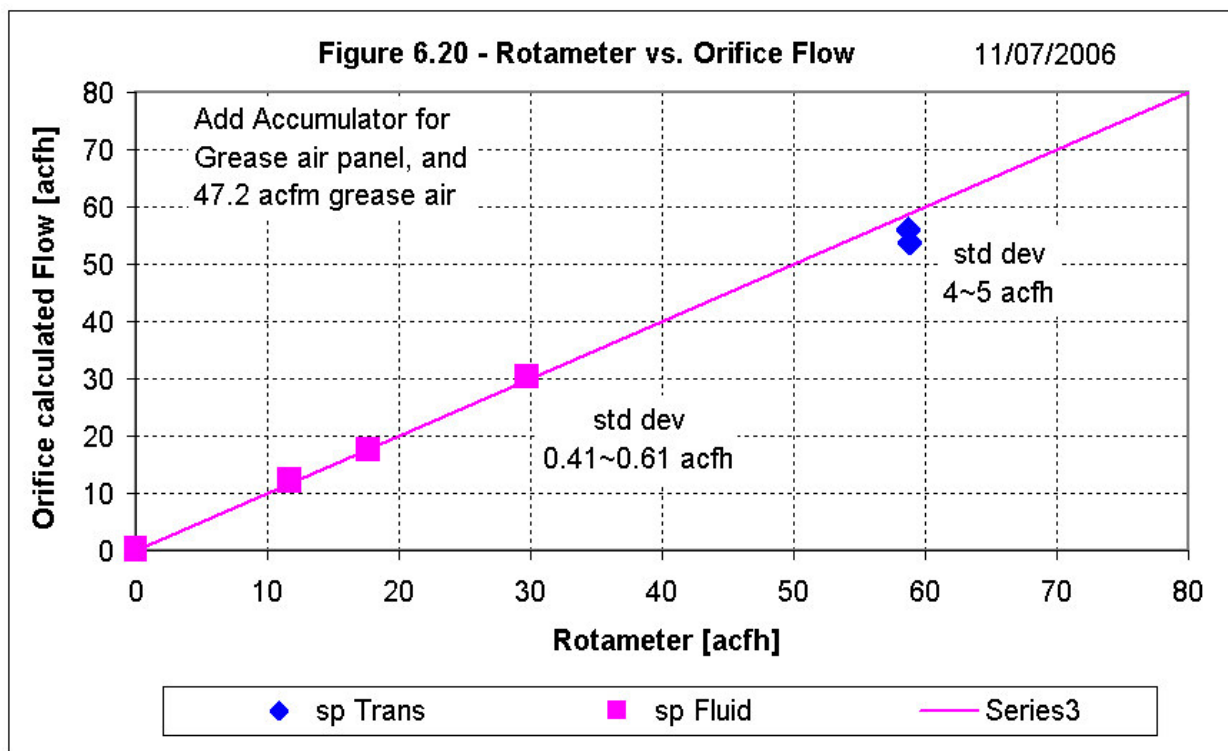
Sealpot fluidizing airflow and sealpot transport airflow were measured independently by rotameters and by orifice calculations based on the ASME recommended method. Orifice calculations provided continuous recording for each second of time through the data acquisition PC. With a stable air supply system, the agreement between rotameter readings and orifice calculations was good, as shown in **Figure 6-14** to **Figure 6-17**, for different air supply system set-up conditions.

**Figure 6-18** to **Figure 6-21** show the deviations of the test airflow rate between rotameter readings and orifice calculations. In general, the deviation in airflow rate increased as airflow rate increased. As shown, the difference was small for all cases after adding the grease air header and GTF (Grease/Fluidize/transport) accumulator. This is due to the relatively small value of grease airflow added to assist solids aeration along the dipleg. The improvement in stability gained by adding GTF accumulator is small. For most cases in the design velocity range, the rotameter flow reasonably agreed with the orifice calculated flow rate. Both of the instruments were used in analysis as a check.





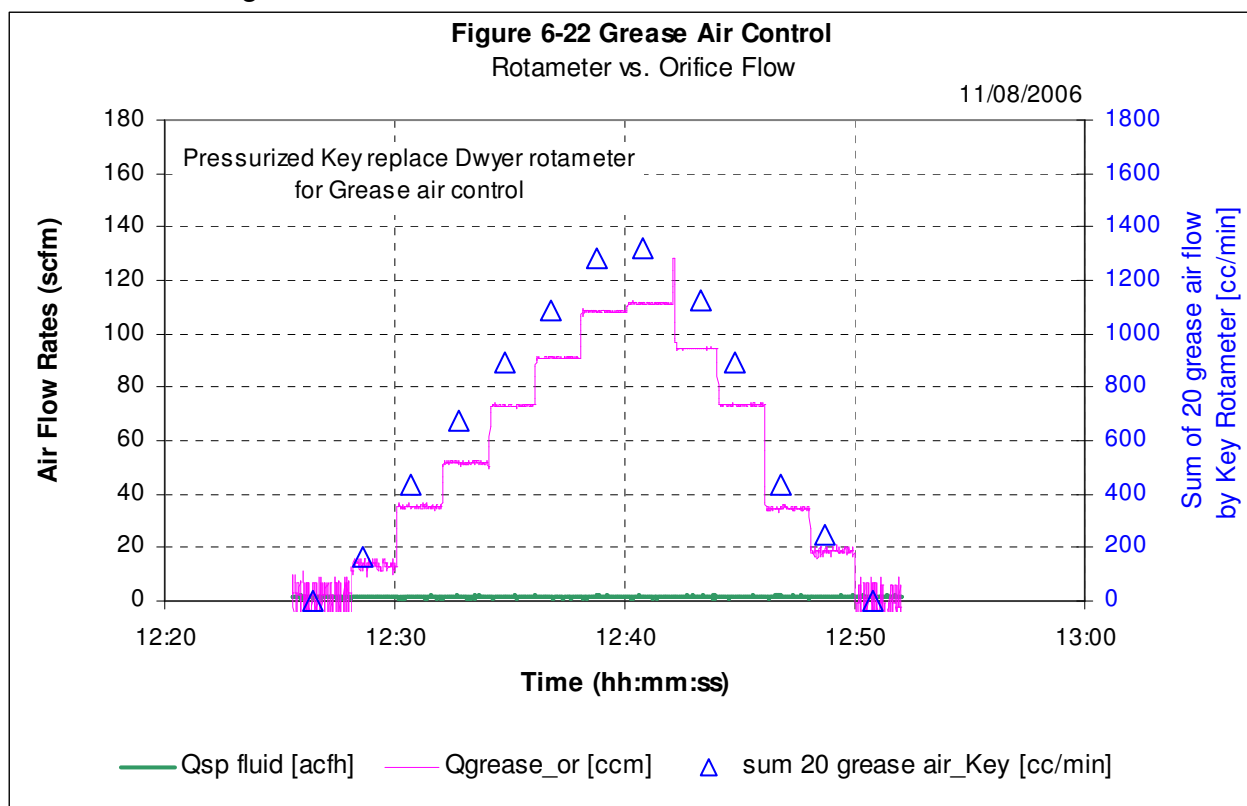


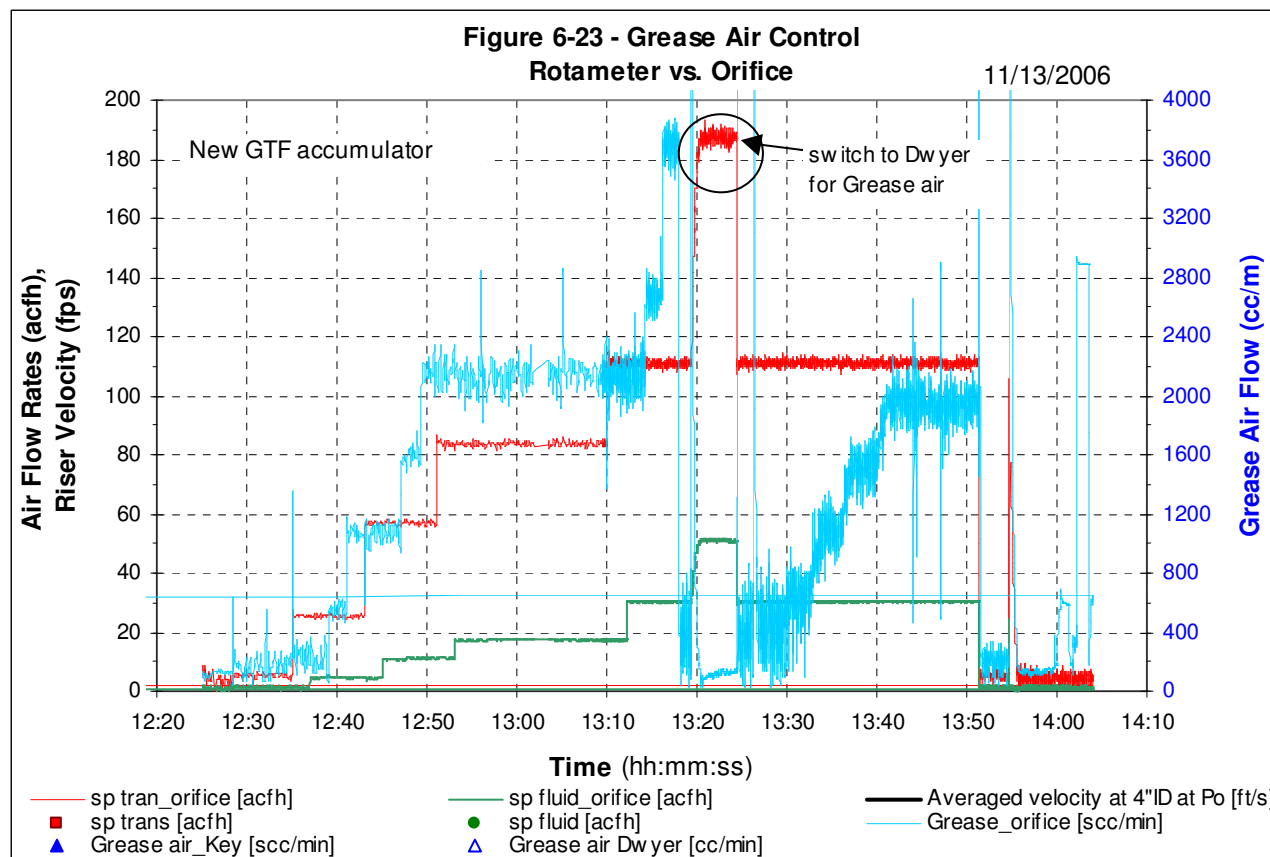


## Dipleg Grease Air Flow Measurement

Originally, the total grease airflow, calculated by the orifice method, did not agree very well with the sum of 20 individual rotameter grease airflow readings. Leakages were found in the grease air supply lines to the rotometer panel and at some of the 20 grease air injection points. A new accumulator header was installed at the inlet of the grease air rotometer control panel. Air leakage was eliminated with the new feed header and grease airflow stability was improved (**Figure 6-22 to Figure 6-23**).

Part of the reason for the disagreement between the rotometer readings and the orifice flow was attributed to the meter itself. This was tested first by using the meter made by Key with the meter outlet pressurized to simulate the Dwyer meter, so the reading was independent of the down stream process. The test depended on the inlet pressure not being affected by the down stream pressure drop. Then, the meter was switched to the Dwyer meter. It was found that the Dwyer meter agreed with the orifice calculated airflow for small airflow rates and had a larger difference from the orifice-calculated value at a higher flow rate. The Key flow meter seemed to have consistent agreement with the orifice-calculated airflow although it did not totally agree. A Key flow meter controlled by inlet pressure, with a wider range than the Dwyer, was then installed and used in the testing.

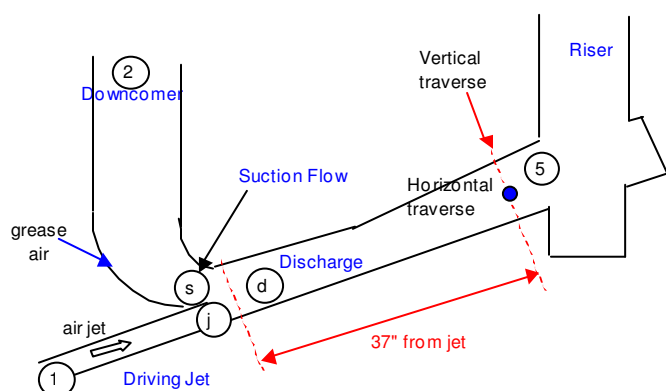




## Design of the Solids Pickup Device in the Lower Leg

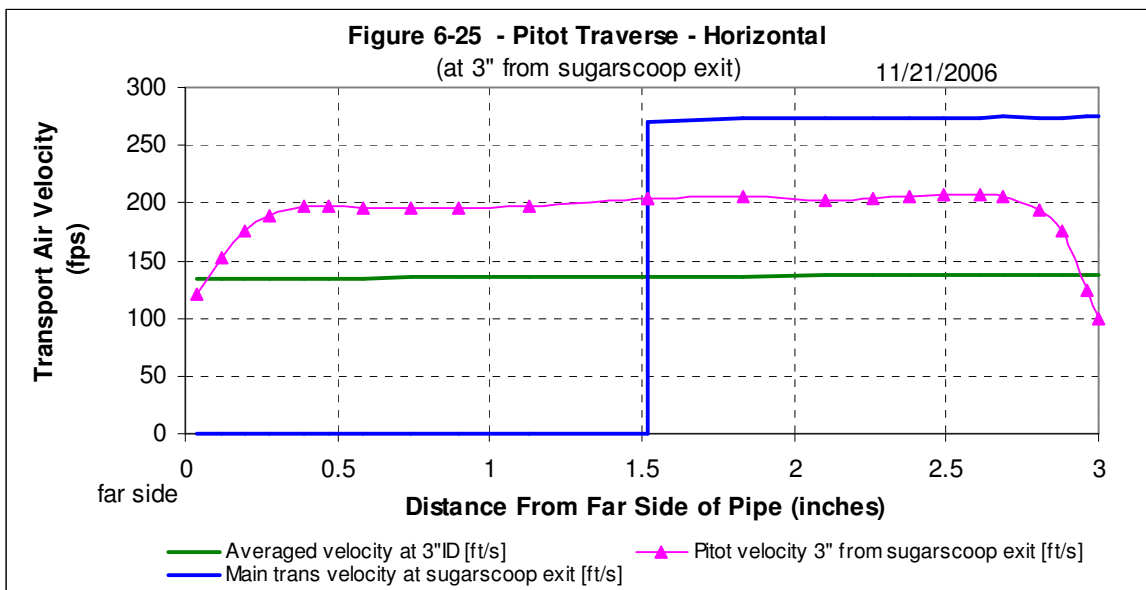
The 'sugar-scoop' concept was originally designed to promote even flow in the mixing of solids and gas before the lower elbow turn. It was also designed to avoid solids saltation along the lower leg and high pressure-drop. This would provide better protection from uneven velocity induced erosion. The schematic design is shown in **Figure 6-24**. This concept was checked with pitot-tube traverse testing across the lower leg tube at 3 inches from the pickup point and also at 37 inches from the pickup point. **Figure 6-25** to **Figure 6-30** show the testing results. As shown, the mixing zone was very effective in converting a skewed velocity distribution at the inlet of the driving jet to a reasonably even flow distribution at the end of the mixing zone.

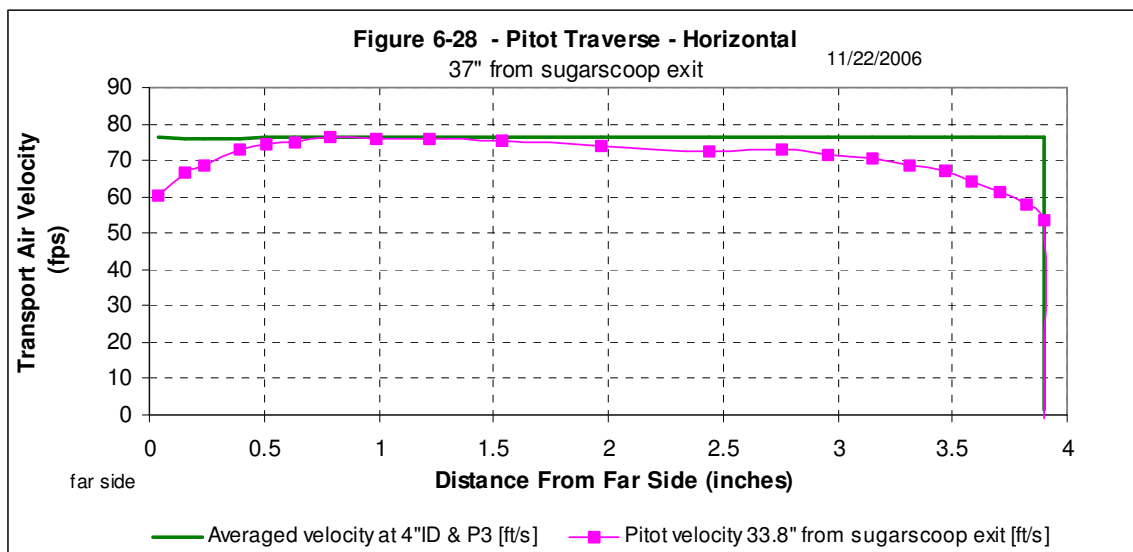
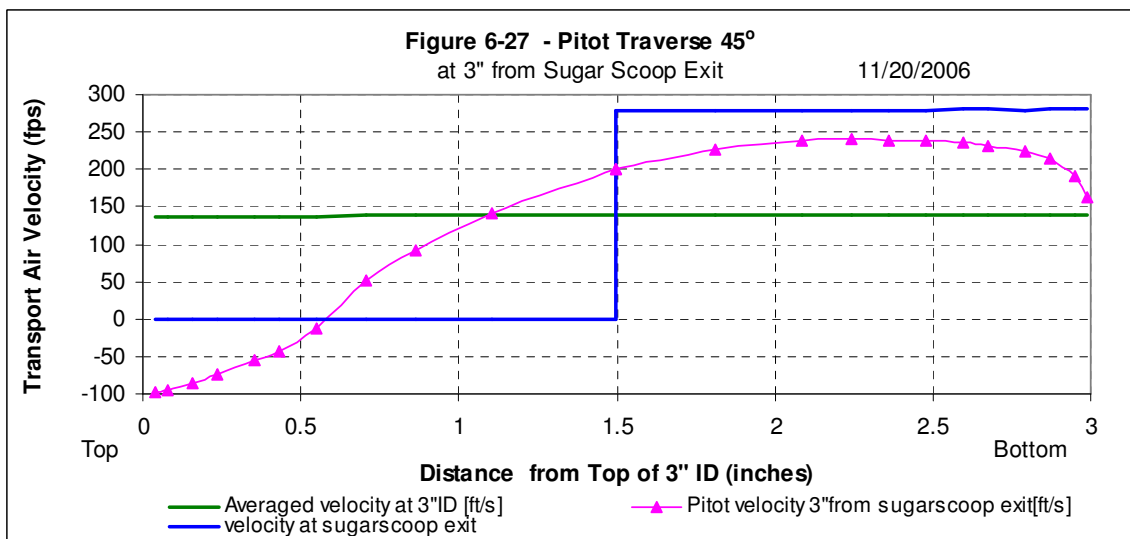
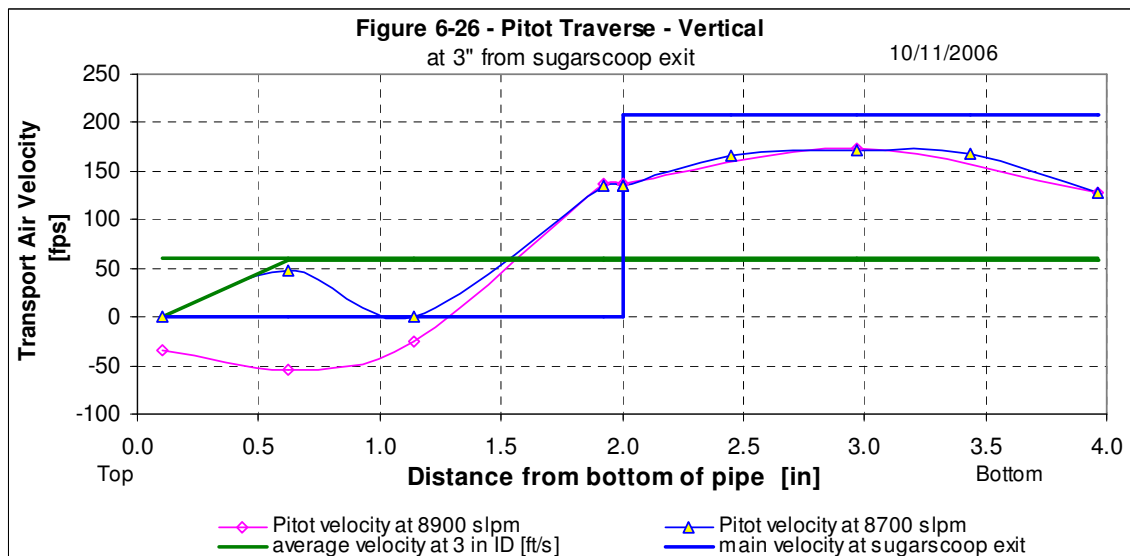
**Figure 6-24 Original Sugar Scoop Design**

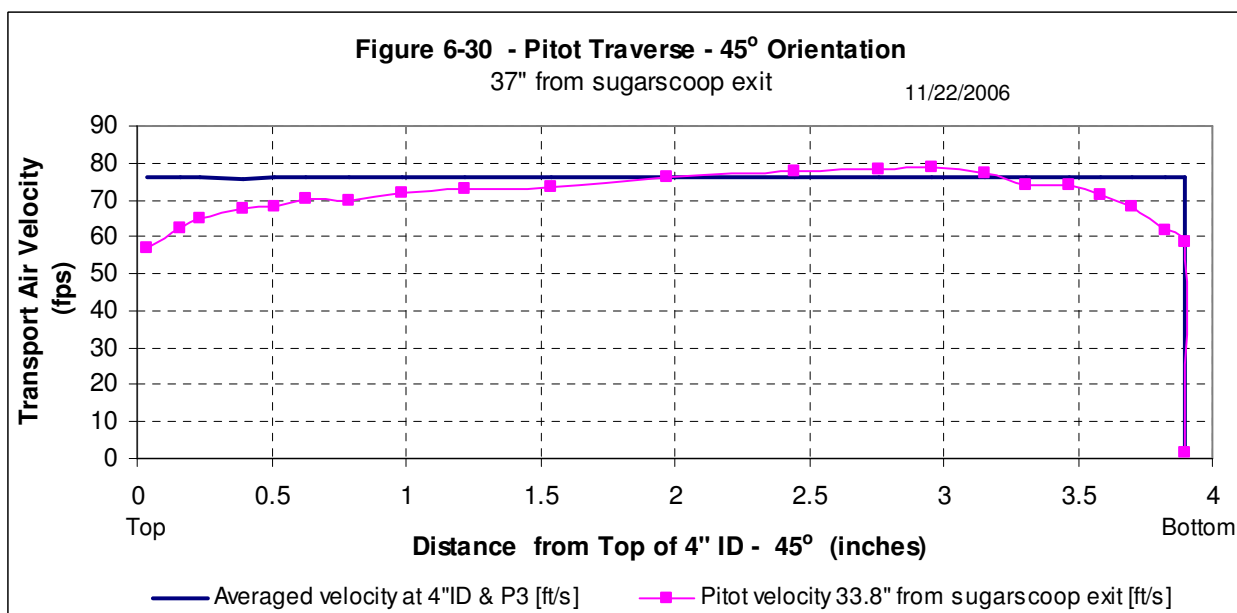
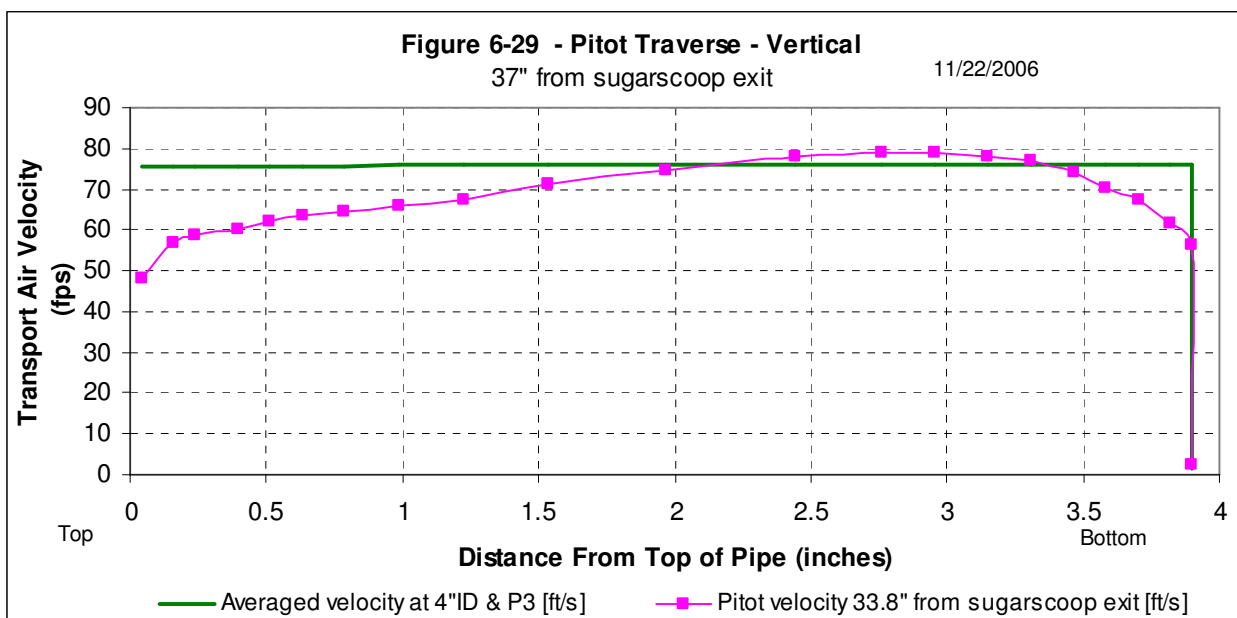


During testing, the original pickup device showed an orifice effect and limited circulating solids flow rate in the mixing zone. When it was tested with higher solids flow circulation, the mixing zone was nearly saturated with solids. Eventually, the high pressure drop due to the saturated solids in

the mixing zone caused the pressure to backup toward the SPCV. Solids started to build up above the sugar scoop with an approximately 25 degree angle of repose. The solids resting above the sugar scoop reduced the opening for solids to go from the return leg to the lower leg. Instead of enlarging the lower leg a new device with a constant diameter was tried. This allowed a higher circulation flow rate but it required locating potential erosion spots.







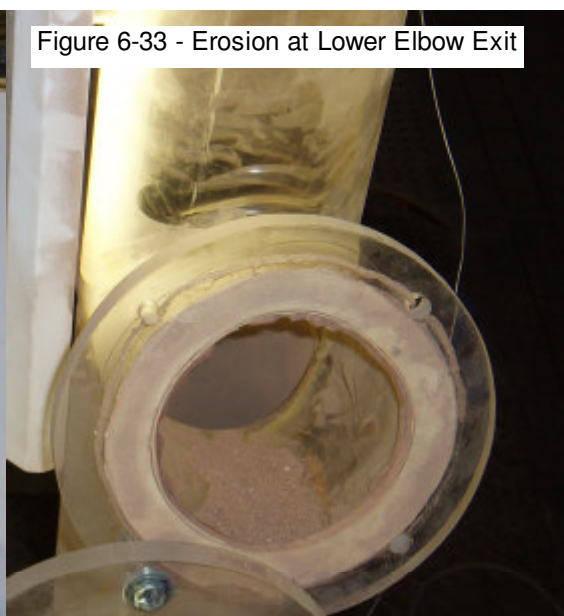
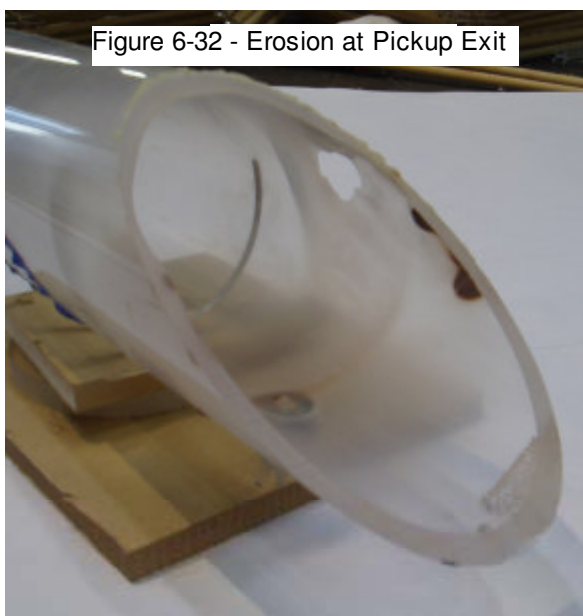
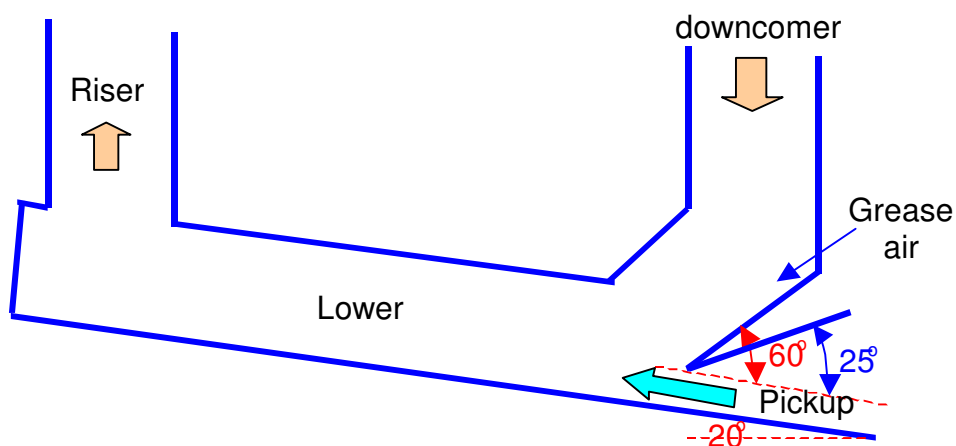
The new pickup device with constant diameter is shown in **Figure 6-31**. Solids pick up and acceleration in the lower leg is steady at velocities above the saltation velocity. At lower velocities (less than 20 ft/s for the tested particle size distribution) solids begin to settle out along the bottom of the lower leg. This increases pressure drop. Saltation starts near the turn of the vertical riser. Accumulation of solids stretches down to the inlet of the pickup jet. Higher solids loading eventually builds up around the turn, and the pressure drop increase accelerates.

The saltation limit of solids under the allowable pressure drop in the lower leg was not

demonstrated during the test campaign. The oscillation of solids flow in the loop during upset conditions may damage the plexi-glass CFM due to a drastic change in pressure. Testing for the choking limit and the saltation limit will be performed later.

The maximum solids flow allowed under the corresponding operating conditions is determined by the available system pressure and an economic trade-off. Test observations show that this design is simple and effective for solids circulation. However, erosion did exist near the pickup point on the side wall of the constant diameter lower leg (see **Figure 6-32**) and at the turn directly above the T-buffer zone (see **Figure 6-33**). This means that erosion resistance material should be applied in these locations in the prototype design.

**Figure 6-31 Constant Diameter Sugar Scoop Design**



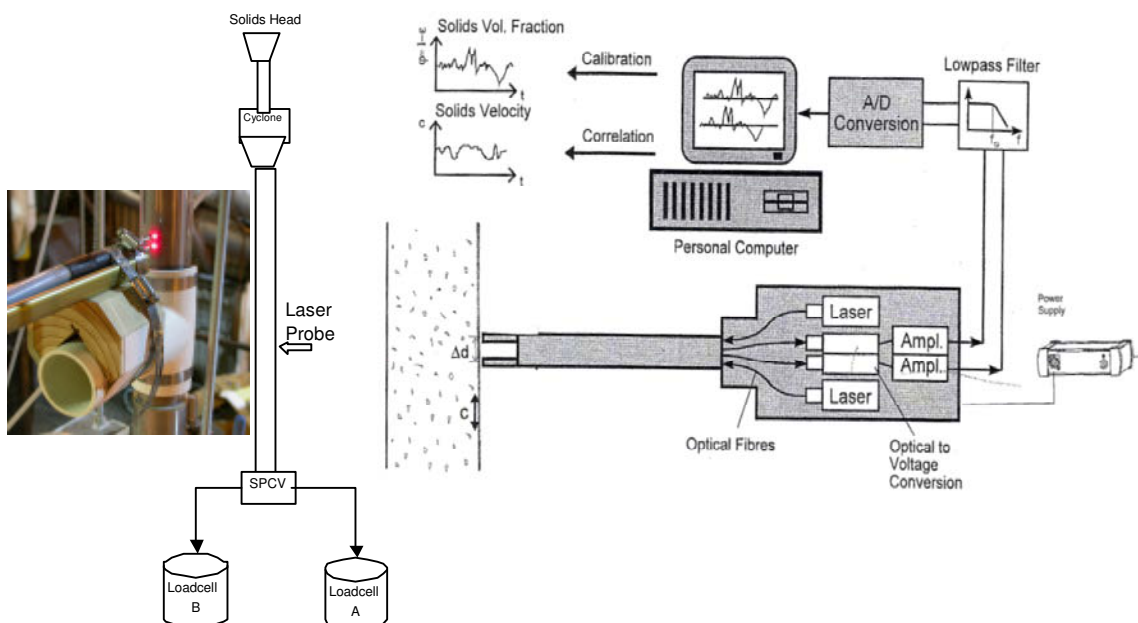
## Solids Flow Measurement and Calibration

### Laser Diode Based Measurement of Solids Velocity in the Dipleg

Measuring the correct solids flow rate in a loop is an important issue not only in solids transport but also for the chemical reactions. To avoid interfering with the flow field in a small tube at high temperature operation (up to 2200°F), intrusive measuring devices are ruled out for solids flow measurement. The flow in the dipleg is very close to the flow in a moving bed. Solids flow is calculated by measuring the solids velocity in the dipleg. The measured solids velocity and the solids bulk density in the dipleg are used to calculate solids flow. Once the solids flow is calibrated, it can be correlated to the associated pressure drop. The correlation can then be used to monitor the solids circulation in hot conditions and in cold conditions.

A laser-diode based probe (by Multiphase System Engineering) was installed on the dipleg just above the SPCV, as shown in **Figure 6-34**. The two solids flows of the cross over solids flow and the main circulating solids flow were measured by load cells A and B respectively. A gap between the probe and the plexi-glass outside wall is reserved to simulate potential cooling requirements when the probe is eventually applied to the hot loop operation. This device is therefore non-intrusive in the solids flow field. A similar type of probe will be installed in the hot loop by using a quartz window to monitor solids flow.

**Figure 6.34 - Laser Diode based Solids Flow Measurement for the 15 ft-Loop**



The laser-diode probe has two laser beams to detect solids flow movement in the dipleg. The software supplied by the vendor analyzes the solids flow pattern to detect the time traveled by solids in a given distance. The resulting analog signal voltage is

then sent to a PC for continuous recording. This non-intrusive set-up was successfully calibrated first in the 15-foot CFM. A typical frequency analysis of the "detected flow" is shown in **Figure 6-35**.

**Figure 6.35 - Example of Frequency Analysis for Flow Detection**

**Analysis Test Data 'Alstom' - 'Flow-Detection'**

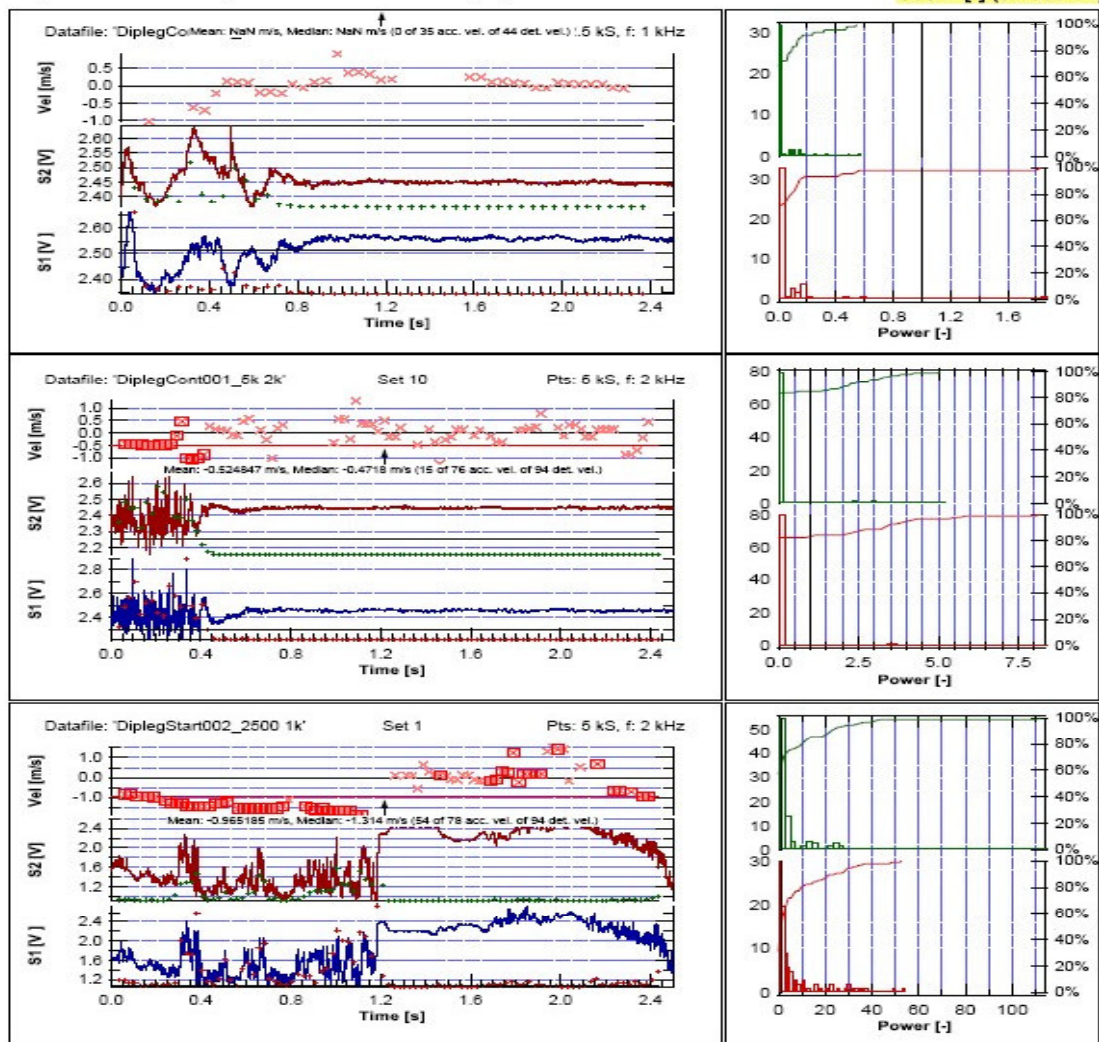
Customer: Alstom Inc., Power Plant Laboratories  
Product: Bauxite 300  $\mu\text{m}$   
Experiment: Labasys® 100 at 'Chemical Looping CFM' Unit

**Method: Freq Ana**

Win. Len Vel: 256, Win. Adv. Vel: 50

Win. Length: 128, Win. Adv.: 50

Cut: 1 [-] (0-1000 Hz)



Flow Detection Analysis Freq Ib.eps

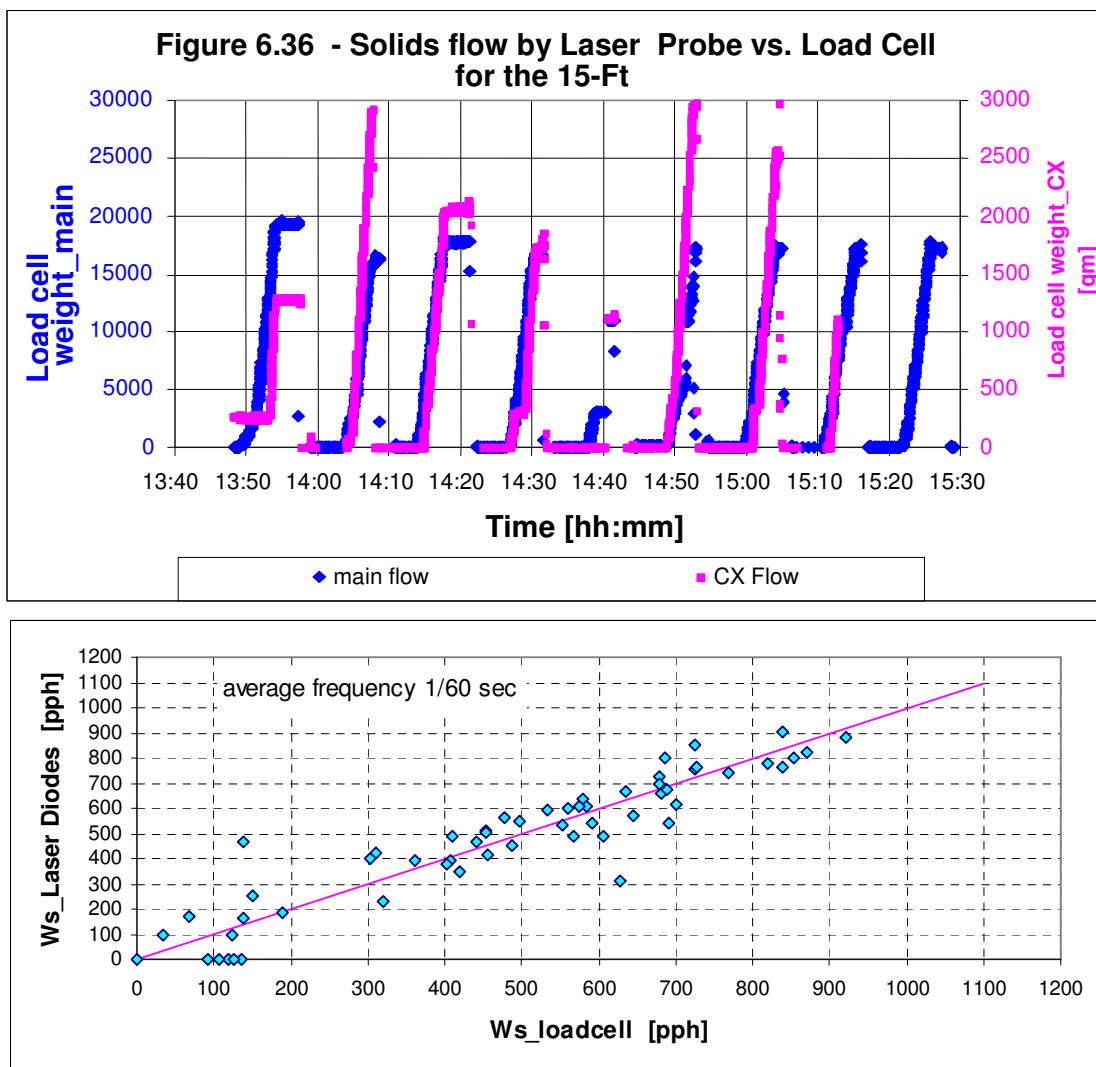
- 1 / 1 -

23. Aug 2005

## Calibration of Solids Flow

Solids flow for the 15-ft-loop CFM was calibrated based on the set up as shown in **Figure 6-34**. Solids were fed continuously from the top hopper by adjusting the control fluidizing air in the SPCV. Two separate load cells were used to continuously measure the solids weight accumulation for the primary circulating loop and the crossover loop.

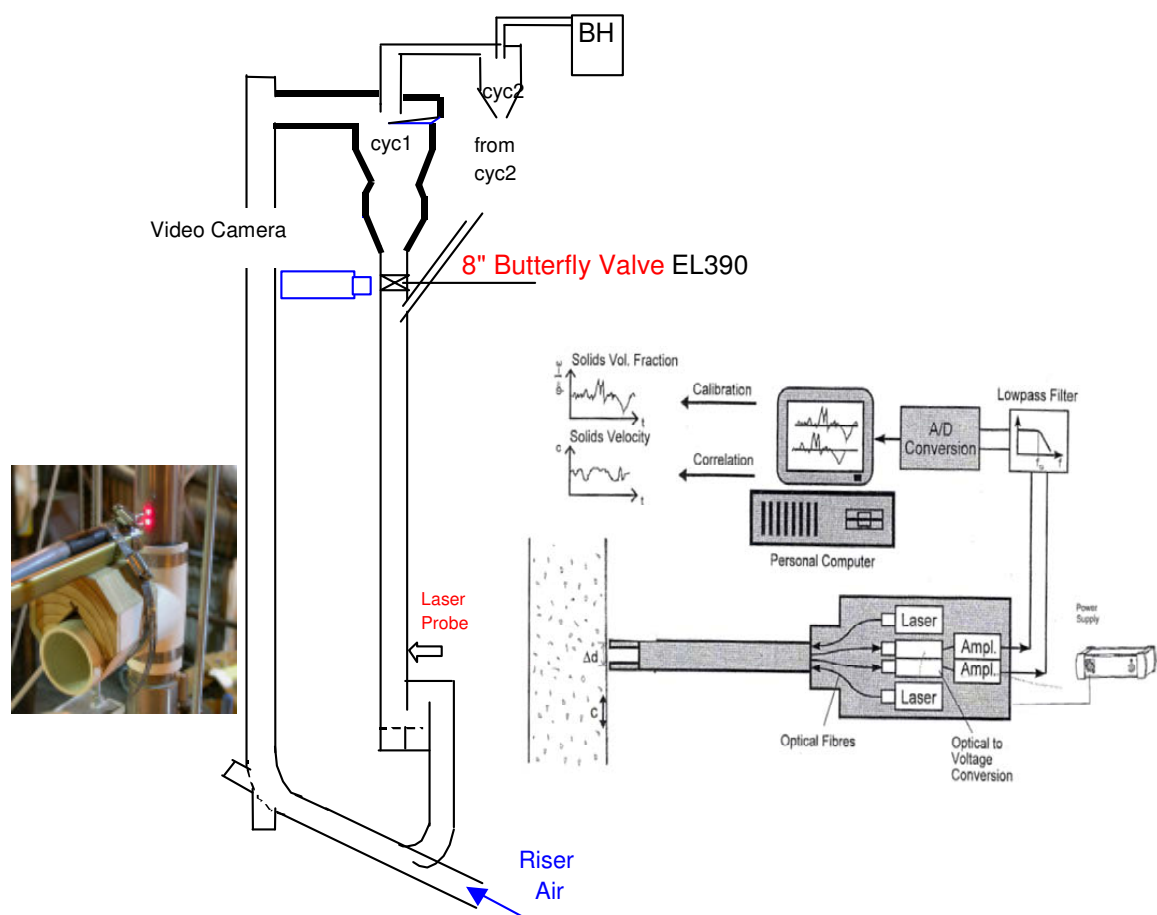
**Figure 6-36** compares the solids flow calculated from the laser measurement to the solids flow based on load cell measurements. The calibration also demonstrated that the laser flow meter was reasonably accurate in measuring average solids flow with a sampling cycle of 60 seconds, as compared to the solids flow based on load cell measurement.



To further reduce the cycle time required to average the data, the correlation used in the software may have to be further calibrated for the lower velocity conditions. Other factors may also affect the detection of solids, such as the background light around the test facility.

Solids flow for the 40-ft-loop was calibrated based on the setup shown in **Figure 6-37**. It was not practical to use a load cell because of the large solids flow in the 40-ft-loop. An 8-inch diameter butterfly valve was installed 390 inches above the SPCV. During solids flow testing, the butterfly valve was closed and solids were allowed to build up in the dipleg to a marked distance and time was measured by a stopwatch. Due to the fast solids build-up in the dipleg, a video camera was used to record the solids rising in the dipleg. The distance and time were correlated by counting each video frame. Since these tests were rather short, the effect of a precise time reading on solids circulation was significant.

**Figure 6.37 - Laser Based Solids Velocity Measurement for the 40-ft Loop**

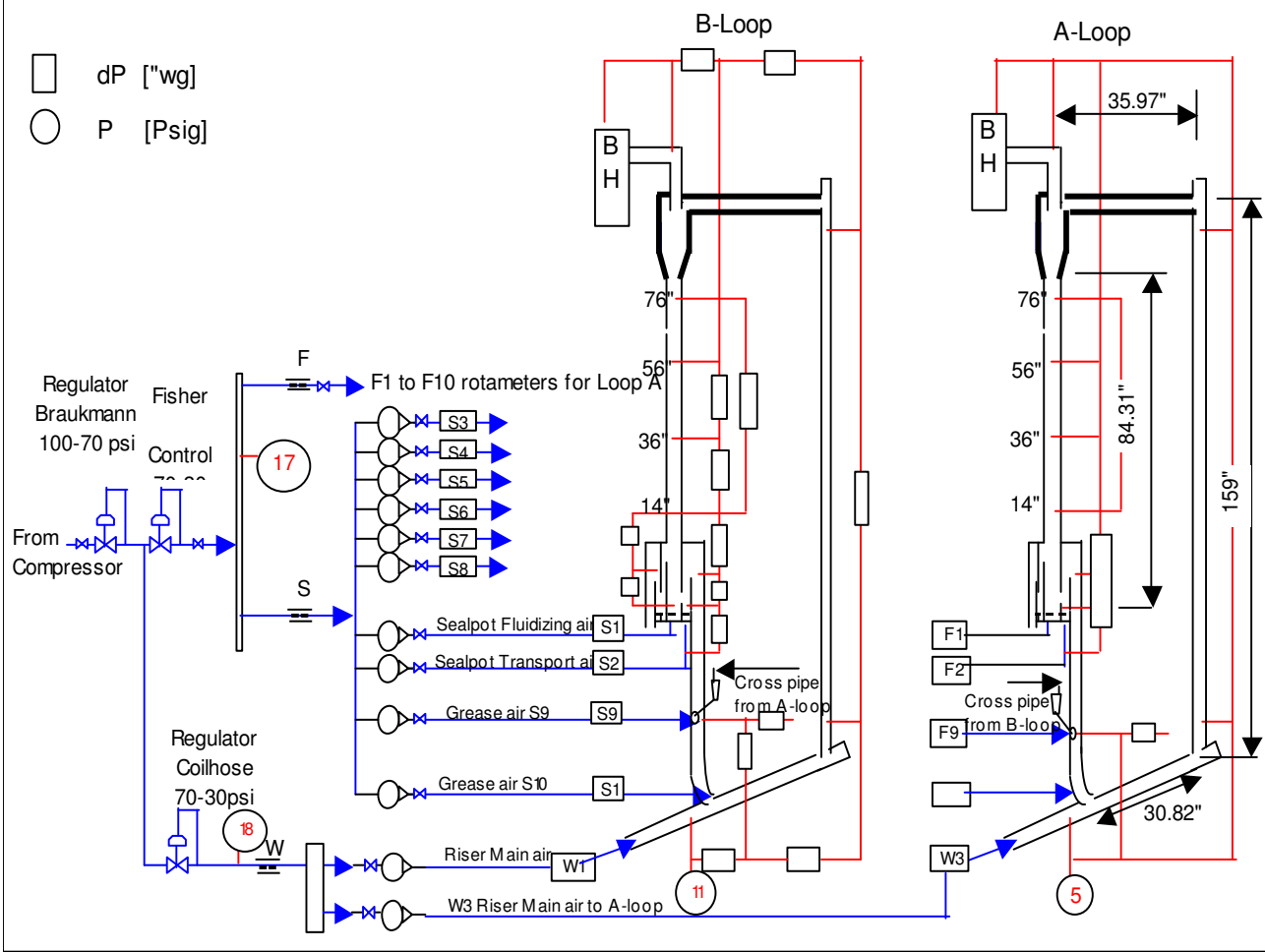


## 6.2.2. 15-Foot CFM Test Facility

The 15-ft CFM Test Facility was modified to have two identical loops. It is nearly identical to the hot PDU (Process Development Unit). This facility can operate in a single-loop mode or in a double-loop mode. A simplified schematic diagram is shown in **Figure 6-38**. The riser vertical section is 159 inches. The dipleg height including sealpot is 84.31 inches. The upper horizontal leg is 35.97 inches. The lower leg is 30.82 inches with a slope of 20° from the horizontal. The inside diameter of the dipleg is 1.5 inches. The rest of the pipes have an inside diameter of 0.75 inches. Solids are loaded into the CFM from the top of the cyclone exit pipe before each test.

Many solids transport concepts and equipment designs were verified at this facility. The data obtained provided valuable input to scale-up studies. It also provided a training facility and was a diagnostic tool for solids transport problems during the hot PDU operation.

**Figure 6.38 Flow Measurement and Pressure Taps for the 15 Ft-Loop**

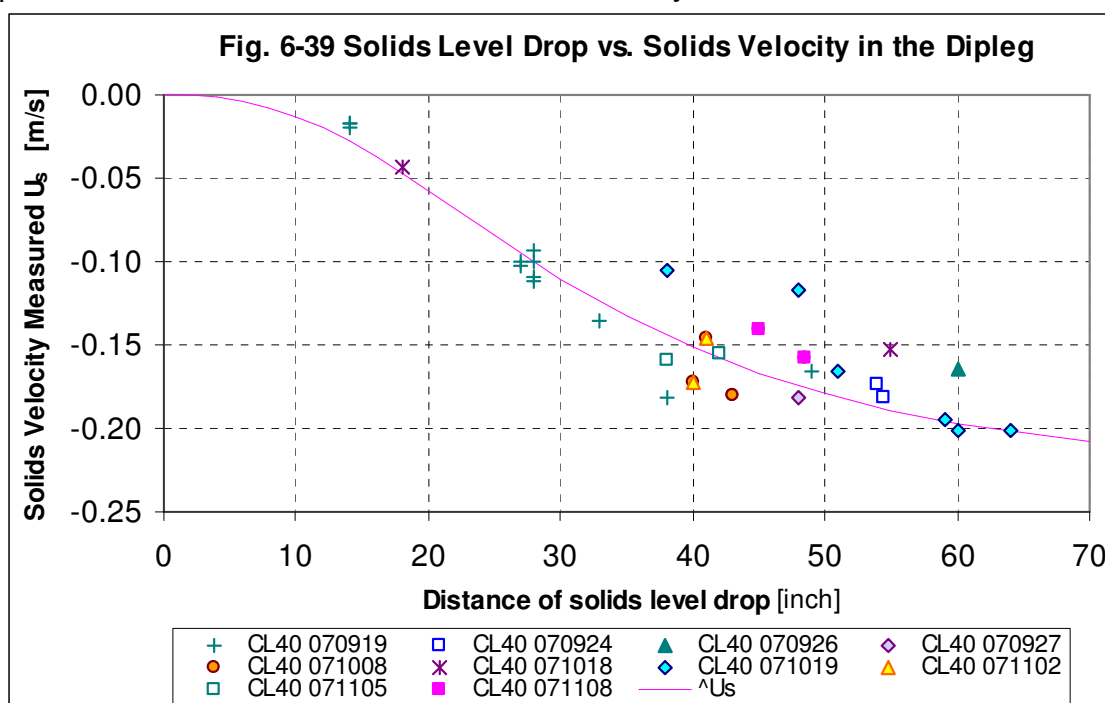


## 6.3. Test Summary and Analysis

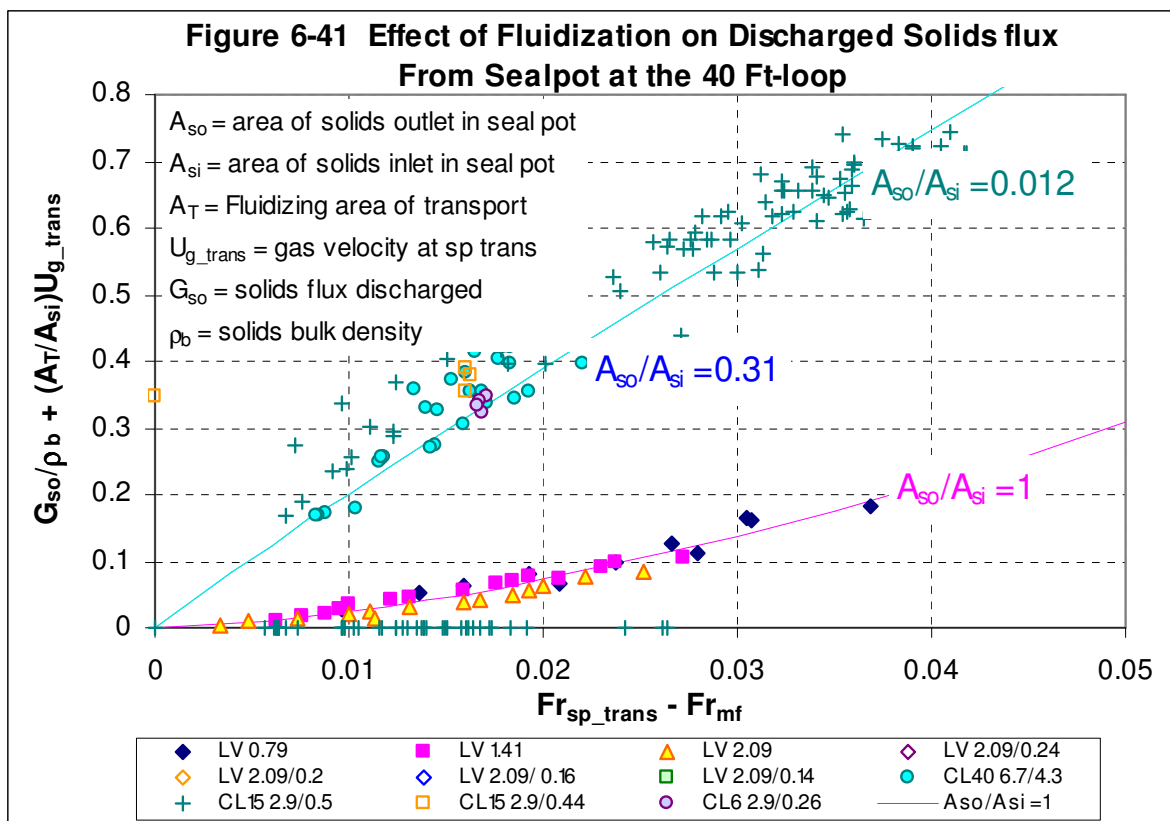
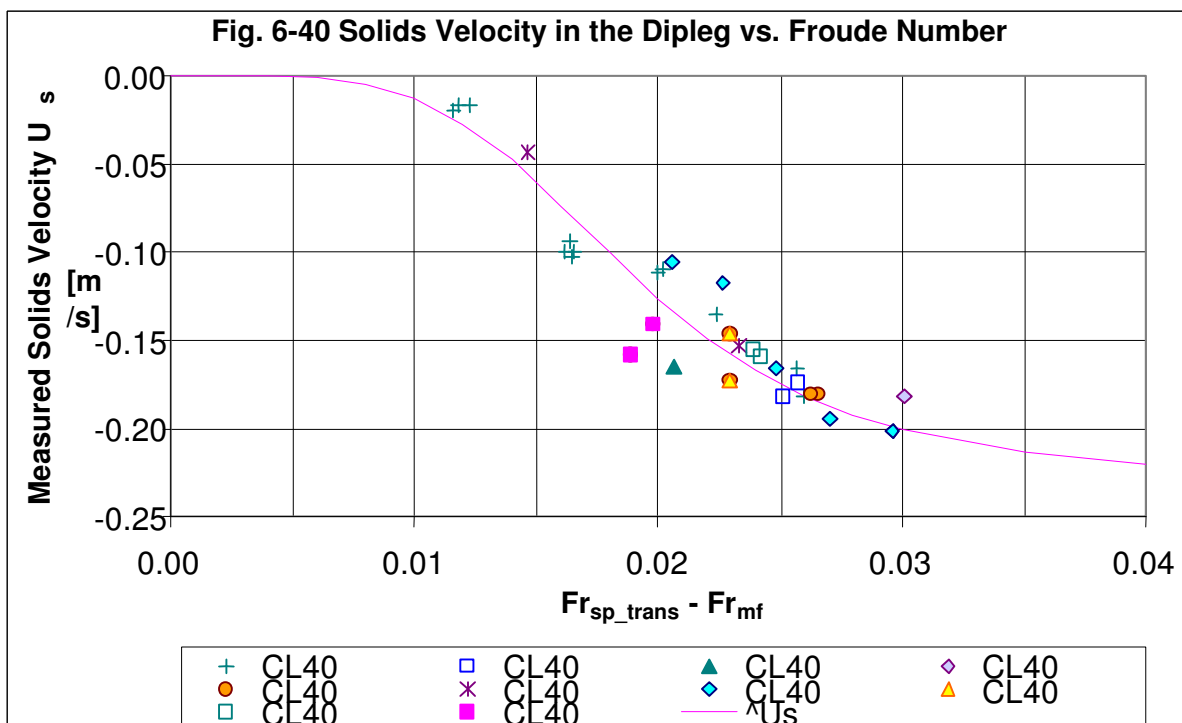
### 6.3.1 Solids Flow Recirculation

The solids velocity along the dipleg was measured by the laser probe. Solids flow in the 15 ft CFM was calibrated by load cell measurements. Solids flow in 40-ft-loop was calibrated with the closed-valve test by using the known bulk density of the solids in the dipleg. During the 40-ft-loop test the initial dipleg height and the drop of the solids height in the dipleg were recorded.

Solids velocity  $U_s$  was closely related to the drop of solids height in the dipleg as shown in **Figure 6-39** for the 40-ft-loop. Test data showed that a larger drop in solids height in the dipleg corresponded to a higher solids velocity in the dipleg, and hence more solids flow. In addition to the measurement of solids velocity by the laser probe, the correlation between the amount of dipleg solids drop and solids velocity provided an additional independent check to the closed-valve solids velocity test.

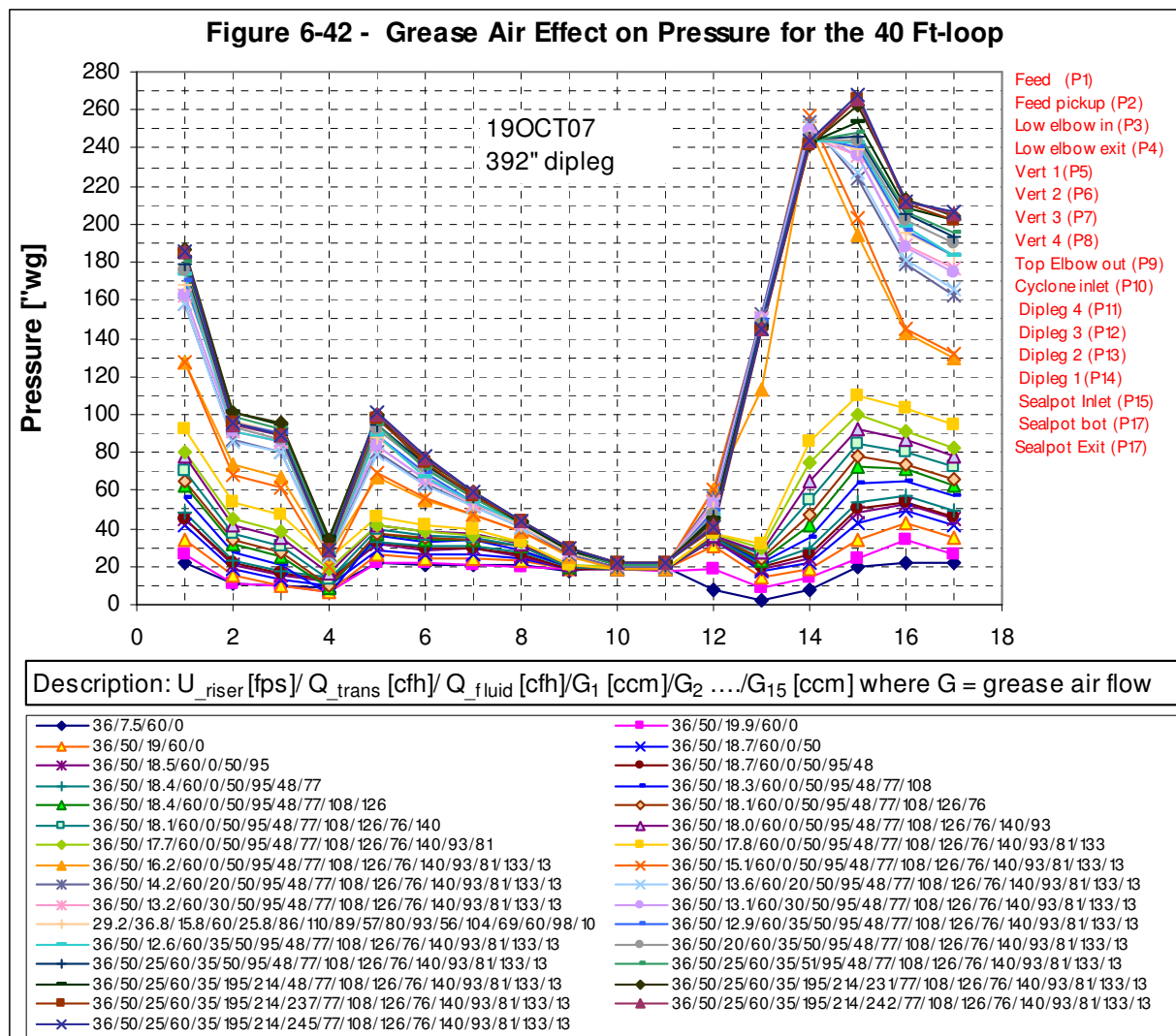


The SPCV provides control of the dipleg solids velocity and therefore the circulated solids flow. This is done by controlling the sealpot fluidizing air and the dipleg grease air. **Figure 6-40** shows the correlation of solids velocity in the dipleg of the 40 ft-loop, as a function of the difference between the Froude number in the sealpot transport chamber and minimum fluidization. The effect of fluidizing velocity (shown as Froude number) on the discharged solids flow is shown in **Figure 6-41**. As Froude number increases with increasing fluidizing velocity, the fluid bed in the SPCV expands and the solids discharge flow increases for the same particle size distribution and dipleg grease airflow. Also shown in **Figure 6-41** is the published data for the L-valve, which is similar to the SPCV.

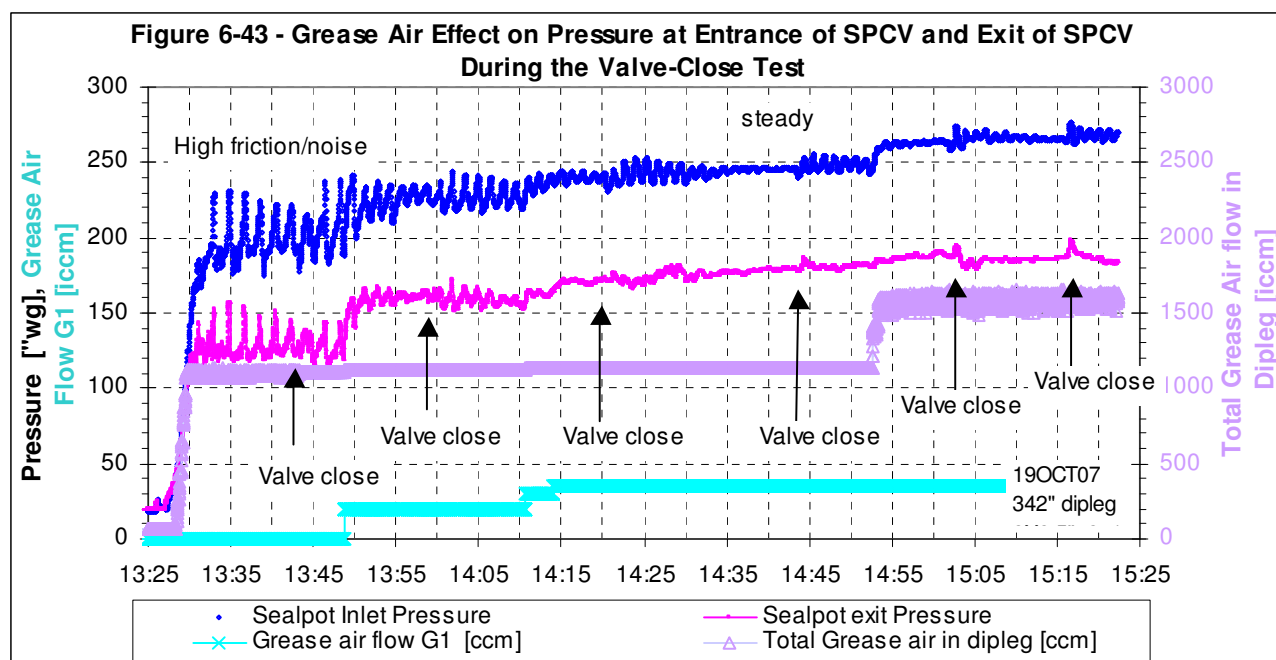


### 6.3.2 Dipleg and Sealpot Performance

The pressure drop along the dipleg was closely related to the amount of grease air injected and the solids downward velocity. Grease air was gradually increased in the 19 OCT 2007 test to determine the effect of grease air on dipleg pressure drop and pressure drop around the loop. **Figure 6-42** demonstrates the overall effects of grease air on pressure measurement for all pressure taps along the 40-ft-loop. Before grease air was injected, the dipleg had a lot of friction between the bed material and the tube wall and in the bed itself.



The vibration and noise detected during the test without grease air was reflected in the large pressure fluctuation measured at the entrance and the exit of the SPCV. This is shown in **Figure 6-43**. The solids velocity in the dipleg reached a minimum when grease air was off. Without grease air, the sealing capability was mainly controlled by the static head of the solids and the friction force between the wall and the moving solids. Solids flow was limited by the dipleg size and friction.

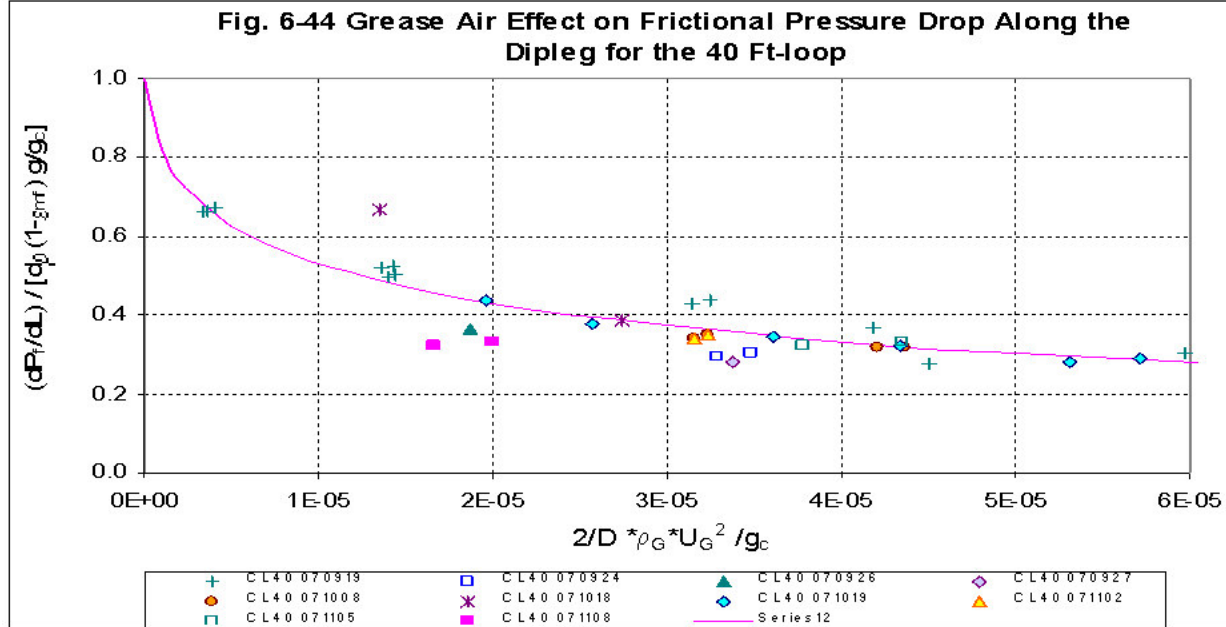


Audible noise was induced by the compression of solids and gas. The compression of gas at the bottom of the dipleg was caused by the static head of solids and the dynamic head due to the solids acceleration. Grease air allowed the pressure to be dissipated along the length of the dipleg. This avoided the excessive compression of gas. Without sufficient grease air noise built up during the compression period and then diminished when the pressure dissipated. The cyclic phenomenon of compression and dissipation continued until more grease air was injected, which effectively established a pressure dissipation passage. With more grease air, noise was reduced and the vibration gradually reduced until it disappeared.

The level of solids in the dipleg reached a steady-state during the test after a short transition period (about 10 seconds) after a change in operating conditions. Pressure readings for measuring ports eventually reached a steady state. Solids flow in the loop was under control and remained steady. Further increases in grease air made little difference in the pressure readings. Tests showed that grease air acted as one of the key elements to increase solids flow circulation but also reduces the seal capability of solids in the dipleg.

Further calibration showed that grease air increased the solids downward velocity improving solids flow. However, as solids moved more rapidly, pressure drop due to friction between the wall and solids actually decreased due to the grease air effect. This is shown in **Figure 6-44**. As grease air further increased, the whole dipleg reached a minimum fluidization. The total pressure drop was then equal to the static pressure drop. In this case, the frictional portion was zero and the solids velocity reached a maximum.

In an actual application, the amount of grease air will be optimized to obtain the design solids velocity for a required seal capability. The evaluation will be based on the solids flow requirements in the chemical reactions in the reactors and on the auxiliary power required with more grease air.



The pressure drop due to the frictional effect was analyzed for the 40-ft-loop, the 15-ft-loop and some publicly available data. Solids movement in the 40-ft and the 15-ft was similar to solids in a moving bed. The stress on the wall due to friction was assumed proportional to the kinetic energy of the gas velocity as follows:

$$(1) \quad \tau_o = f \frac{\rho_g U_g^2}{2}$$

$$(2) \quad \delta P_f \frac{(\pi D^2)}{4} = \tau_o (\pi D \delta L)$$

$$(3) \quad \frac{\delta P_f}{\delta L} = f \frac{2 \rho_g U_g^2}{g_c D}$$

$$(4) \quad \delta P_f = \delta P_{dip} - \delta P_s - \delta P_a$$

$$(5) \quad \delta P_s = \frac{\rho_g g}{g_c} \delta L$$

$$(6) \quad \delta P_a = \frac{U_g^2}{2 g_c}$$

$$(7) \quad \text{Re}_p = \frac{\rho_g U_g D_p}{\mu_g}$$

where,

D = diameter of dipleg [ft]

$D_p$  = Harmonic mean particle diameter [ft]

L = dipleg length [ft]

$U_g$  = superficial gas velocity [ft/s]

$\rho_g$  = gas weight in dipleg void space [ $\text{lb}_m/\text{ft}^3$ ]

$\mu_g$  = gas viscosity [ $\text{lb}_m/\text{ft} \cdot \text{s}$ ]

g = gravity acceleration [ $\text{ft}/\text{s}^2$ ]

$g_c$  = conversion factor [ $\text{lb}_f \cdot \text{s}^2/\text{lb}_m \cdot \text{ft}$ ]

$\Delta P_f$  = frictional pressure drop [ $\text{lb}_f/\text{ft}^2$ ]

$\Delta P_s$  = static pressure drop [ $\text{lb}_f/\text{ft}^2$ ]

$\Delta P_a$  = acceleration pressure drop [ $\text{lb}_f/\text{ft}^2$ ]

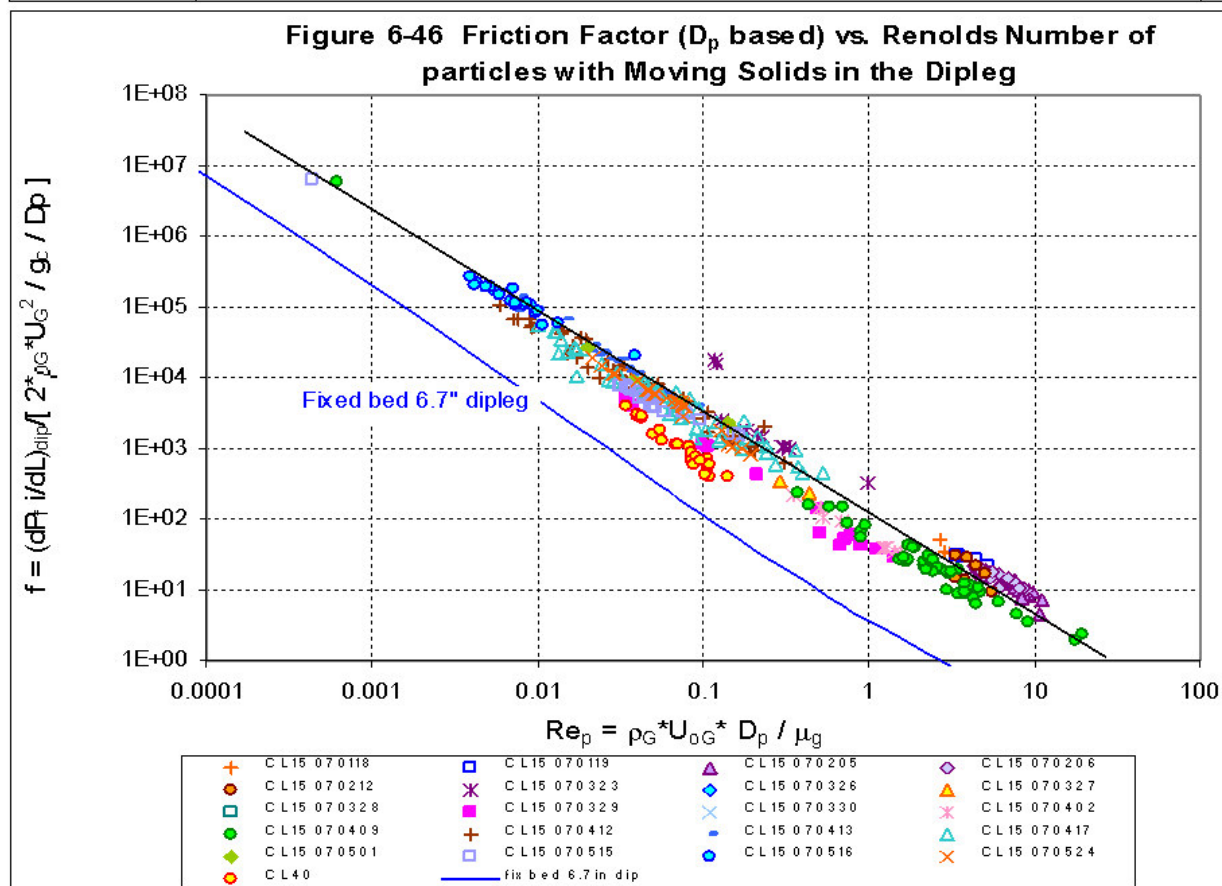
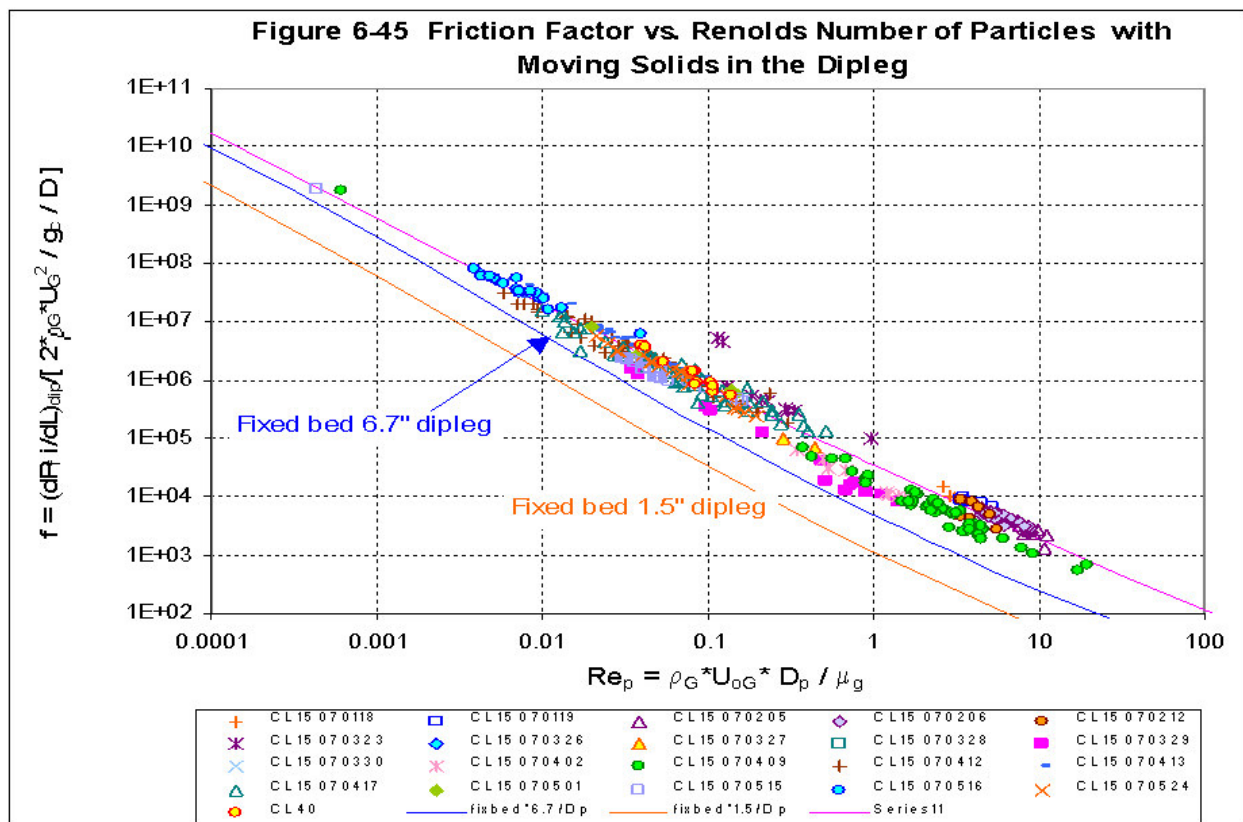
f = friction factor

$\tau_o$  = stress due to friction on dipleg wall

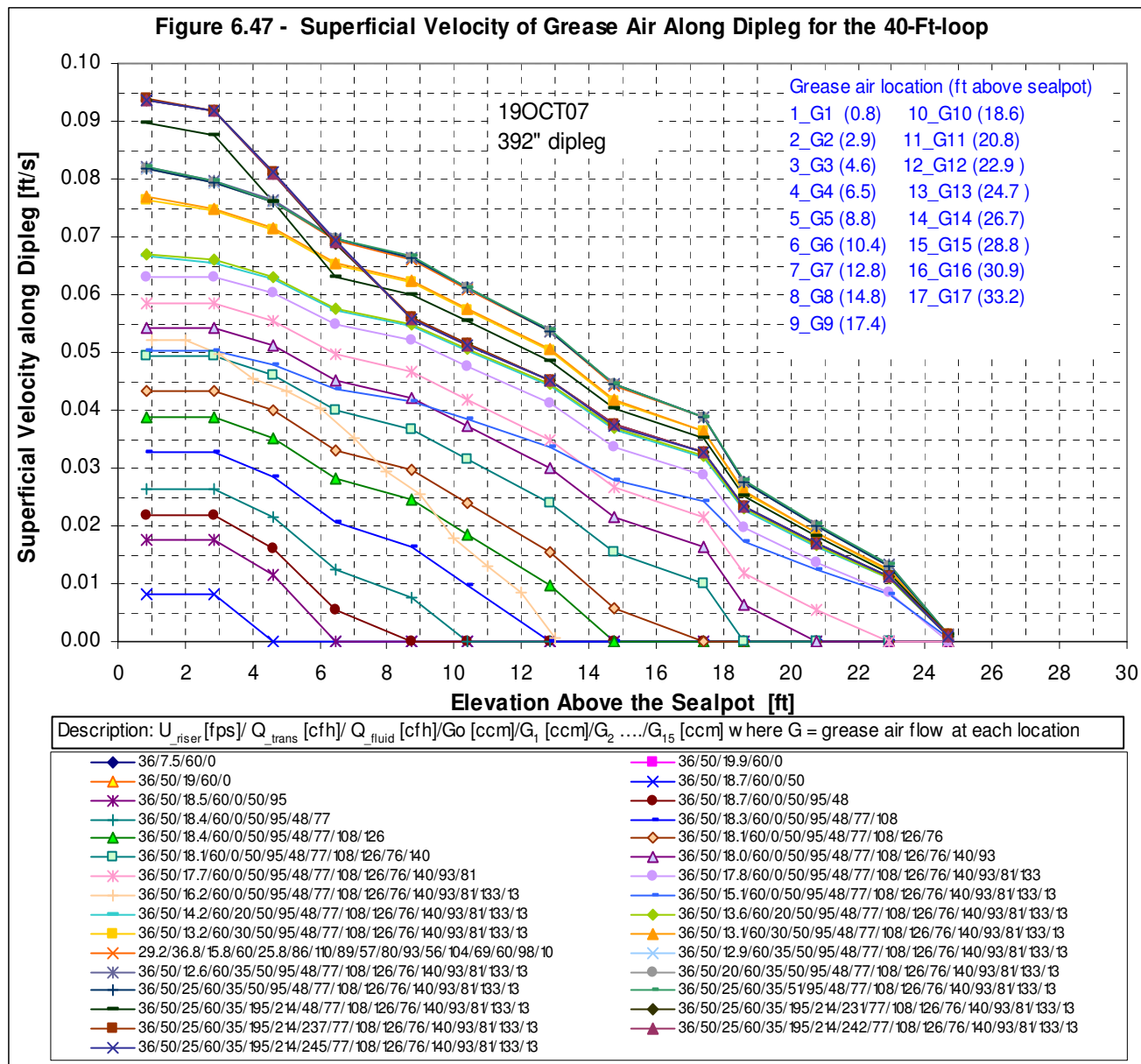
The friction factor, as defined in Equation (3), is correlated to the Reynolds number based on the harmonic mean particle diameter. **Figure 6-45** shows that the friction factor is strongly related to the particle Reynolds number. As the Reynolds number of the particle increases, the friction factor is dramatically reduced. This means, for a given particle size, increasing the grease air increases the particle Reynolds number and reduces the friction factor accordingly.

The test data was very close to the correlation derived by Zenz (1960) for solids in a fixed bed based on Carman's correlation (1933) (for  $\text{Rep} < 0.1$ ), and Bakhmeteff and Feodoroff's data (1937) for  $1 < \text{Rep} < 100$  (**Reference 6**). The calculated friction factors based on the Zenz fixed bed correlation are also shown in **Figure 6-45** for dipleg diameters of 1.5 inches and 6.7 inches respectively.

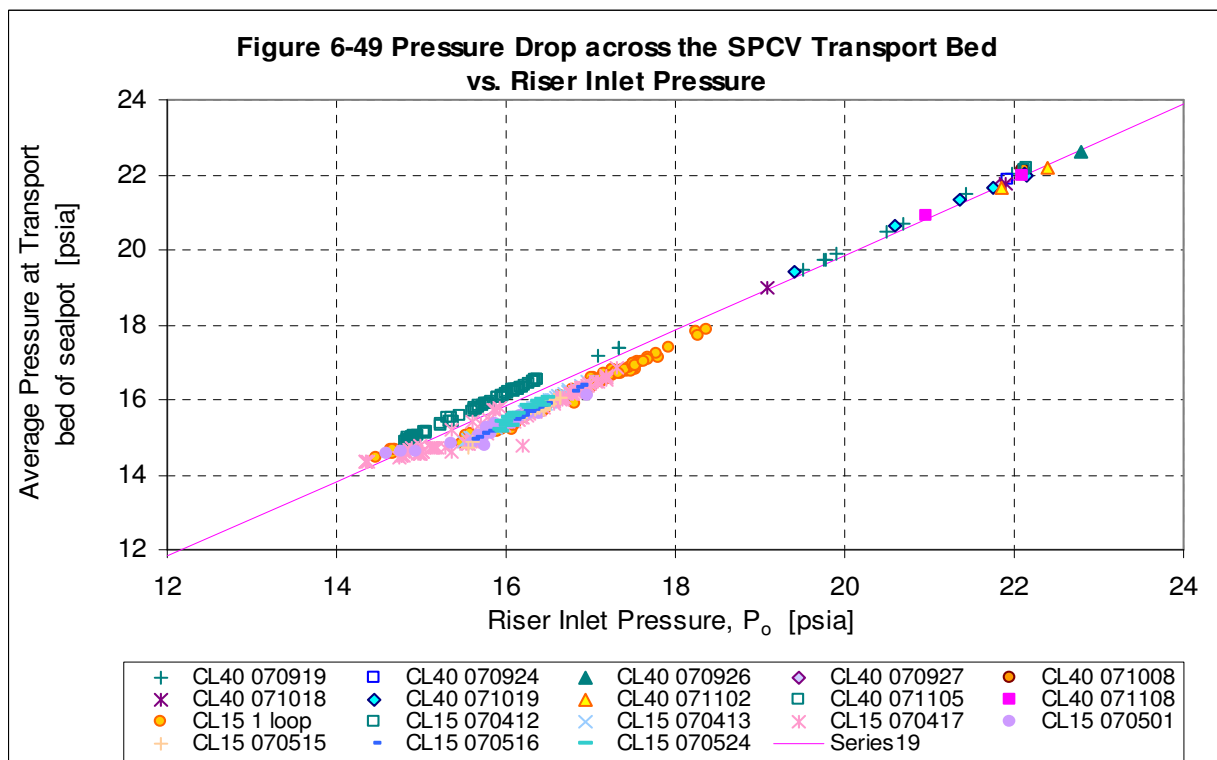
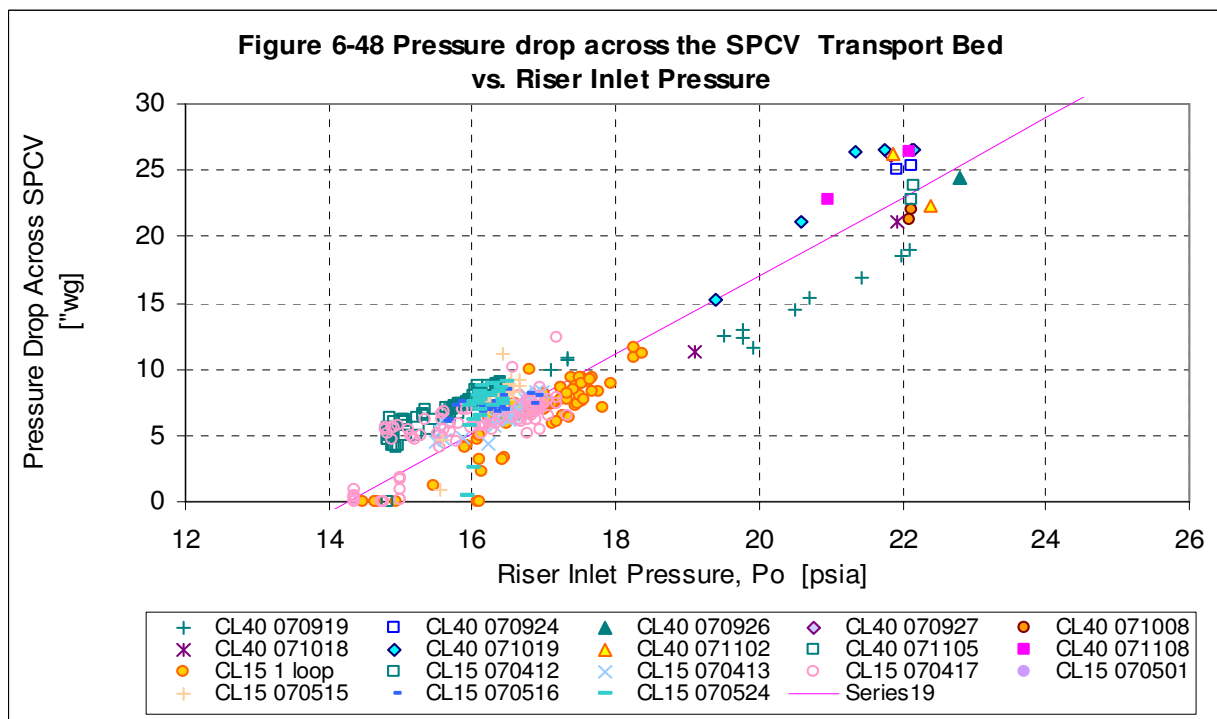
It is interesting to note that in equation (3) the dipleg pipe diameter correlates pressure drop better than the particle diameter as typically used in fixed bed studies. **Figure 6-46** shows that the friction factor based on particle diameter correlates well for each different pipe itself, but pipe size apparently is a factor. This is evident in **Figure 6-46** as data obtained from the 40-ft CFM (6.7 inches diameter) apparently deviates from the performance of the 15-ft CFM (1.5 inches diameter).

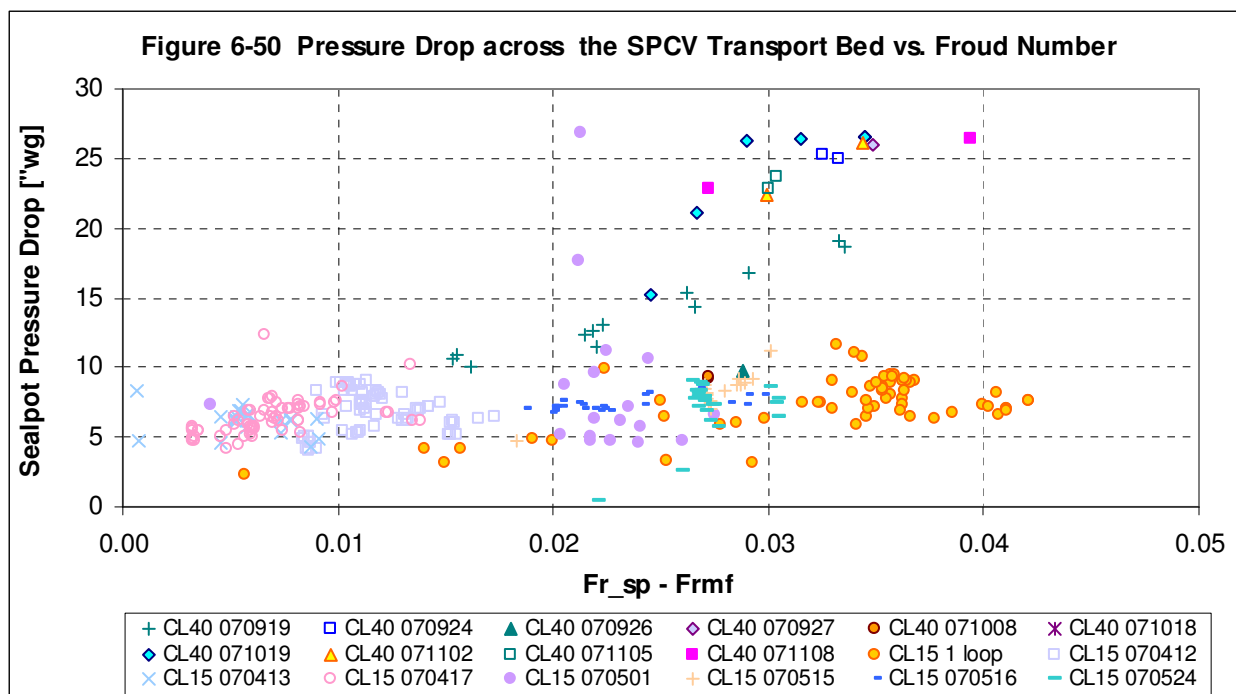


The amount of grease air injected is shown in **Figure 6-47** as superficial velocity along the dipleg elevations.



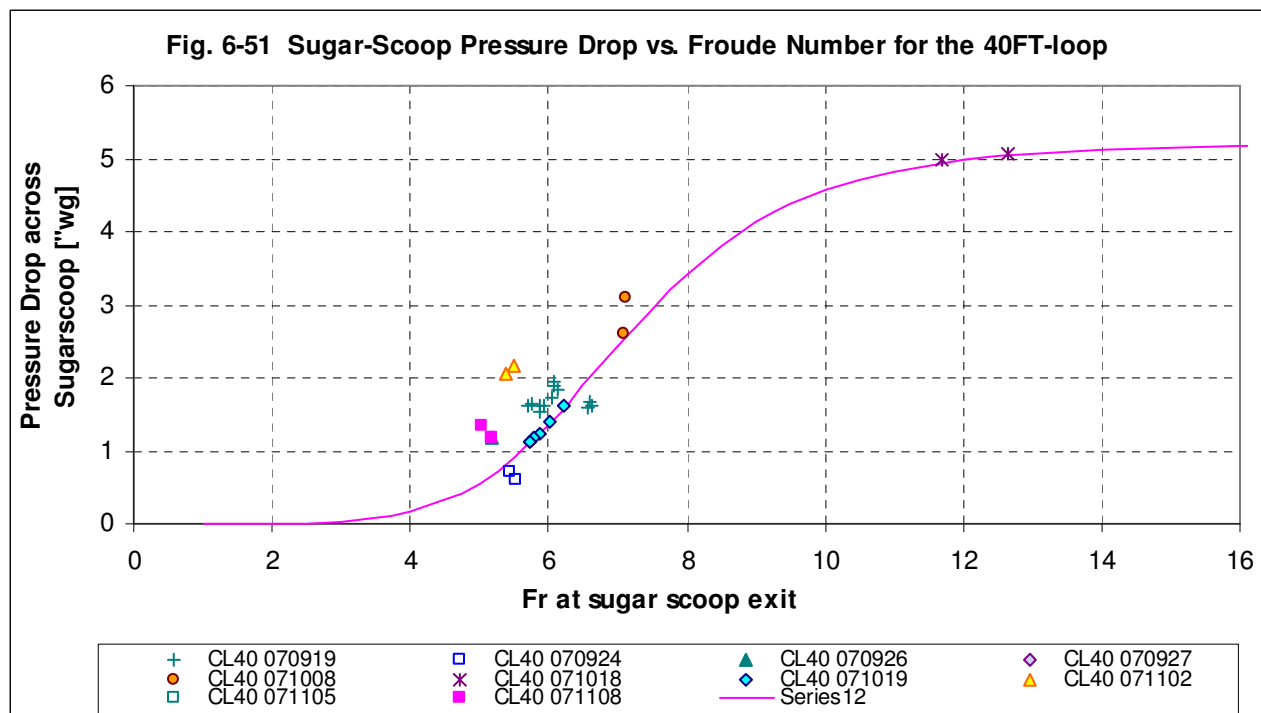
The pressure drop in the transfer bed of the SPCV represents the driving force for discharging solids from the SPCV. This is controlled by the bed fluidizing velocity. **Figure 6-48** shows the pressure drop across the transport bed of the SPCV as a function of the riser inlet pressure. As the fluidizing velocity in the SPCV increases, the bed expands. This increases the solids exit velocity and the pressure at the down-comer leg. **Figure 6-49** shows that the inlet pressure of the SPCV is closely related to the riser inlet pressure. **Figure 6-50** shows the pressure drop across the transport bed of the SPCV as a function of the Froude number for the 40-ft CFM and 15-ft CFM.





### 6.3.3. Sugar-Scoop

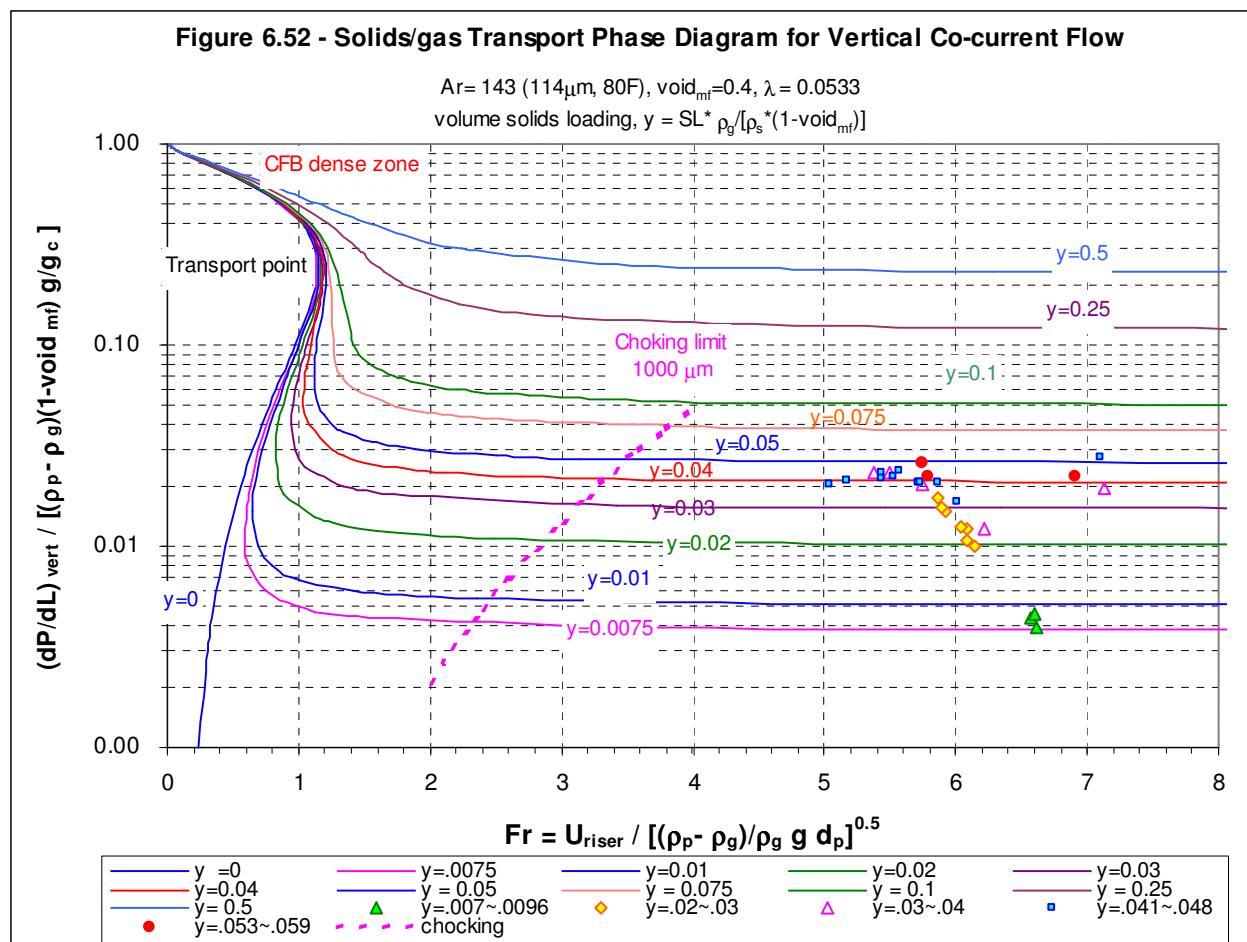
Pressure drop across the sugar scoop increased as the velocity at the riser inlet increased. **Figure 6-51** shows the pressure drop across the sugar-scoop as a function of Froude number based on the riser velocity for the 40-ft tests.



### 6.3.4 Vertical Riser Pressure Drop

The pressure drop in the vertical section of the riser is similar to the typical vertical co-current two-phase problem. In addition to the prediction of pressure drop, a main focus of the CFM tests was to find the choking point which made the pressure drop increase drastically. This can cause stoppage of the solids transport or cause the failure of the SPCV seal.

**Figure 6-52** shows the model prediction vs. test data under different solids loading for a mean particle size of 114 microns with varying Froude number. The test data maps very well in most cases with the normalized pressure drop, Froude number and volumetric solids loading. This solids transport map is essential for scale-up of the prototype design as well as an operational guideline.



The choking limit and the saltation limit of the solids transport in the horizontal leg define the safe region for operation before reaching the limit of solids transport. The actual choking limit was not tested for fear of damaging the test facility due to drastic pressure fluctuation before other test conditions were completed. However, a slip test between

solids and transport gas was later performed and the test facility withstood the impact of the solids during an abrupt shut down of the transport velocity.

As shown in **Figure 6-52**, the operating range can be extended by either reducing the transport velocity until the vertical pipe reaches the choking limit or simply increasing the solids loading by SPCV control until the system pressure cannot support the required pressure drop. These conditions are possible as long as the seal limit in the SPCV can seal against the additional pressure. The volume solids loadings tested ranged from 0.007 to 0.06 for the 40-ft loop. Both the solids loading and riser velocity will be further tested in the future to specify critical ranges of operation.

In an actual application, however, the increase of solids circulation should be evaluated with the performance of the other sections in the loop. For example, the lower leg may reach the solids saltation limit first before choking actually happens in the vertical section. The scaled up unit can be designed with a small pipe to operate at a high solids loading, saving some initial cost. Alternately, it can be designed with a lower solids loading for a lower operation cost but with a higher initial cost.

### 6.3.5 Lower-Leg and Elbow Pressure Drop

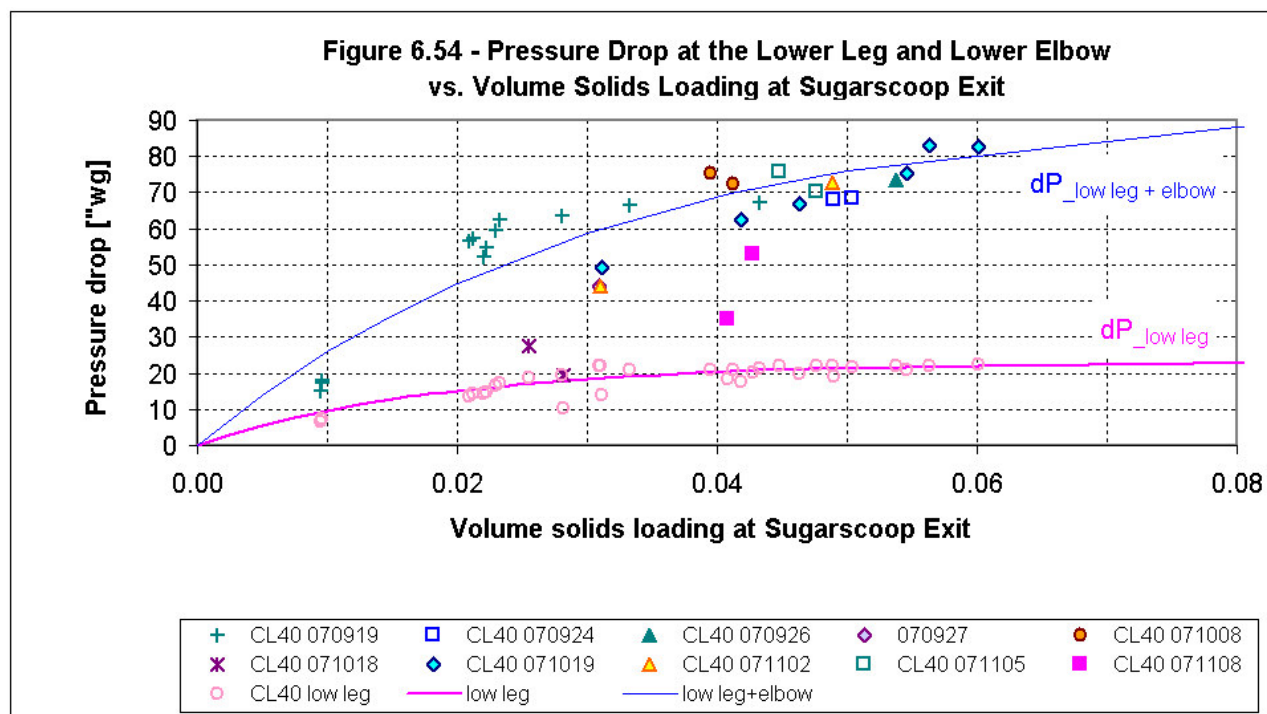
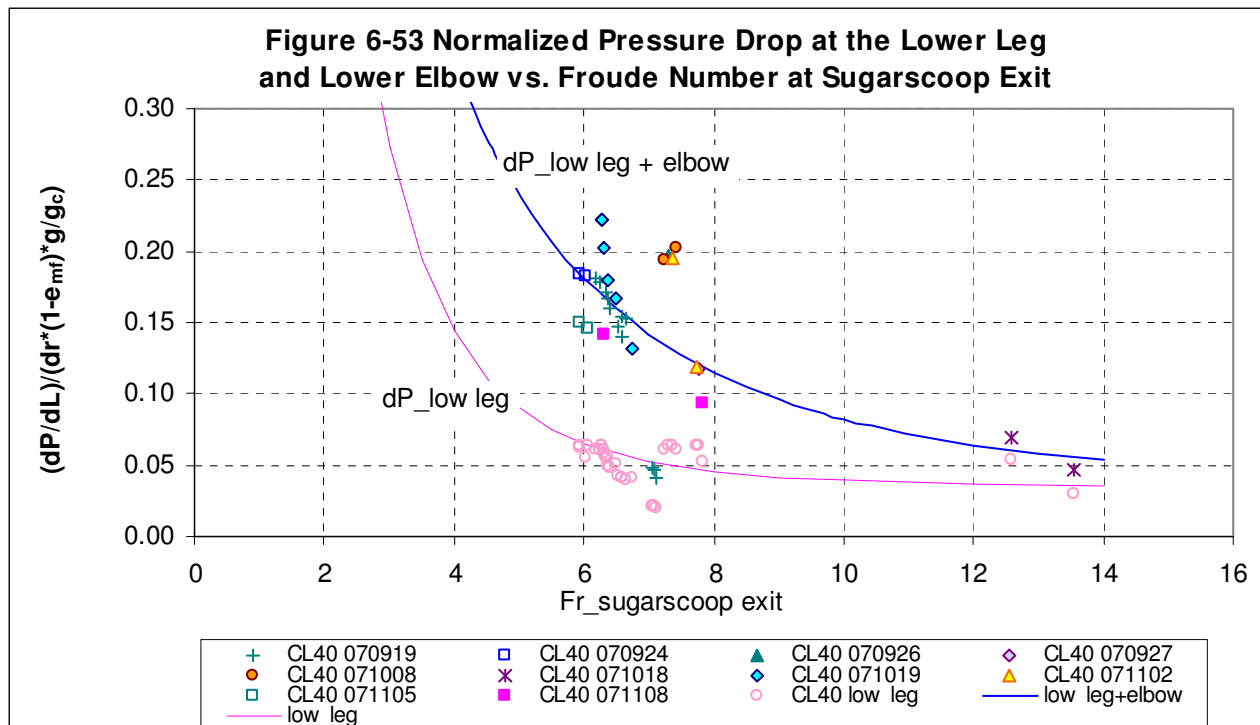
Pressure drop along the lower-leg is similar to the solids flow transport in a horizontal pipe. Test data showed that as the velocity was reduced in the pipe, pressure drop at the lower-leg segment started to increase, probably due to the saltation effect of the large particles along the bottom of the pipe. Once the velocity was near the saltation velocity of the larger particles (about 30 ft/s), solids saltation was observed at the lower elbow turn. The solids slowly built up along the bottom of the lower-leg toward the sugar-scoop, forming a wedged shape.

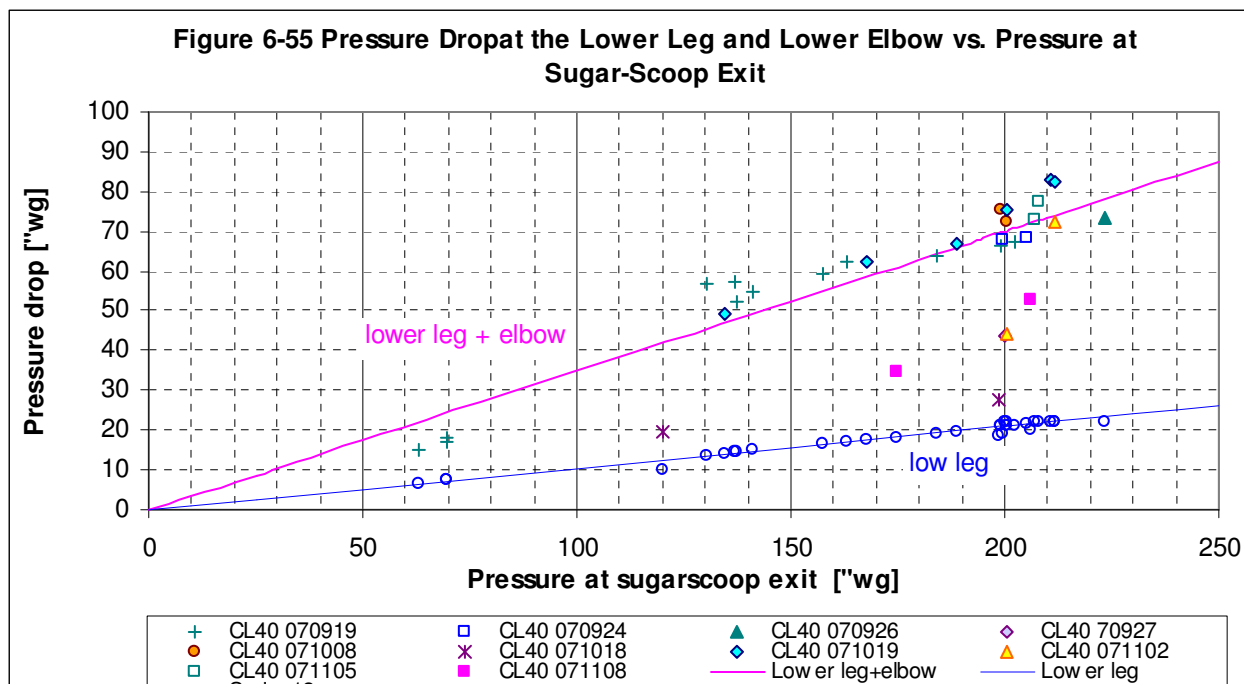
**Figure 6-53** shows the normalized pressure drop of the lower-leg as a function of the Froude number. The sum of the pressure drop at the lower-elbow turn and lower-leg is also shown in the figure.

**Figure 6-54** shows that as volume solids loading increased, pressure drop also increased in the lower leg and lower elbow turn, as expected. It is interesting to note that pressure drop at the lower-leg with a 20° slope increased as solids loading increased, but held at a maximum during all tests. At the same time, the total pressure drop, including the lower-leg and lower-elbow turn, continued to increase as the solids loading increased. This indicates that further pressure drop was added by the closing of the solids passage at the lower elbow turn. Higher solids loading increased pressure drop and built up inlet pressure as shown in **Figure 6-55**. The pressure at the sugarscoop exit increased linearly with the pressure drop for the lower-leg and lower-elbow.

This reflects the observation in tests that solids first started to build up around the turn of the lower-elbow, which left less area for solids to get by. The higher solids build-up around the turn induced higher pressure drop. The lower-elbow turn was probably the most critical element in raising the pressure drop to the saltation limit. Once the saltation

limit condition was reached, the pressure drop was so high that the system supply pressure could no longer support the increased pressure drop. The back pressure induced by saltation could have gotten high enough to over-power the seal design capability.

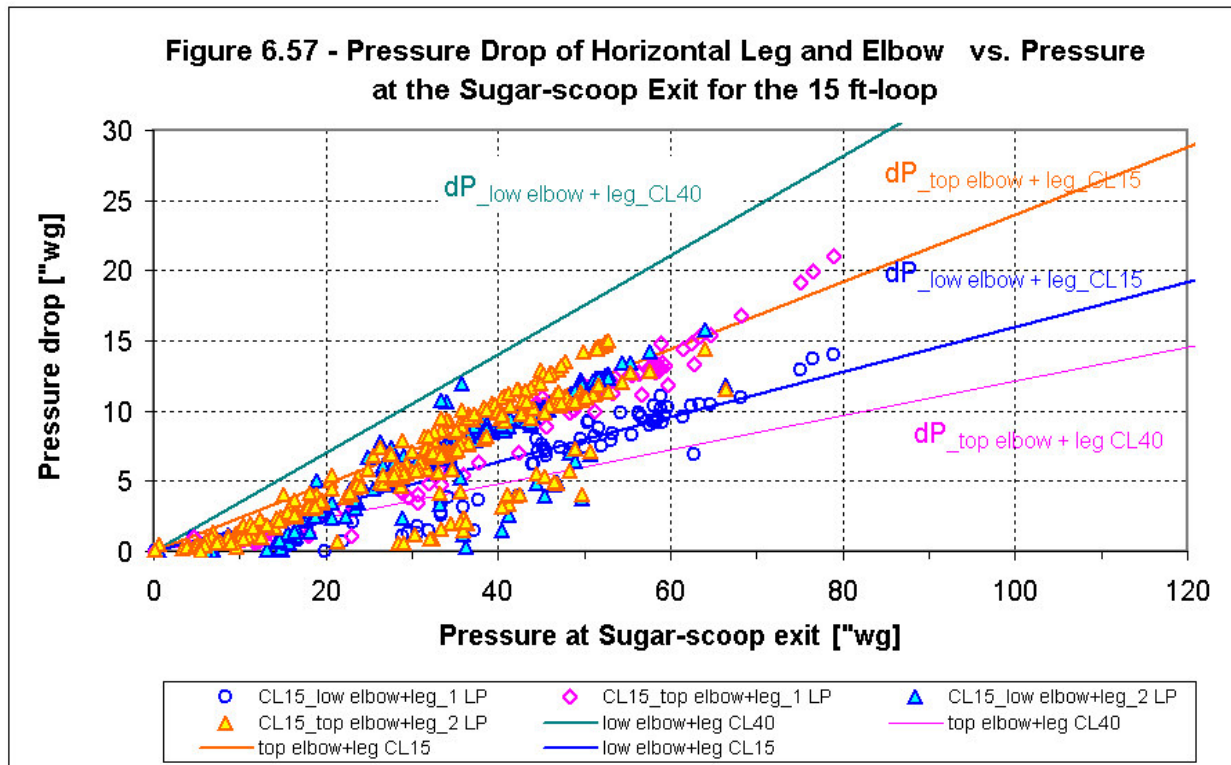
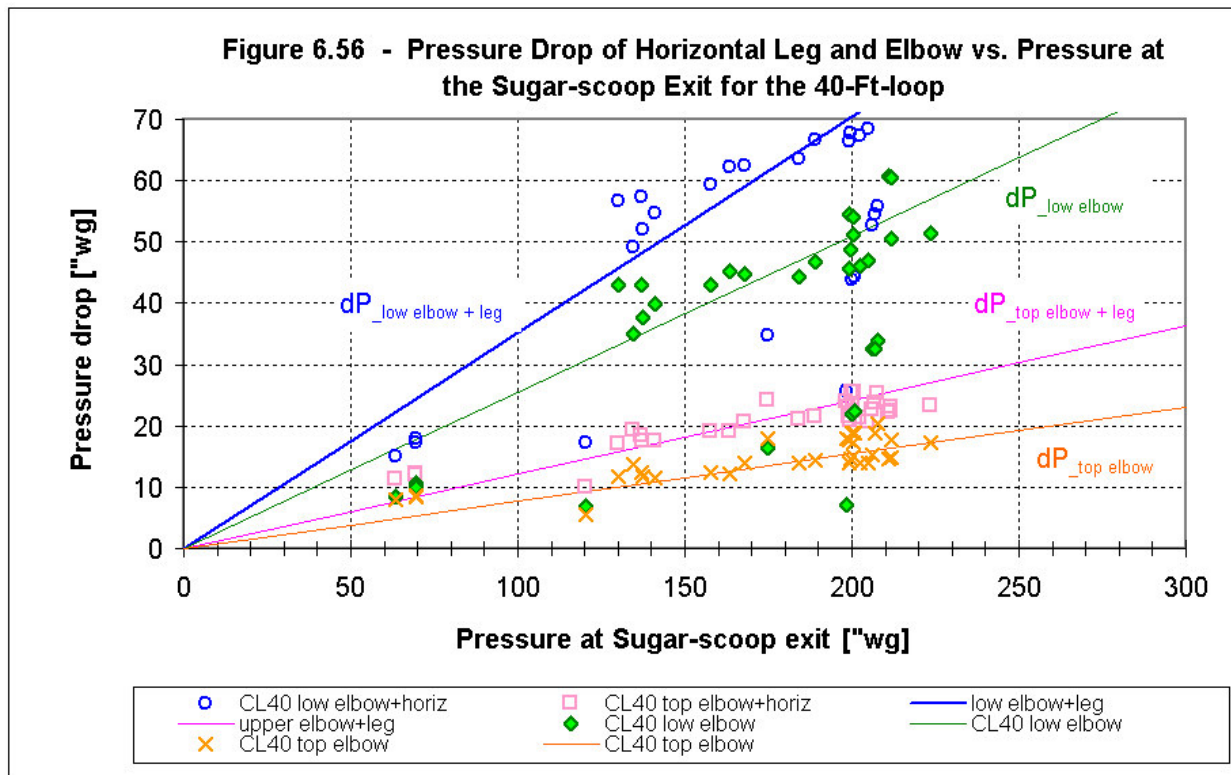




### 6.3.6 Upper-Leg and Lower Elbow Pressure Drop

**Figure 6-56** shows the comparison of the pressure drop at the upper elbow and lower elbow as a function of the pressure at the sugar-scoop exit in the 40-ft loop. The pressure drop at the upper elbow was about 30% of the pressure drop at the lower-elbow for the 40-ft loop testing. This trend reverses the trend in the 15-Ft loop results, which is shown in the **Figure 6-57**. It should be noted that in the 40-Ft loop, the upper elbow goes from a round shape riser to a rectangular horizontal leg, which comes off tangentially to the riser circle. The geometric change from round to rectangular shape seems to reduce the pressure drop. More studies may be needed to find the real reasons. This is unexpected good news in reducing the spent energy for the pressure drop and shall be used in designing the large-scale unit.

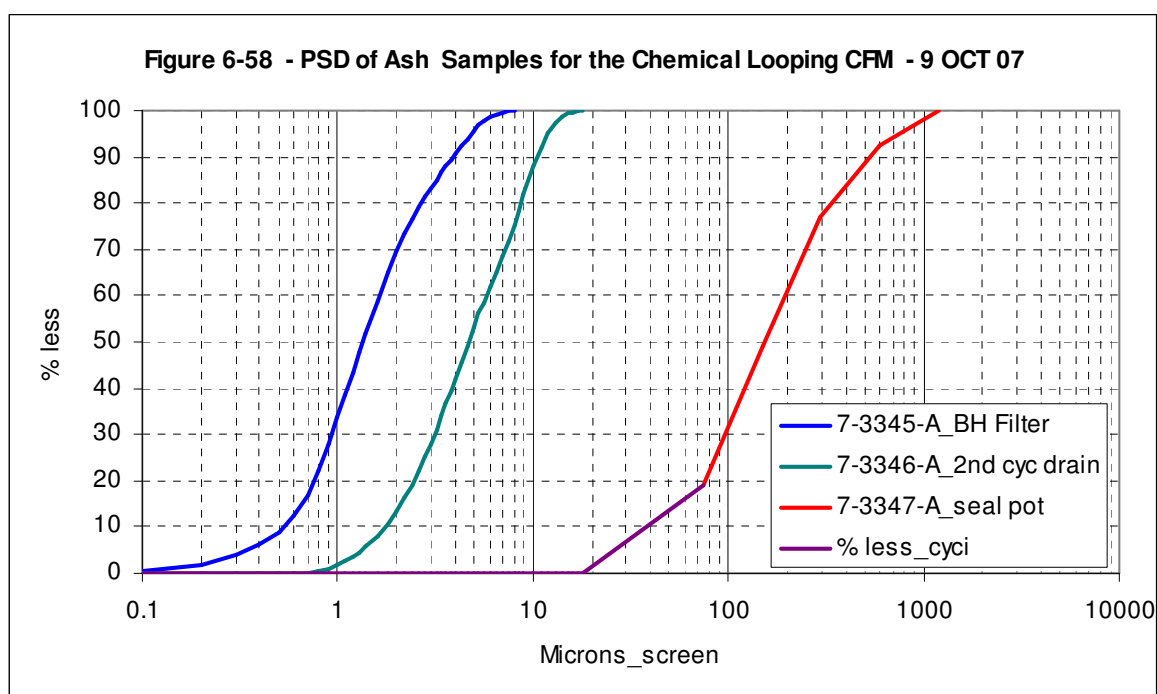
**Figure 6-57** shows a comparison of the pressure drop at the upper elbow and lower elbow as a function of the pressure at the sugar-scoop exit for the 15-Ft loop. The test data from 15-Ft loop (indicated by the symbols in **Figure 6-57**) showed that the pressure drop of the upper elbow was greater than the pressure drop of the lower elbow. For the 15-ft loop case, the upper elbow remains round from the riser to the horizontal leg. The trend of the sum of the pressure drops for the horizontal leg, including the elbow, for the 40-Ft loop, is also shown in **Figure 6-57** to compare with the data from the 15-Ft loop.



### 6.3.7 Cyclone Performance

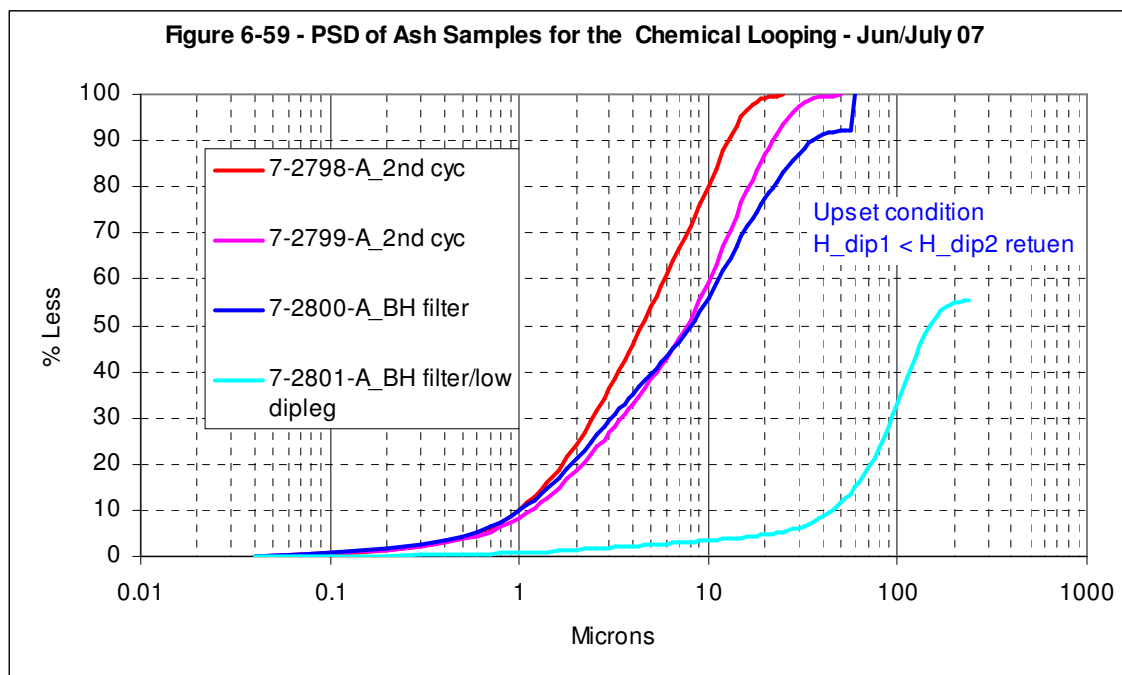
The cyclone for the 40-ft loop has two stages. The cyclone has a very high fractional efficiency for solids separation. When the operating primary dipleg height is above the junction of the secondary cyclone dipleg, the primary cyclone and the second stage cyclone collect all particles with size greater than 7 microns. The particles that escape from the cyclone have a 'd50' of 1.5 microns as collected in the bag-house.

**Figure 6-58** shows the measured particle size distributions (PSD) entering the primary cyclone, captured at the secondary cyclone, and at the bag-house, respectively. All data was obtained by operating the primary dipleg higher than the junction of the secondary cyclone return port in.

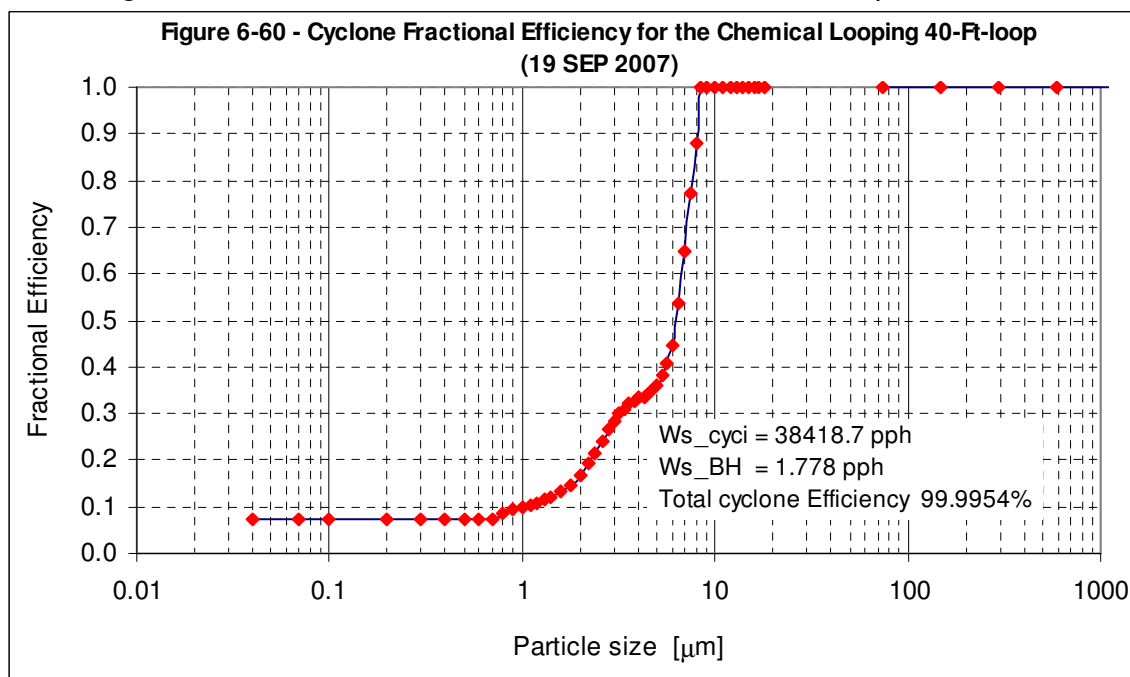


The return leg of the secondary cyclone was designed without a seal in the bottom of the return port. The reason was to find out under what conditions the downward solid flow of the primary cyclone could be maintained without losing solids through the secondary cyclone dipleg. Test results indicated that as long as the primary dipleg solids operating height was above the junction of the secondary return port, the seal was effective. The solids downward flow could be maintained in a steady condition without a seal device at the bottom of the dipleg of the secondary cyclone. Once the operating solids height in the primary dipleg was lower than the junction with the secondary cyclone return, some solids would escape through the secondary cyclone dipleg to the bag-house. **Figure 6-59** shows the measured particle size distribution (PSD) when the CFM was operated with the primary dipleg solids height lower than the junction with the secondary cyclone return leg. As shown in the light blue curve of

**Figure 6-59** some larger particles (greater than 100  $\mu\text{m}$ ) escaped through the secondary cyclone dipleg during upset conditions.



The fractional efficiency of the combined primary and secondary cyclone can be calculated by knowing the ash PSD, solids circulation flow rate and the accumulated bag-house solids weight during the test. **Figure 6-60** shows the typical calculated cyclone fractional efficiency. The total calculated efficiency for this test was 99.9954%. All particles greater than 7 microns remained in the circulation loop.

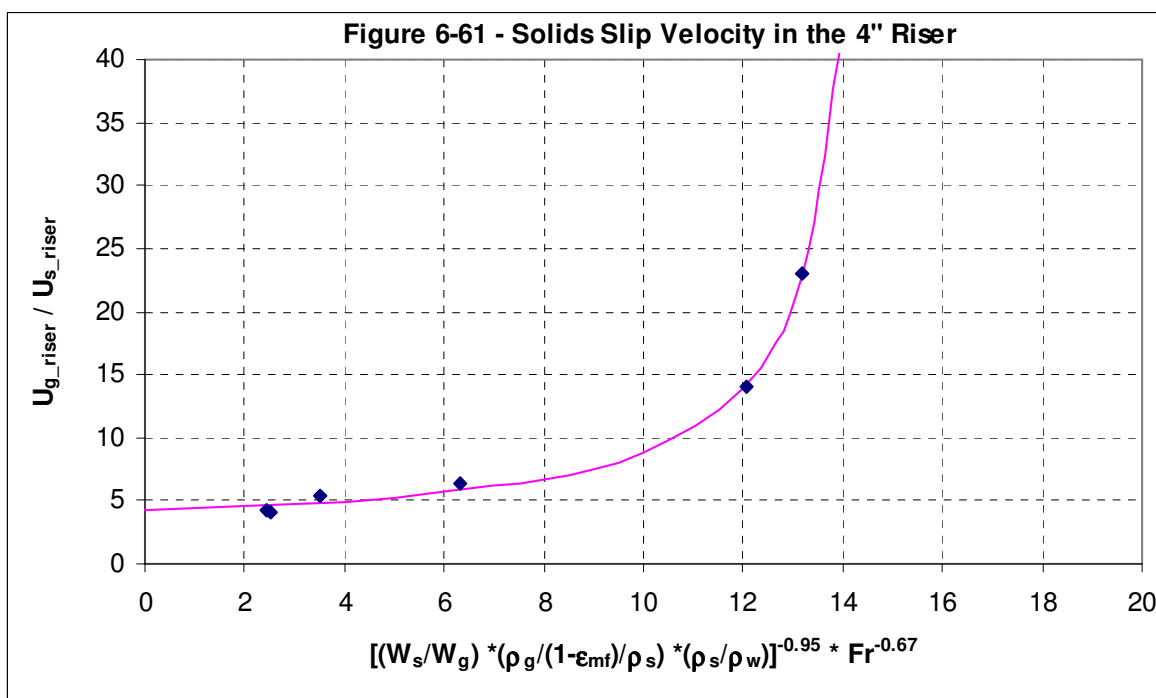


### 6.3.8 Slip between Solids Flow and Gas Flow

It is important to know the slip velocity between gas and solids in the riser. This is essential both for calculation of chemical reactions and for modeling of the solids transport. Because the 15-ft loop has a much smaller margin to test the slip between solids velocity and gas velocity in the riser, the slip velocity was tested only in the 40-ft loop.

Once the 40-ft loop was running in a steady-state condition, the loop was shut down abruptly by turning off all of the supply air at the same time. Solids accumulation at each leg was carefully marked and measured to estimate the solids weight in each location. Solids velocity was then calculated to reflect these accumulations. The plexi-glass loop survived the impact of these up-set operations. This test also provided a close look at loop behaviors during emergency shut down conditions. As expected, the solids column in the riser collapsed and fell to the bottom of the riser and then gradually slid toward the sugar-scoop. The cyclone inlet duct built up some solids. The solids level in the dipleg first dropped, but then rose to stay as the solids weight and momentum in the riser section pushed air backward and eventually through the SPCV upward toward the dipleg. All this happened in a few seconds.

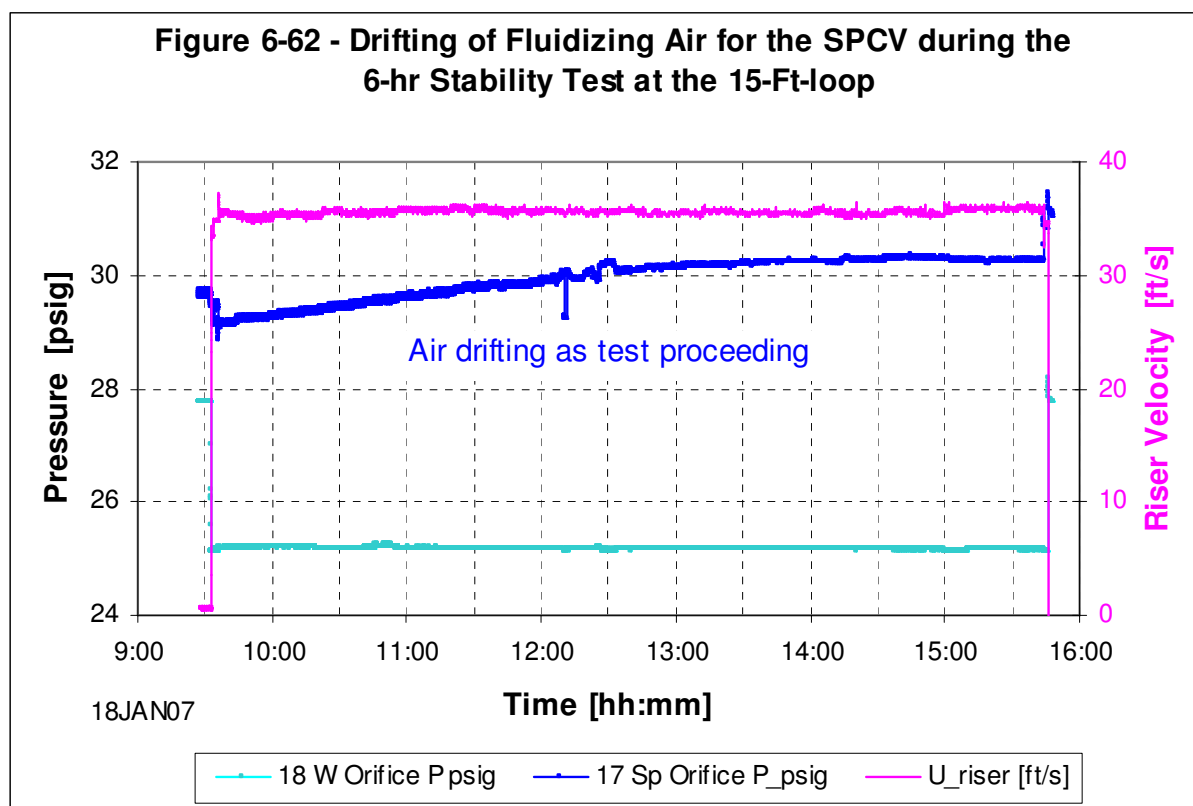
**Figure 6-61** shows the slip velocity ratio, which is defined as the ratio of gas velocity to solids velocity. The slip velocity ratio is correlated with the volumetric solids loading and Froude number. In most of the tested solids transport regions, the velocity slip ratio was about 4 to 5 for the vertical riser section.



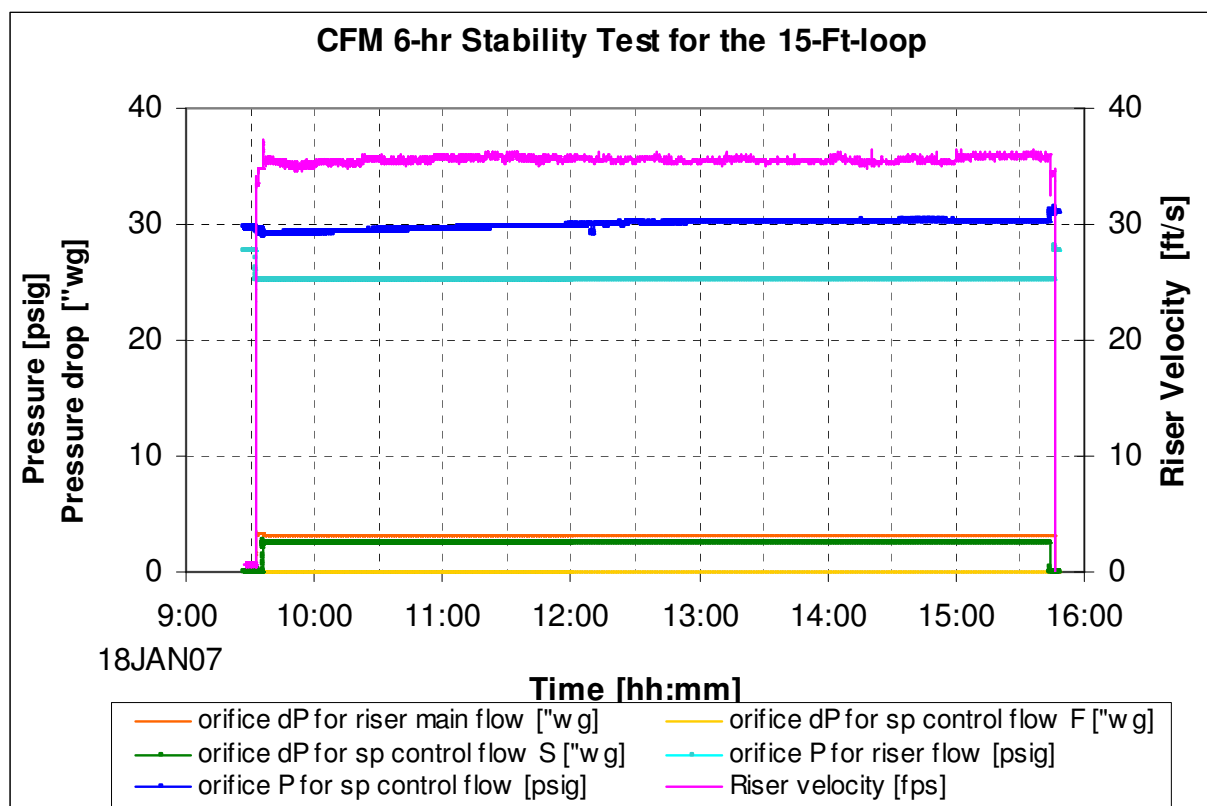
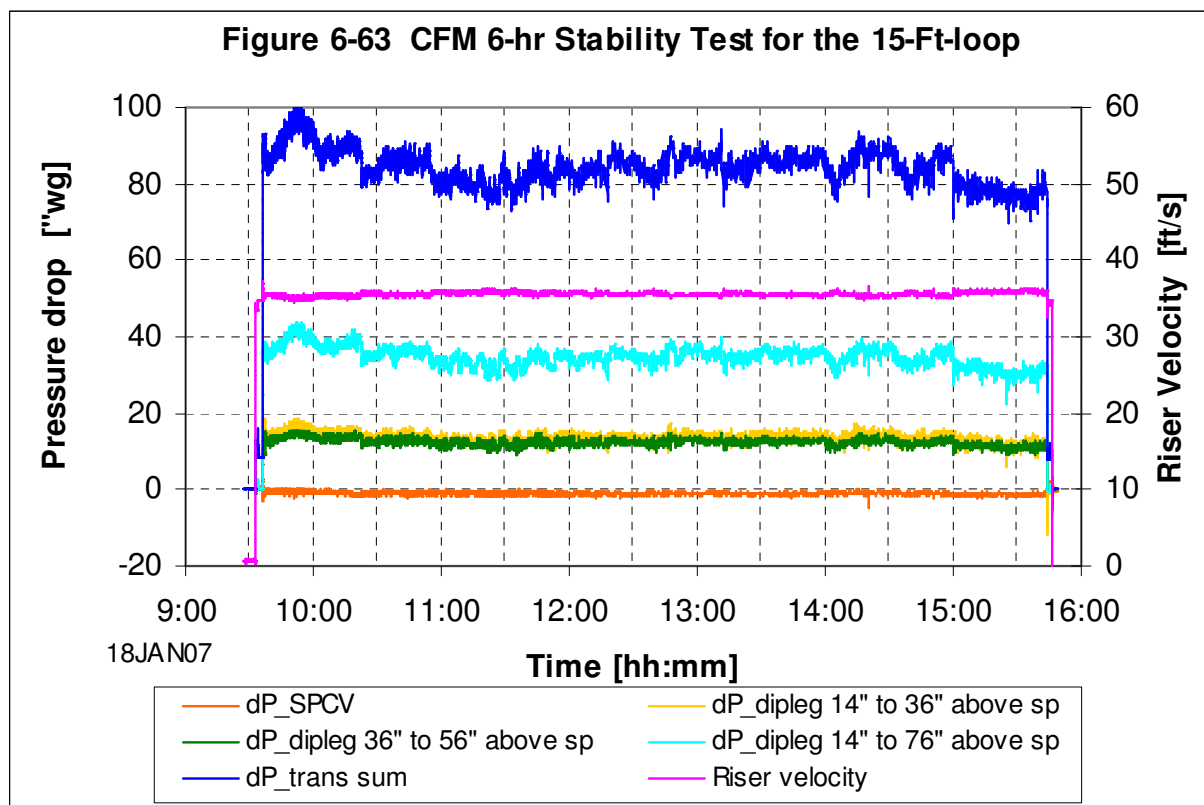
### 6.3.9 Demonstration of Solids Flow Stability with the Seal Pot Control Valve (SPCV)

The fluidizing air supply is critical to the control of the SPCV. The 15-ft loop was run continuously for 6 hours under the given conditions to check the stability of the loop pressure response and solids transfer rate. It was observed that the air supply system for the seal pot control had a tendency to drift over time.

**Figure 6-62** shows the pressure measured at the flow orifice. It drifted from 29.2 psig to 30.2 psig after a 6-hour run. However, the response of the loop was quite steady for the rest of the measured locations. The test proves that the system is robust in keeping solids in stable circulation. **Figure 6-63** shows the operating conditions and the corresponding pressure response in the transfer leg and seal leg. As shown, the dipleg seal pressure was stable during the 6-hour test, which means the solids transfer in the circulation loop was steady. The riser velocity was stable. The sum of the transfer leg pressure drops from the sugar-scoop to the cyclone exit varied about  $\pm 5$  "w.g., which was considered acceptable.



The segregation of large particles in the bottom of the seal pot may contribute to the drifting of supply air pressure at the measuring orifice. This phenomenon was eliminated in the 40-ft loop design with the proper angle on the seal pot wall and modified air supply system. The unstable air supply system was further studied and later modified successfully in the 40-ft loop testing.



### 6.3.10 Dual Loop Operation

The 15-ft loop was set up to simulate the operation of three cases: 1) independent two loop operation without solids exchange, 2) constant exchange of solids flow between the two loops and 3) biased solids flow from one loop to the other loop.

**Figure 6-64** shows one of the typical tests. As shown in **Figure 6-64**, the pressures of the two loops from the SPCV bottom to the discharge port of the other loop remained relatively steady (green and pink curve). The pressure drop of the dipleg for loop A and loop B were also shown to reflect the level of solids flow in the dipleg for each loop.

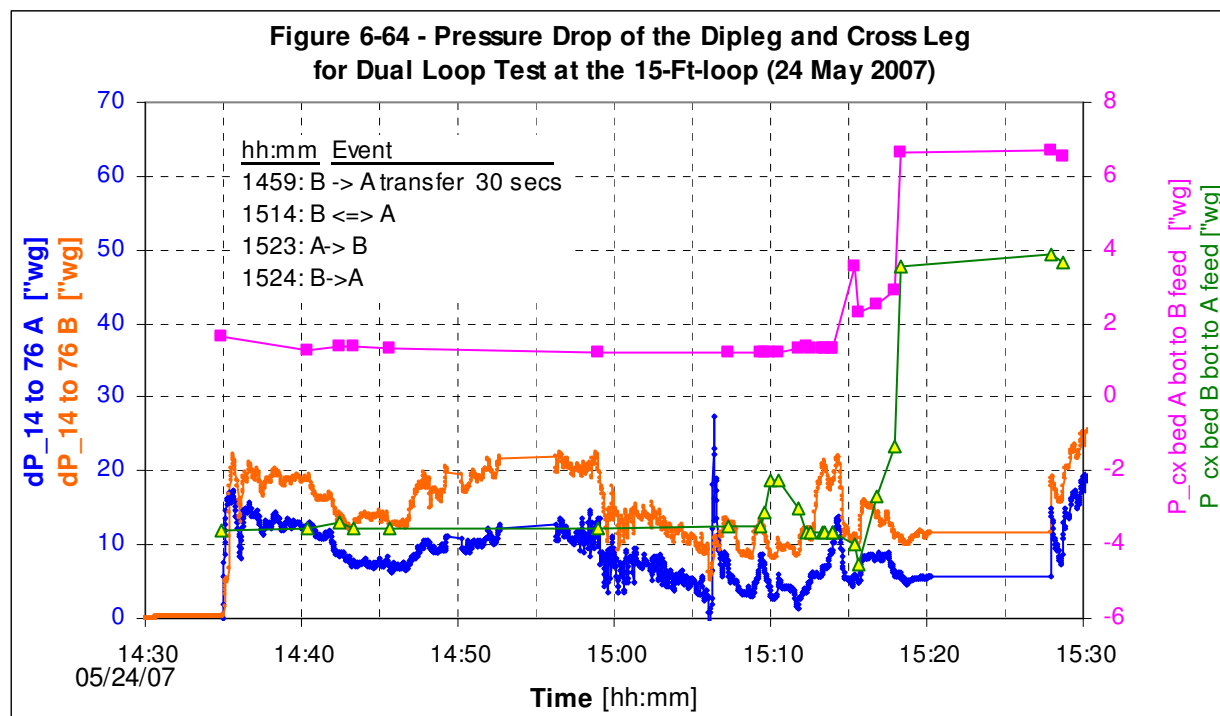
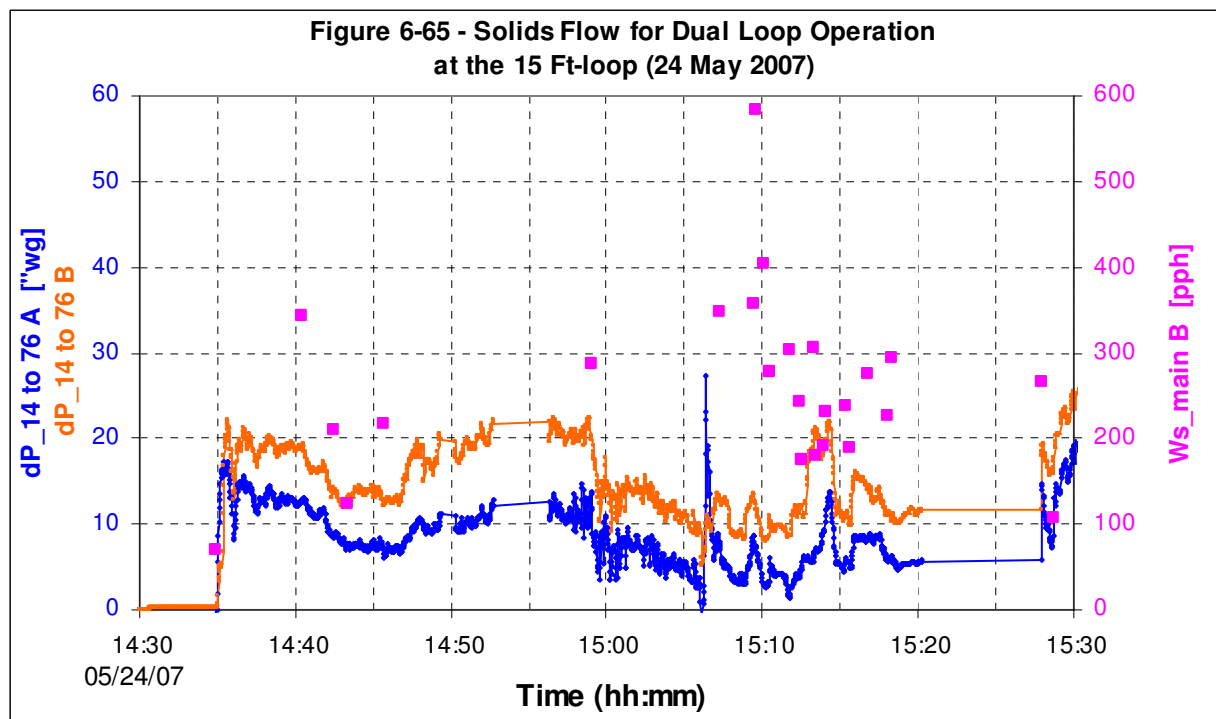


**Figure 6-65** shows the solids flow measured by the laser probe during the test in the B loop. Lower pressure drop along the dipleg and hence lower solids level means, more solids were circulated in the riser vertical section. Therefore, a higher solids velocity (higher solids flow) was measured in the dipleg. This solids measurement was made with a sampling cycle of about 60 seconds per averaged value.



## 6.4 Scale-up

The most critical issues for scale-up in the design of solids transport are:

- Solids saltation in the horizontal sections and elbow turns
- Solids choking in the vertical section
- Seal capability and height of the seal leg
- Solids/gas separation

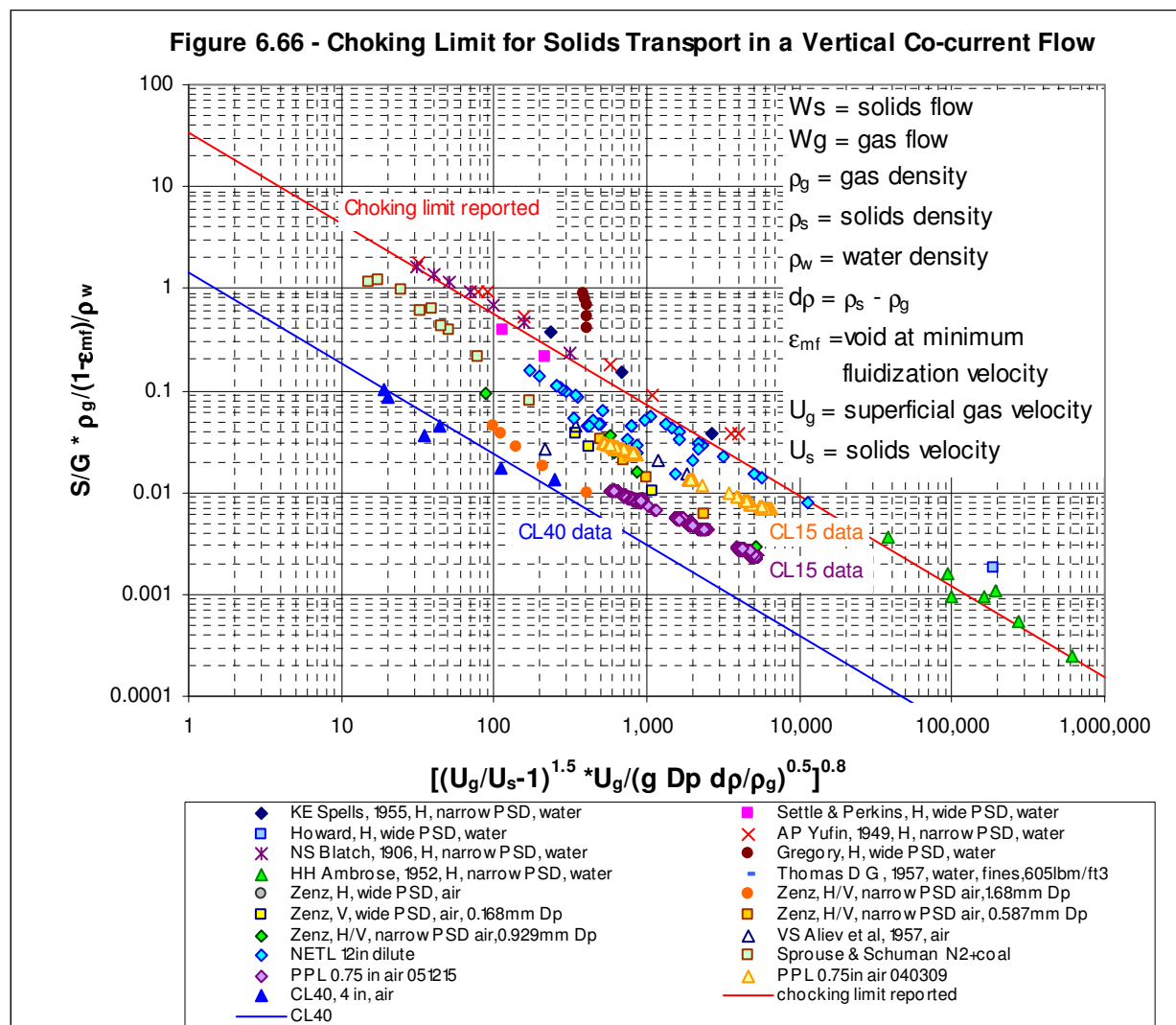
Saltation and choking of solids can cause a sudden increase in pressure drop and therefore cause the solids flow to collapse if the supporting power is not designed correctly. This can happen when the system is operating with a higher transport media flow. This makes the pressure drop too high and it exceeds the seal capability. The system can also be operated with too low a transport velocity. This can result in solids saltation in the horizontal leg or choking in the vertical riser. The solids induced saltation or choking eventually causes a sudden increase in pressure drop. The volume solids loading can simply be too high for the transport system. In addition, solids and gas separation is closely related to the conservation of solids inventory, so the cyclone performance must be integrated into the system design.

All of the above technical issues should be considered together as a system and need to be checked against the requirements for the chemical reactors, the cost of auxiliary power, and the initial cost of the equipment.

The solids loading data for the vertical section obtained from the 15-ft loop and 40-ft loop are compared to published data from the literature as shown in **Figure 6-66**. To

make a meaningful comparison, the sealing capability of the systems tested for the reported data needs to be included to distinguish the sealing limits or pressure drop limits. Some of the referenced data was tested in near choking conditions, where pressure drop increased dramatically due to a small change in velocity for the vertical co-current flow. **Figure 6-66** indicates that solids loading could be further increased for the vertical section of the 40-Ft loop, before reaching the choking limit, provided the seal leg could still maintain the seal. The 15-Ft loop was actually operated very close to the choking limit. This also explains why the 15-Ft loop was more sensitive to the operating conditions and easier to up-set solids circulation.

For the future choking tests, the limiting value of solids loading and their corresponding pressure drops will be tested. Under the choking conditions, the loop transport system including the lower, upper and vertical legs will be examined against the seal capability of the dipleg and the operating conditions in the seal pot control valve.





## **7. PDU Testing**

### **7.1 Chemical Looping Phase III Automatic Controls Feasibility Study:**

The areas of Automated controls investigated in Phase III are:

1. Inter-Loop Pressure control
2. Process Temperature Trim of Injection Air control
3. Solids Transport Rate control

#### **7.1.1. Automated Control Testing Area Definition:**

##### **Inter-Loop Pressure control**

A two-part control design was developed for pressure control. The first part was to vary the speed of the reducer vacuum pump using a Proportional-Integral-Derivative (PID) controller to control the reducer outlet pressure to a set point. In the second part, the oxidation loop pressure control was slaved to the reducer pressure using a reducer loop-to-oxidizer loop differential pressure measurement at the crossover elevation. Loop pressure equalization was achieved by having a set point of zero for the loop differential variable.

##### **Process Temperature Trim of Injection Air Control**

In order to maintain the correct process stoichiometry, the solids velocity in the loop vertical riser and reaction residence time must be kept constant. In order to keep the solids velocity at a constant value the injection airflow rate must be adjusted to account for the gas density change caused by changes in the process temperature. The main injection airflow trim adjustment was set based on a function of reactor process temperature.

##### **Solids Transport Rate Control**

Individual loop solids recycle flow for each reactor is achieved by introduction of transport and fluidizing air into the recycle chamber of the SPCV. Crossover flow between reactors is achieved similarly by introduction of transport and fluidizing air into the SPCV crossover chamber.

The user selects the reducer to oxidizer solids crossover rate. The oxidizer to reducer crossover rate is set based on a user specified loop inventory ratio. This inventory ratio will be based on the ratio of the reducer riser differential pressure to the sum of reducer and oxidizer vertical riser differential pressures. This differential pressure ratio is used as the oxidizer crossover flow controller set point.

#### **7.1.2 Initial Control Loop Tuning**

As part of the automated control feasibility testing, a course of loop characterization tests were performed. These tests were conducted in order to develop the PID loop tuning parameters. Step response testing was performed as the primary system identification tool. PID parameters were selected based on response time and overshoot requirements for each controlled process variable. The following are observations from the loop tuning activities.

### **Automated Pressure Control**

1. Repeatable loop pressure curves were developed at each flow rate. Pump speed was restricted to the pump inlet vacuum manufacturer's limit.
2. The proportional constant of the reducer loop PID controller was derived from analysis of the pressure response to changes of injection flow rates.  $K = -0.020$ .
3. A map of the inter loop differential pressure (PDT 2247) versus oxidizer vacuum pump speed was developed.
4. Performed the initial tuning of the oxidizer vacuum pump PID loop to hold loop-to-loop differential pressure at zero. The proportional constant of the PID algorithm was manually derived.  $K = 0.0001$
5. Additional tests indicated that the first oxidizer controller proportional value produced a response that was too slow. This was corrected by changing the proportional constant to  $K = 0.0005$ .
6. After setting the oxidizer PID values, the reducer tests were repeated to assess loop interactions. The final reducer proportional gain value was  $K = 0.01$ .

### **7.1.3. Chemical Looping Automated Process Control Feasibility Tests**

The chemical looping process automated control feasibility testing areas were:

1. Inter-Loop Pressure Control
2. Process Temperature Trim of Injection Air Control
3. Solids Transport Rate Control

A description of each test conducted and the results observed are provided.

### **Automatic Loop Pressure Control Tests (Air Flow Only)**

Six pressure control tests were conducted between September 25<sup>th</sup> and 27<sup>th</sup> 2007 in order to establish the feasibility of using dedicated vacuum pumps, one per loop, to control the PDU pressure.

All of the tests were conducted without any solids flow (air flow only). Each SPCV was filled with solids but no solids were recycled. It was necessary to keep solids in the SPCV to keep the gas flow from short-circuiting the riser.

Collectively, the automatic pressure control tests were conducted to generate test data to establish the feasibility of reliable automatic loop pressure control of the PDU facility.

### Automatic Loop Pressure Control Implementation

The automatic pressure control strategy utilizes two loop controllers to achieve the goal of maintaining the two loops at the same pressure.

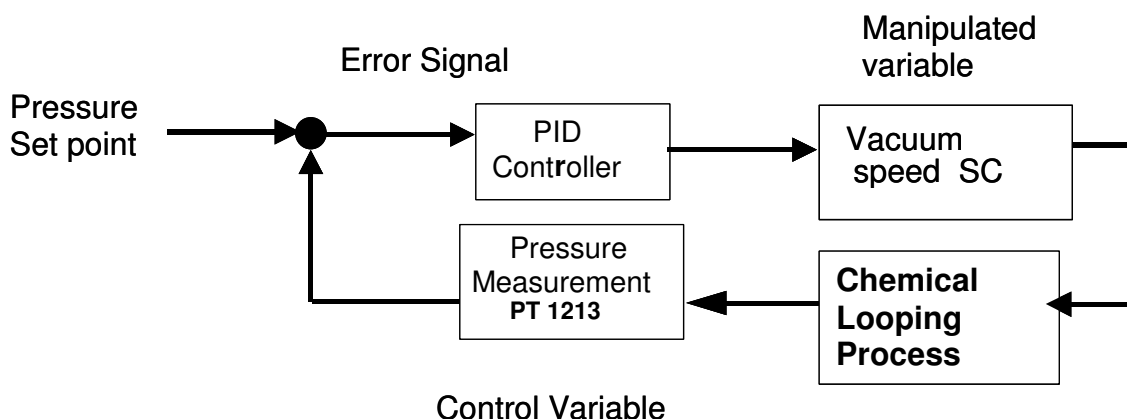


Figure 7-1 - Reducer Pressure Control PID Loop

The reducer loop pressure controller maintains a set point pressure (psia) using the reducer loop pressure (PT1213), as the control variable. The reducer vacuum pump speed controller (SC2425) is the manipulated variable, **Figure 7-1**.

Inter loop pressure equalization at the loop crossover elevation is achieved by having a set point of zero for the oxidizer loop PID controller. The differential pressure between loops (PDT 2247) is the control variable and the oxidizer loop vacuum pump speed controller (SC2416) as the manipulated variable. Manipulation of the oxidizer vacuum pump speed moves the oxidizer loop absolute pressure to track the reducer loop pressure at the solids crossover elevation. The control objective is to control the differential pressure between loops to within  $\pm 3$  " H<sub>2</sub>O (0.1 psia).

The automatic pressure PID controllers used for reducer and oxidizer loops are detailed in **Figure 7-2**. The reducer controller uses an absolute pressure transducer PT 1213 as the control signal. In order to keep the two loop absolute pressures as nearly identical at the critical solids crossover elevation, the oxidizer control sensor was chosen to be a high-resolution narrow range differential pressure sensor, (DPT2247). This differential pressure sensor has a narrow differential pressure range ( $\pm 10$  " Wc).

By measuring the inter loop differential pressure with a narrow range pressure transducer the oxidizer loop differential pressure set point can be set to zero keeping the two loop pressures very closely matched at the PDT 2247 elevation.

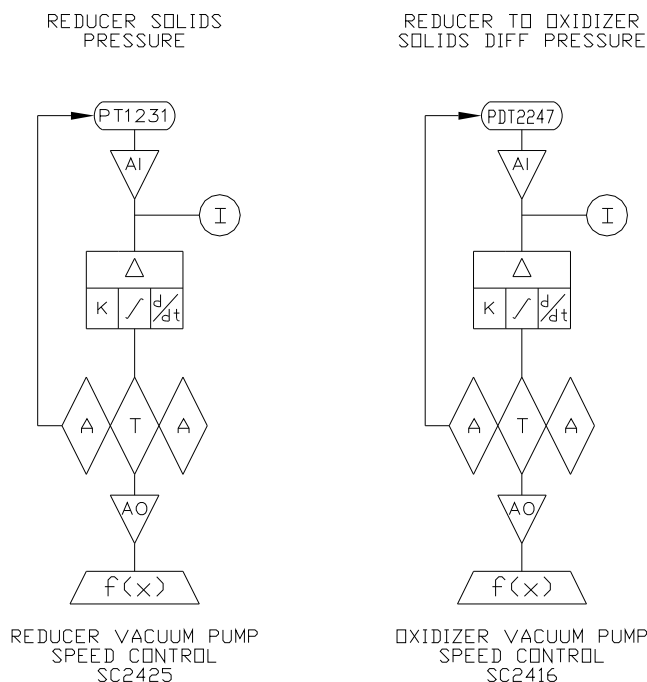


Figure 7-2 - PID Controllers for the Reducer and Oxidizer Pressure Control

## Automatic Loop Pressure Control Tests

### Load Ramp Rate Test (September 26<sup>th</sup> 2007 @15:30)

The test objective was to evaluate the stability of the automatic pressure control using injection air as an indicator of load change. The injection airflow steps were ten standard liters per minute (10 SLPM). Each step was nominally a 10% load change.

### Load Ramp Rate Test Results

As seen in **Figure 7-3**, the oxidizer and reducer loop vacuum pumps were able to maintain the two loops at the same balanced absolute pressures during the test when the loop injection air (riser air) was changed at 10 SLPM per minute. This injection airflow change would be required in the event of a 10 % load change. Stable pressure control was achieved through a load (injection air) change of 10%/min.

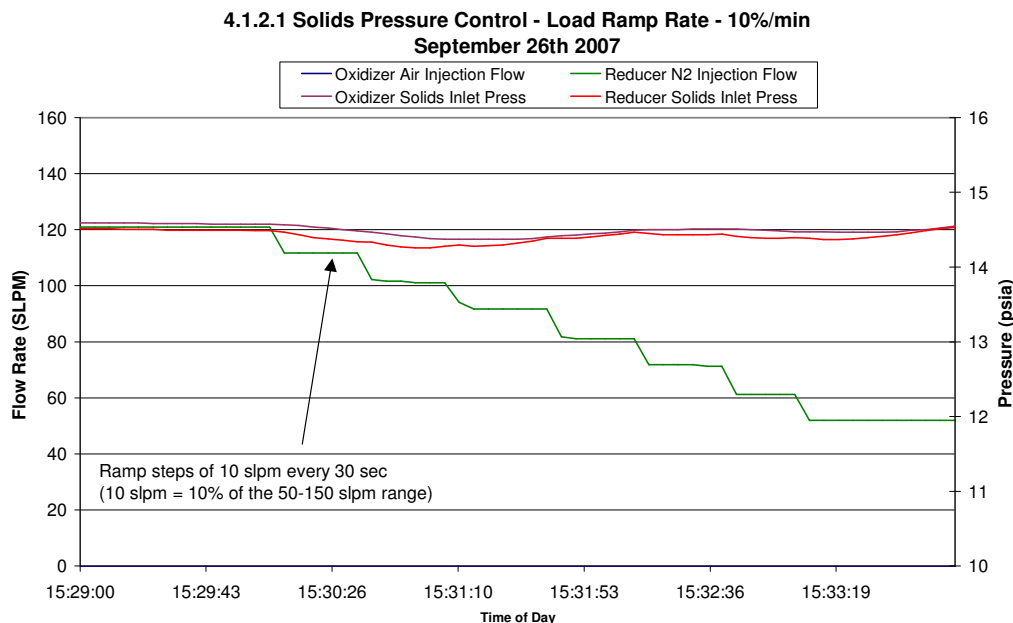


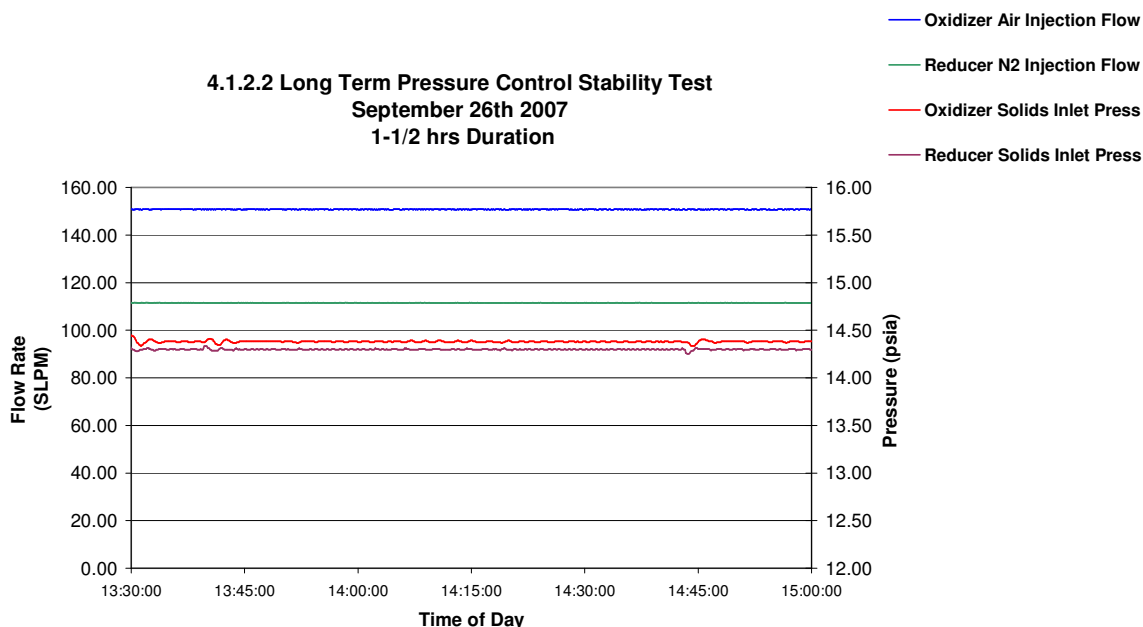
**Figure 7-3 - Oxidizer and Reducer Loop Pressure during load ramp test**

### Long Term Stability Test (September 26<sup>th</sup> @ 13:30)

With both loop injection airflow rates constant and the loop pressure controllers in automatic, this test evaluated the longer-term performance stability of the two, automatic loop pressure controllers.

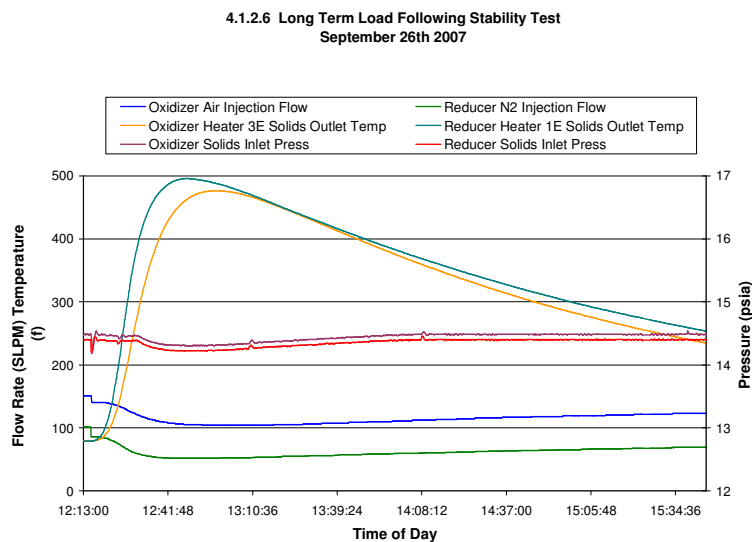
### Long Term Stability Test Results

As presented in **Figure 7-4** both of the loops (oxidizer and reducer) were maintained at their set point values for a 2-hour period under automated control. For this air only test, the reducer loop pressure and the oxidizer loop pressure controllers both worked correctly to maintain both loops at their set points for the entire test period.



### Load Following Stability Test (September 27<sup>th</sup> @ 15:20)

For this test, the process temperature was utilized as the load change variable. A process temperature change produces an injection air change (see test 4.2). This test was used to assess the loop pressure controllers' performance while the process temperature was trimming the injection airflow rate. (**Figure 7-5**)



### Load Following Stability Test Results

During this test the process temperature was changed in the range of 80-500°F. This resulted in an injection air trim to for each loop. During both the process temperature increase and decrease, the loop pressure controllers maintained the loop pressures at their set point values.

## Loop Pressure Disturbance Recovery Test

This test evaluated the response of the oxidizer loop pressure controller to a step change in the reducer loop pressure set point. This test also introduced two reducer injection airflow step changes. Both loop pressure controllers were in automatic.

## Loop Pressure Disturbance Recovery Test Results

The oxidizer pressure set point was held at its set point in the presence of a disturbance caused by a set point change to the reducer loop pressure, **Figure 7-6**. Both loop pressure controllers held their set point values during a disturbance caused by a change in injection flow rate.

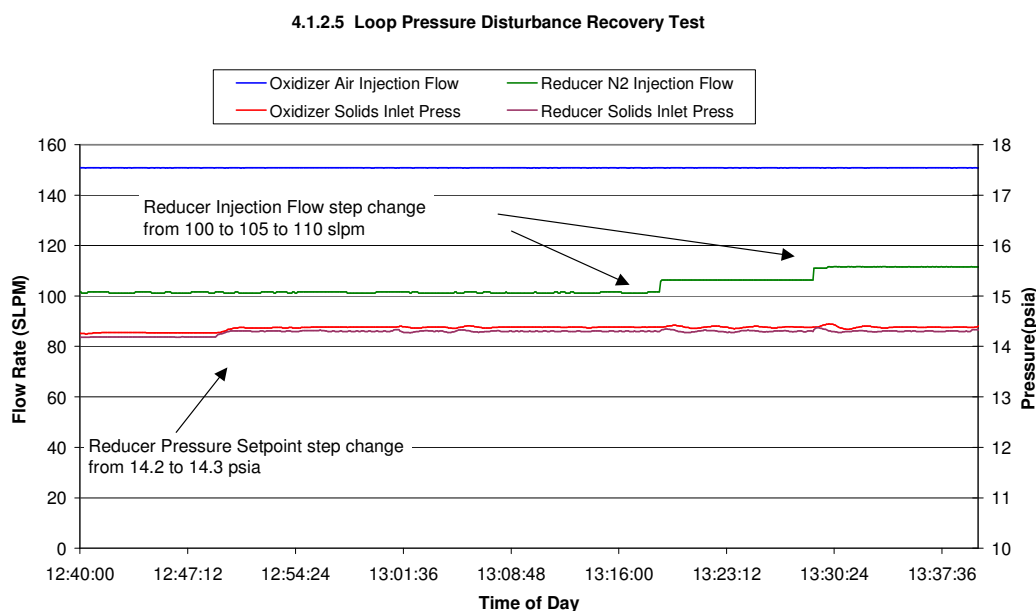


Figure 7-6 - Loop Pressure Disturbance Recovery Test

## Shutdown Pressure Control Test (Sept 26<sup>th</sup> @ 16:30)

Loop pressure control must be maintained during the shutdown of the process. Solids transport shutdown for the PDU consists of ramping the two vacuum pumps down while maintaining the zero inter-loop differential pressure. When the vacuum pumps are at their minimum speeds, both vacuum pump bypass valves are opened. The injection air that remains on for a short time sweeps any inadvertent solids flow that might occur as

a result of the opening of the vacuum pump bypass valves out of the two flow circuit risers. Finally, the injection air is stopped and the solids shutdown is complete.

## Shutdown Pressure Control Test Results

Automatic pressure set point controls were used to successfully shut down the process without pressure excursions, **Figure 7-7**. The shutdown concept was to use the automatic pressure control loop (which controls vacuum pump speed) to bring the vacuum pump to their minimum speed shutoff.

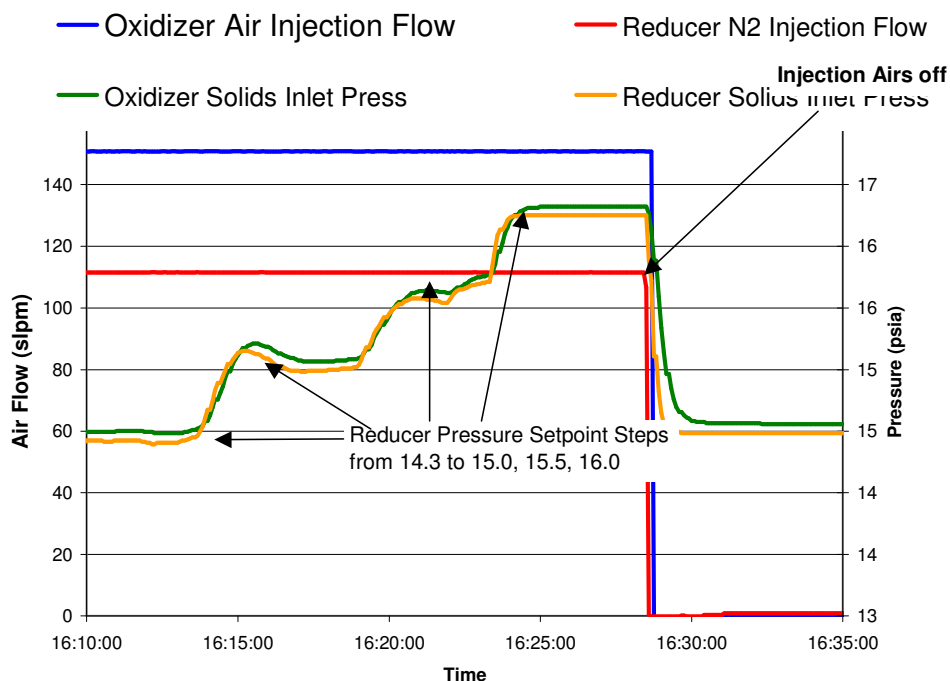


**Figure 7-7 - Shutdown Test Loop Pressures**

The shutdown test was initiated from the point where there were no crossover or recycle solids flow, main injection airs to both loops were on and both vacuum pumps were in automatic, commanding a 14.3 psia solids pressure in both loops. The reducer solids pressure set point was stepped from 14.3 to 16 psia. The automatic pressure controls held the loop-to-loop differential pressure at the zero set point. At the final 16-psia set point, the vacuum pump speeds were low enough that the pump bypass valves could be opened without pressure excursions. With bypass valves open, the main injection airs remained on for a final loop solids sweep out and then turned off. **Figure 7-7** shows that there was no inter-loop pressure imbalance during the set point changes and the PDU was shutdown without a single significant inter-loop differential pressure event.

## Process Temperature Trim of Injection Air Control

The primary control variable of the riser injection air is the unit load (steam demand or MWe) set point. In order to control the solids velocity within each reactor riser the individual loop process temperature further trims the injection air mass flow. Using a control function block, the individual loop process temperatures generate the adjustment trim for the injection air mass flow rate. During this test, both the injection airflow trim control and the loop pressure controls must both be in automatic mode. The loop pressure set points must be maintained while the injection air flow rate is modified by the process temperature changes.

## Injection Air Trim Control Implementation

For both the oxidizer and reducer loops, a function block for process temperature to injection air mass flow rate trim was implemented. Using a power series function, the individual loop riser temperature (TE2008 reducer, TE2025 oxidizer) generates a loop temperature based trim for the injection air mass flow rate, which is input to the mass flow controllers (FCV 1413 reducer and FCV 1421 oxidizer).

## Injection Air Trim Control Results

Changes to the loop process temperatures introduce a change in the loop injection air mass flow rate. The proper operation of the injection air trim function block causes a reduction of the injection air as the process temperature increases. The proper injection air trim can be identified in **Figure 7-8**.

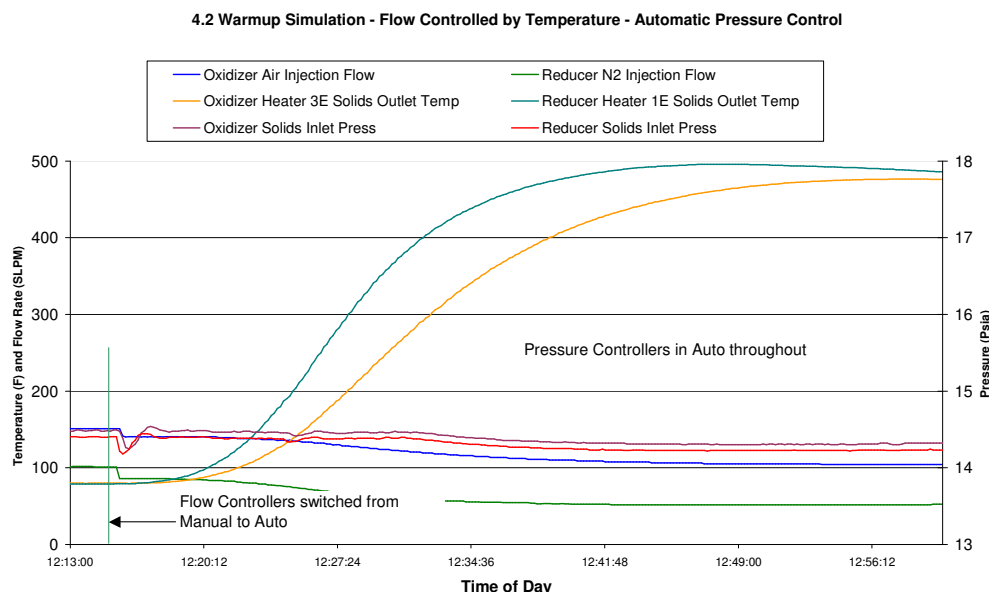


**Figure 7-8 - Riser Temperature vs Injection Air mass flow rate (SLPM) Trim**

## Solids Transfer Rate Control (September 27<sup>th</sup> 2007)

The solids transfer rate test was the only Phase III control feasibility test that involved solids transport. This test is the first attempt at the automated solids flow control. It is important for the Phase IV pilot scale facility to be able to implement a reliable control method for both loop solids recycle and inter-loop solids cross-over.

The controls method implemented for this study used the experimentally developed relationships between the loop riser differential pressures and solids flow rate. Similarly, the SPCV used an experimentally derived relationship between cross-over transport airflow rate and crossover solids mass flow rate.

The Phase III solids transfer rate control testing utilized the individual loop vertical riser differential pressures (PDT 2203 for the reducer and PDT 2219 for the oxidizer) to act as the control variables for the loop solids recycle rate. The manipulated variables were the Seal Pot Control Valve recycle transport air mass flow controllers (FVC2433 & 2434 for the reducer and FCV2429 & 2430 for the oxidizer) to establish a stable solid recycle rate (lb/hr) in both loops. The loop pressure controllers were in automatic mode to maintain the individual loop pressures at their set point values.

## Solids Transfer Rate Control Implementation

The primary requirement for reliable automated reactor solids crossover control is the ability of the two loop vacuum pumps to maintain both loops at identical pressure, as measured by the loop differential pressure (PDT 2247) located at the solids cross-over elevation. This zero loop differential pressure control must be maintained even when instantaneous solids recycle pressure pulsations exist within each loop.

The individual reactor loop riser solids inventory is monitored through the two riser differential pressure transducers (PDT 2203 on the reducer side and PDT 2219 on the oxidizer side). These two riser differential pressures are functionally related to the individual loop riser solids inventory.

After automatic pressure control was established with the pressure controller in automatic, the next step was the initiation of stable solids recycle in the reducer and oxidizer loops. The crossover solids rate (lb/hr) from the reducer to the oxidizer loop, **Figure 7-9**, is entered as Solids Flow in the crossover panel (blue circle). On the oxidizer side, the rate of crossover flow, based on the calculated loop differential pressure ratio, is entered as a set point value in **Figure 7-10**, (red circle).

The solids crossover flow controller PID loop, **Figure 7-9**, has as an input structure with the reducer and oxidizer riser differential pressures as the process variables. A function block then establishes the differential pressure ratio value that is used as the control variable. This is a proxy for the loop solids ratio. A user specified differential pressure ratio is used as the controller set point value. Any set point error is corrected through the action of the oxidizer side solids transfer PID adjustment of the oxidizer crossover

air mass flow controllers (FCV 1424 fluidizing air and FCV1426 transport air) as the manipulated variables.

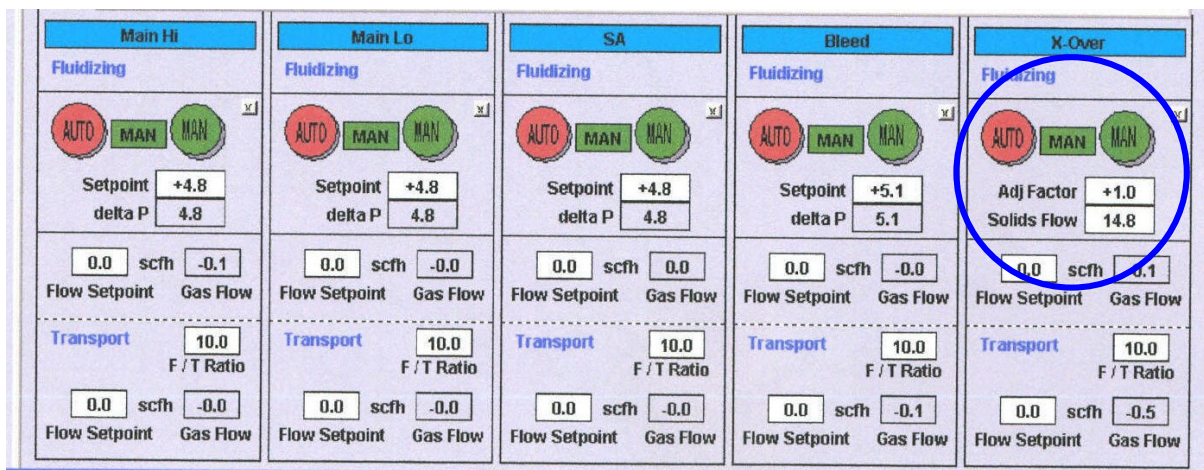


Figure 7-9 - Reducer to Oxidizer Crossover Rate control screen

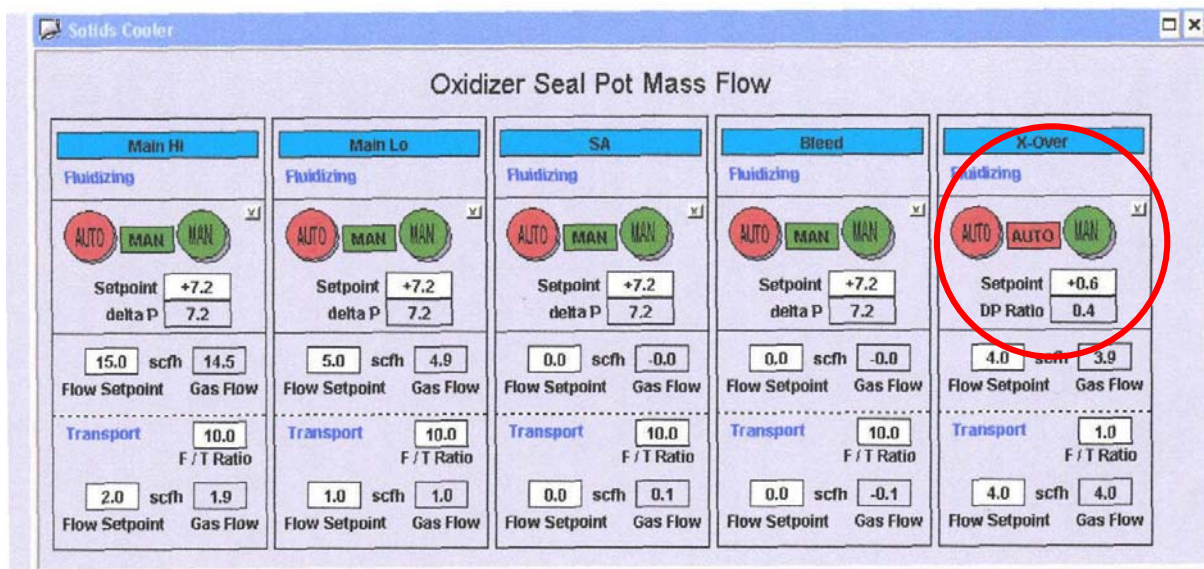


Figure 7-10 - Oxidizer Solids Crossover Rate Control screen

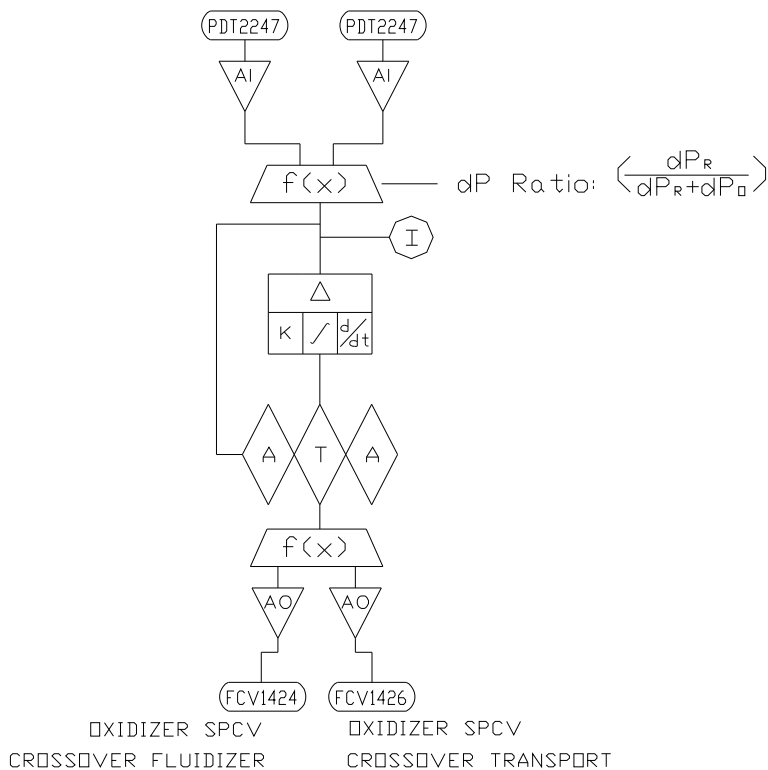


Figure 7-11 - Oxidizer Solids Flow Rate PID controller logic

## Solids Transfer Rate Control Test Results

Once the two chemical looping reactor circuits were in the recycle mode with both of the loop pressure controllers in automatic, (reducer pressure at set point value and oxidizer controller at the required 0 psi inter-loop differential pressure set point) the crossover rate from the reducer to oxidizer was set on the reducer Seal Pot Mass Flow screen, **Figure 7-10**.

Lastly, oxidizer crossover controller using the DP ratio set point, **Figure 7-11**, was placed into the automatic mode.

**Figure 7-12** and **Figure 7-13** are data traces of the PDU facility from 1600 until 1620 on September 27<sup>th</sup> 2007. During this interval, the PDU was operating with both of the loop pressure controllers and the oxidizer solids crossover controller in the automatic mode. In **Figure 7-12**, it can be seen that the solids are being transported, with both recycle and crossover, while the automatic pressure controllers maintain both loops at their set point values.

This finding is significant. Unlike the air only tests conducted previously, solids transport was occurring in this test. This solids flow rate test directly shows that the automated pressure controllers works correctly with solids transport active.

#### 4.3.2 Solids Flow Rate Control Test September 27th 2007

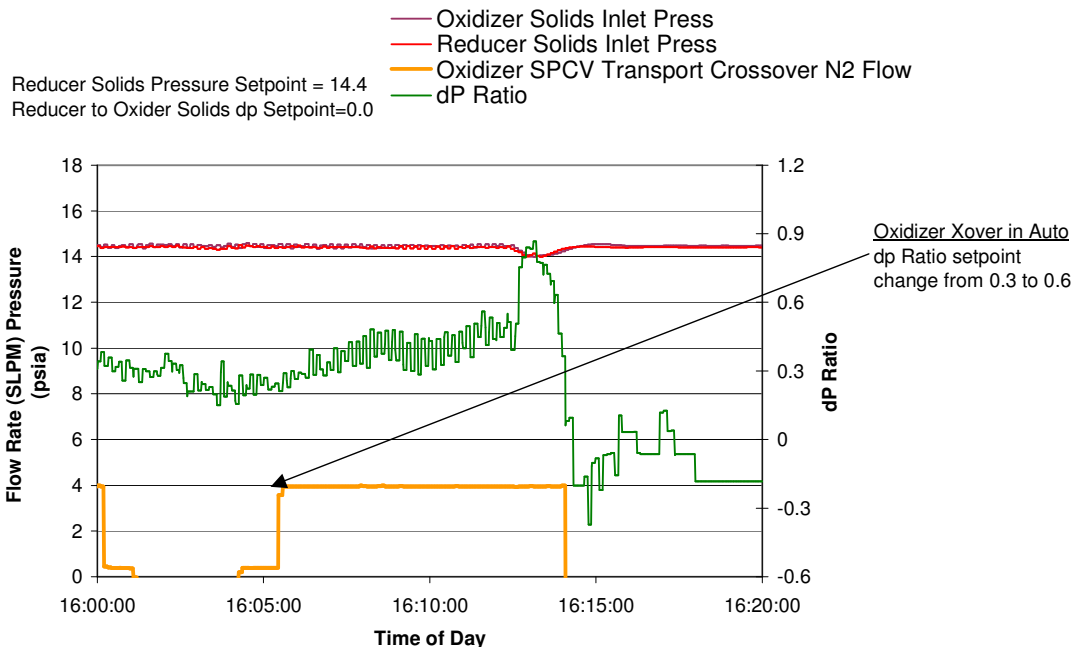


Figure 7-12 - Solids Flow Rate Testing Pressure and Flow Rate

#### 4.3.2 Solids Flow Rate Control Test September 27th 2007

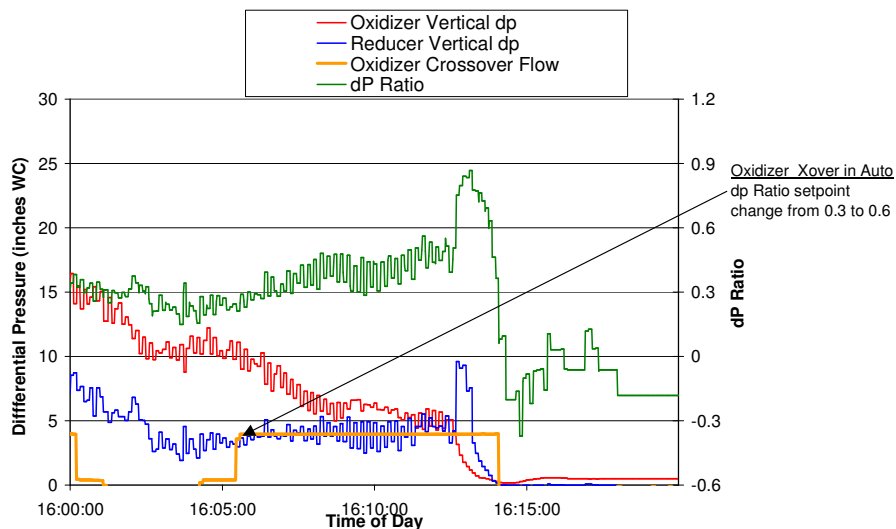


Figure 7-13 - Solids Flow Rate Testing Riser Pressure and dP Ratio

**Figure 7-13** is over the same time period and test conditions as **Figure 7-12**. With the dP ratio set point at 0.6 and the actual dP ratio of 0.3 the initial reaction of the solids transport controller, **Figure 7-11**, is to ramp up the oxidizer solids crossover transport air (orange trace) to its maximum value of 4 SLPM. This results in a decrease in the

oxidizer solids inventory (red trace). This test was conducted without any reducer to oxidizer crossover flow so the inventory of the reducer riser must increase (blue trace) as the oxidizer solids inventory decreases due to oxidizer to reducer solids crossover flow.

When examining the individual loop riser differential pressures, the decrease in the oxidizer riser differential pressure (6 inches WC) is different from the increase in the reducer riser differential pressure (2.3 in WC). This differential pressure difference can be explained by examining **Figure 7-14**. The reducer loop air injection rate (red trace) is nominally 75 SLPM and the oxidizer injection airflow rate (blue trace) is 130 SLPM. The injection air flow ratio and air velocity ratio between the two loops (reducer relative to oxidizer) is 0.58. The solids transport velocity in the reducer is only 60% of the oxidizer loop solids transport velocity. The associated velocity induced differential pressure would be the 0.3. This implies that an amount of solids transferred from the oxidizer to the lower velocity reducer loop would result in a differential pressure change of 30% the change in the oxidizer loop.

Therefore, by accounting for the lower reducer loop solids velocity a differential pressure increase of 2.0" WC is predicted based on a 6" WC decrease in the oxidizer riser differential pressure. The observed value of a 2.3"WC increase in the reducer riser differential pressure is quite close to the predicted change value.

#### 4.3.2 Solids Flow Rate Control Test September 27th 2007

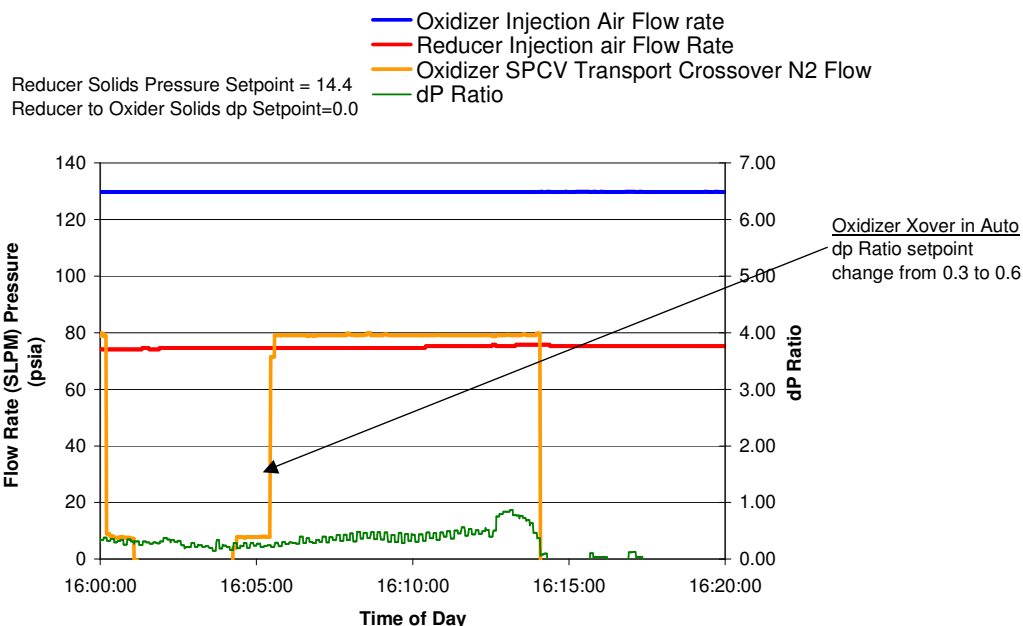


**Figure 7-14 - Solids Flow Rate Testing Injection Air**

Despite the very limited duration of the automatic solids transfer rate testing the results are positive. In the process of reviewing the solids transfer rate test results a question

has arisen regarding the adequacy of the tested “differential pressure ratio” controller strategy. The test results indicate that a revised controller strategy is needed in order to account for any difference in two loop’s injection airflow rates. Establishing this adjustment factor for the solids flow rate controller will be done in Phase IV.

#### **7.1.4. Overall Automatic Control Feasibility Testing Conclusions**

The Phase III Chemical Looping program had a very modest controls objective: to demonstrate that an automated controls strategy towards solids transport was feasible. On this single objective, the phase III effort met with success. The testing of the automatic pressure control strategy proved encouraging.

The air only automatic pressure control test results are bolstered by the observation that during the solids flow rate test the automatic pressure controllers were able to maintain their respective process pressures at the desired set points even while recycle solids and crossover solids were being transported.

To the extent that loop injection air flow rate can be set to “boiler load” the Phase III testing is viewed as a positive indicator of automated control feasibility during a plant startup, load change and shutdown.

The second area of automated controls testing established the feasibility of providing a process temperature trim on the loop injection airflow rate. The adequate performance of the tested process temperature trim on the injection airflow rates must be confirmed in Phase IV over the full range of process temperatures.

The final area of controls investigation undertaken in Phase III attempted to assess ability of a solids transport rate controller to automatically control the movement of solids between CL loops. The feasibility testing of this controller was promising but needs to be developed in Phase IV.

The implemented control strategy for inter-loop solids transfer was logical from both the process and a regulatory controller standpoint. The control methodology, labeled dP ratio, appears to have good promise for providing loop solids inventory control but will likely require modification to accommodate reducer and oxidizer loop injection air differences.

Phase III was not expected to provide the final answers with regards to the applicability of automated controls to the chemical looping process. The success of the testing conducted during this phase does provide the promise that automated solids transport control can be achieved.

Additional Phase IV controls testing and controller tuning is needed to build on the Phase III results and to verify the performance of the Phase III developed automated controls designs.

### **7.1.5. Remaining Process Controls Challenges for the Chemical Looping Project**

There are clear controls challenges, which must be addressed during Phase IV before a commercial plant control design can be finalized.

The following tests will be included in the Phase IV work plan:

1. Automatic pressure balance and controls test with solids flow in both loops. These tests should include solids load change with automatic air injection control in automatic mode.
2. A matrix of solids load changes that covers the anticipated solids flow ranges encountered during all anticipated load changes.
3. Both detailed startup and the shutdown procedures must be developed and tested. This requirement is for the full multiple loop configuration.
4. Both cold flow and hot flow tests of process stability with solids cross over should be first conducted at the PDU and again in the prototype.
5. During the prototype testing, the integrated CL chemical performance (steam / syngas) controller and final solids transport control strategy must be evaluated simultaneously to prevent any possibility of system interaction problems.

## 8.0 Prototype Engineering

The goal of Phase III was to obtain enough information to design, build and operate a prototype Chemical Looping facility. This prototype facility will be the first time that the Alstom's Chemical Looping Concept can be operated and tested with all of the commercially important systems operating in an auto-thermal (i.e. without external heat) integrated manner. The information gathered from testing in the PDU and in the cold flow models was applied to a very preliminary design for the prototype plant.

Several engineering studies were performed to supplement the pilot test program. The first engineering study was to size and estimate the prototype performance. This is described in **Section 8.1**. The prototype was scaled from the Chemical Looping plant described in the Greenhouse gas report. Case 13 from that report was used as the basis for the prototype design. The prototype was initially sized to fire about the same amount of coal as Alstom's Multiuse Test Facility (MTF), about 1000 lb/hr..

Heat transfer issues for the three major gas streams are addressed in **Section 8.2**. The design of air heaters to recover sensible heat in the main process discharge lines will be addressed in detail in the engineering activities for Phase IV. This engineering study was done to determine what the main issues will be.

Calcination tests were done as described in **Section 8.3**. These tests were done to investigate the effect of solid-to-solid reactions and the generation of gas in the calciner on solids transport.

Based on the Greenhouse Gas Report Case 13 specifications, a study was done to determine which materials will be used for any of the equipment which is a new application of standard Alstom products or a new design. This is discussed in **Section 8.4**.

Material recommendations were applied to the design of the prototype plant. A study was done to determine if the prototype plant was reasonably sized. The selected plant size must be able to heat up in a reasonable time. The plant must also minimize heat loss for the process temperature to be maintained without external heat sources. This is discussed in **Section 8.5**.

Additional chemical looping applications are discussed in **Section 8.6**. This was done to determine if any considerations needed to be included in the design of the prototype.

A preliminary design of the prototype was then developed and discussed in **Section 8.7**.

CFD modeling was investigated as a tool to help analyze chemical looping. This is discussed in **Section 8.8**.

## 8.1 Prototype Performance Estimate

The prototype facility will be designed based on Chemical Looping Option 3 described in **Section 2**. In this option, the plant will produce hydrogen as a fuel and will remove CO<sub>2</sub> as a separate stream. This is the option described by Case 13 in the Greenhouse Gas Report (**Reference 2**). Designing the prototype for this option gives the most flexibility. All of the equipment used in all three options will be installed and therefore the prototype can be operated to characterize any of the three options.

The nominal size for the MTF is used because that size is large enough to operate all of the plant equipment at commercially significant sizes. It is also large enough to operate the process with heat generated from the process fuel. It will not have the external heating required at the PDU. The size is small enough to make a relatively cost effective fully operation chemical looping system.

The MTF is sized for about 1000 pounds per hour of coal feed. The prototype will be sized for a nominal coal feed of about 2000 pounds per hour. This will give the prototype the ability to operate in the hydrogen-producing mode and produce enough product gas to characterize performance. When operating in the other modes, coal flow will be lower.

Performance from Case 13 of the GHG report was used as the basis for scaling the performance of the prototype. A simplified process flow diagram for the prototype is shown in **Figure 8-1**, and the flow streams are listed in **Table 8-1**.

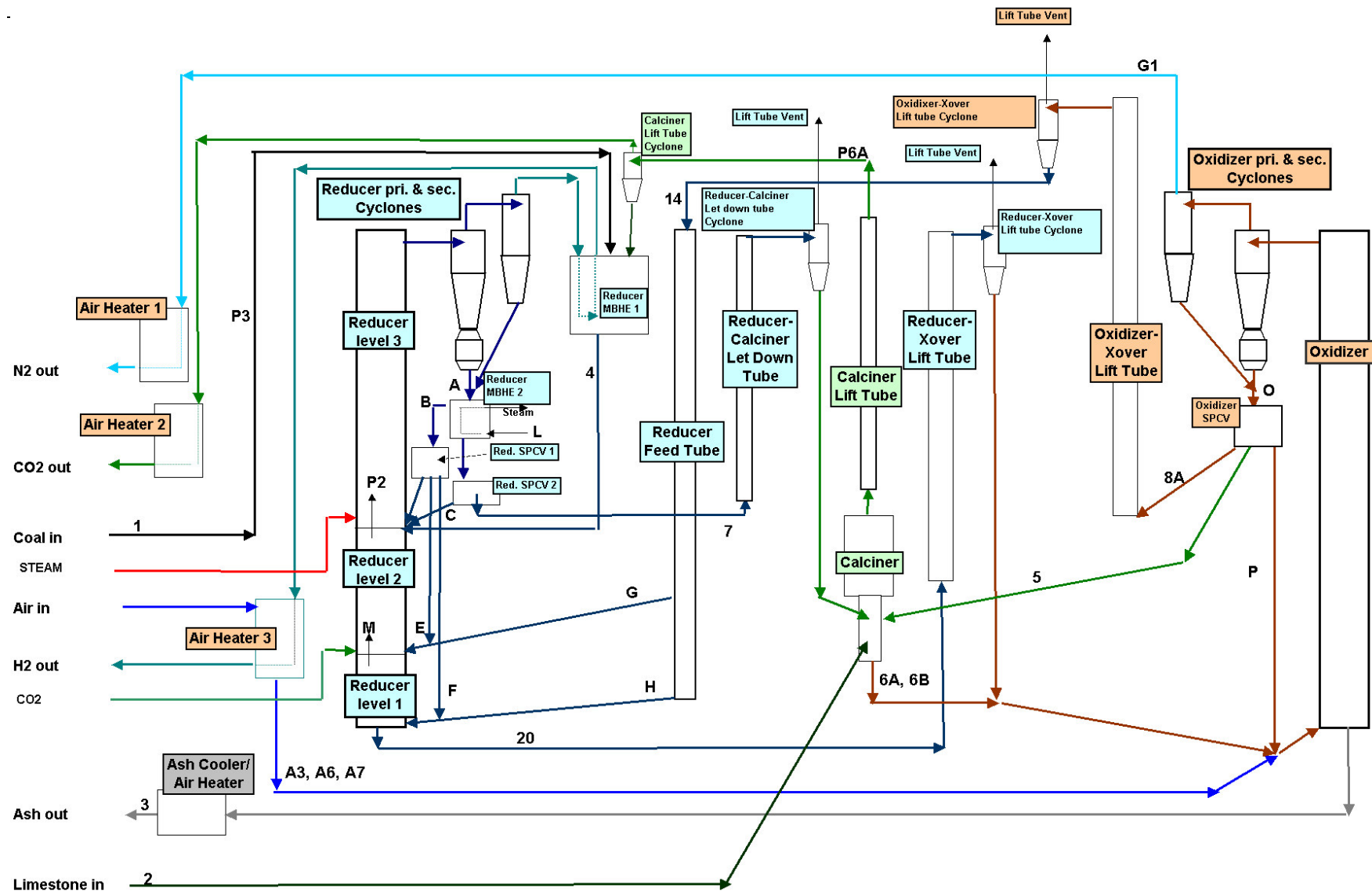


Figure 8-1 - Chemical Looping Prototype Simplified Process Flow Diagram



**Table 8-1 - Chemical Looping PFD Flow Streams (Scaled from Case13)**

Stream		Gas (lbmole/hr) lb/lbmole			Solid (lb/hr)
1	Coal				3000
2	Limestone				461
3	Disposal				1172
4					107720
A					1510808
B					1258631
C				758	139848
D					629315
E					604143
F					25173
G					26027
H					20028
I	CO2	1.40	44.01	62	
J	CO2	12.64	44.01	556	
K	Steam	168.27	18.02	3032	
L	Steam	42.07	18.02	758	
M		10.91	43.97	480	1345
P2		277.20	22.49	6235	625836
P3		269.43	2.80	755	
P6A		172.91	44.01	7610	
A3,A6,A7		263.50	28.63	7544	
G1		218.33	27.93	6099	
14	Hot CaSO4				46055
20	CaS				43438
7	CaCO3				112330
8A	CaO				104720
5	Calciner Heat				163333
6A,6B	Calciner Cold				163333
O					91484
P					45428

## 8.2 Heat Exchangers

The prototype will have three outlet gas streams when operating in the hydrogen production mode. These are a nitrogen rich stream from the oxidizer, a hydrogen stream from the reducer and a CO<sub>2</sub> stream from the calciner. All three of these streams will be leaving the process equipment at temperatures of 1800 degrees F to 2000 degrees F.

In the commercial plant design, the sensible heat from these streams will be recycled back into the process. The equipment for doing this will be developed in Phase IV. The prototype will need to use some of this heat to preheat the air to the oxidizer and the coal and limestone feed to the reducer. Phase IV will have a design effort to develop the heat exchangers to be used in the prototype.

The purpose of this engineering study in Phase III was to investigate the feasibility of using high temperature heat exchangers to preheat the air to the process, and to identify the issues that need to be resolved in the Phase IV heat exchanger design effort. Gas-to-gas heat exchangers in power plants are usually not designed to operate with gas temperatures as high as 2000 degrees. The problems anticipated include differential expansion of the tubes in the heat exchangers and materials of construction.

A specification was created for two heat exchangers. One was sized for the anticipated CO<sub>2</sub> stream in the Case 13 size plant. The other was sized for the N<sub>2</sub> rich stream in the prototype plant.

The specifications for the heaters are provided below:

Demo size:

Air flow:	70,000 lbs/hr
Air inlet temperature	1380F
Air inlet pressure	500" H <sub>2</sub> O abs
Flue gas flow:	65,000 lbs/hr
Gas inlet temperature	2000F
Gas outlet temperature	1500F
Gas inlet pressure	100" H <sub>2</sub> O abs
Gas composition:	CO <sub>2</sub> (100%)

No leakage is allowed. It was assumed that there are no particulates in the gas stream.

Pilot scale size:

Air flow:	10,000 lbs/hr
Air inlet temperature	1380F
Air inlet pressure	500" H <sub>2</sub> O abs
Flue gas flow:	9,500 lbs/hr

Gas inlet temperature	2000F
Gas outlet temperature	1500F
Gas inlet pressure	100" H <sub>2</sub> O abs
Gas composition:	N <sub>2</sub> (95%) , O <sub>2</sub> (5%)

No leakage is allowed. It was assumed that there are no particulates in the gas stream.

The specification was sent to an AlstomPower company, called Alstom Power Energy Recovery that supplies air heaters. This was done to determine the availability of commercial products that could meet these requirements. Alstom Power Energy Recovery supplies HRSGs that can accommodate the differential expansion caused by the high temperature differences.

The rough cost estimates that came back were very high. The commercially sized air heater was \$5.4 million and the prototype was \$1.2 million. The physical size of the equipment was also very large. However, this exercise showed that commercial equipment exists that can be used for this application.

The prototype has special needs for flexibility that the commercial design doesn't have. The prototype will not have to operate at 90%+ reliability for 20 years. This means that Alstom Power Plant Labs will internally design the heat exchangers for this application and either fabricate them on site or have them custom built.

In addition, an internal study also sized equipment for the prototype application and showed the same result. This indicates that the air heaters for the prototype will require a significant design effort to reduce costs and weights but that the concept is feasible.

## 8.3 Calcination Tests

### 8.3.1 Calcination Experiment

In the chemical looping process, CO<sub>2</sub> is absorbed from the process gas through the chemical reaction:

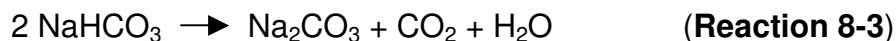


The solids containing the formed CaCO<sub>3</sub> are separated from the process gas and fed to a calcination reactor. In this process step, the reaction conditions (CO<sub>2</sub> partial pressure and/or temperature) are changed to favor the reverse of **Reaction 8-1**:



Depending on the design of this process step, the reaction can be rather instantaneous and sometimes referred to as “flash calcination”. The gas evolution could potentially create very high linear gas velocities in the reactor and as a result uncontrolled particle entrainment.

It was deemed necessary to study the process difficulties caused by this gas evolution from **Reaction 8-2**. If CaCO<sub>3</sub>-chemistry was used for these calcination experiments, the reactor temperature would have to be above 1700-1800 °F. To simplify the experimental set up, a new approach was developed using NaHCO<sub>3</sub>. This compound calcines at roughly 520 °F according to the reaction:



The fluidized bed reactor used for these tests was made in glass and the bottom of the bed was made from sintered glass (see **Figure 8-2**). The height of the glass tube was 13 3/8 inches, measured from the sintered glass bottom and the inner diameter was 7/16 inch. The bottom 20 to 25 % of the reactor was heated by heat tape and the temperature was monitored by a thermocouple attached to the glass wall close to the fluid bed bottom. A layer of insulation was applied outside the heating tape. No fluidizing gas was used through the fluid bed bottom. **Figure 8-2** shows a drawing of the test setup.

Al<sub>2</sub>O<sub>3</sub> was used in the experiments together with the NaHCO<sub>3</sub>. It had a dual function: a) it acted as a heat carrier for the calcination reaction and b) it simulated inert ash.

Some pre-tests were needed to establish the final procedure. Thermal control had to be checked and the physical integrity of the glassware had to be checked by gradually increasing temperature to control the heat up and cool down phases.

Final test procedure was:

- The glass test rig was heated to 617 °F.

- 1.8 cm<sup>3</sup> of Al<sub>2</sub>O<sub>3</sub> was heated to 932 °F in a furnace.
- 0.8 cm<sup>3</sup> of NaHCO<sub>3</sub> at ambient temperature was simultaneously added and quickly blended with the pre-heated Al<sub>2</sub>O<sub>3</sub> through the funnel.
- The effects were observed and documented.

Visibly, it was obvious that very rapid calcination took place in the reactor within less than a second. Generated gas blew out some of the solids through the funnel and the side of the tube at the top.

After the cool down, some of the powders were attached to the walls. With as little time delay as possible, the solids in the reactor were transferred over to a small sample container for analysis.

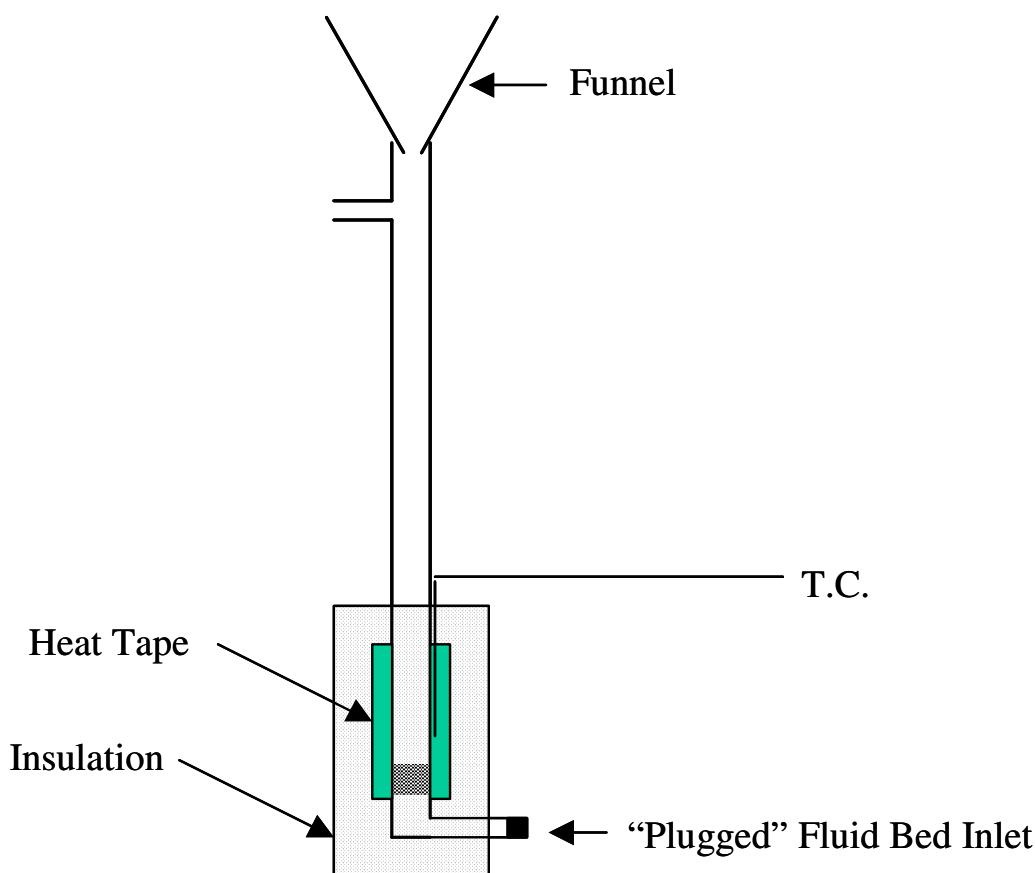


**Figure 8-2 Calcining Test Setup**

PPL Sample No.	7-3338-M	Al <sub>2</sub> O <sub>3</sub>	NaHCO <sub>3</sub>
Sample I.D.	Test 4 Bed Residue	Fisher ACS Reagent	Fisher ACS Reagent
Total Mass (grams)	1.7496		
Composition			
% Al <sub>2</sub> O <sub>3</sub>	73.5		
% NaHCO <sub>3</sub>	7.0		
% Na <sub>2</sub> CO <sub>3</sub>	18.6		
% Total	99.1		
Sieve Sizing			
+ 60 mesh		0.3	0.0
+ 100 mesh		15.7	0.6
+ 200 mesh		51.3	39.2
Pan		32.7	60.2
Bulk Density			
grams/cm <sup>3</sup> (compact)		1.15	1.27

**Table 8-2 Analysis of Calcination Product.**

The total mass collected after the test was 1.75 g. An analysis of the product is given in **Table 8-2**. The charged amounts for each test was measured volumetrically, but was recalculated to weight, using the above bulk densities. The result can be summarized in the following **Table 8-3**.

Component	Charge [g]	Charge [mole]	Recovered [g]	Recovered[mole]
Al <sub>2</sub> O <sub>3</sub>	2.07		2.49	
NaHCO <sub>3</sub>	0.102	0.0121	0.123	.00146
Na <sub>2</sub> CO <sub>3</sub>	0	0	0.326	0.00301
Na		0.0121		0.00748

**Table 8-3 Summary of Test Results**

It is clear from both visual observations and video documentation that material blew out of the reactor due to the gas generated by the calcination. The chemical analysis shows that about half of the NaHCO<sub>3</sub> was calcined and responsible for the generated gas. The fact that more Al<sub>2</sub>O<sub>3</sub> was recovered than charged at before the test can have many physical explanations, such as particle shape and electrostatic adherence to the glass walls.

## 8.4 Materials

The Chemical Looping Concept uses many components that are used in the power industry and a few that are new designs. Most of the components in the chemical looping gasifier island have specifications that are different from conventional applications. The main concerns are the reactor vessels and interconnecting piping. While the technology to build these components has been in use for a long time, it was decided to determine if design practices and materials needed to be modified for the specific needs of the Chemical Looping process.

A specification for the chemical looping components that were new designs or new applications of existing equipment was made for the commercial size equipment. The commercial-sized equipment was described based on the Case 13 application from the GHG report (**Reference 2**). These Specifications were sent to Alstom Global Refractory Applications for review and to make recommendations.

The main areas of concern were

1. High temperature refractory lined vessels without water walls are used. These are used in CFB boilers. However, CFB boilers operate at temperatures up to about 1700 F in the reactor, with possibly higher local temperatures. The three reactors in the Chemical Looping concept will operate at temperatures between 1800F and 2000F.
2. High temperature refractory lined transfer lines are used. The issue of thermal expansion is a concern.
3. The reducer will have high concentrations of hydrogen at elevated temperatures. Both refractory materials and vessel wall materials need to be selected to account for the hydrogen.

The results of the review were used to confirm the feasibility of constructing the chemical looping island components, check the cost estimates of these components to determine a preliminary design for the Phase IV Prototype and to verify the initial cost estimates for the prototype.

### 8.4.1 Refractory Requirements for Chemical Looping Process Equipment

This specification is based on the Greenhouse Gas Report (**Reference 2**) Case 13, which is the commercial chemical looping plant with CO<sub>2</sub> removal. The requirements for Case 13 are presented in the appendix, “High Level Equipment Specification for the Chemical Looping Process” which was taken from the Chemical Looping Spec Gate Review and Peer Review (**Reference 4**).

The design requirements listed in this document were used to recommend the refractory design for the equipment listed.

## **Oxidizer**

Transport reactor.  
Rectangular Vessel, 15 ft. w, 7 ft. d, 38 ft. h. No water-walls  
Temperature 1800 F  
Pressure atmospheric  
Various input pipe penetrations and solids discharge pipe penetrations  
(Temperature of pipe penetrations can vary from Oxidizer)  
Air in, N<sub>2</sub> out  
Solids to gas ratio: 200 to 1 velocity up to 100 fps.  
Solids: CaSO<sub>4</sub>, CaS, CaCO<sub>2</sub>, CaO, inerts

## **Reducer**

Transport reactor  
Cylindrical Vessel, 10 ft. dia., 38 ft. h. No water-walls  
Temperature 1800 F  
Pressure 75 psia  
Various input pipe penetrations and solids discharge pipe penetrations  
(Temperature of pipe penetrations can vary from Reducer)  
Gas Composition: Steam, CO<sub>2</sub>, CO, H<sub>2</sub>, H<sub>2</sub>S  
Solids to gas ratio: 200 to 1, velocity up to 100 fps.  
Solids: CaSO<sub>4</sub>, CaS, CaCO<sub>2</sub>, CaO, inerts

## **Calciner**

Fluid bed reactor  
Cylindrical Vessel, 12 ft. dia., 24 ft. h. No water-walls  
Temperature 1570 F  
Pressure: 7 psia (operates below atmospheric)  
Various input pipe penetrations and solids discharge pipe penetrations  
(Temperature of pipe penetrations can vary from Reducer)  
Gas Composition Steam, CO<sub>2</sub>  
Solids to gas ratio: 200 to 1, velocity up to 100 fps.  
Solids: CaSO<sub>4</sub>, CaS, CaCO<sub>2</sub>, CaO, inerts

## **Moving Bed Heat Exchangers (MBHE)**

Moving bed reactor.  
Two separate vessels.  
Outer wall refractory lined  
Rectangular Vessel, 12 ft. d, 12 ft. w, 24 ft. h. No water-walls  
Temperature: 1800 F solids inlet. 500-900F solids out.  
Various input pipe penetrations and solids discharge pipe penetrations  
(Temperature of pipe penetrations can vary from Reducer)  
Gas Composition :Steam, CO<sub>2</sub>, CO, H<sub>2</sub>  
Moving solids, velocity up to 100 feet per hour  
Solids: CaSO<sub>4</sub>, CaS, CaCO<sub>2</sub>, CaO, inerts

### **High Temperature Heat Exchanger**

Tubular Air heater.  
Outer wall refractory lined  
Rectangular Vessel, dimension to be determined. No water-walls  
Temperature: 1800 F Flue gas inlet. 500-900F Flue gas out.  
Gas Composition: N<sub>2</sub>, CO<sub>2</sub> on one side of the tubes, air on the other

### **Calcliner Particulate Removal**

Refractory lined cyclone or other refractory lined device.  
Outer wall refractory lined  
Dimensions to be determined  
Temperature: 1600 F Flue gas inlet.  
Gas Composition: N<sub>2</sub>, CO<sub>2</sub>  
High solids loading.  
Solids: CaSO<sub>4</sub>, CaS, CaCO<sub>2</sub>, CaO and inerts.

### **Oxidizer and Reducer Particulate Removal**

Refractory lined cyclones, or ring cone separators  
Dimensions tbd  
Temperature: 1800 F Flue gas inlet.  
Gas Composition: N<sub>2</sub>, CO<sub>2</sub>, for Oxidizer and CO<sub>2</sub>, CO, H<sub>2</sub>, Steam  
High solids loading.  
Solids: CaSO<sub>4</sub>, CaS, CaCO<sub>2</sub>, CaO and inerts.

### **Seal Pot Control Valves (SPCV)**

Refractory lined rectangular vessels, one for Oxidizer and one for Reducer  
Dimensions to be determined. (guess: 12ft. by 12ft., by 12ft.)  
Temperature: 1800 F at solids inlet.  
Gas Composition: N<sub>2</sub>, CO<sub>2</sub>, for Oxidizer and CO<sub>2</sub>, CO, H<sub>2</sub>, Steam  
High solids loading.  
Solids: CaSO<sub>4</sub>, CaS, CaCO<sub>2</sub>, CaO and inerts.

### **Oxygen Transport Chemical Loop**

Refractory lined pipes.  
Three major lines:  
    oxidizer to cyclone,  
    cyclone dipleg to seal pot and  
    line to reducer feed  
Dimensions: 12inch ID by up to 150 ft long  
Temperature: 1800 F at solids inlet.  
Gas includes Steam, N<sub>2</sub> and CO<sub>2</sub>,  
High solids loading. Flowing solids with interstitial gas  
Solids: CaSO<sub>4</sub>, CaS, CaCO<sub>2</sub>, CaO, inerts.

### **CO<sub>2</sub> Capture Chemical Loop**

Refractory lined pipes.

Six major lines:

Reducer to cyclone,  
cyclone dipleg to seal pot and MBHE  
line to oxidizer feed  
line to calciner  
Calciner to calciner cyclone and  
Calciner cyclone to MBHE

Dimensions: 12inch ID by up to 150 ft long

Temperature: 1800 F at solids inlet.

Pressures: up to 75 psia down to 7 psia

Gas includes:  $H_2$ , CO, Steam and  $CO_2$ ,

High solids loading. Flowing solids with interstitial gas

Solids:  $CaSO_4$ , CaS,  $CaCO_2$ , CaO, inerts.

### **Flue Gas Lines to High Temperature Heater**

Refractory lined pipes.

Dimensions: 12inch ID by up to 150 ft long

Temperature: 1800 F.

Gas includes:  $N_2$   $CO_2$ ,

### **Coal and Limestone Feed Lines**

Similar to CFB design

## **8.4.2 Refractory Design Requirements**

The issues and requirements related to the refractory linings within the chemical looping process will be discussed in this section. The topics include:

- Chemical Issues
- Refractory Lining Constructability
- Design of Refractory Linings
- Refractory Material Recommendations
- Process Component Linings

### **Chemical Issues**

Hydrogen, steam and carbon monoxide are three issues within the described chemical looping process that will have detrimental effects on the refractory linings.

The hydrogen rich atmospheres within the reducer represent challenges for the refractory lining as well as the steel shell.

Hydrogen is a much more highly conductive gas than air, so the thermal conductivity of the refractory materials is adversely affected. As a result, thicker refractory linings are required in order to achieve the same thermal performance and steel shell temperatures when hydrogen is present. The higher the concentration of hydrogen, the worse the effect will be on the insulating ability of the refractory.

The hydrogen can be very chemically reactive with refractory materials, particularly constituents, such as iron and silica. The refractory products selected for use in the applications areas with hydrogen atmospheres must be low iron regardless of the operating temperature.

In hydrogen atmospheres, at temperatures greater than 2000°F and with increasing hydrogen content, silica will be extracted from the refractory matrix, weakening the refractory and leading to failure. In addition, the leached silica is likely to be deposited downstream in the process. It is important in these conditions to use high alumina, low silica refractory products. See **Figure 8-3** for additional information.

It should be noted that hydrogen will penetrate to the outer steel casing at refractory expansion joints, construction joints as well as through the porosity of the refractory materials themselves. As a result, the selection and design of the steel shell should take this into account to ensure against hydrogen embrittlement.

High pressure steam is also capable of extracting silica from refractory materials at temperatures above 1600°F, so again, high alumina, low silica refractory products should be used in these areas to form the hot face refractory layer.

In reducing conditions, concentrations of carbon monoxide will react with iron oxide present within the refractory lining to form iron carbide deposits. These deposits will grow within the refractory matrix causing cracking and failure. Only refractory materials containing low iron should be used in these conditions. Fortunately, in our chemical looping process, it should also be noted the presence of hydrogen has been shown to inhibit the carbon dioxide disintegration process.

### **Refractory Lining Constructability**

The refractory linings inside larger vessels within the described chemical looping process may be cast, gunited or bricked.

In the smaller components and the transfer lines, the refractory linings will need to be constructed by forming and casting from the outside. The transfer lines will need to be segmented into manageable pieces, i.e., approximately 8 to 10 foot lengths. This approach would also offer easier maintenance of these components in the future. This also would allow for the transfer lines and smaller components to have the refractory lining shop installed and then shipped to the plant site for final assembly.

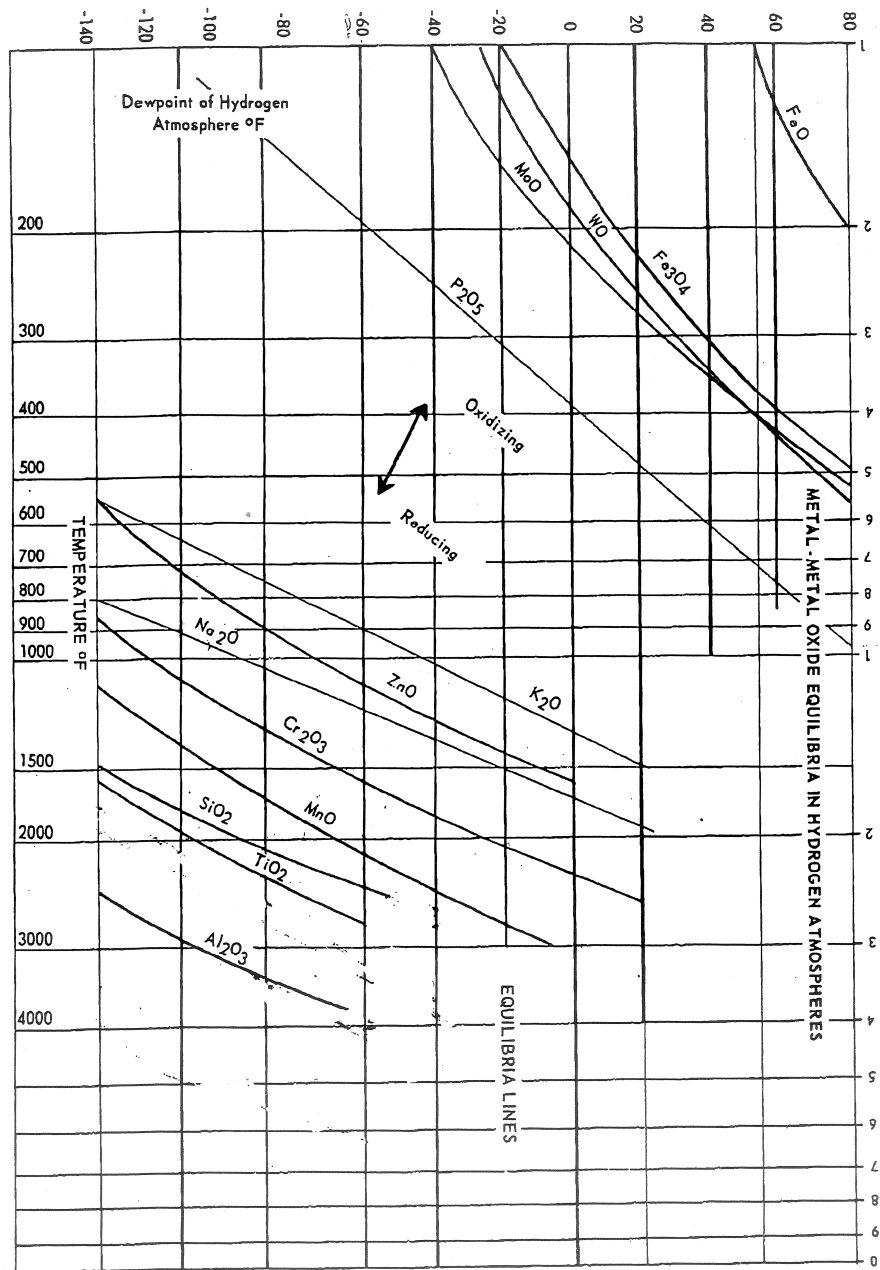


**Figure 8-3 – Refractory Properties**

The refractory lining will grow due to thermal expansion and allowance for this must be made in the lining design. The thermal expansion is typically taken into account by creating an expansion joint at regular intervals and packing with ceramic fiber blanket. Unfortunately, this also provides more opportunity for hydrogen to reach the steel shell and the more porous backup refractory layers. In CFB Boiler experience, in order to

minimize “pinch-spalling” caused by bed material infiltrating the expansion joint, the joints are kept smaller than 0.5 inches. This is shown in **Figure 8-4**.

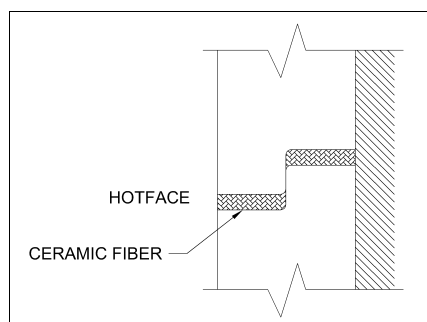


**Figure 8-4 - Typical Refractory Expansion Joint**

Once the construction is complete, the refractory linings will need to be initially heated at a carefully controlled rate in order to dryout the materials without damaging the lining. The actual dry-out rate will be determined by the type and thickness of the refractory materials selected. Typically, the dry-out rate will be at temperature ramp rates no greater than 50 to 75°F per hour to approximately 1500°F.

### Design of Refractory Linings

As previously described, hydrogen atmospheres adversely affect the thermal conductivity of the refractory materials. For example;

1) In a large vessel, (80°F ambient and no wind) the results would be as follows: With a 6” thickness of High Alumina Dense castable and an 8” thickness of Lightweight, Low Iron castable, an air atmosphere would have a shell temperature of 230°F, where a 100% hydrogen atmosphere would have a shell temperature of 348°F.

2) In a 12” diameter pipe, (80°F ambient and no wind) the results would be as follows: With a 4” thickness of High Alumina Dense Castable and an 8” thickness of Lightweight, Low Iron Castable, an air atmosphere would have a shell temperature of 200°F and a 100% hydrogen atmosphere would have a shell temperature of 299°F.

In addition, allowance must be made for thermal expansion of the refractory lining that will be greater than the steel shell. For the 12” diameter pipe with 100% hydrogen example above, the thermal expansion results will be as follows:

1) 95% Alumina Dense Castable at 1800°F of a 10 foot long section;  
 Thermal Expansion = (rate of thermal expansion) x (temperature difference) x (length)  
 – (permanent linear change of the refractory material)  

$$= 5 \times 10^{-6} \times (1800 - 80) \times 10 \times 12 - (10 \times 12 \times .002)$$
  

$$= 0.792 \text{ inches}$$

2) Stainless Steel Shell, 10 foot long section;

$$\begin{aligned}\text{Thermal Expansion} &= (\text{rate of thermal expansion}) \times (\text{temperature difference}) \times (\text{length}) \\ &= 10.5 \times 10^{-6} \times (299 - 80) \times 10 \times 12 \\ &= 0.276 \text{ inches}\end{aligned}$$

The refractory material selections for the hot face layer must be capable of providing adequate abrasion resistance due to the nature of the fluid bed combustion process and the movement of solids through the transfer lines. It is believed that the abrasive nature of the media within the chemical looping process will be no greater than our experience in conventional CFB boilers to date. As a result, the hot face material should have an abrasion resistance of less than 12 cc (cm<sup>3</sup> of volume loss in the test sample) when tested according to ASTM C-704.

The refractory linings within the larger components will need to be anchored. The anchoring can be conventional “Y” type anchors **Figure 8-5**, or combination MS/YF type anchors, **Figure 8-6**. The advantage of the MS/YF system is that it allows for easier installation of the backup, insulating refractory castable.

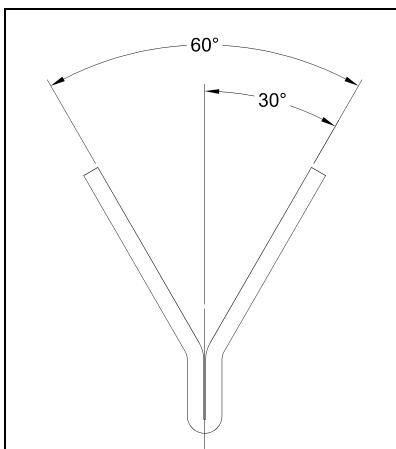


**Figure 8-5 - Y Anchor**

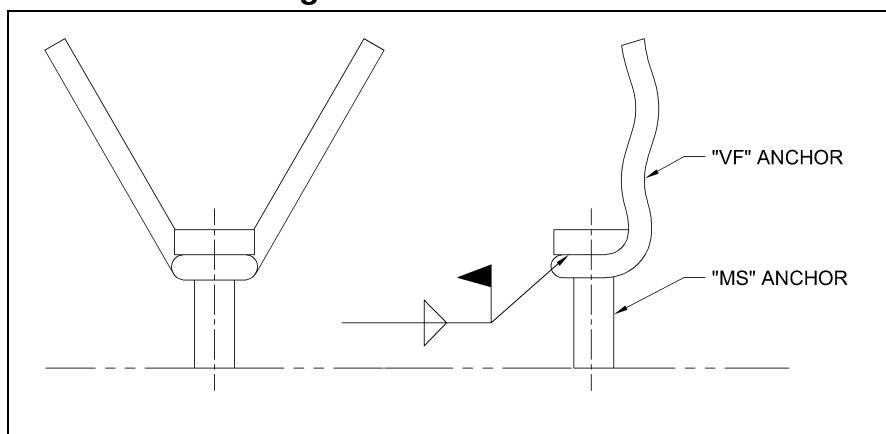


**Figure 8-6 - MS / YF Anchor Combination**

In the reducing portion of the chemical looping process with the hydrogen atmosphere, the use of Inconel 601 for the refractory anchoring is recommended. In the remainder of the process, the use of 330SS or Inconel 601 for the refractory anchoring is recommended.

In the small diameter transfer pipes, anchors will typically be required only at one end of each straight section to be constructed.

It is noted that the sealpot components may include a divider wall suspended from the roof. This is not recommended with refractory castable construction. However, it should be possible to construct a refractory brick checker wall that incorporates openings in the lower portion to accomplish the same objective.

It should also be noted that personnel protection in the form of metal standoffs will be required in all accessible locations on the outside of the components due to the predicted shell temperatures being greater than 140°F.

## Refractory Material Recommendations

**High Alumina Dense Castable** – minimum 95% alumina content, 0.1% or less iron content, abrasion < 12 cc, dried density 170 to 190 lb/ft<sup>3</sup>. (Kao-Tab 95 or HP-Cast Ultra) It should be noted that high alumina refractory products have a greater susceptibility to thermal shock. Rapid changes in temperature will have an adverse affect on the service life of the refractory lining.

**Lightweight Low Iron Insulating Castable** – iron content < 0.9%, thermal conductivity at 1500°F < 1.85 BTU\*in/hr<sup>2</sup>\*°F, dried density < 60 lb/ft<sup>3</sup>, Service Use Temperature 2000°F minimum. (Kaolite 2300-LI or Kast-O-Lite 20 LI)

**Erosion Resistant Low Cement Dense Castable** - abrasion < 12 cc, dried density 135 to 150 lb/ft<sup>3</sup>, Service Use Temperature 2600°F minimum. (Uni-Shot 45 or equal)

**High Alumina Severe Duty Brick** - minimum 90% alumina content, iron content < 0.3%, abrasion < 12 cc, density 185 to 195 lb/ft<sup>3</sup>. (SR-90 or Korundal XD)

**Bitumastic High Temperature Coating** –Service Use Temperature 400°F minimum (HT Mastic). Consideration should be given to the use of a Bitumastic coating on the inner surface of the steel shell in order to assist in its protection from sulphuric acid attack during shut down periods.

## Process Component Linings

**Reducer** – 6” High Alumina Dense Castable, 8” Lightweight Low Iron Insulating Castable – anchors on walls 9” x 9” spacing (1.78 /sf), roof 6” x 6” (4/sf)

**Cyclone** (Hydrogen) - 6" High Alumina Dense Castable, 8" Lightweight Low Iron Insulating Castable - anchors on 9" x 9" spacing (1.78 /sf), roof 6" x 6" (4/sf)

**MBHE** - 6" High Alumina Dense Castable, 8" Lightweight Low Iron Insulating Castable - anchors on 9" x 9" spacing (1.78 /sf), roof 6" x 6" (4/sf)

**Transfer Lines** (Hydrogen) - 4" High Alumina Dense Castable, 8" Lightweight Low Iron Insulating Castable

**Oxidizer** - 6" Erosion Resistant Low Cement Dense Castable, 6" Lightweight Low Iron Insulating Castable - anchors on 9" x 9" spacing (1.78 /sf), roof 6" x 6" (4/sf). Thicknesses based on maintaining a shell temperature > 250°F sulphur dew point

**Cyclone** - 6" Erosion Resistant Low Cement Dense Castable, 6" Lightweight Low Iron Insulating Castable - anchors on 9" x 9" spacing (1.78 /sf), roof 6" x 6" (4/sf)

**Calciner** - 6" Erosion Resistant Low Cement Dense Castable, 6" Lightweight Low Iron Insulating Castable - anchors on 9" x 9" spacing (1.78 /sf), roof 6" x 6" (4/sf)

**Transfer Lines** (non-Hydrogen) - 4" Erosion Resistant Low Cement Dense Castable, 5" Lightweight Low Iron Insulating Castable

**Tubular Air Heater** - 6" Erosion Resistant Low Cement Dense Castable, 6" Lightweight Low Iron Insulating Castable - anchors on 9" x 9" spacing (1.78 /sf), roof 6" x 6" (4/sf)

**Sealpots** - 6" High Alumina Dense Castable, 8" Lightweight Low Iron Insulating Castable & High Alumina Severe Duty Brick for divider walls - anchors on 9" x 9" spacing (1.78 /sf), roof 6" x 6" (4/sf)

The recommendations contained within this section represent design concepts based on the information currently available. These concepts and issues will be considered as the detail design of the chemical looping prototype components is undertaken. When this is complete, it will be possible to develop detailed refractory lining designs.

## 8.5. Refractory Heat Up

This study was done to determine if a prototype chemical looping plant can be constructed and operated without using external heating of the process equipment as was done in the pilot plant. Heat up rates were determined to verify that a refractory-lined design could be heated up in a reasonable time, and that the steady state heat loss would not cool the process to the point where the process could not maintain temperature.

### Preliminary Prototype Plant Equipment Design

The prototype preliminary design was estimated by taking Case 13 from the Greenhouse Gas Report and scaling the flow rates of the individual streams to the expected prototype heat input of 10 million btu/hr. This is roughly the heat input to the Multiuse Test Facility (MTF). The Case 13 heat and mass balance from the GHG report is summarized in the document 'High Level Equipment Specification for the Chemical Looping Process'. This can be found in **Reference 3**.

Five main pieces of process equipment were considered: The upper reducer, the lower reducer, the oxidizer, the calciner and the feed pipes. These make up most of the refractory-lined pieces in the process.

The coal used is Pittsburgh #8 with an HHV of 13390 Btu/#. Therefore 10MM Btu/hour is 746.8 #/hour.

#### Reducer

The reducer will be constructed of two parts. The lower reducer will serve as a carbon burnout chamber and will operate as a bubbling fluid bed. The upper reducer will be an entrained flow reactor with a velocity high enough to transport solids and keep them from falling back into the lower reducer.

The lower reducer will be fluidized by the CO<sub>2</sub> generated by burning the carbon. The maximum amount of gas that can be generated by 746.8 lb/hr of coal is approximately 1540 lb/hour of CO<sub>2</sub> gas. The lower reducer will operate at 6 psig and 1800 F. This will require a vessel ID of 18.8 inches to maintain a fluidizing velocity of 6 feet per second. The vessel height will be 10 feet.

The upper reducer vessel will be designed with a velocity of 30 fps to keep solids from falling directly into the lower reducer. The maximum gas flow will be the amount of product gas generated which is 146.8 lb/hour. The CO<sub>2</sub> will be absorbed by the CaO. The diameter of the upper reducer will be 10.8 inches and the height will be 50 feet.

Both upper and lower reducer vessels will have a 6-inch refractory layer, a 1-inch insulation layer and a 0.25-inch thick steel vessel wall.

## Oxidizer

The oxidizer will be sized for the maximum amount of air at 100 fps, 1.0 atm, and 1800 F. For 746.8 lb/hr of coal this corresponds to 2472 lb/hr of air. The diameter of the oxidizer will be 8.6-inches, and the height will be 60-ft. The oxidizer will have a 6-inch refractory layer, a 1-inch insulation layer and a 0.25-inch thick steel vessel wall.

## Calciner

The calciner will be designed as a fluidized bed reactor similar to the lower reducer. The vessel will be designed based on the amount of CO<sub>2</sub> generated which is calculated to be 1540 lb/hour. For the purposes of this heat transfer study, the design of the calciner vessel will be identical to the lower reducer.

## Feed Pipes

The feed pipes are assumed to have a 2-inch ID and a total length of 150 ft. They will have a 6-inch refractory layer, a 1-inch insulation layer and a 0.25-inch thick steel vessel wall.

## MTF Design Check

A calculation was done for the MTF design as a check for the Chemical Looping prototype heat transfer. It is known that the MTF heats up to near operating condition in 15 to 18 hours. The MTF is 40-inches in diameter and 60 feet long. It has 10-inches of refractory and 1-inch of insulation and a 0.25-inch vessel wall. The performance of the MTF is used as a model to determine at which point the prototype is to be considered warmed up.

## Steady State Heat Transfer

The steady state heat transfer through the vessel walls is given by the following equation (Reference: Alan J. Chapman, "Heat Transfer, Second Edition")

$$U=L*2*PI*(T_{process} - T_{air})/[ (1/r1h1) + (ln(r2/r1)/k1) + (ln(r3/r2)/k2) +(ln(r4/r3)/k3) + (1/r4h4) ]$$

U	= overall heat transfer coefficient through a layered cylinder.
T <sub>process</sub>	= reactor process temperature.
T <sub>air</sub>	= air temperature
r1	= vessel inside radius = refractory ID
r2	= refractory OD = insulation ID
r3	= insulation OD = vessel wall ID

- r4 = vessel wall OD  
h1 = inside film coefficient. This is assumed to be 30 Btu/hr-F-ft<sup>2</sup> based on the Chemical Looping PDU test results.  
h2 = outside film coefficient = approximately .67 Btu/hr-F-ft<sup>2</sup> for still air or approximately 2.5 BTU/hr-F-ft<sup>2</sup> for 7 mph wind. To be conservative the higher value is used.

Heat flux is defined as:

$$Q/A = h1 * (T_{process} - T_{inside\ surface})$$

### Transient Heat Transfer during Heat-Up

During startup, the heat flux from the process gas is higher than during steady state. The extra heat removed from the process heats up the vessel walls. At some time during startup the extra heat flux is close enough to the steady state that the process temperature can be maintained at a reasonable level. In the MTF startup this seemed to occur when the heat flux was down to about 115% above the steady state condition (Using the same calculation procedure as this).

The transient start up was calculated by considering each vessel to be made of ten concentric rings of refractory, 1 ring of insulation and 1 ring of steel wall. An initial temperature of 80 degrees was used for the vessel and the outside air. At time equal zero the process temperature was assumed to be 1800 F. Each time increment recalculated the temperature distribution in the vessel using the heat transfer properties and the temperature differences from the previous time increment. A time step of 20 seconds was fast enough to allow the calculation to proceed without temperature extremes and slow enough to give reasonable results with less than 2500 iterations for all of the vessels.

### Results

The results of the calculation are shown in **Table 8-4**.

The steady state heat loss calculation for the MTF using this method is about 253,000 Btu/hr. The observed warm up period is 15 to 18 hours. It can be seen that it takes 16.89 hours for the heat loss value in the MTF during warm up to get down to 115% above steady state. Therefore, this is the target value for the prototype vessels. That is, the prototype vessel warm up will continue until the heat loss gets down to 115% above the calculated steady state condition. After that condition is reached, it will be assumed that heat loss from the process will be low enough to allow the process to maintain a reasonable operating temperature.

The total steady state heat loss from the five major prototype components was calculated to be about 3.59% of the input heat. 115% more heat loss is 7.71% of the input heat. The heat loss from each component was calculated individually. It was seen that the longest time to meet the warm up criteria was about 8.4 hours for the lower reducer vessel. This is reasonable considering that this vessel has the largest diameter (approximately 19 inches). This is also conservative compared to the MTF calculation (which has a diameter of 40 inches).

Warm up curves are shown in the attached graphs for each component **Figure 8-7** through **Figure 8-12**.

## Conclusions

1. The prototype can be heated up and operated within a reasonable time. The warm up will require up to 8.4 hours.
2. The steady state heat loss is low enough to allow the process to maintain process temperature. The steady state heat loss from the major components is about 3.6%.

Heat loss Summary			
	Steady state:	Target Heat loss for warm up	
	Btu/hour	Btu/hour	warm-up time -hours
Combustor	63,458.94	136,436.73	5.15
Reducer upper	70,368.98	151,293.32	6.03
Reducer Lower	25,050.20	53,857.93	8.46
Feed pipes	149,750.79	321,964.21	0.83
Calcliner	50,100.40	107,715.86	8.41
Total losses	358,729.32	771,268.04	
% of input	3.59%	7.71%	
reference :			
MTF	253,070.01	544,100.53	calc 16.89 data 15.0 - 18.0
% increase in heat loss to get target for warm up		115%	

**Table 8-4 - Heat Loss Summary**

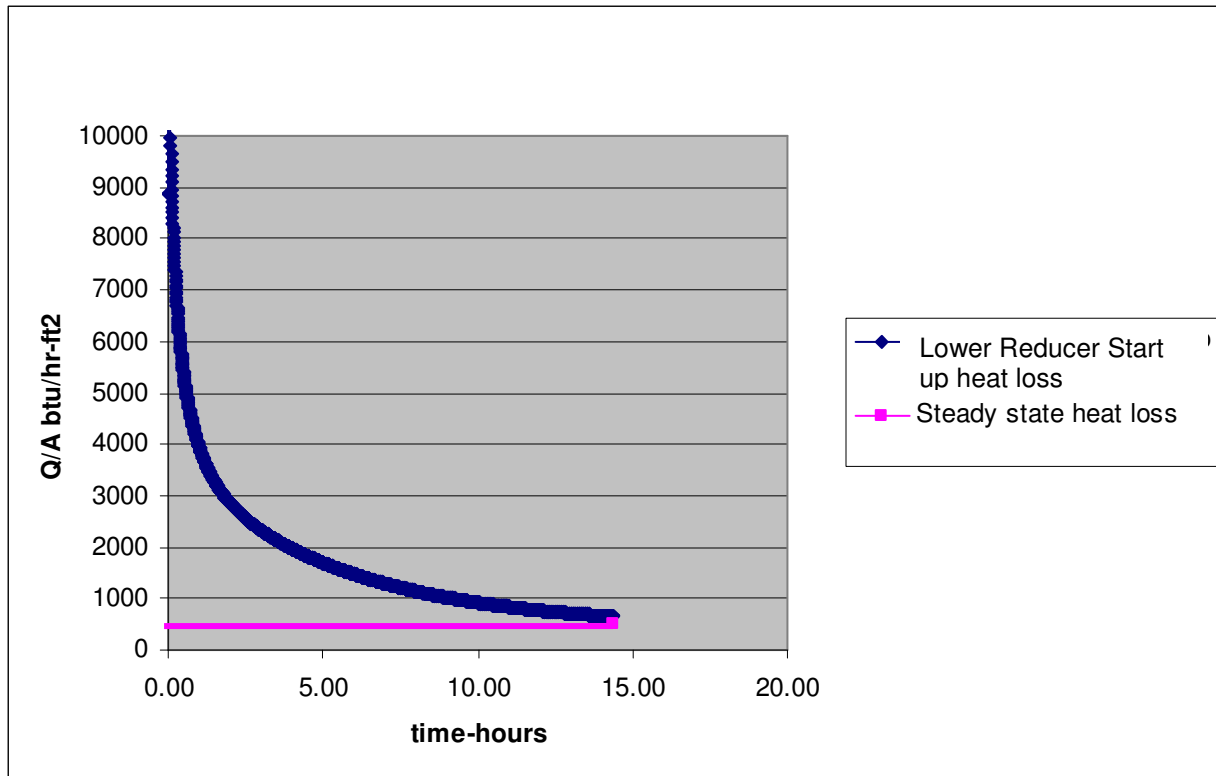


**Figure 8-7 – lower reducer Startup Heat Loss**

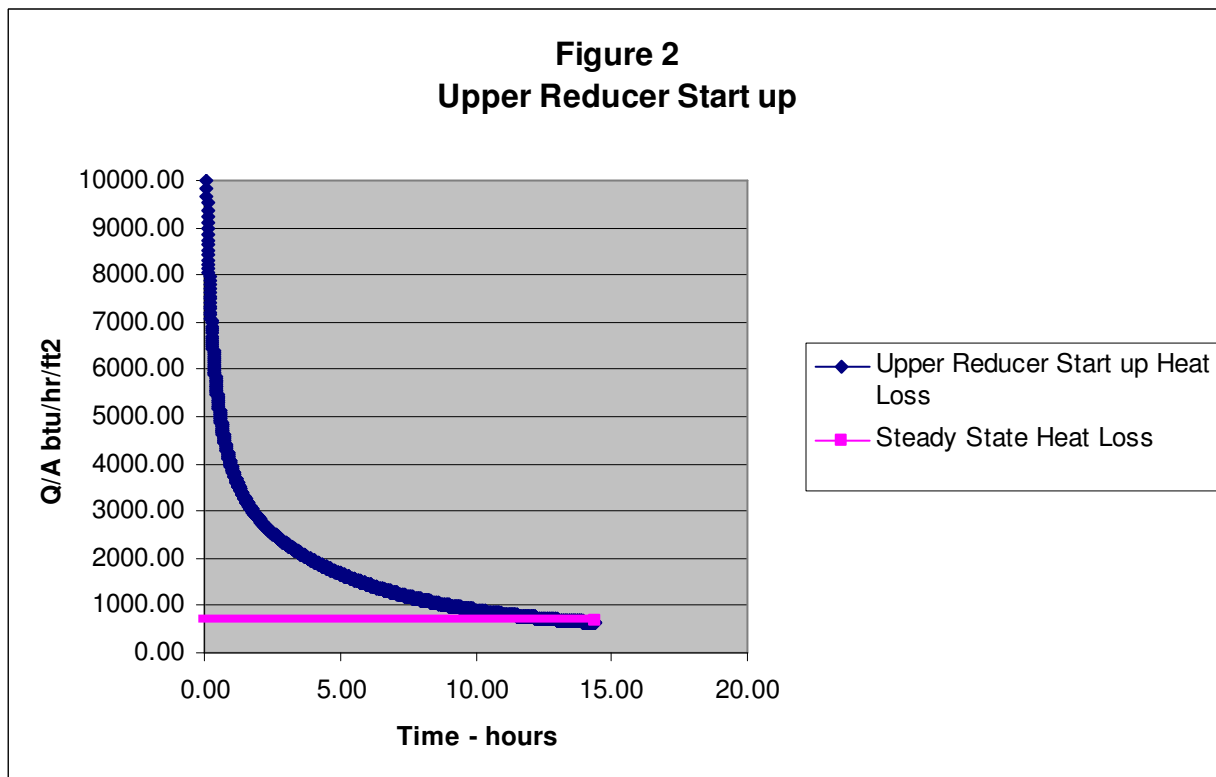


**Figure 8-8 – Upper Reducer Startup Heat Loss**

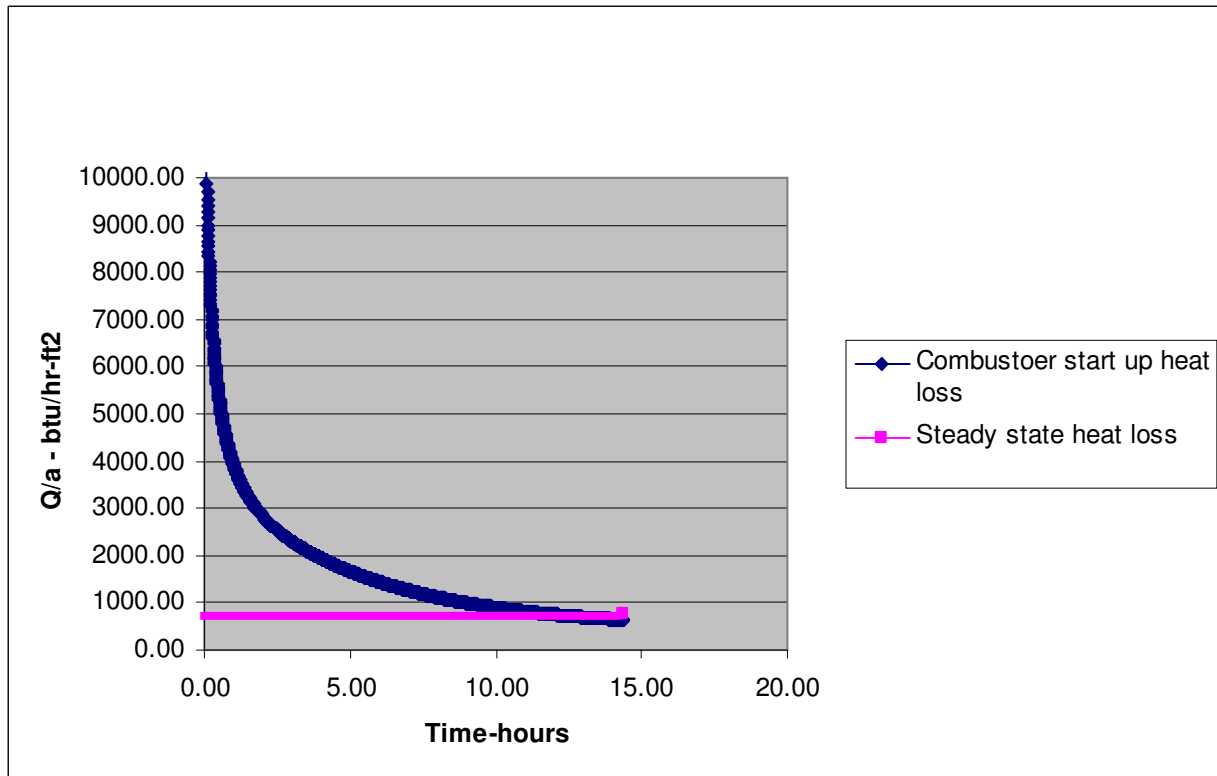


**Figure 8-9 – Oxidizer Startup Heat loss**

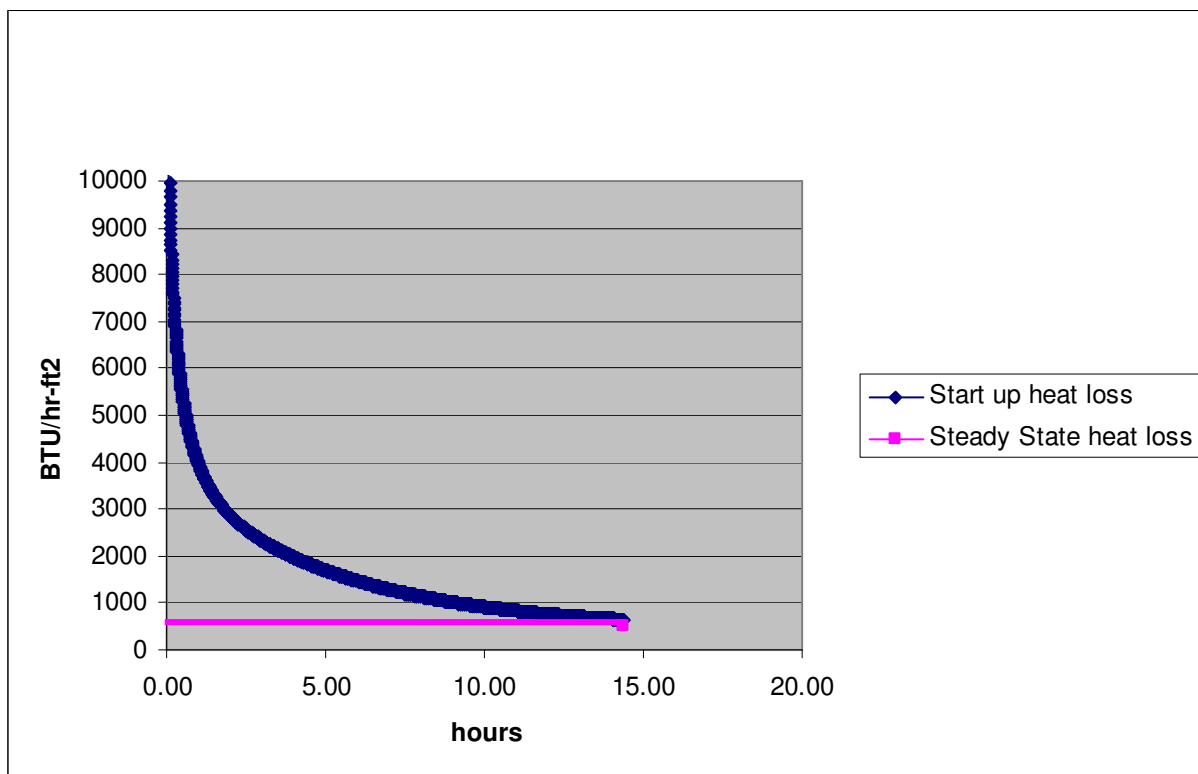


**Figure 8-10 – Calciner Startup heat Loss**

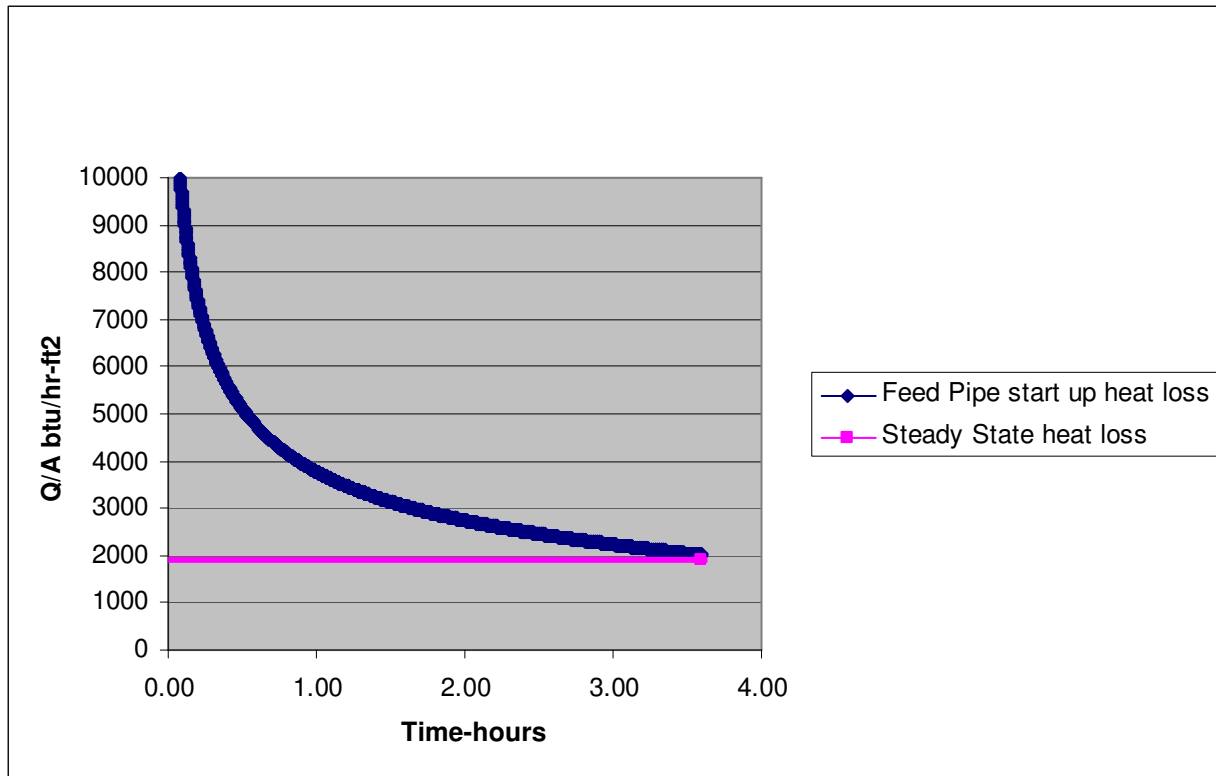


Figure 8-11 – Feed Pipe Startup Heat Loss

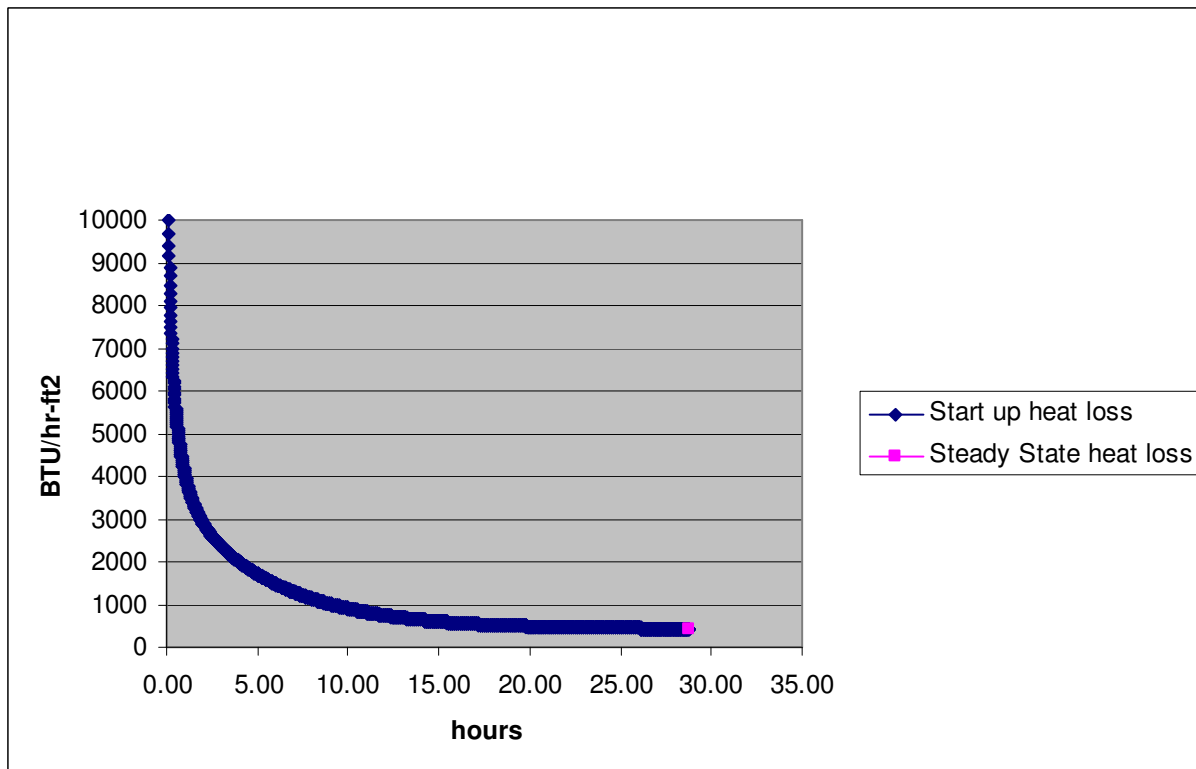


Figure 8-12 – MTF Startup Heat loss

## 8.6. Chemical Looping Applications

### 8.6.1 Integration of a PC Fired Boiler with Hydrogen from a Chemical Looping Gasification System and CO<sub>2</sub> Capture

The objective of this brief study was to examine the impact of firing a synthetic-gas fuel, consisting of nearly CO<sub>2</sub> free hydrogen produced by the Chemical Looping gasifier, on boiler performance in a PC designed boiler. In addition, the study assessed boiler island equipment modification requirements and any potential barriers to boiler conversion and integration with the chemical looping system.

Since the main driver for boiler conversion is CO<sub>2</sub> emission reduction, economic comparison with other potentially competing technologies, such as O<sub>2</sub> firing with a CO<sub>2</sub> (flue gas) recycle system and ammonia-scrubbing system was made. To this end, approximate investment costs and performance were estimated for the three retrofit technologies and an economic analysis was carried out. Since detail analyses were beyond scope of this study, much of the technical and cost information was prorated from previous reports described in **Reference 2**.

#### Base Case Unit

A base case unit, a state-of-the art supercritical sliding pressure PC fired boiler, was selected for performance analysis. It is an 800MW (nominal) rated capacity, open upper furnace unit with the outlet steam conditions of 1055<sup>0</sup>F/1105<sup>0</sup>F/3732psig. **Figure 8-13** illustrates the boiler arrangement. The boiler is equipped with two 34.5', Ljungstroem<sup>®</sup> air heaters, 92"deep, and 6 HP1043 model pulverizers. A normal mode of operation includes 5 mills in service with each mill operating at a grinding capacity of 82.41% when grinding the design PRB coal. The coal analyses are shown in **Table 8-5**. The boiler is fired with 18% excess air and operates at a boiler efficiency of 87.05%. It consumes approximately 825,800 lbs/hr of coal.

#### 1. Boiler Conversion

**Reference 2** Case 13 lists various performance ratios in relation to coal heat input in the chemical looping system. These ratios are:

- a) 10.8% of total energy released in the chemical looping system goes into production of steam for power generation
- b) Chemical and sensible energy contained in the synthetic gas is 85.5% of the total energy released
- c) Gasifier heat losses are 3.7% of the total energy released
- d) Internal steam consumption used in the production of synthetic fuel is 1.034 lbs of steam/lb of coal
- e) Air requirement for the chemical looping system is 3.31 lbs/hr/lb of coal

**Table 8-5 – Coal Analysis**

	Caballo
DESCRIPTION	Mean
Coal Rank	Sub C
Proximate, Wt. %	
Moisture	29.90
Volatile Matter	31.10
Fixed Carbon	34.00
Ash	5.00
TOTAL	100.00
LHV, Btu/lb	7,835
HHV, Btu/lb (calc'd)	8,500
Lb Ash/10 <sup>6</sup> Btu	5.88
Ultimate	99.99
Moisture	29.90
Hydrogen	3.43
Carbon	48.84
Sulfur	0.35
Nitrogen	0.70
Oxygen (dif)	11.77
Ash	5.00
Grindability	59
Ash Fusibility	Reducing
I.T. Deg. F	2,130
S.T.	2,140
H.T.	2,150
F.T.	2,160
Ash Fusibility	Oxidizing
I.T. °F	2,195
S.T.	2,205
H.T.	2,215
F.T.	2,225

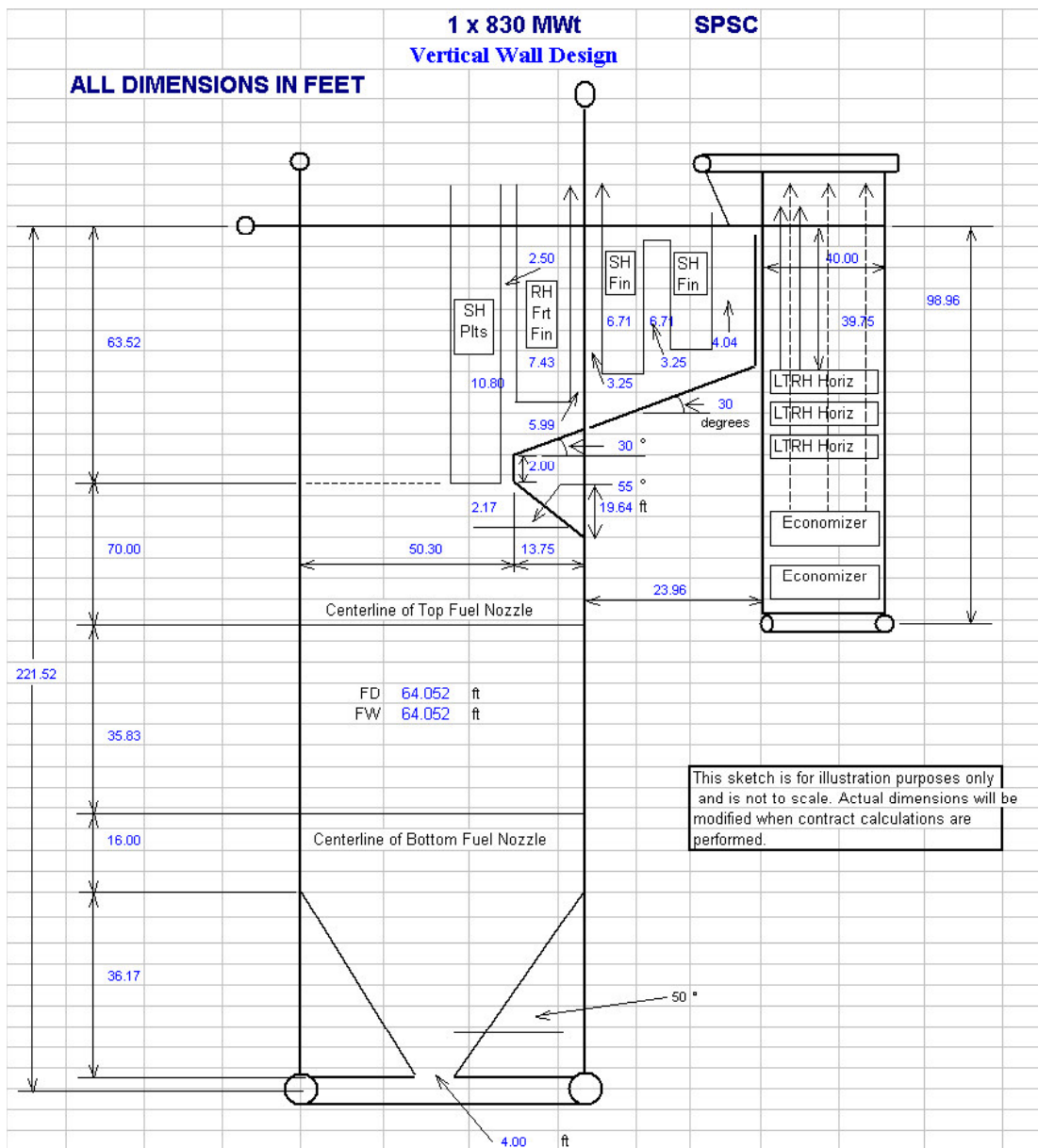


**Figure 8-13 – PC Steam Boiler**

It was assumed that these ratios would apply for the conversion case also. The synthetic fuel analysis produced in **Reference 2** and used in this study is as follows:

Composition	%Weight
H <sub>2</sub>	97.09
N <sub>2</sub>	1.34
CO	.61
H <sub>2</sub> O	.96
HHV= 44,899Btu/lb	

It was also assumed that when the PC boiler is constructed provisions will be made for a future chemical looping system installation and that the system could be installed within 100-150 ft from the existing boiler.

Two chemical looping gasifier integration schemes were considered. In the first one, the boiler and chemical looping systems integration was limited to the water/steam side and coal handling and preparation systems only. Consistent with the assumptions listed above, 10.8% of the total energy released in the chemical looping system was converted to power steam. Consequently, the boiler generating output was de-rated to maintain the same steam turbine generator gross output as for the base case. Steam produced in the retrofit boiler was combined with the steam from the chemical looping and the combined steam was routed to the steam turbine.

Steam turbine heat load was 6110 mmBtu/hr of which 825 mmBtu/hr was produced within the chemical looping system and the balance, 5285 mmBtu/hr, was generated in the boiler by firing the synthetic gas. To facilitate the required steam and synthetic gas production, approximately 7635 mmBtu/hr of coal heat input was fired in the chemical looping system.

Boiler performance was estimated and critical components such as the boiler fans and their capacities were checked. The existing primary air and secondary air fans had sufficient capacities to provide boiler combustion air. The primary air was decoupled from the mills and the flow from the air heater, was directly re-routed to the windbox.

The windbox, which has coal piping and coal nozzles along with the air compartments, may require some modification to accommodate synthetic gas fuel firing. While the exact modification is yet to be determined, it is not envisioned to be significant or requiring any pressure parts modifications. Coal piping together with the pulverizers need to be either retired from service or converted for use in the chemical looping system.

The air heaters depth was increased from 92" to 104" to increase heat transfer surface and to improve boiler efficiency and reduce the synthetic gas-firing rate. Generally, the air heaters have additional space at the cold end to enable additional surface installation.

The existing ESP system was not required to meet boiler particulate emission requirements since there was no ash in the synthetic gas fuel. The best use for this component needs yet to be determined.

The flue gas contained a significant amount of water vapor generated from burning H<sub>2</sub> in the fuel, which reduced boiler efficiency by approximately 6%. If the water vapor were condensed and reclaimed from the flue gas, it would require a number of additional systems and components including condenser, a water treatment plant and a water condensate recycling system. However, in this study, no recovery system was

used and the process water was a consumable. Future studies will need to address the most appropriate strategy for this issue.

Since some power steam was generated in the chemical looping system, the boiler generated approximately 86% of the MCR load. Performance comparison between the coal fired boiler and the retrofit Case 1 is shown in **Table 8-6**.

**Table 8-6 – Performance Comparison  
between the Base Case and Retrofit Case 1**

	Base Case	Retrofit Case 1
Boiler Heat Duty (10 <sup>6</sup> Btu/hr)	6110	5285 (+825 in the Chem Loop.)
Steam Conditions	1055 <sup>0</sup> F/1105 <sup>0</sup> F/3732psig	1055 <sup>0</sup> F/1105 <sup>0</sup> F/3732psig
Q fired in the Boiler ( 6110*10 <sup>6</sup> Btu/hr)	7019	6535 (7635 in the Chem Loop)
Boiler Eff. %	87.05	80.89
Coal flow in the system Lbs/hr	825,779	898,235
PA Fan Flow lbs/hr	1,532,000	1,044,000
FD Fan Flow lbs/hr	4,789,000	4,914,000
ID Fan Flue Gas Flow lbs/hr	7,418,000	6,397,000
Excess Air %	18	20
Tilt	-20 <sup>0</sup>	21 <sup>0</sup>

In the second Case study, the integration between the boiler and the chemical looping system was expanded as shown on **Figure 8-14**. In this design case, the coal piping was modified and the primary air-coal mixture was piped to the gasifier vessel where the “wet” air was separated from the coal and was piped back to the boiler windbox. In this design the following components were affected and needed to be modified or added:

1. The coal piping was re-routed from the boiler to the gasifier. The coal piping diameter could be the same since the primary air flow was approximately the same as in the Base Case.
2. The mills were modified to yield coarser size particles for transport to the chemical looping system.
3. A cyclone was installed to separate primary air from coal. (Materials of construction should be consistent with the air and coal mixture temperature of 140F.)
4. An air duct was provided from the gasifier to the windbox for the primary air.
5. A booster fan was provided for the primary air.
6. The windbox and windbox internals were modified to accommodate the new synthetic gas fuel.

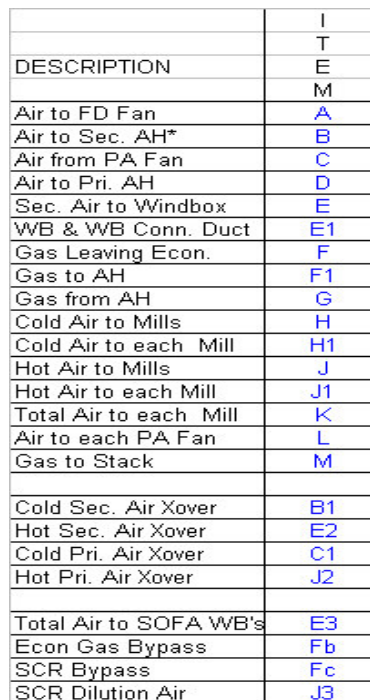
7. The air heaters depth was increased from 92” to 104”.

The boiler generated approximately 86% of the MCR load. A performance comparison between the coal fired boiler and the retrofit is shown in **Table 8-7**.

**Table 8-7 - Performance Comparison  
between the Base Case and Retrofit Case 2**

	Base Case	Retrofit Case 1
Boiler Heat Duty (10 <sup>6</sup> Btu/hr)	6110	5297 (+813 in the Chem Loop.)
Steam Conditions	1055 <sup>0</sup> F/1105 <sup>0</sup> F/3732psig	1055 <sup>0</sup> F/1105 <sup>0</sup> F/3732psig
Q fired in the Boiler ( 6110*10 <sup>6</sup> Btu/hr)	7019	6562 (7536 in the Chem Loop)
Boiler Eff. %	87.05	80.65
Coal flow in the system Lbs/hr	825,779	885,790
PA Fan Flow lbs/hr	1,532,000	1,290,000
FD Fan Flow lbs/hr	4,789,000	4,161,000
ID Fan Flue Gas Flow lbs/hr	7,418,000	6,334,000
Excess Air %	18	19.5
Tilt	-20 <sup>0</sup>	20 <sup>0</sup>

The comparison between Cases 1 and 2 indicates some small differences in boiler performance between them. It is believed that these differences should get even smaller with more accurate heat and mass balances for the total plant systems. Regardless of the design choice, either Case 1 or Case 2 is feasible. The boiler can be converted to firing the synthetic gas fuel and with very modest modifications. While the ultimate choice between the two cases comes down to the cost, the analyses didn't show any obvious superiority of one system over the other.



September 30, 2008

## Conclusion

This brief study examined boiler performance and key barriers to re-powering PC fired boilers to fire the CO<sub>2</sub> free hydrogen synthetic fuel produced by the chemical looping system gasifier. The boiler performance was achieved with minimum boiler island modifications and no barriers were found to boiler re-powering or integration with the gasifier system. The economic comparison with other potentially competing technologies such as an advanced post combustion CO<sub>2</sub> scrubbing system and O<sub>2</sub>/recycle flue gas system illustrated that the chemical looping technology is more cost effective than the O<sub>2</sub>/recycle flue gas system and is similar in cost to the ammonia scrubbing system. The small differences in cost are believed to be well within the accuracy range of the analysis. As these technologies mature, the analysis should be revisited for a more thorough examination.

## 8.7. Prototype Preliminary Design

The simplified process flow diagram (PFD) for the prototype was shown in **Figure 8-1**. The main process equipment internal dimensions were given in **Table 8-2**. Refractory recommendations were given in **Section 8.4**. Based on this information a preliminary prototype mechanical design was generated.

The refractory recommendations for the heated lines and vessels were modified based on the calculations performed in **Section 8.5**. The refractory thickness was set at 6 inches with another one inch of insulation and a vessel shell thickness assumed to be  $\frac{1}{4}$ ". The smaller refractory thickness was used because the MTF vessel, which has a similar heat input, uses that construction. The refractory heat loss calculations done in **Section 8.5** predict an outside surface temperature about the same as the material recommendations for the commercial plant listed in **Section 8.4**. Finally, the smaller refractory dimensions give a faster heat up time for the prototype plant than the MTF.

Very rough sizes were estimated for other process equipment such as cyclones and the moving bed heat exchangers. While these estimates were rough, the dimensions used are based on valid flow calculations for the prototype mass flows. Since the details of these designs are not complete, the actual dimensions are not listed.

The prototype design was generated to develop a first estimate of the building dimensions and to check the cost estimates for the Phase IV program. The plant is shown in **Figures 8-15 and 8-16**. The main process vessels are relatively small compared to the MTF unit. It is interesting that there are pipes that seem to be very large. The internal diameters of these pipes are quite small but they need to have thick refractory linings and are more noticeable.

The reducer in the prototype plant will operate at a slightly elevated pressure compared to the oxidizer and calciner. The pressure difference will require that the transfer lines between vessels will have to include lift lines, standpipes and let down lines. This adds to the number of lines shown in the drawings.

The prototype design generated a list of material weights that was used to check the cost estimates for Phase IV. The Phase IV design study will optimize the prototype design so this design should not be considered the final design.

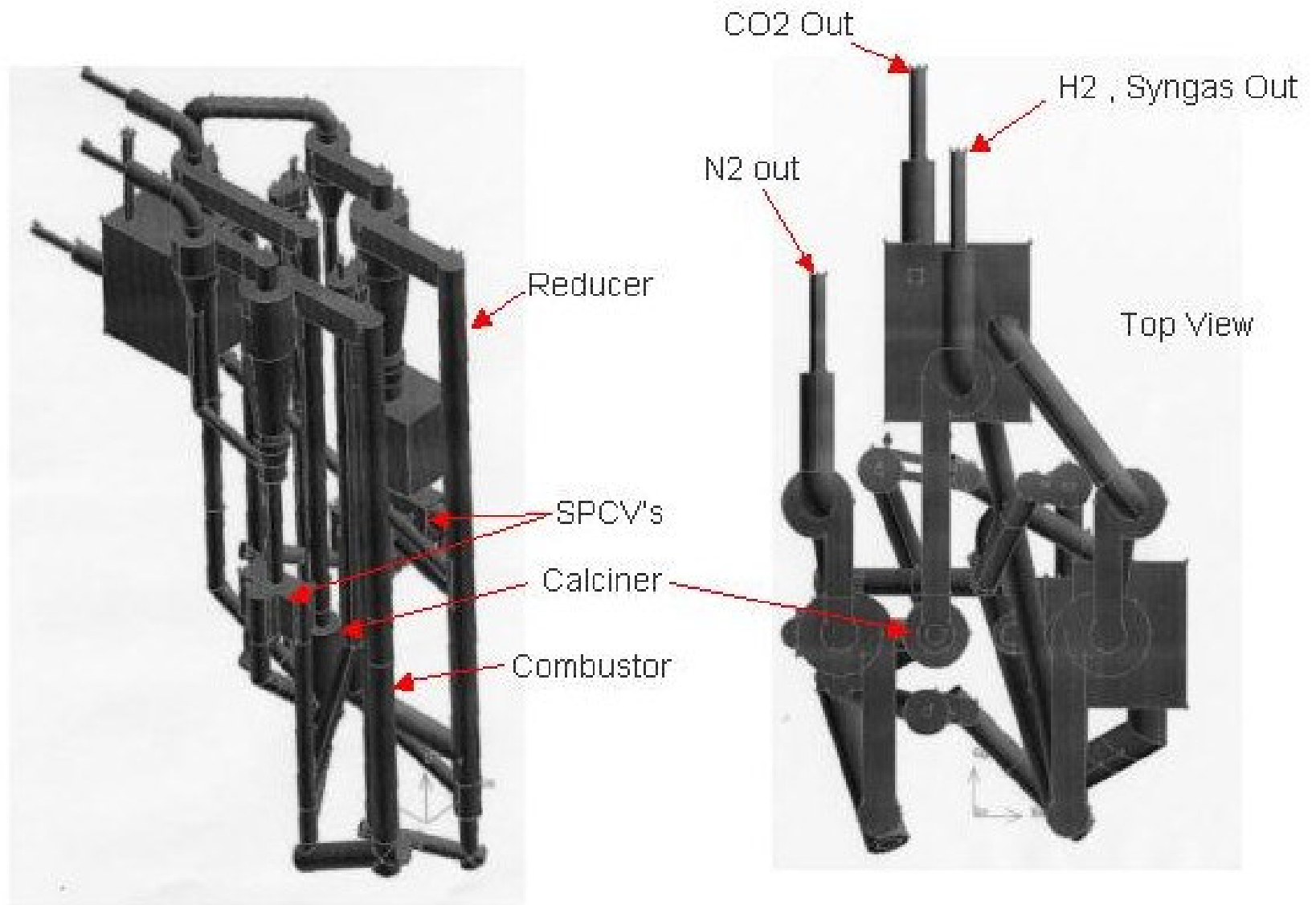


**Figure 8-15 - Preliminary Prototype Design Isometric View and Top View**

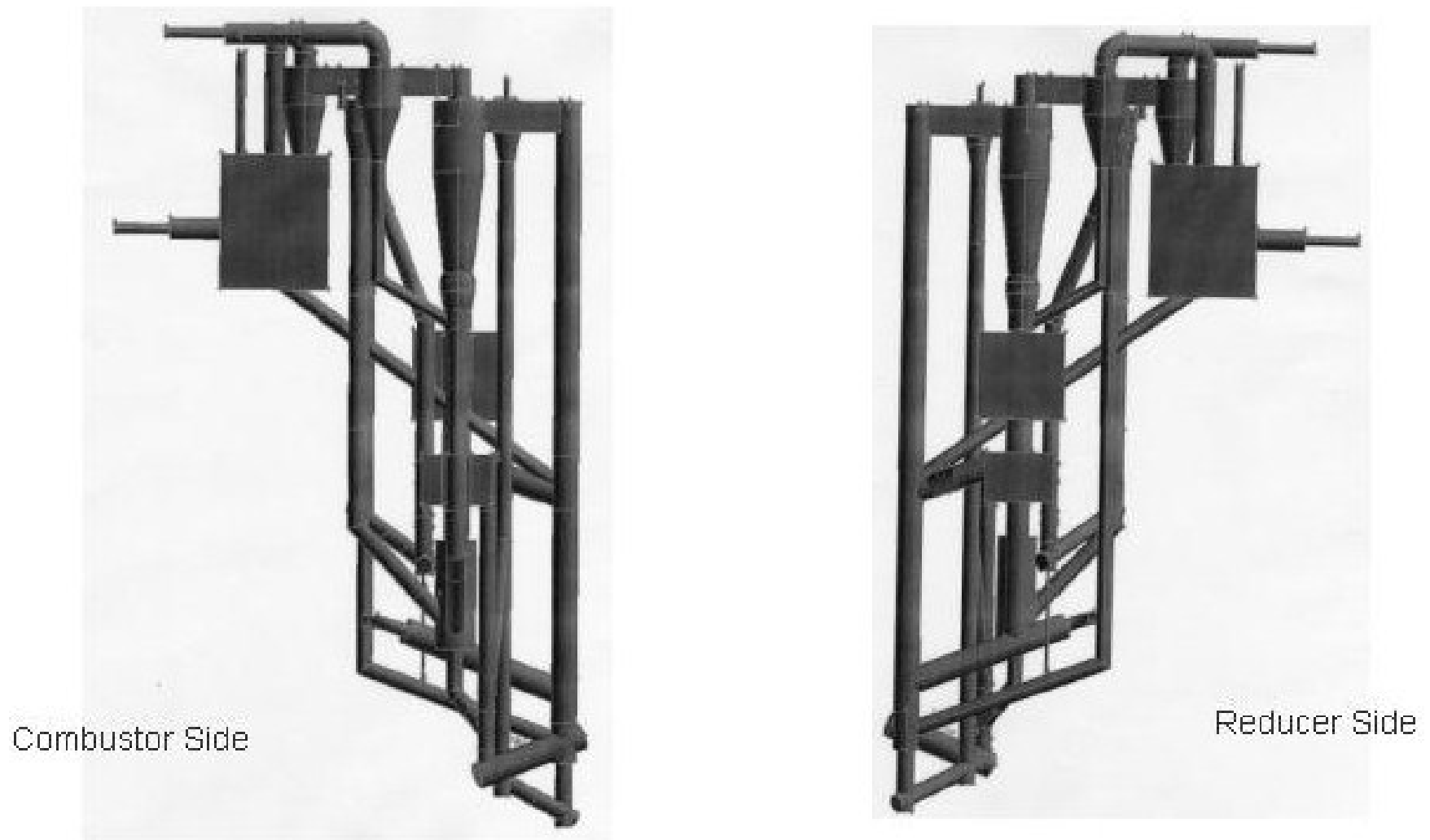


**Figure 8-16 -Preliminary Prototype Design Side Views**

## 8.8. CFD Modeling

### 8.8.1 Introduction

Alstom evaluated the performance of selected geometries to determine the viability of CFD techniques to assist in the development of Alstom's chemical looping system.

This section describes the application of Barracuda to the 4-inch diameter, 40-foot cold flow model described in **Section 6**. The lower portion of the loop was modeled and run for two different gas/solids ratio conditions for which the solids flow rate was determined. These simulations represented 40 seconds of model operation. From the predictions, temporal distributions of gas velocity, particle velocity, solids concentration and pressures were extracted and analyzed.

Predicted pressure profiles were compared to measurements at 10 different positions. The predictions were found to correlate reasonably well to the data. Overall pressure drop was matched to within 10% (see light blue overall DP curves of **Figure 8-37** and **Figure 8-38**, where charted measured values are approximately 150 inches H<sub>2</sub>O +/- 5 inches versus 162 inches H<sub>2</sub>O +/- 10 inches predicted, which is within 10%). Sectional pressure drops were reasonable in the upper riser section as well. Some discrepancies were noted near the solids pick-up, which are described in the context of the modeling assumptions and boundary conditions. Qualitative comparison of the particle flows showed that the model is able to capture some of the more interesting features.

This specific application of CFD modeling to chemical looping using Barracuda provides a useful benchmark study to assess the feasibility and predictive accuracy of the software.

It is clear that CFD is not suitable to replace cold flow modeling for several reasons. In contrast to CFD modeling of single-phase flow geometries such as ductwork, modeling two-phase systems requires several orders more computer time. To achieve only 40 seconds of simulation time required 3 weeks of CPU time for a subset of the cold flow loop. Alstom currently does not have the computational resources to fully exploit the potential of this software. However, this application initiative is important to extrapolate how Barracuda could be applied to subsequent phases of the chemical looping project.

Barracuda appears to be a powerful simulation tool that could be applied to equipment scale-up and component optimization. There is still a need for additional validation. The pressure-cells, data sampling and logging system and associated flow visualization observations were not designed for CFD model validation. Subsequent tests could be performed in the cold flow model to better validate this set of Barracuda predictions.

### 8.8.2. Description of BARRACUDA Software

Barracuda utilizes an innovative numerical technique to couple a vast collection of discrete particles trajectories in a gas/solids system. Using a transient solution technique, the concentration of solids in any given computational cell is correlated to a pressure term that controls the trajectory of individual particles and limits the ultimate packing density.

This approach allows the effect of individual particles to feel the impact of other particles, without resorting to calculation of specific particle-to-particle impaction and rebounds. Particle impaction and rebound from surfaces is determined by prescribed normal and tangential restitution coefficients. A maximum solids concentration (packing density) must be defined for the solids mixture.

Barracuda is different from other commercial CFD software that can simulate a collection of individual particles by sequentially integrating the laws of motion coupling the particle momentum forces back to the gas phase in an alternating fashion. Typically, the collection of particles is tracked through the domain from the injection point all the way through to the exit. The resulting momentum exchange is updated.

Barracuda's transient particle tracking moves all of the particles by a single time increment only. The incremental movements from each time step generally represent a small displacement. After the set of particles are displaced during each time step, the mass and momentum equations for the continuous phase and local solid volume fraction are updated and converged. This appears to be a quite stable algorithm. The solver can automatically reduce time step size based on local convergence rates, current number thresholds or other condition as needed, then increase the time step interval to the prescribed value without intervention. This makes the solver robust and efficient. However, a transient CFD model requires sufficient simulation time to encompass a desired transient event or to capture the characteristics of relatively steady-state flow systems. Depending upon the geometry, this could result in very long run times.

The software consists of the main solver, the mesh generation tool, and a separate post-processor that reads compact graphics files

A general purpose post-processor called GMV is included. A view of the modeled U-tube geometry appears in **Figure 8-17**, illustrating the surface mesh with the flux planes defined in the lower section. Surface triangles are used to represent the trimmed hexahedral computational cells. A range of display options and utilities are found in under the various pull-down menus. Inside the object window, traditional pan-rotate-zoom controls allow manipulation of the object.

At the problem setup, the specific Eulerian or Lagrangian variable to be included in the incremental output "gmv" files needs to be prescribed. Once this set is defined, it cannot be modified without restarting the calculation. The output files contain all the data for the pre-selected variables. A nice feature of this approach is that the entire record of data can be reloaded after the run is done to generate animations or plots from any viewpoint. This is quite powerful, considering that most commercial CFD packages typically generate a fixed set of plots for each time step and does not save all the data at multiple time intervals.

These binary gmv files are relatively compact, depending upon the grid size and number of variables to be written at selected time intervals. The GMV post-processor is also

public-domain software, and does not require a license. Thus, extensive post-processing can be conducted on multiple machines, without the licensing limitations of the solver.

Other output files, such as flux planes are predefined in the setup phase and can provide detailed breakout of the particles passing each plane. Also include are gas flow rates, fluxes and others.

To monitor the pressures in the same locations that the pressure taps are located, transient monitor probe points were defined. These probe points recorded pressure at each time step.

Associated with the generation of animation sequences, a time index is included in the upper right. There is no control over the format of this number, and the units are always in seconds. Several different methods are available to the user for representation of particles. These can be based on a pixel representation for each particle, or the particles can be scaled to their relative size.

A limited range of different particle variables, including volume fraction, radius, and velocity are available. Currently, only the total velocity magnitude, not component velocities can be plotted. Other features include the ability to calculate custom variables, iso-surfaces, planes and clipping utilities in Gmv. For an animation sequence, a specific view and variables are selected. An automated reader pulls the data in from a set of gmv files written at intervals. The batch of images files can be merged into a MPG animation file with included utilities.

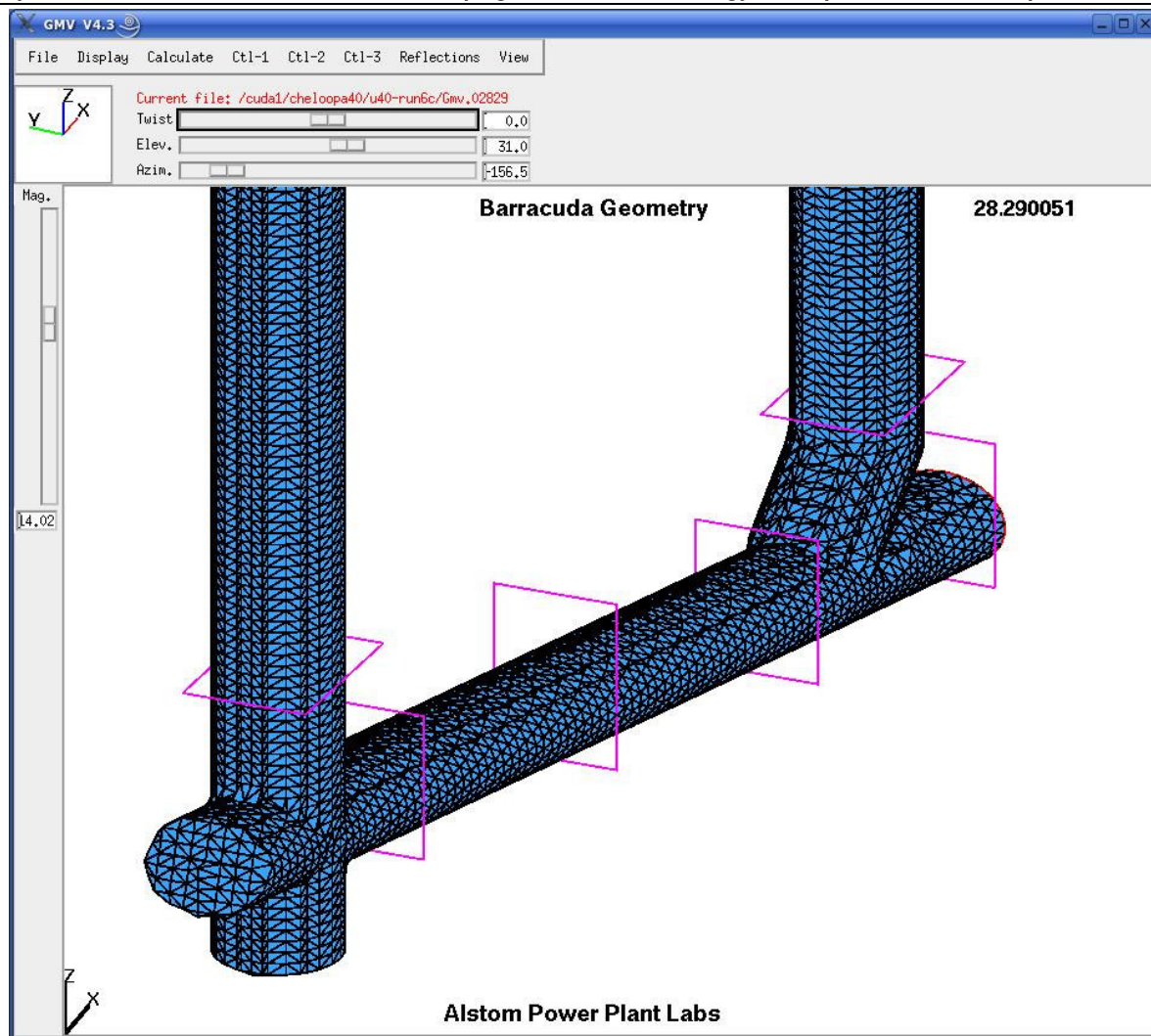


**Figure 8-17 - View of the GMV post-processor window showing the surface mesh and flux planes**

### Geometry of Model

Barracuda was used to simulate the 4-inch diameter, 40-foot tall cold flow model of the Chemical Looping system. A schematic of the loop is shown in **Figure 8-18**. The aspect ratio of this geometry, combined with the existing equipment in the area of the test loop makes it difficult to photograph. Details of the lower section are expanded in the figure to show the important lower section of the test loop that was modeled. The solids return from the two cyclones collects in a 6.875" diameter return pipe into the SPCV. The control valve regulates the solids flow into the pick-up section where transport air entrains solids in a mixing tee near the end of the 20° inclined pipe.

The SPCV was not modeled in these Barracuda simulations. Instead, the solids were fed into the pipe at the location corresponding to the discharge of the solids control valve. The transport airflow is accelerated at the solids pick-up point with a tapered constriction known as the sugar scoop. The solids are blown up the inclined pipe through a tee up the

vertical riser. The riser is approximately 40 feet tall. The geometry modeled with Barracuda is shown in **Figure 8-19**.

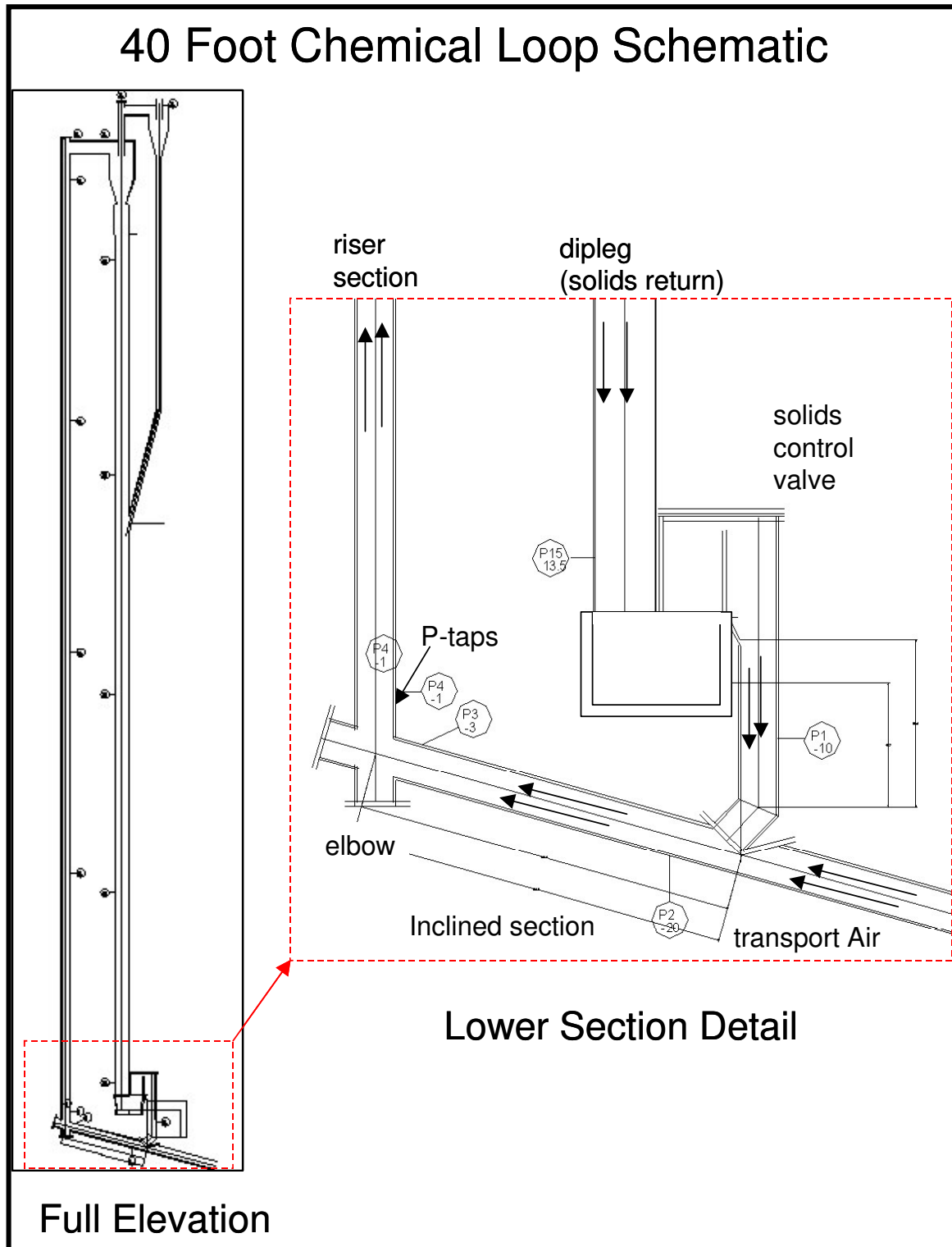


**Figure 8-18 - Schematic of the Chemical Looping 40ft Flow Model**

The mesh was generated from a CAD file generated from measurements of the flow model geometry. The lower section of the model is shown in **Figure 8-20**. The blue dots in this figure are monitor points for which pressure data was extracted. The locations of these dots are aligned with the pressure taps in the cold flow model. In addition, the boxed zones are flux plane surfaces that monitor the gas and solids flows passing. These planes also provide information about the particle size distribution passing each plane, which is useful in some cases to examine size segregation effects.

A mesh was applied to the model that was finer near the lower section and coarser in the upper straight pipe as shown in **Figure 8-21**. This allows the gradients near the transport air solids pick-up and mixing elbow to be refined. The single block mesh included 212,800 cells (96 x 8 x 280). After the mesh tool processed the cellblock to carve out the relevant cells, only 26,745 cells were calculated. A much finer mesh would typically be used for a CFD flow calculation using body fitted coordinates to better represent the geometry. However, because of the extensive computational effort to attain these solutions, the goal was to use as coarse a grid as possible to accelerate the process. This limitation is relevant to future studies.

### Test Conditions:

Two different test conditions were selected. The two runs represented a “high” and “low” solids to gas ratio condition. The normal solids to gas case was representative of a condition that transported a significant level of solids on a continuous basis. The low solids to gas test was included to evaluate the differences in solids distribution and pressure drop. The solids flow was measured in the loop by rapidly closing a butterfly valve in the solids return leg and calculating solids flow based on the accumulated weight over the period the valve was closed (See **Section 6**). During the solids flow test, the transport airflow and pressure measurements were stable both before and after the solids flow determination. For reference, the two model runs were based on test loop experiments conducted on two different days. The flow rates for these two tests are listed in **Table 8-8**.

**Table 8-8 – Test Conditions for Barracuda Simulation**

Run	Solids	S/G	Transport	Solids	Test	Time
Number	Levels	Ratio	Air - lb/hr	lb/hr	Date	HH:MM
1	High	39.3	1164	45,691	9/28/2007	14:24
2	Low	21.5	840	18,083	9/19/2007	13:17

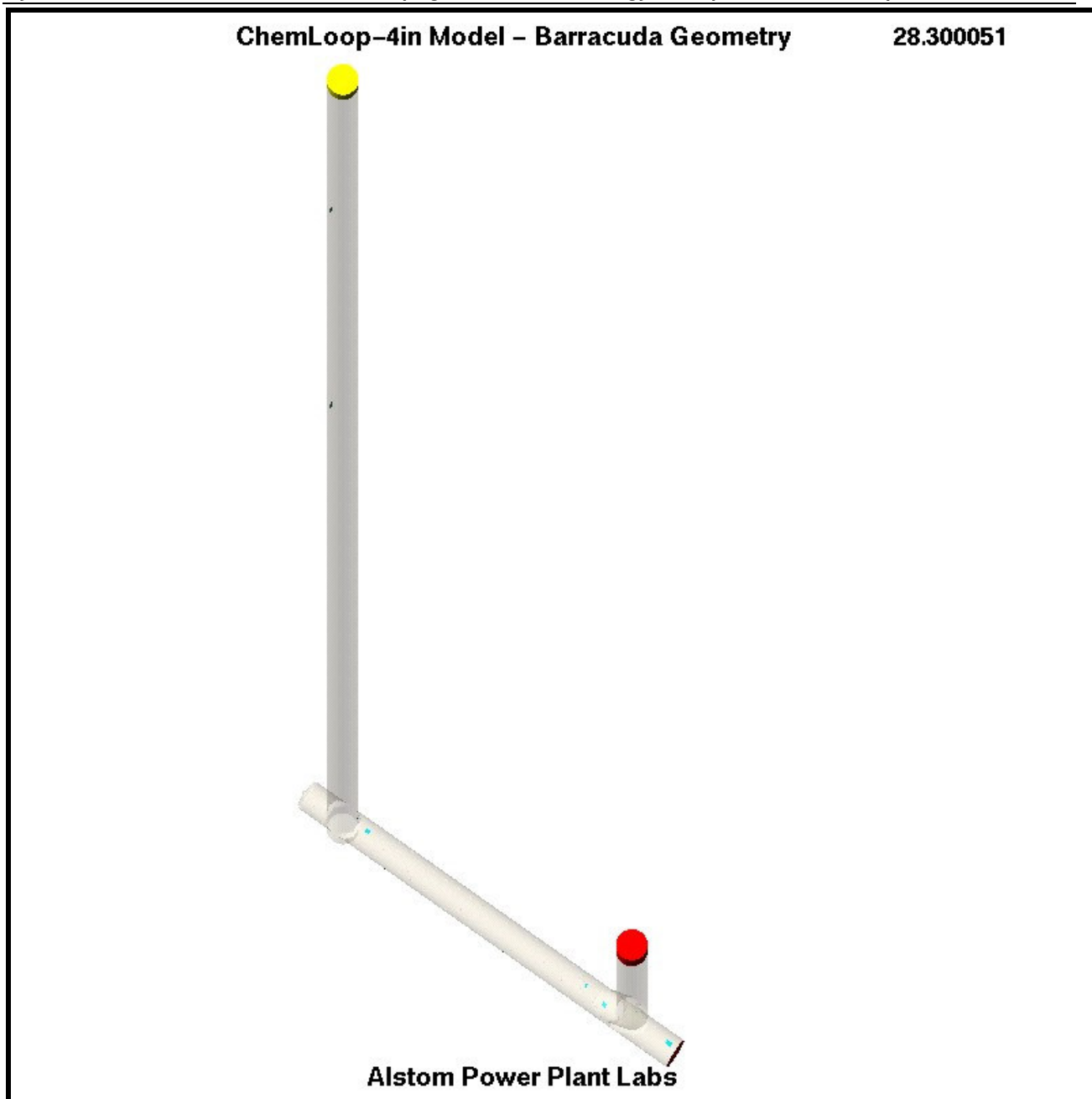


**Figure 8-19 - Geometry of the modeled section of the cold-flow loop**

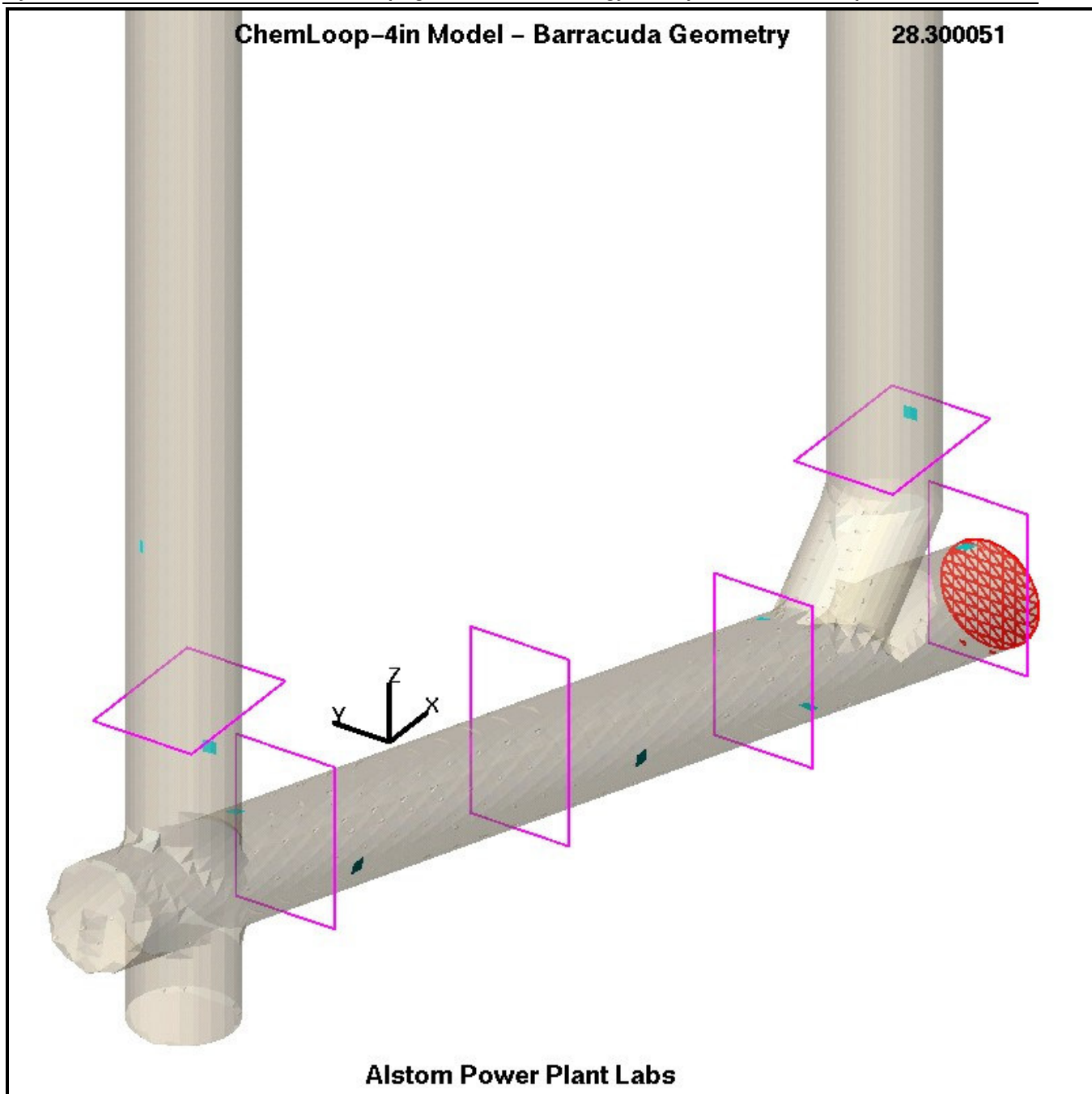


**Figure 8-20 - Geometry of Lower Section**

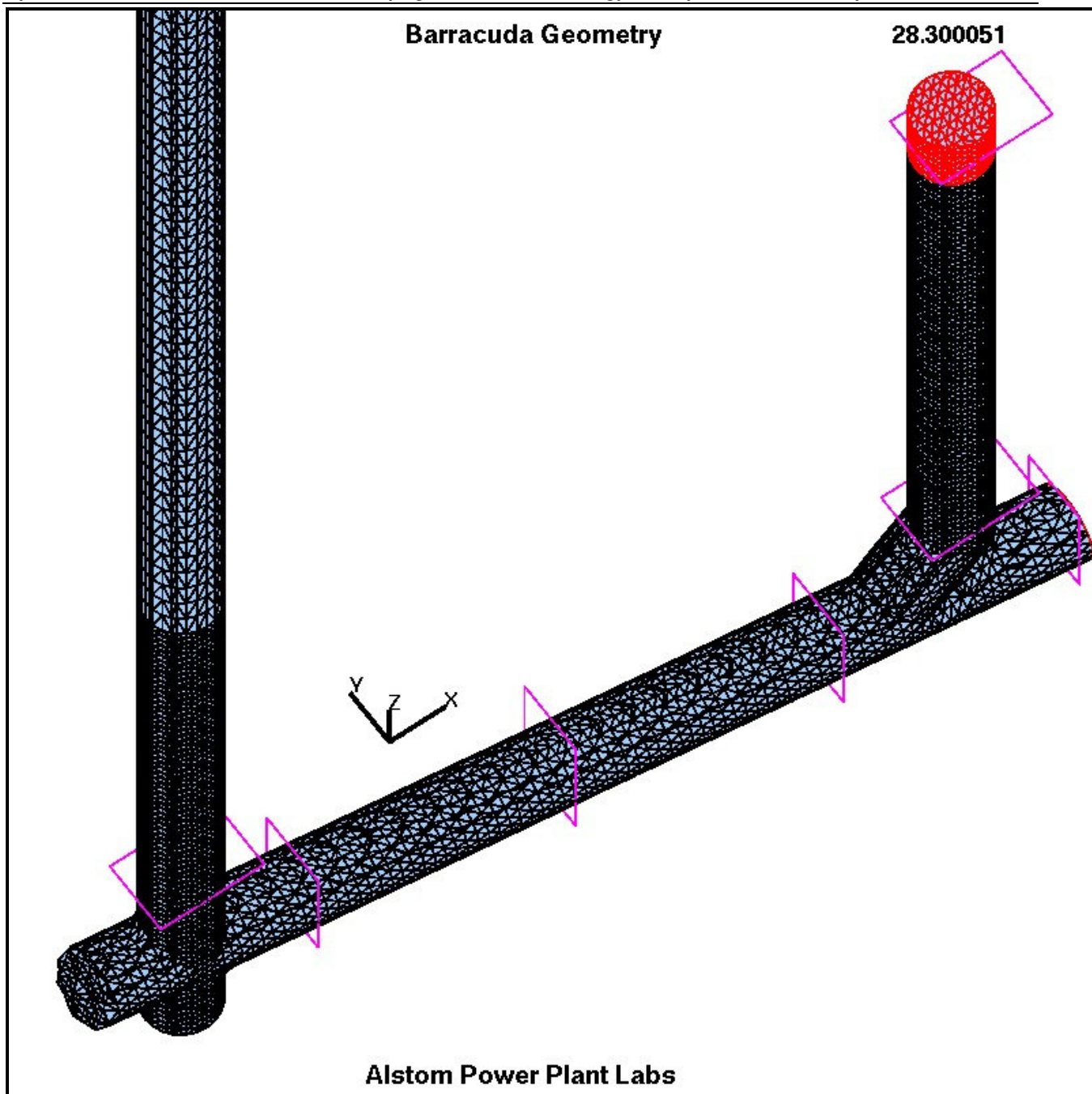
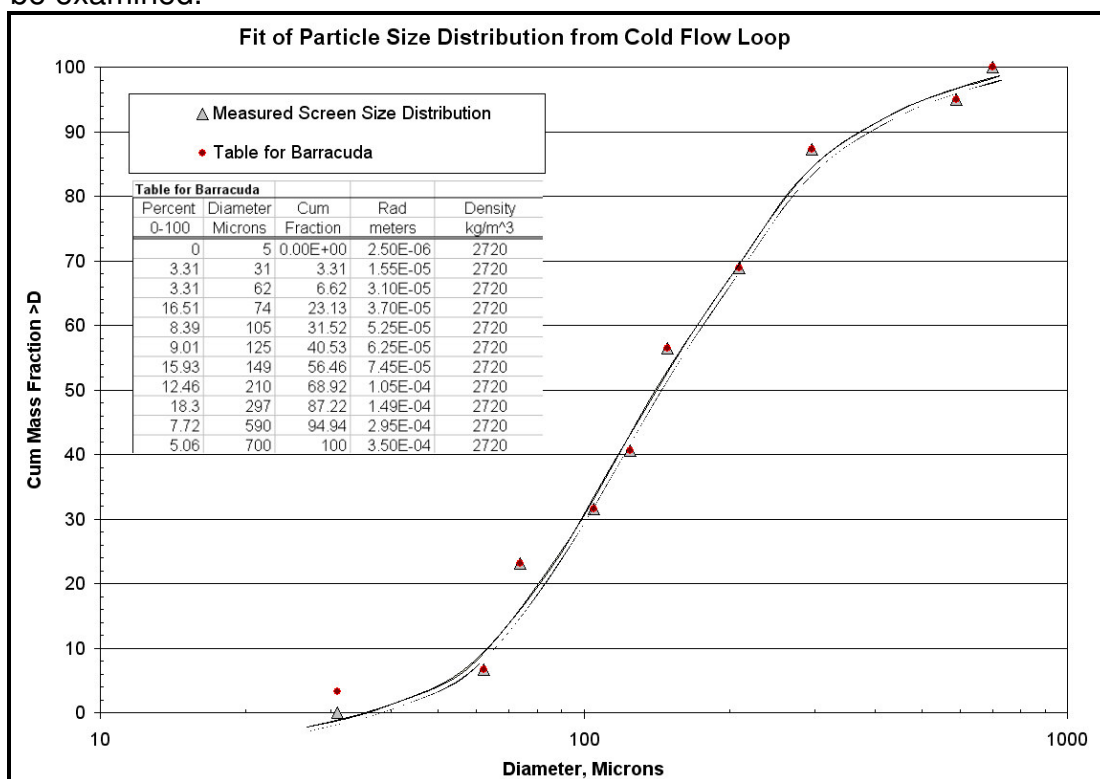


Figure 8-21 - Mesh for the lower section of model.

The solids description used in this simulation was based on an analysis of the typical flow model ash. A definition of the particles is required by Barracuda to generate the population of particles. The program requires particle size distribution, particle density, close pack volume fraction and shape factor.

A sieve analysis of the material was performed. A plot of the size distribution is shown in **Figure 8-22**. The actual data points as measured were used for the definition of the particle size group file in Barracuda, rather than fitting the data to Rosin-Rammler function and mapping that function to the size distribution input to Barracuda. The particle density was measured experimentally. The particle specific gravity was found to be 2.72. Particle groups from different screen cuts were examined with a microscope to observe the general shape as this may impact drag coefficients.

After examining the microscope photograph of **Figure 8.23**, it was decided that the particles in the model can be represented as spheres. There is an option to input a non-spherical particle factor for the drag calculation, however it appears this applies to all particle groups uniformly. The program allows the user to define many different particle types that are defined by their size distribution curve, and specific gravity. These different particle groups can be initialized in different zones or fed from different locations. These particles of different types are classified as different “tracer species”. This allows for mixing and dispersion to be evaluated and monitored as a function of time. For example, coal and sand species could be imposed at the starting point, and the dispersion of each could be examined.



**Figure 8-22 - Size Distribution for typical solid material used by Barracuda.**



**Figure 8-23 - Particle shapes for 120mesh screen sample**

Some additional setup factors used in this Barracuda simulation were set without detailed analysis. For example, the close-pack void fraction for many particle types was suggested by CPFD-Software to be in the range of 0.6-0.7. Without more information, a value of 0.65 was assumed. Particle restitution coefficients impact the rebound of particles is dependent on many factors and is not constant. For the model inputs, the rebound of particles is set for both normal and tangential components. The factor for the normal direction was defined to be 0.2. This is the fraction of the momentum retained in the normal direction. For the tangential component, the momentum fraction retained was set to 0.70. These restitution coefficients were a reasonable guess.

In the definition of gas and solid flow rates, velocity or pressure boundary conditions are prescribed. At present, there is no mass-flow boundary condition option in Barracuda. After running the calculation for some interval of time, the flux reports provide an indication of the mass flow. Adjustments are necessary to match the target flow rates, and there are two different methods to calibrate the flow rate at a boundary. One option is to restart the calculation with correction factor to the initial guess. The other is to use an external boundary condition file that can be tuned and incremented at different times. For tuning of the solids flow rates, the choices are more limited. The actual solids flow rates are not explicitly defined. Rather, the solids are carried into the calculation domain with some fraction of the gas velocity set. This fractional value cannot be modified after starting the run. To modify the solids flow rate, the user must change the gas velocity as

the means to impact the solids flow. It was found that using external boundary condition files was necessary to allow calibration of the solids flow without restarting the entire calculation. These input files can also toggle the feeding of solids at different time values. So feeding solids after some specific time value can simulate a transient. This method of interacting with the solver via the “Interact” panel allows other changes to be made mid-stream. These include outputs from the program, solver time step, and restart file dumps, planar data file dumps, as well as solver tuning parameters.

## RESULTS

### Qualitative Assessment

Two different conditions were modeled with Barracuda. The high solids case (run1) was modeled with qualitative observations and comparison to measurements. The low solids run included only relative pressure drop data. To best evaluate the relative differences in the flow and solids flow patterns, a series of animation files were created. These are very big, typically in excess of 100 MB. The animation files are useful for visualizing the solids flow patterns.

The gas flow distribution on the surface of the model is shown in **Figure 8-24**. This provides some evidence of the gas flows near the wall. Unfortunately, the flow pattern inside the duct reveals much more variation as evidenced by the vertical slice through the center of the model in **Figure 8-25**. Based on the transport airflow alone, a bulk average velocity of 36 ft/s is expected. The predicted gas flow distribution at this particular time ( $t=28.3$  seconds in simulation time) is far from uniform. Regions of low flow in the inclined section and vertical riser correspond to areas where solids are concentrated.

At the flux plane just before the vertical elbow, the velocity distribution is more uniform than in all other locations. While there is a top-to-bottom gradient, the average is nominally about 36 ft/s. In the feed pipe, the fluidizing airflow is very low, and the solids basically fall down into the pickup section. The peak velocities are on the order of 100ft/s (or 3.6x higher than the bulk average) in the center of the riser. These threads of high velocity are moving upward while the solids can be moving in different directions or speeds. The velocity stratification continues up the full 10-meter column height, but the peak velocity decreases further away from the elbow as shown in **Figure 8-26**. These two figures may appear different, but they are the same data viewed from different vantage points.

Direct comparison of gas flow velocity distribution to these predictions of the flow model is not possible, because there are no direct velocity measurements from the 40 ft model. The movement of the solids in the inclined duct and riser seems to be consistent with lightly loaded observations of particles in the inclined pipe and lower riser. It is also important to recognize that these snapshots show dynamic flow structures. To illustrate, contours of velocity near the base of the riser are shown 1/2 second apart in **Figure 8-27**.

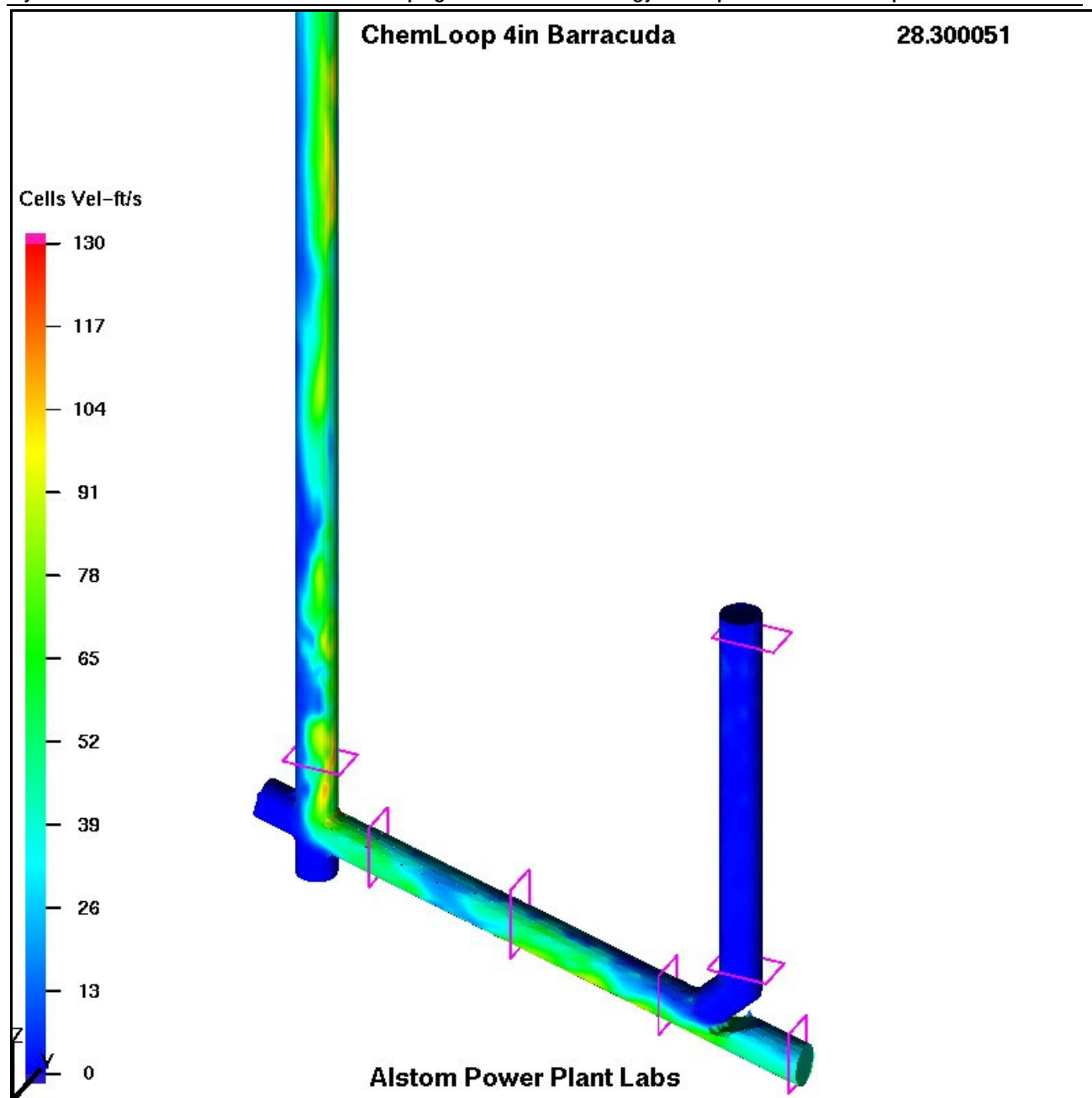
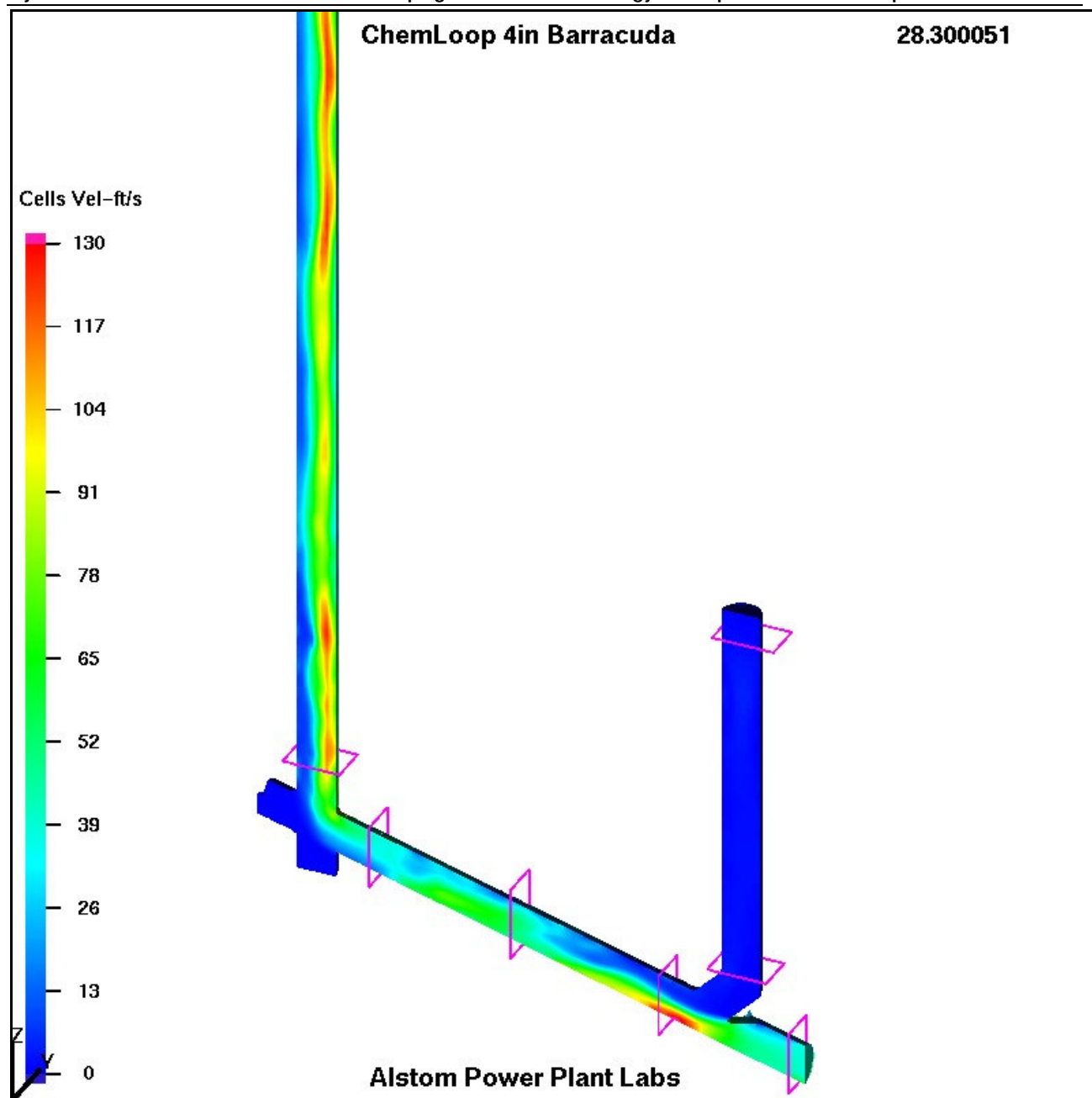


Figure 8-24 - Velocity distribution near the surface of the tube.



**Figure 8-25 - Centerline gas velocity distribution – lower portion**

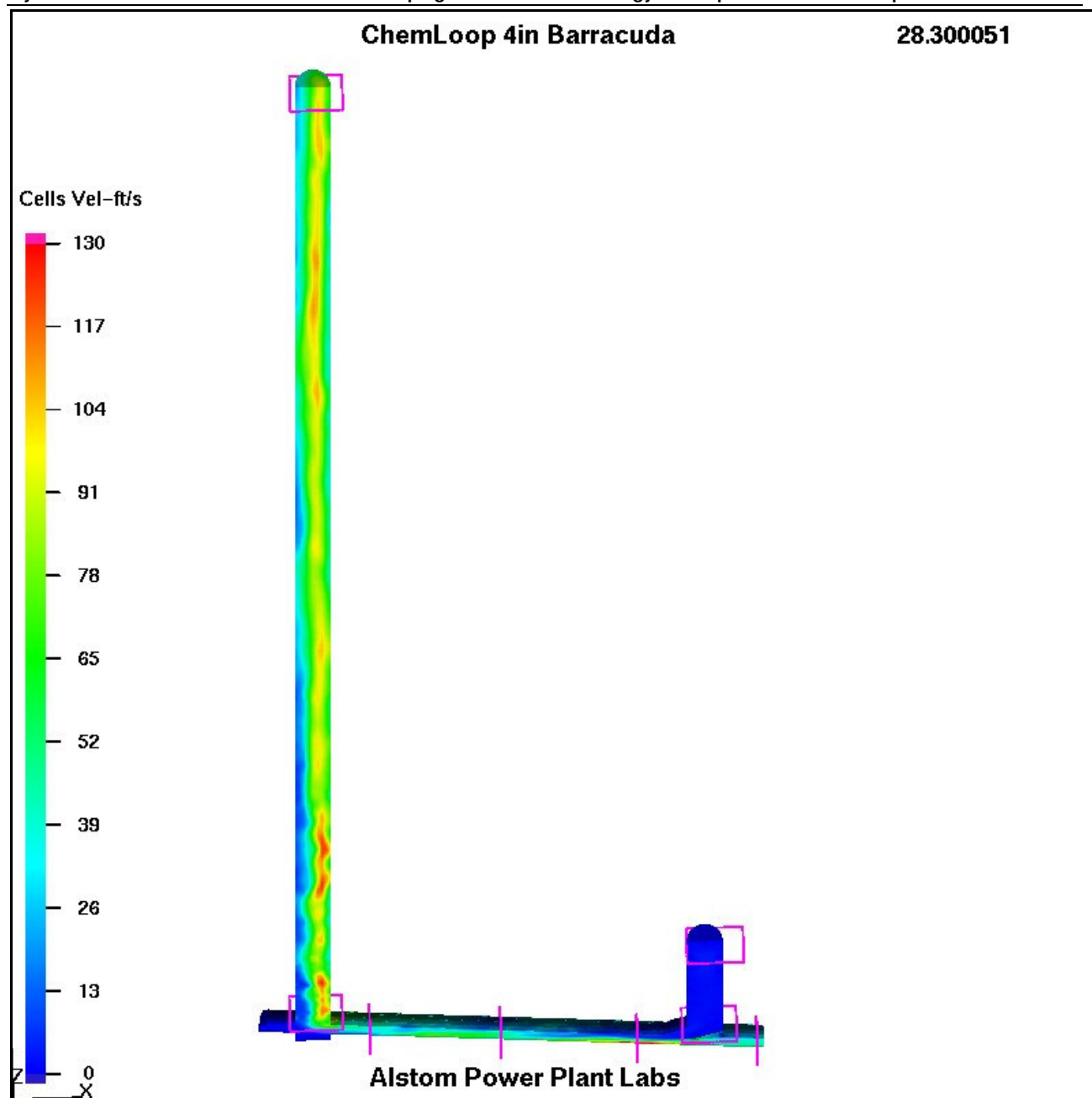
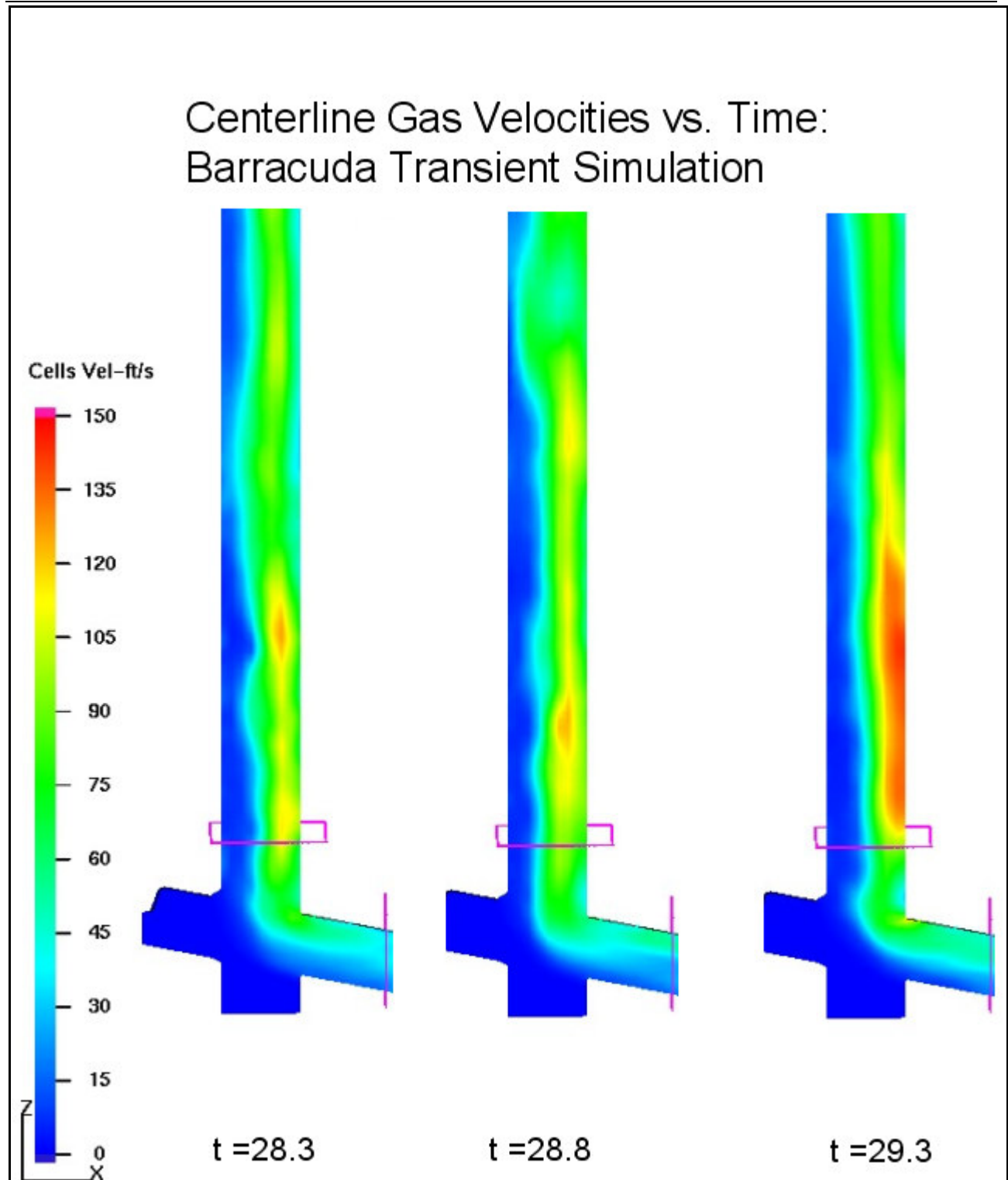


Figure 8-26 - Centerline gas velocity distribution – lower portion



**Figure 8-27 Flow Velocities near base of riser vs. time.**

Flow of solids inside the pipe can be seen through the Plexiglas with proper illumination. Hence, it is useful to use particle plots in the qualitative comparison. The flow of solids in the lower section of the model reveals interesting attributes. A plot of the solids as colored by particle velocity are shown in **Figure 8-28**. The size of the colored dots is proportional to the particle size. A close-up view is needed to discriminate the size variation more

clearly. The low velocity zones and concentration of particles in the dead branches of the tee appear consistent with the flow model observations. In addition, the threads of particles ejected from the pickup pipe seem consistent with observations under lightly loaded conditions. It is difficult to discern the roping of solids at higher solids loadings in the flow model. The velocity gradient of the smaller particles (blue to light blue), up this inclined duct, after the pickup, is shown by color, as the particles are accelerated away from the pick-up.

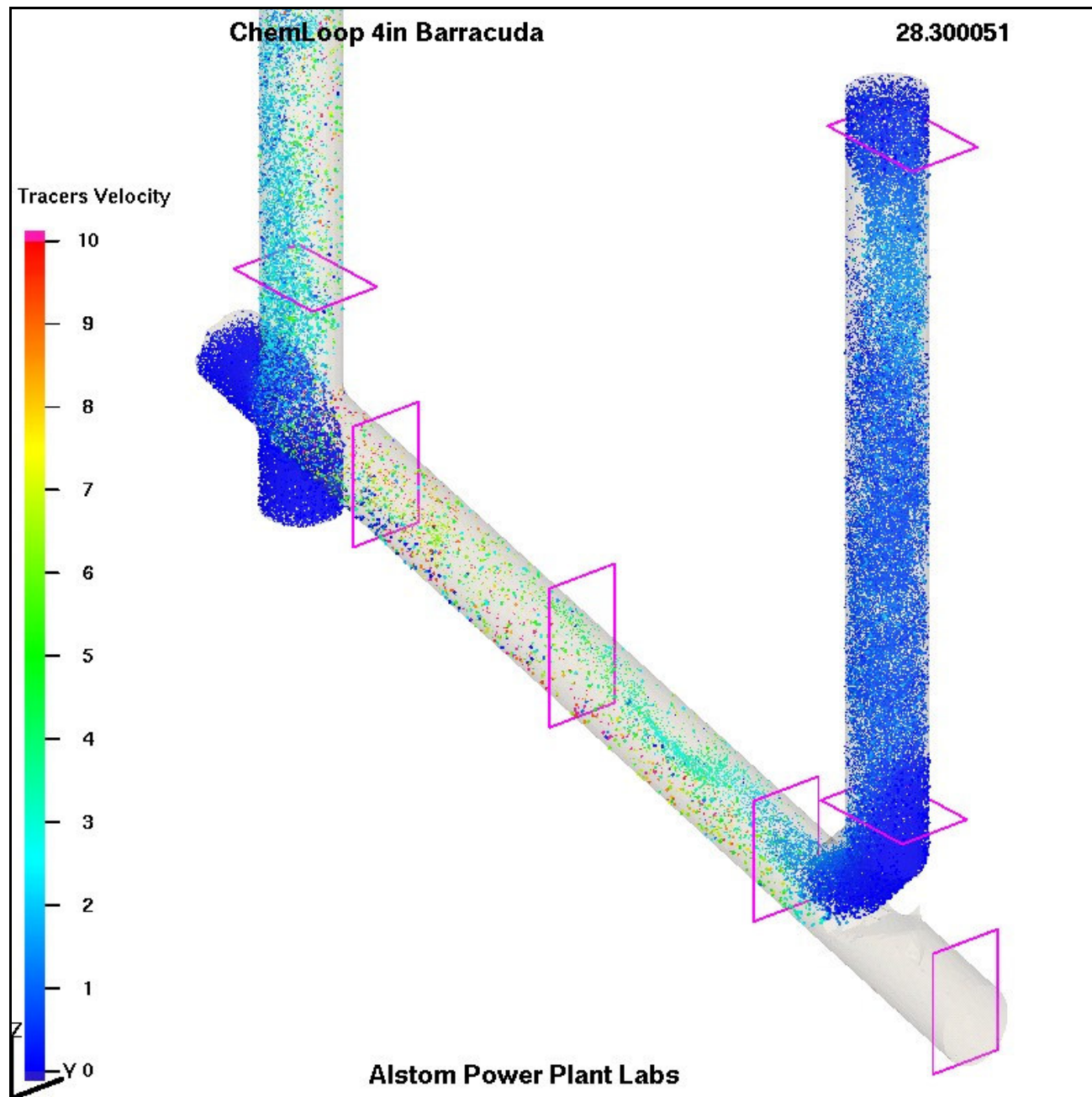
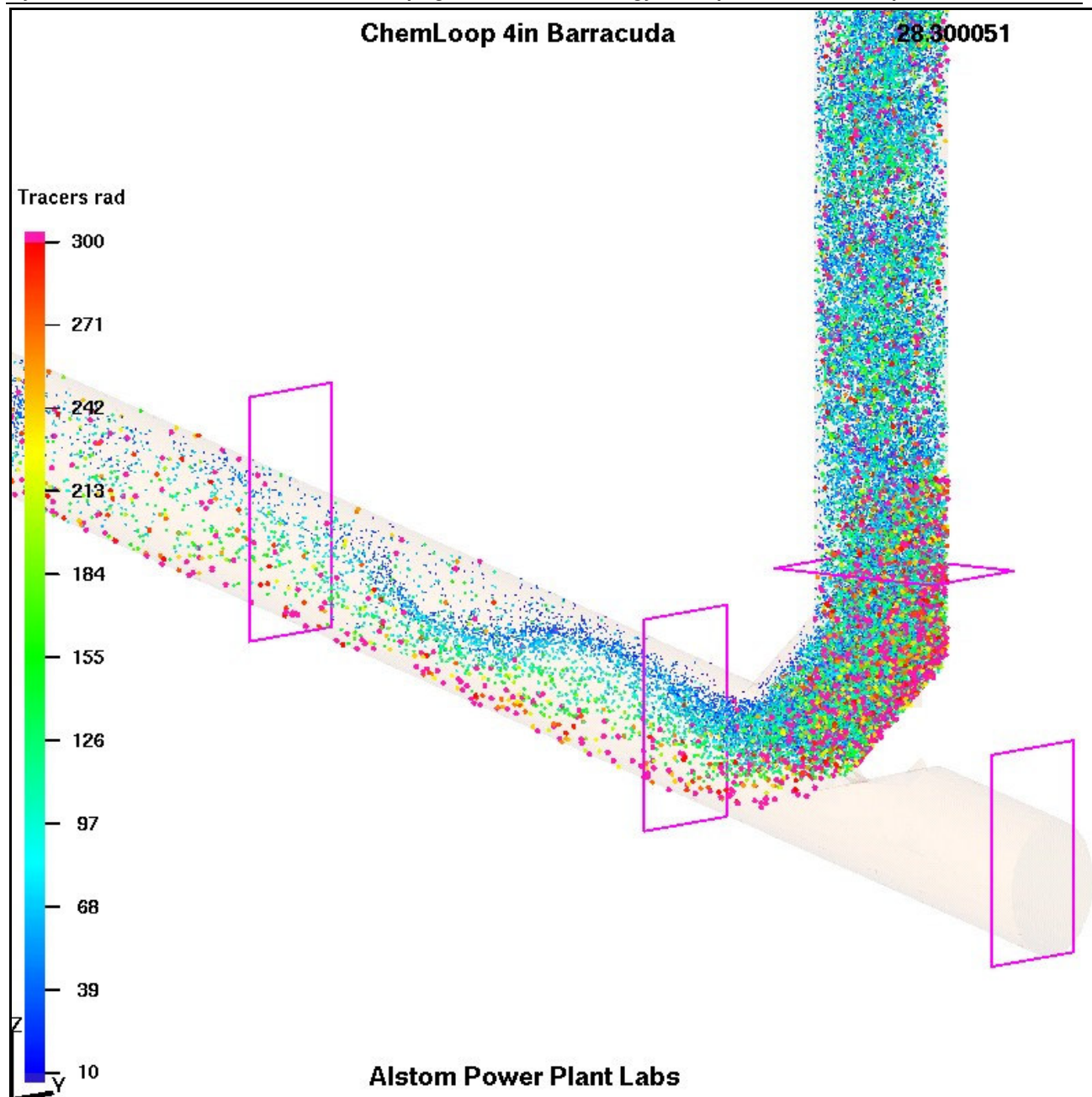


Figure 8-28 - Solids colored by particle velocity in the lower section



**Figure 8-29 - Particle Size Distribution near the 45° solids pick-up pipe.**

A close-up view of the solids in the lower section near the sugar scoop is presented in **Figure 8-29**, colored by particle radius. Note that the legend indication “tracer rad” is the particle radius. For some reason, radius not diameter is used as a variable in Barracuda. The options to display custom variables for the particles are limited in GMV.

The solids accumulate in the feed pipe and segregate as they turn into the transport air stream. This segregation is not obvious in the flow model. Recirculation and roping of the particles streams can be observed at the top of the pipe junction. In this figure, clusters of smaller particles wind along the upper part of the inclined pipe. Larger particles that were segregated on the bottom due to the turn appear to mix in with the fine particle thread in the zone near the legend of this plot. This seems to be realistic.

Another area of interest is the impact tee. Build up of solids on the outside that pack the end of the incline may reduce the erosion potential by blanketing the impact zone. A plot of the particle radius near this tee is shown in **Figure 8-30**. The solids have packed both dead legs of the tee. The solids are also concentrated on the outside of the turn.

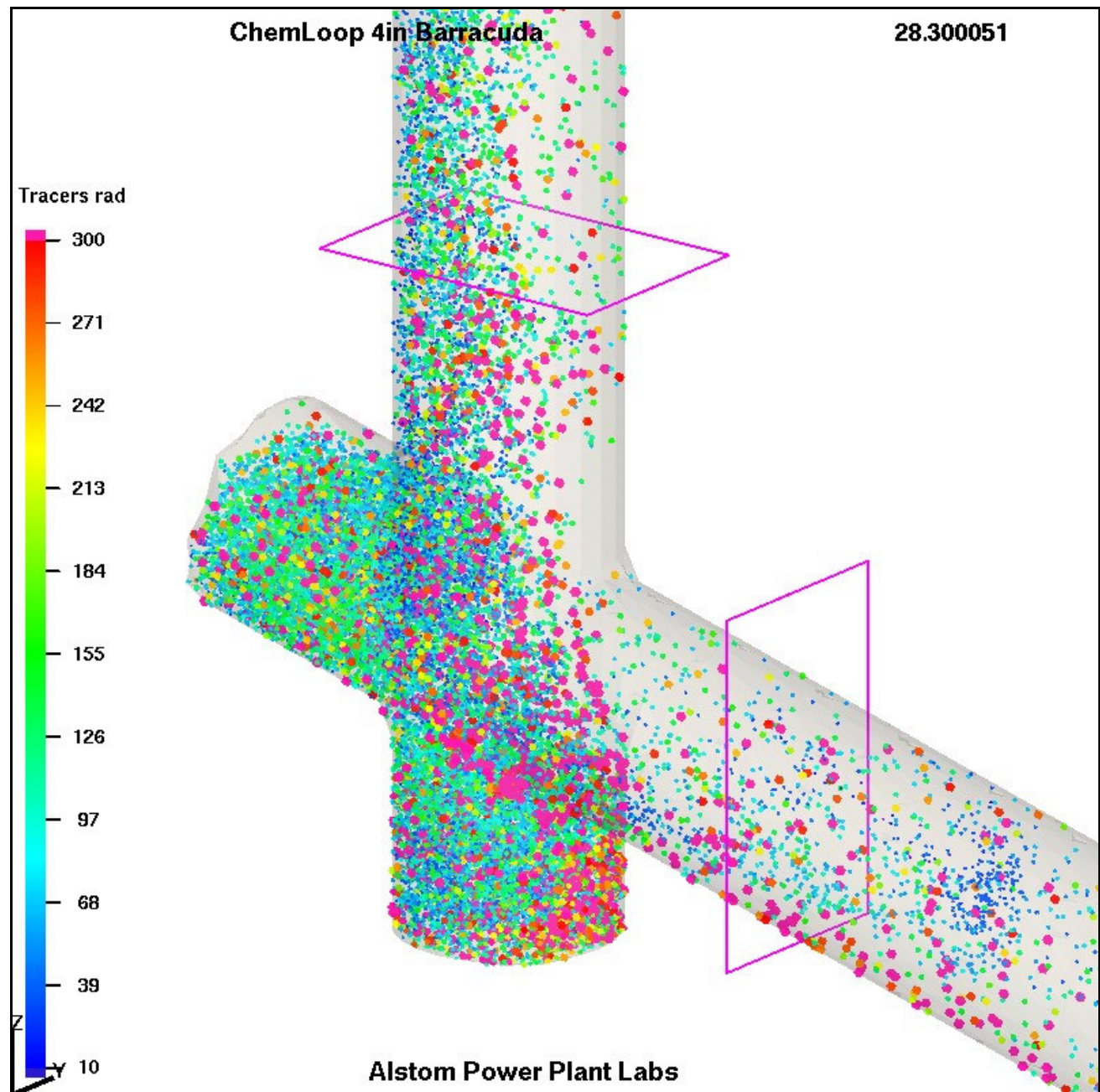
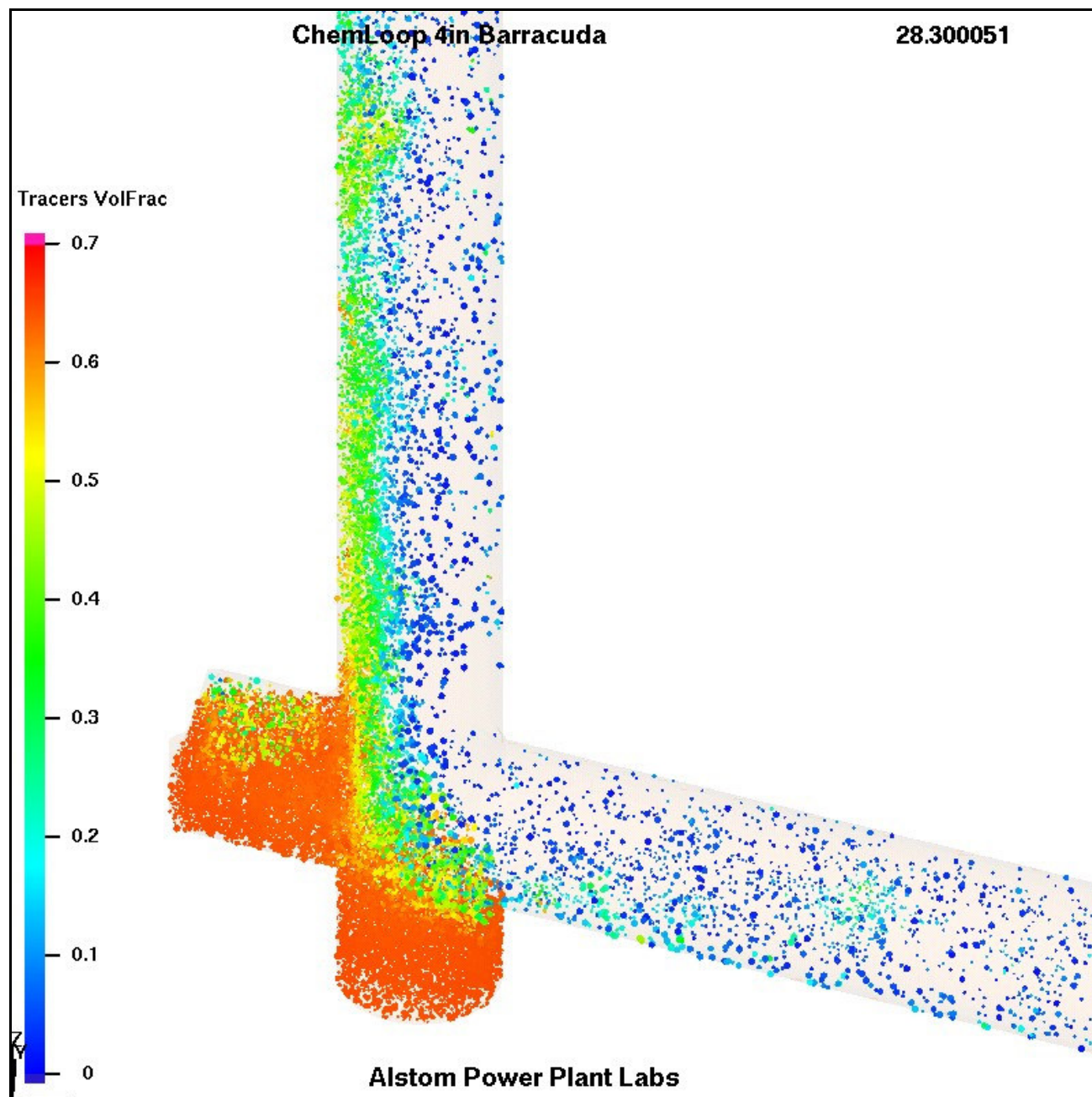


Figure 8-30 - Solids colored by radius in the mixing tee.



**Figure 8-31 - Particle Solids colored by volume fraction**

The observed segregation is more clearly shown with a plot of the solids concentration. **Figure 8-31** shows the same region with particles colored by volume fraction. The maximum allowable volume fraction for this solids mixture was set to be 65%. Based on the figure, it is clear that the dead ends are filled to the allowable level of solids. The volume fraction across the lower portion of the riser is quite interesting. It suggests that the solids concentration is very low on the inside of the turn, and this extends upward some distance. The predicted solids concentration profile here may be critical to the predicted tee pressure drop.

An isometric view of the particle velocities in the entire riser section is shown in **Figure 8-32**. There is a large variation in particle velocities up the riser. The variation in velocity also varies widely with time.

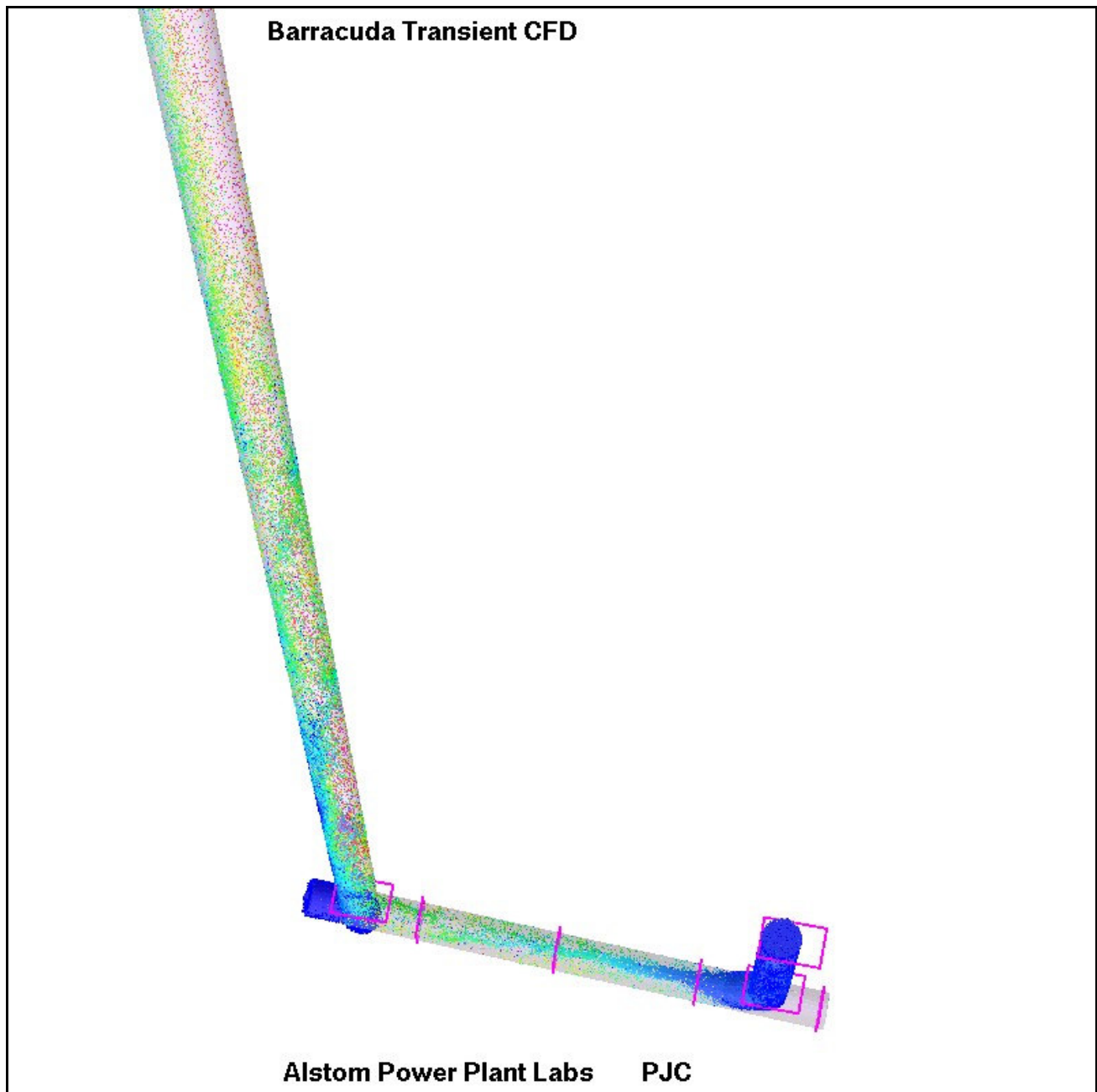


**Figure 8-32 - Particle Velocity Distribution colored by velocity magnitude**

## Pressure Drop Evaluation

A considerable amount of pressure data has been recorded in the 40-foot cold flow model. Extraction and processing of the data to determine the match between CFD predictions and measurement was performed. From the data logged, pressures and differential pressures were extracted from specific time intervals associated with the solids flow measurement tests. The location of these pressure taps is shown in **Figure 8-33**.

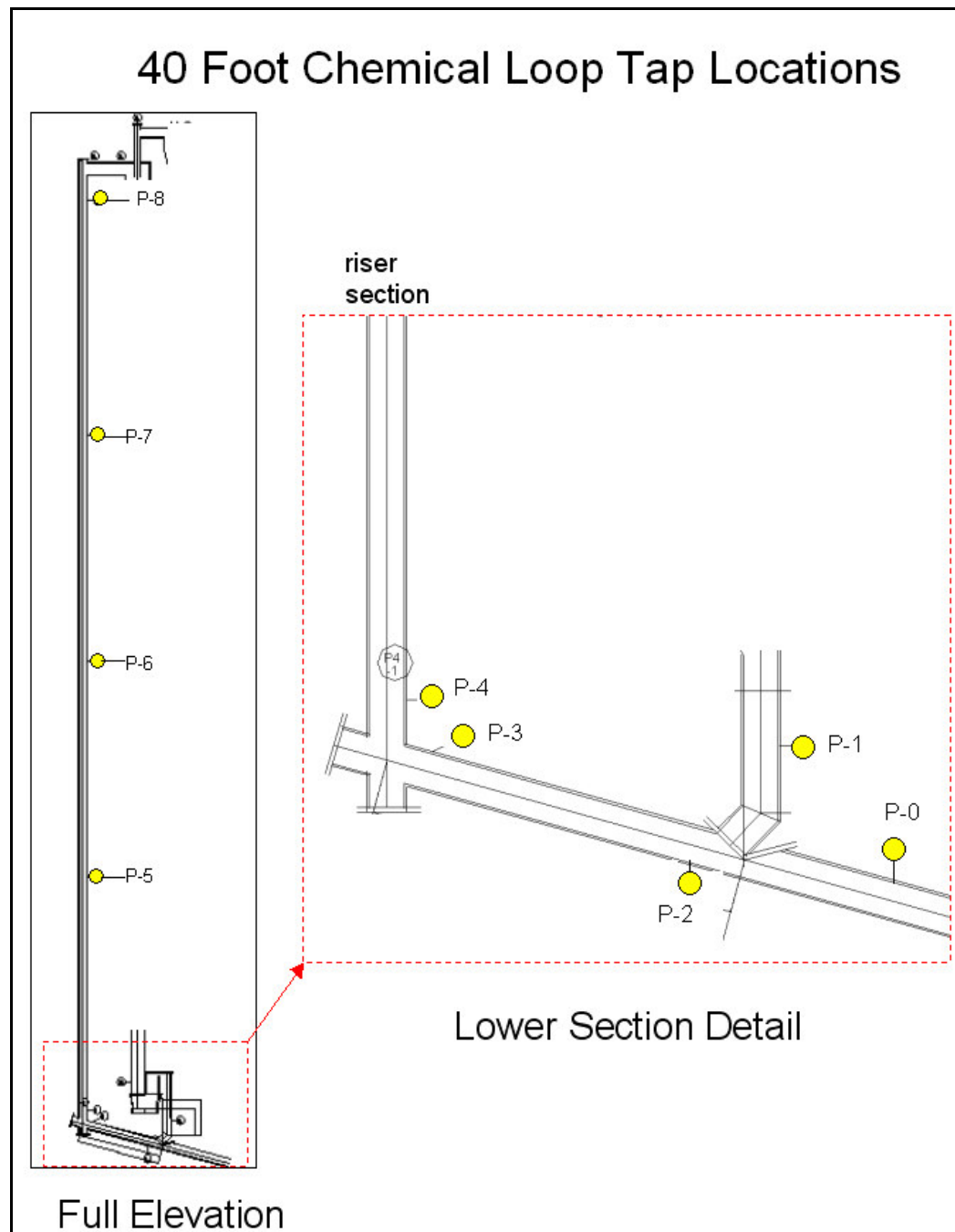


**Figure 8-33 - Position of relevant pressure taps**

The measured data was logged as a series of either gauge pressures, or differential pressures. The data was processed to develop a set of DP's relative to the transport air pressure. The transport air pressure was relatively stable after the initial tests (see **Section 6**) and insensitive to solids concentrations in the feed pipe and was therefore a better reference point for this comparison.

Using the Barracuda predictions, a similar set of data was developed for each of the tap locations from P0 to P8 in **Figure 8-33**. In the Barracuda model, the riser height was approximately 1 meter shorter than the flow model riser, thus the location of P8 in the Barracuda model is too low.

During the time interval of the high-solids test, the pressures were relatively constant. A plot of the pressure profile over the full range of the simulation appears in **Figure 8-34**, with a close-up of the lower inclined pipe in **Figure 8-35**. The solids concentration in the lower elbow, which is relevant to the discussion of the predictions, appears in **Figure 8-36**.

A plot of the measured differential pressures, (P1-P0) through (P8-P0) is charted for a 400 second interval in **Figure 8-37**. From this data, the pressures at P1 and P3 were nearly identical, so the curves for these DP's (30 inches) are almost identical. P2 was slightly lower than P0. Looking at the other curves, the pressure drop of the tee can be determined from the offset of the red and copper/beige curves. A significant DP results between P4 and P5 as the solids are accelerated up the column. The incremental DP's between P5/P6, P6/P7 and P8/P7 are very similar, which is expected given that the elevation rise between the taps is the same. The more significant DP is generated in the bottom of the riser.

By comparison, the predicted Barracuda curves are shown for a shorter time interval in **Figure 8-38**. This data was plotted with a portion of the entire sample. Examining this set of data, several observations can be made. First, the temporal variation in the differential pressures is much higher than for the cold flow data. The pressure cell response rates, pressure line lengths, particle filter pressure drop, and other experimental factors need to be examined to determine what the true pressure fluctuations are. Despite the fluctuation intensity, these curves indicate some nominal pressure drop information when visually averaged.

The total overall pressure drop is nominally 160 inches H<sub>2</sub>O, which compares favorably to the measurement data indicating about 150 inches H<sub>2</sub>O. The sectional pressure drops in the upper riser are also consistent with the measurements. The relatively large pressure drop predicted by Barracuda in the bottom of the riser differs from the other vertical segments of the riser.

The overall inclined pipe DP prediction is nearly identical to the measurements. This is good as well. However, there is an obvious mismatch between the predicted and measured P1-P0 reading. While the (P2-P0) match is very close, the predicted pressure at P1 is far higher than measured. This seems to be connected with the observation of a nearly packed column of solids just above the 45 feed elbow, as shown in **Figure 8-36**. This creates a blockage that isolates the inclined pipe from the short vertical feed pipe.

This allows the solids pressure to build up to a value higher than P2. This is not expected and the source for this discrepancy has not been isolated. There may be issues associated with insufficient grid resolution; solids slip factors or something else. Apart from this feature, the pressure drop profile prediction for the other pressure taps is within about 15% of the measured values.

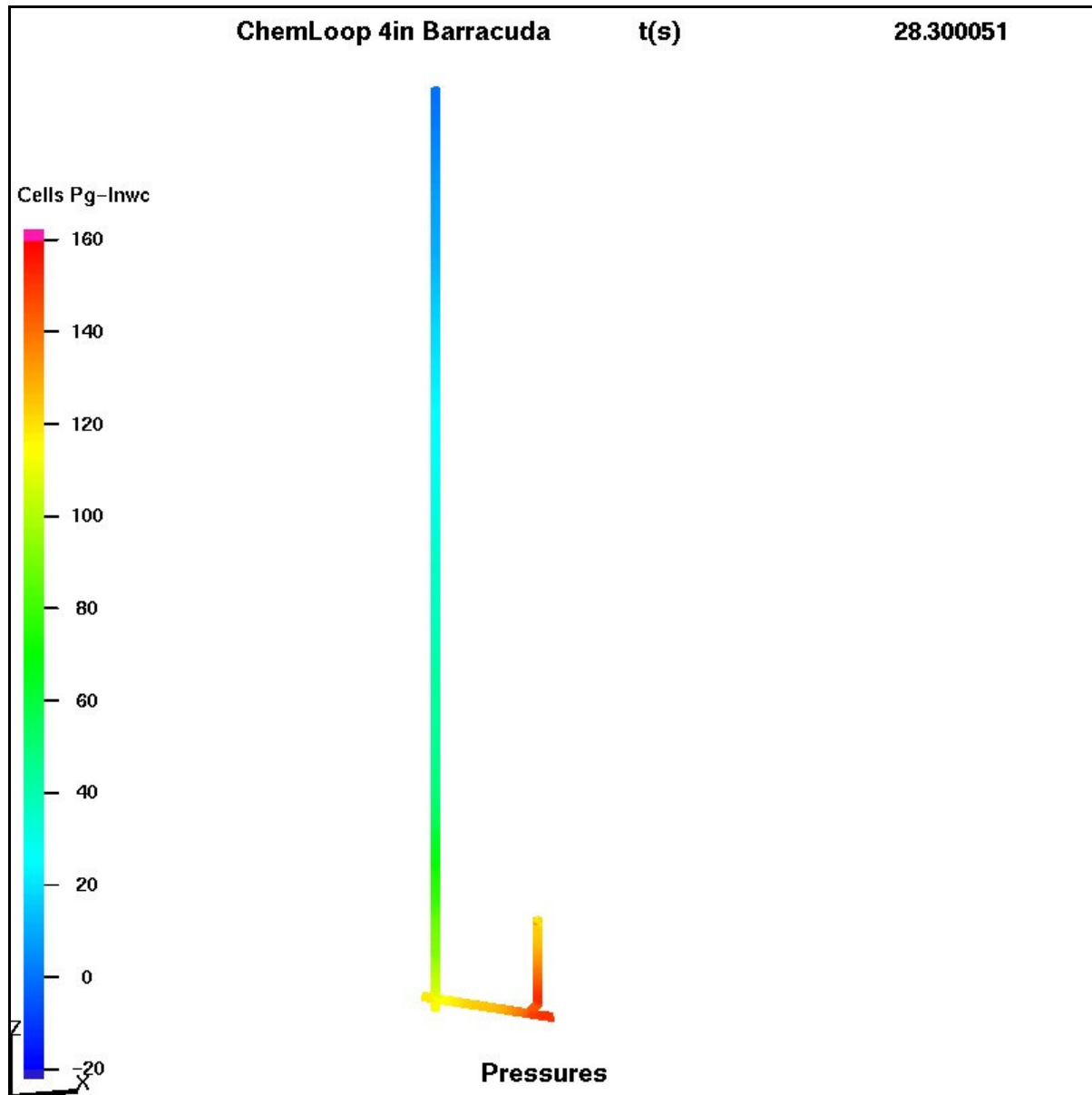
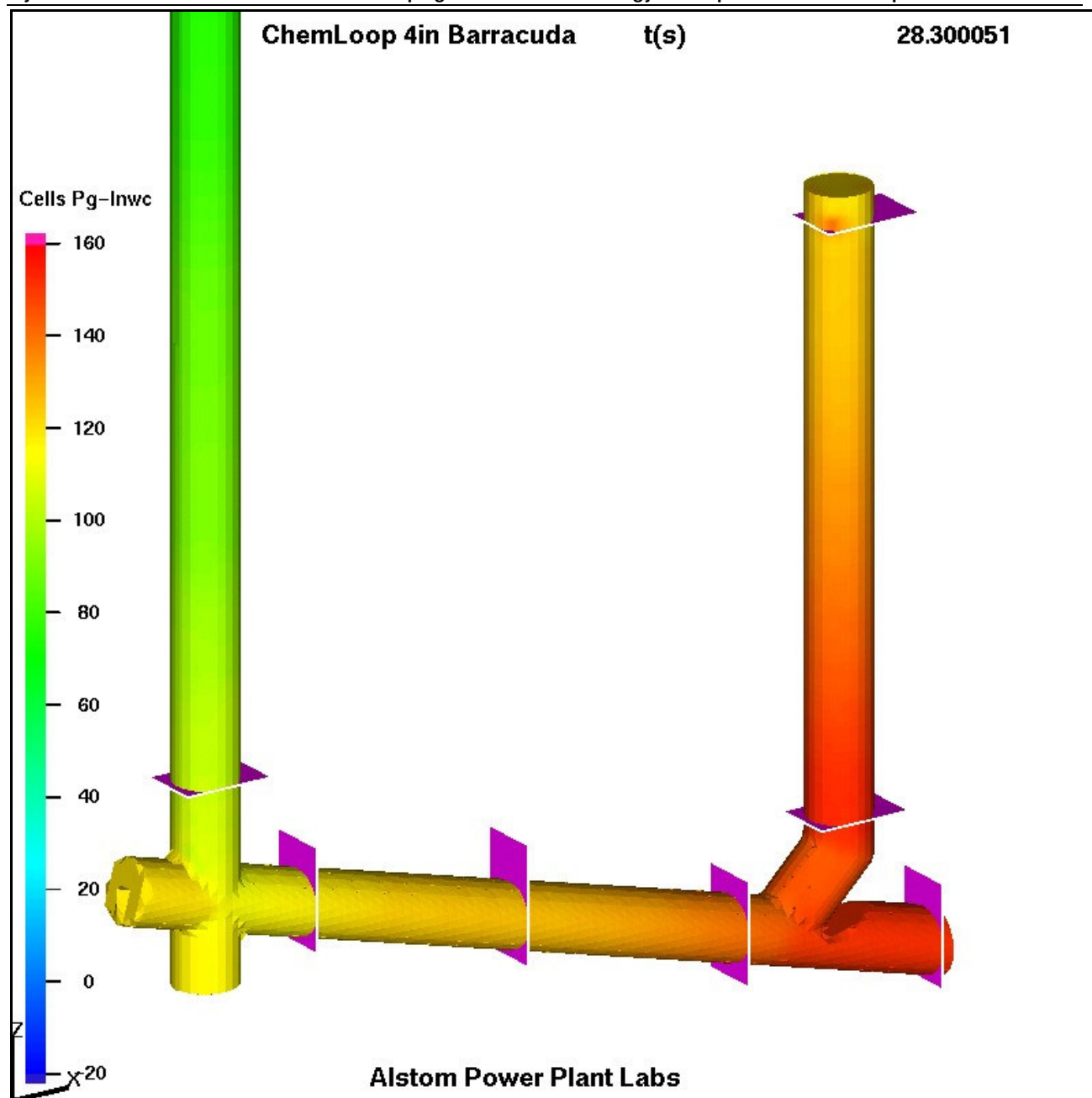
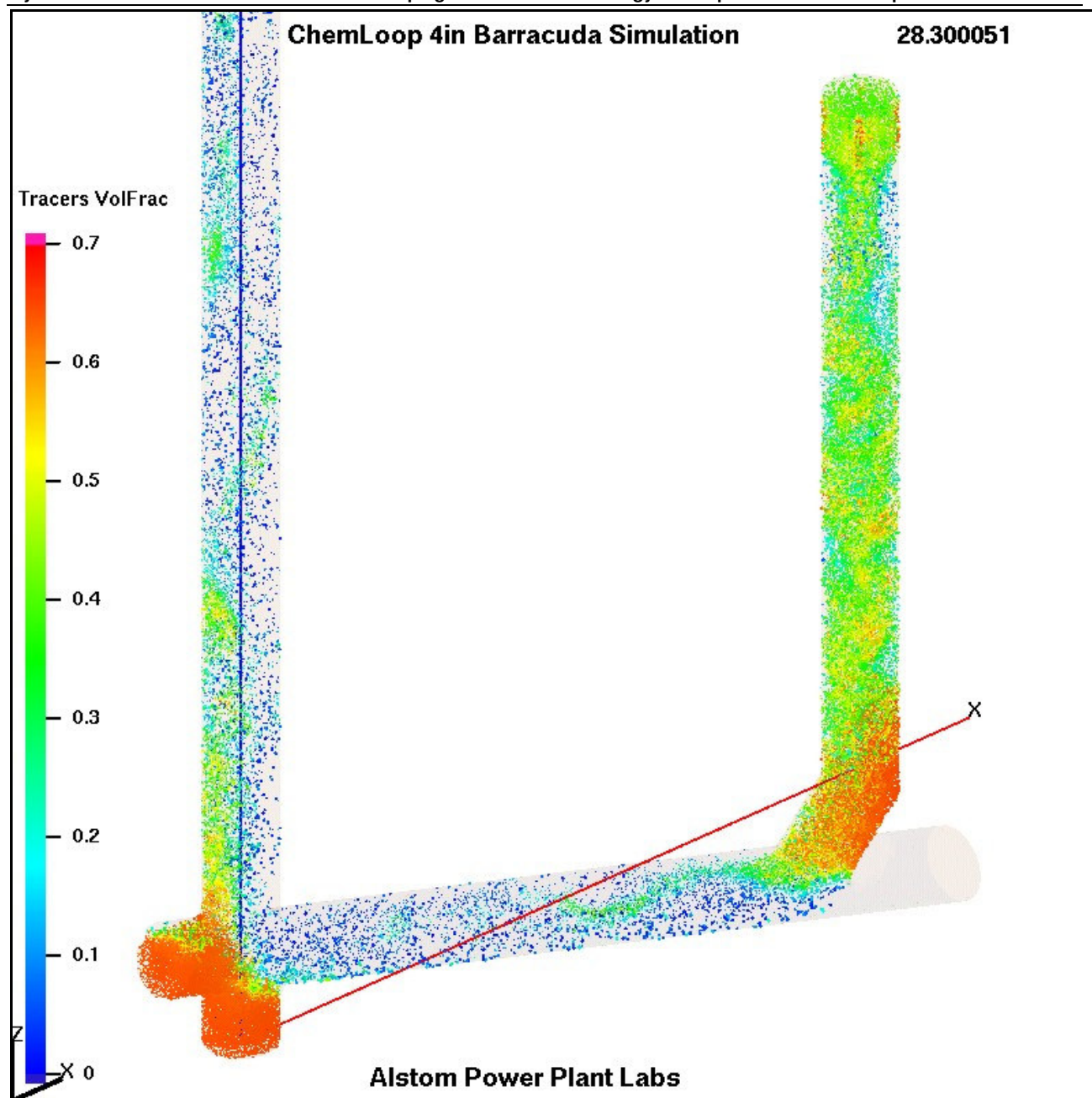


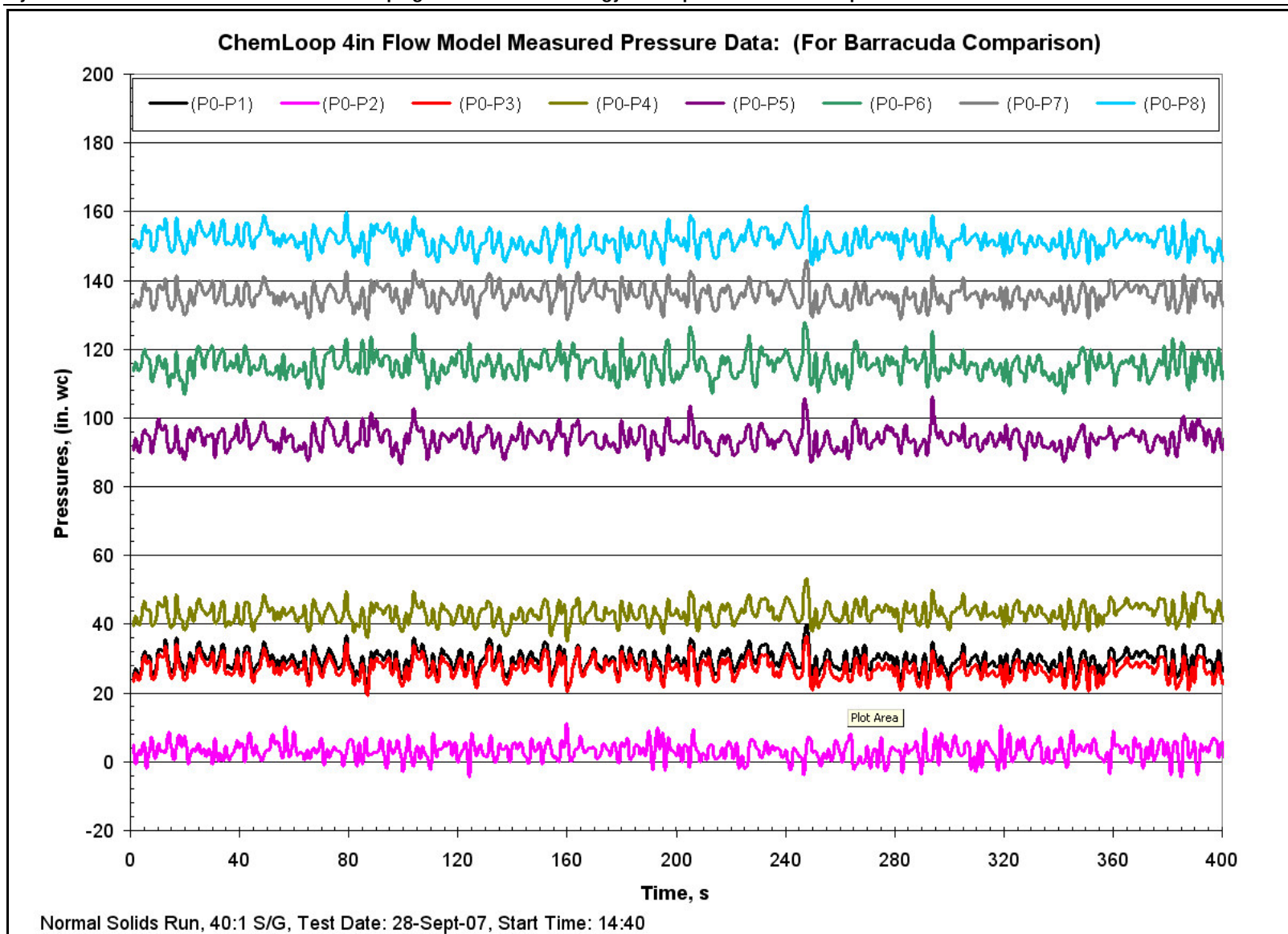
Figure 8-34 - Pressure Distribution over the full height of the flow model

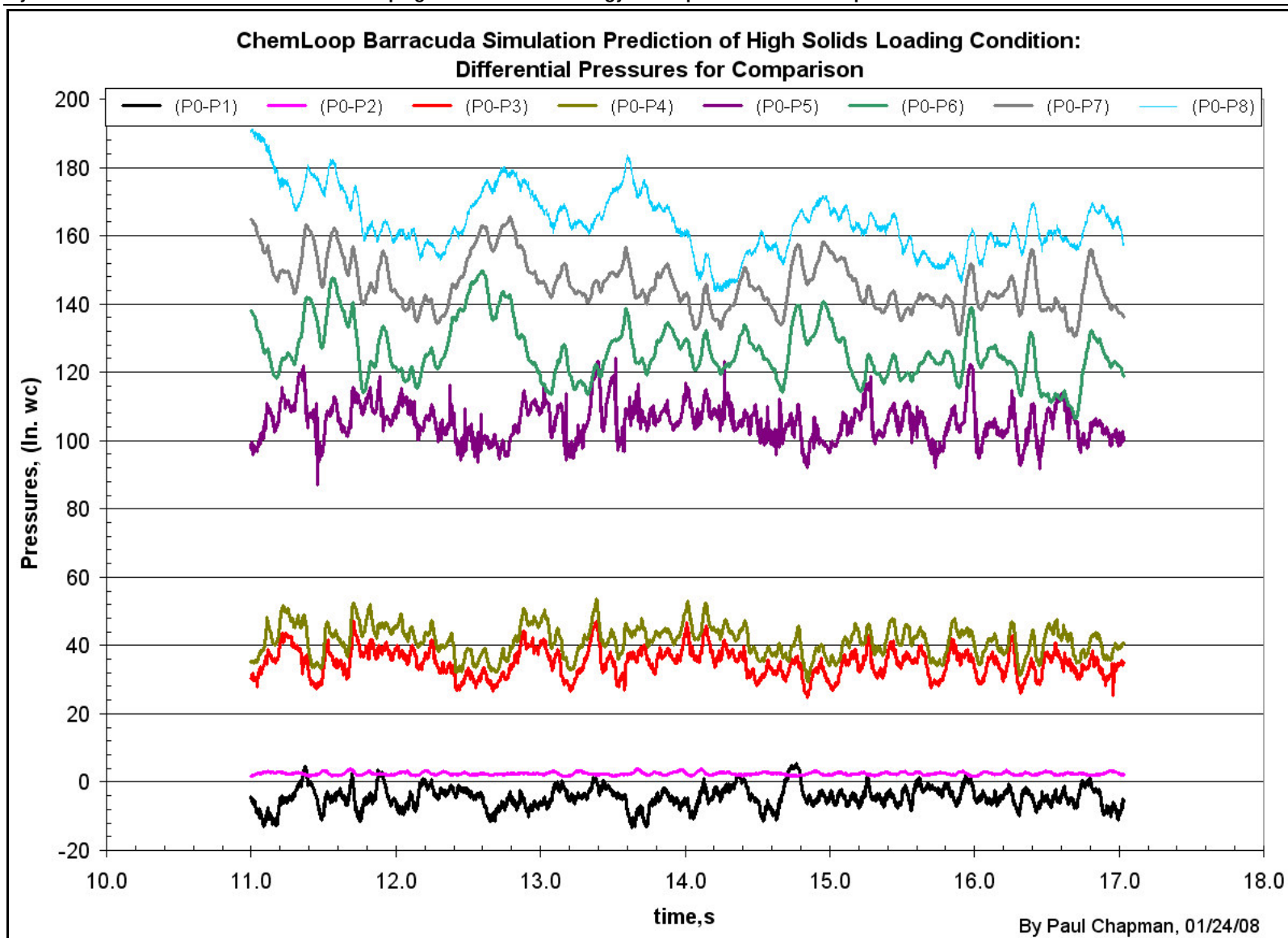


**Figure 8-35 - Pressure distribution near the lower inclined pipe.**



**Figure 8-36 - Solids concentration in the lower inclined pipe section.**



**Figure 8-38 - Measured Differential Pressures**

## Conclusions and Recommendations

In general, Barracuda represents a unique software simulation tool that can provide reasonably accurate predictions of such complex gas/solids flows as in chemical looping. The efficient computational method for representation of a large population of individual particles in flow environments extending from disperse to very concentrated is unlike other commercially licensed CFD software.

The results presented here for the high solids loading case at the 40 ft CFM were obtained without any model “tuning” or calibration factors. While the overall and sectional pressure drops were reasonably well predicted, match to the solids feed leg pressure (P1) did not match the data. The cause of the discrepancy was not determined, and could be due to the oversimplification of the solids feed profile, mesh resolution, particle rebound settings, or some combination of factors.

Despite an efficient algorithm for modeling the motion of millions of particles in a transient gas and solids system, model runs still require vast amounts of computer time. The program currently does not include parallel processing capability and thus the calculation progress is limited by CPU speed and the problem size. These runs were generated on a CFD workstation powered by AMD 64-bit Opteron dual-core processors. These are well suited to large CFD problems and have an efficient memory architecture.

CFD in combination with cold flow modeling allows developing a better understanding of the solids flow behavior. The CFD tool can be further utilized for development of the chemical looping system in Phase IV.



## **9. Technical Reviews**

### **9.1 ASME Peer Review**

NETL's Strategic Center for Coal (SCC) implemented bi-annual peer reviews of the project portfolio for each of its programs. In FY07, the Advanced Power Systems (APS) Program portfolio, which includes gasification (IGCC), turbines, and advanced research projects, were reviewed. The Hybrid Combustion-Gasification Chemical Looping Coal Power Technology Development was selected as one of the projects in the APS portfolio to be reviewed.

In compliance with a directive from DOE-Headquarters, NETL conducted independent reviews of its R&D programs. Individual projects were selected based on the following selection criteria.

1. Congressionally directed projects.
2. Projects existed for at least one year prior and one following the 2007 APS Peer Review
3. The project has not been reviewed in the past 12 months

The scope of the 2007 APS Peer Review was to conduct an independent assessment of the project's activities and accomplishments, based on its own merits, in support of helping the APS Program to achieve its goals and objectives.

On July 16, 2007, Alstom presented 30 minute briefing on the project to an independent Peer Review Panel, followed by a question and answer period.

#### **9.1.1 ASME Peer Review Results**

The results of the review are summarized below.

The reviewers found that the project had the following strengths

1. Alstom has a very large experience base.
2. This builds on Alstom's circulating fluidized bed (CFB) boiler technology experience.
3. Alstom has the capability to commercialize this technology.
4. Alstom appears to be making a strong effort to develop a new approach to CO<sub>2</sub> capture.
5. They have very good testing equipment.
6. Alstom has made significant progress on modest funding.
7. Chemical looping has multiple applications.

The following were listed as weaknesses:

1. The process kinetics appear oversimplified and may not be accurate.
2. Multiple flows may be difficult to control.
3. Delivering CO<sub>2</sub> at low pressure may be a disadvantage.

4. Disposal of captured sulfur as calcium sulfate ( $\text{CaSO}_4$ ) may cause a problem by releasing hydrogen sulfide ( $\text{H}_2\text{S}$ ).
5. Next steps in the schedule are highly compressed.
6. Technical challenges may be harder than the presentation suggests.

In order to address these comments the reviewers suggested the following recommendations and action items:

#### **Recommendations:**

1. Review the Rand Corporation studies on synthetic fuels projects from the late 1970s and early 1980s.
2. Perform CFD modeling of solids flows.
3. Identify risks by category.
4. Continue building a larger and more integrated pilot plant.
5. Identify any shortcomings in GE's Advanced Unmixed Combustion/Gasification Program.
6. Provide a plan for getting to Phase V demonstration.

#### **Action Items:**

1. Demonstrate automated control of solids flows at larger (industrial/commercial) scale.
2. Provide a detailed project report justifying success to-date before moving forward.
3. Review and clarify primary kinetic data.
4. Clarify the issue of  $\text{CaSO}_4$  disposal and release of  $\text{H}_2\text{S}$ .

The overall evaluation from the reviewers in ten categories ranged from 3.5 to 4.6 on a scale of 1 to 5 with 5 being the most favorable. The overall average rating was 3.96.

#### **9.1.2 Response to ASME Peer Review.**

In responding to the reviewer's comments (**Appendix A4**), Alstom has agreed to implement the recommendations and action items listed above.

Recommendation R1 will be discussed in **Section 9.1.2.1 Review of previous studies**.

Recommendation R2 was discussed in **Section 8.8 CFD Modeling**.

Recommendation R3 was discussed in the Phase II Final Project Report (**Reference 3**). The format of the ASME review, especially the time restrictions did not allow us to bring this subject up in the presentation. This subject will be reviewed in **Section 9.1.2.2 Risk Review**.

Recommendation R4 is the subject of a proposal to continue the Chemical Looping project to the next Phase (Phase IV), which is to build a prototype Chemical Looping Plant. This is described in **Section 6 Prototype Engineering** and in **Section 12 Future Developments**. Alstom interprets this recommendation as an endorsement to continue development of the Chemical Looping Project.

Recommendation R5 will be discussed in **Section 9.1.2.3 Comparison with GE's Unmixed Gasification Combustion Process**.

Recommendation R6 is to provide a plan to proceed to a demonstration phase of the Chemical Looping program. This plan is included in the proposal to proceed to Phase IV that was submitted to the DOE in October 2007.

Action Item A1 is the subject of the work done in Phase III and is discussed in **Section 6** and in **Section 7**. It also included in the proposal to proceed to Phase IV that was submitted to the DOE in October 2007.

Action Item A2 will be completed by submitting this report for Phase III.

Action Item A3 was discussed in the Final Report for Phase II (**Reference 3**) and will be discussed in **Section 9.1.2.4 Review of Kinetics Data**.

Action Item A4 was also discussed in the Final Report for Phase II (**Reference 3**) and will be discussed in **Section 9.1.2.4 Review of Kinetics Data**.

#### **9.1.2.1 Review of Previous Studies.**

In making the recommendation to review the Rand Corporation studies on synthetic fuels plants, the review team made the following comment:

**“These studies looked closely at the economics of these projects, particularly what caused cost overruns. One major factor was dealing with solid-gas flow rates. Alstom should get the lessons learned from this previous work.”**

The studies cited (**Reference 23**) concluded, in general, that “pioneer” or first of a kind process plants had under-estimated costs and lower than expected performance. The specific conclusions from **Reference 23** are summarized as follows:

- **Both performance problems and cost-estimation error, measured as the ratio of the estimated costs at various points on a projects development to the actual cost, were common among the plants examined. Both experiences, however, are associated with characteristics of the project or technology – characteristics that are knowable early in project development.**

- **Despite widespread belief to the contrary, unanticipated inflation, unanticipated regulatory changes, scope changes, and other external factors such as bad weather and strikes, are *not* the principal causes of cost underestimation.**
- **Most of the variation found in cost-estimation error can be explained by (1) the extent to which the plant's technology departs from that of prior plants, (2) the degree of definition of the project's site and related characteristics, and (3) the complexity of the plant.**
- **Most of the variation in plant performance is explained by the measures of new technology and whether or not a plant processes solid material.**
- **The statistical analysis of cost-estimation error – cost growth – enables both government and industry planners to gauge the reliability of a given estimate and to assess probable ultimate costs of process facilities.**
- **The performance analysis suggests the routinely high performance assumed for pioneer process plants when financial analyses are done is unrealistic. Over 50% of the plants in our sample failed to achieve their production goals in the second six months after start-up.”**

Throughout the Chemical Looping process development, Alstom has been aware of these issues and has structured the development program to address them. As discussed below and throughout this report, process definition, cost estimates and performance targets have been constantly updated and subjected to various project reviews and risk analyses. Process performance goals will be tested by building and testing the prototype plant in Phase IV.

Alstom has been updating the economics of the original Chemical Looping cost estimate during each of the project phases. These updates have taken into account the information developed during the Chemical Looping project phases, the air-blown gasification programs as well as questions raised during numerous project reviews.

In Phase II the economics were re-considered to account for the possibility that reactor sizes might be different if reaction rates were found to be slower than expected. Also, heat and mass balances and economics were re-considered to account for the possibility that solids transport might require more transport medium than originally assumed.

A reactor that is 10 times the size of the entire gasifier (including the CO<sub>2</sub> removal/H<sub>2</sub> production/water-gas shift sections as well as the fixed-carbon gasification sections) was priced. Solids transport lines were priced at a solids-to-gas ratio of 10. Plant efficiency and auxiliary power were re-estimated in accordance with these very conservative size and performance changes. Both of these more conservative factors combined only increased the cost of the plant by \$64/kW and the cost of electricity by 0.17 cents/kW-hr.

These studies varied the kinetics and transport requirements by orders of magnitude and the total net effect on the economics of the system was on the order of a few percent, which did not change the Chemical Looping rating in the order of comparable projects in either cost or performance. The small cost differences were due to the fact that these changes affected only a small amount of equipment in the overall plant and that this equipment is relatively small in relation to the rest of the plant equipment.

In Phase II, testing indicated that both the originally assumed kinetics and transport schemes appear to still be valid. A detailed account of these studies is given in the appendix to the Phase II final project report.

The Alstom project team has been involved in gasification development since the early 1970's and has been aware of the issues affecting the costs of this technology on an ongoing basis. We are sensitive to the issues raised here and will continue to review them.

Developing practical, economical methods to capture CO<sub>2</sub> from coal-fired power plants is essential to Alstom's business success. Accordingly, Alstom continues to investigate alternative CO<sub>2</sub> capture technologies and develop those which show most promise.

Of all the alternate CO<sub>2</sub> capture technologies investigated to-date, Chemical Looping provides the lowest cost alternative for capturing CO<sub>2</sub> from coal-fired power plants. The economics of various CO<sub>2</sub> technologies being studied at Alstom for new coal-fired power plants are shown in Figure 9-1. This figure also lists the economic assumption, which are used for economic calculations throughout this report.

**Figure 9-1** shows how the cost of electricity (COE) varies as the cost of CO<sub>2</sub> allowances changes. Alstom's limestone-based Chemical Looping process provides the lowest COE measured against all of the alternatives studied to-date. The Chemical Looping COE is nearly constant with CO<sub>2</sub> allowance price because nearly all (over 95%) of the CO<sub>2</sub> can be captured with this technology. The cost of CO<sub>2</sub> capture for Alstom's Chemical Looping coal-fired power plants for these studies is about 11 to 13 \$/Ton of avoided CO<sub>2</sub>.

### **Comparison to Other Type Approaches to Chemical Looping**

Alstom's Chemical Looping technology differs from all other chemical looping technologies involving oxygen transport for the indirect combustion/gasification of coal. Alstom's process uses limestone as the cycling agent. All other developers use a metal-oxide. This difference has important economic, environmental and reliability consequences. Limestone at less than \$20/ton delivered (world-wide) is at least 10 to 100 times less expensive than any of the metal oxide alternatives. The composition and disposal of the solid by-product is exactly the same as for the hundreds of world-wide large commercial CFB boilers in use today. In Alstom's process, the limestone not only transports oxygen, but also captures and purges all of the sulfur in the fuel, captures

nearly all (>95%) of the carbon in the coal (as CO<sub>2</sub>) and produces CO<sub>2</sub>-free hydrogen, all within the chemical looping process. All other metal-oxide-based chemical looping processes only transport oxygen. They can be used for chemical looping combustion or to make syngas (CO/H<sub>2</sub>), but they cannot capture the sulfur in the fuel or produce CO<sub>2</sub>-free hydrogen without adding additional, expensive down-stream sulfur removal and hydrogen production systems.

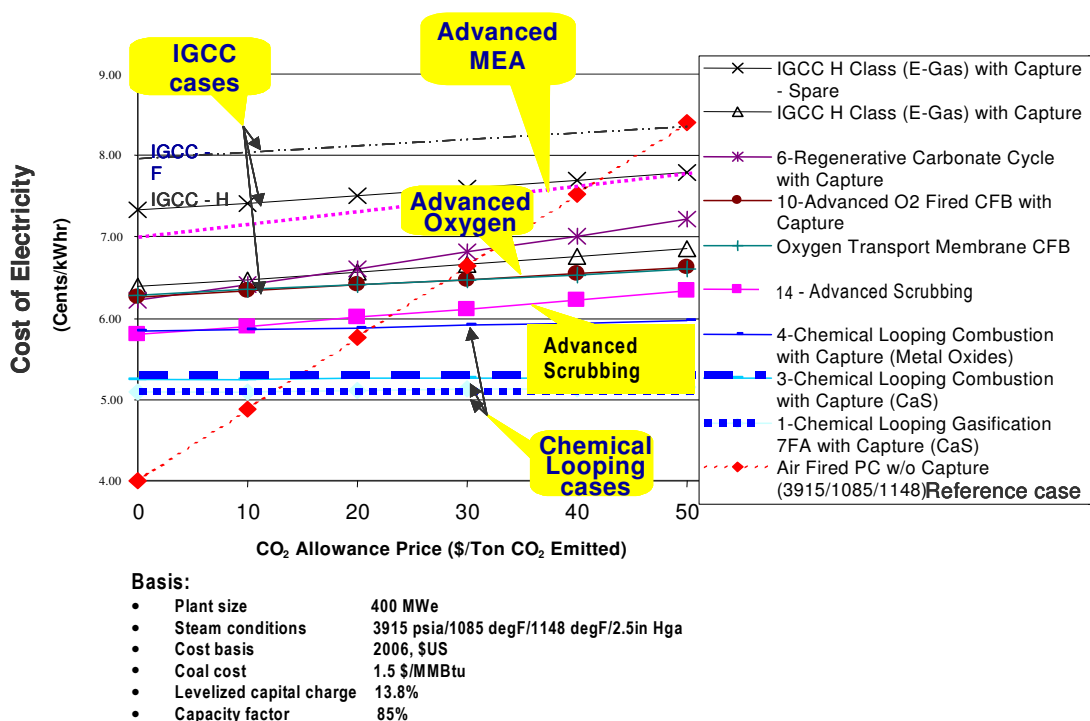


Figure 9-1 – Cost of Electricity for Advanced CO<sub>2</sub> Capture Technologies

Alstom's limestone-based process can use any limestone or dolomite or even CFB disposal solids as the oxygen carrier with only crushing required for preparation. Since solids are bled from the system (as CaSO<sub>4</sub>, CaO and coal ash) to purge and dispose of coal ash and sulfur, limestone is continually added to replenish lost calcium. This requirement continually renews the circulating sorbent/oxygen-carrier. The molar ratio of calcium-to-sulfur (Ca/S) in the solids feed is about 2 to 2.5 (about the same as in commercial CFBs). Alstom's process depends on sorbent attrition to enhance sorbent reactivity by increasing available particle surface area, as in CFBs. Solids reactivity is also enhanced using a proprietary sorbent activation step, which was employed to reduce the Ca/S ratio in Alstom's CFBs. Because limestone is cheap and also removes sulfur, there is no need to physically separate either the coal carbon or coal ash from the oxygen carrier particles. The problem of coal contaminants such as sulfur, carbides or mineral matter from the coal are well known by Alstom to blind and decrease reactivity of the sorbent. Accordingly, Alstom separately developed and commercialized its sorbent activation process, which continually renews the solid reactant surface. Environmentally, the process removes all of the sulfur and produces no measurable NO<sub>x</sub> in the Pilot. Mercury emission results await the Prototype.

In contrast, the metal-oxide-based chemical looping processes require more preparation for the oxygen-carrier. If the carrier is an ore like iron-ore or ilmenite, it must be double screened to a narrow size distribution to allow it to be more effectively separated from coal ash and carbon. On average, transportation legs can be expected to be about 10 times farther than for limestone because ore sources are much farther apart (world-wide) than limestone quarries. If the carrier is a manufactured carrier, a manufacturer must be located, contracted and more transportation arrangements must be borne. Carbon and ash must be separated from the solids that are bled from the system with the ash because the solids are too expensive to replace. Blinding by materials in the coal becomes critical because the carrier must be maintained in the system for several thousand hours to make the process economical. Solids disposal is costly. For sorbents such as nickel, the waste is hazardous and nickel is too valuable to discard. Therefore, another industry must be involved to reclaim and recycle the waste. For iron, the disposal question is unclear because iron is less valuable. However, it is probable that spent iron sorbent will have to be reclaimed as well. Environmentally, NO<sub>x</sub> should not be a problem, but down-stream sulfur removal will have to be added.

These differences and others make Alstom's limestone-based Chemical Looping system more economical than any of the metal-oxide alternatives. Referring to **Figure 9-1**, the most expensive chemical looping case is a metal oxide case. The two lowest cost chemical looping cases are Alstom's limestone-based system. The difference amounts to about a 0.8 cents/kW-hr increase in the cost of electricity relative to the limestone-based case.

#### **9.1.2.2 Risk Review**

A summary of the risk discussion is given below in **Table 9-1**. Some of the risks have been discussed in the preceding responses. A detailed discussion of the risks has also been presented in the Phase II report in the appendix as part of Alstom's internal concept review.

A list of 'show stoppers' was made. Plans were made to address R&D needs to resolve them. All areas of the plant were evaluated and no potential 'show stoppers' were identified. Several other areas of the plant are addressed in the list. The list is included in **Table 9-1**.

At the beginning of Phase II in the development of the Chemical Looping process there was only one identifiable potential 'show stopper'. That is the rate of CO<sub>2</sub> capture via the water gas shift and CaO in the reducer with and without sorbent activation. The commercial plant study required a rate of CO<sub>2</sub> capture (i.e. rate of CaO conversion to CaCO<sub>3</sub>) of 5%/sec-ata. During Phase II we determined the rate of these reactions to be over ten times faster (for the normal-sized sorbent - nominally 700 microns) than that required for the commercial plant concept.

There is a fundamental difference in the Chemical Looping concept between metal oxides, as used in some processes (including a separate process being developed by Alstom in Europe), and limestone based CaS/CaSO<sub>4</sub> looping, even though they may have similar uses in some regards. The durability issue with metal oxides is that metal oxides are expensive and therefore need to last in the process for a large number of cycles. In the Alstom DOE program, calcium sulfate, calcium sulfide, calcium carbonate and calcium oxide are recycled to transfer oxygen and to remove sulfur from the process. Bed material is removed from the oxidizer to remove sulfur and ash from the process in exactly the same way that is done in a CFB boiler. Limestone is added to make up the bed supply. The length of time that the bed material in the calcium based Chemical Looping concept needs to be retained in the system is on the order of hours instead of months as in the metal oxide case. In addition to sorbent activation, the attrition of particle size actually provides more surface area for chemical reactions. Therefore, the durability of the oxygen carrier is not an issue in Alstom's DOE project. The durability of other parts of the process is discussed in **Table 9-1**.

### 9.1.2.3 Comparison with GE's Unmixed Gasification Combustion Reactor

The DOE sponsored chemical looping competition includes several other processes. The most notable is GE Global Research's Unmixed Fuel Processor (UFP) process. Alstom does not have any detailed information about the UFP process. The information in this comparison is based on publicly available sources (**References 14 through 18**).

In the UFP process, coal, water and air are converted into hydrogen, CO<sub>2</sub> and vitiated air streams. The reported high-risk areas are: economics, solids attrition and lifetime and product gas quality for turbines.

The UFP process uses a prepared sorbent for oxygen transport. Alstom's process uses calcium compounds, which use the same chemistry as used in CFB boilers. The cost of the prepared oxygen transport compounds is in the order of 10 to 100 times the cost of the limestone used in Alstom's process. Because of the costs, the prepared sorbent must be cycled continuously for very many cycles in order for the economics to be reasonable. This requires that the prepared sorbent has a low attrition rate.

The UFP process also uses a separate prepared sorbent for the CO<sub>2</sub> removal. This requires that the solids will need to be separated at some point in the cycle and also ash will need to be separated from both sorbents for disposal. Sulfur removal apparently requires an additional downstream step

By comparison, Alstom's process uses limestone chemistry for both oxygen transport, SO<sub>2</sub> removal and CO<sub>2</sub> capture. This is the same chemistry that occurs in CFB boilers and is described elsewhere in this report. Limestone has the following advantages:

1. Limestone is less costly than the prepared sorbents by orders of magnitude.

2. Limestone is constantly added to remove sulfur as in a CFB. Therefore, it is removed constantly to maintain a solids balance. The bed material is constantly being refreshed. The residence time is on the order of hours instead of months. Because the cost of the limestone is low, this is economical.

**Table 9-1 – Potential Show Stoppers**

Item	Reason this is not a problem
<b>Kinetics issues</b>	
CO <sub>2</sub> Capture via the water gas shift and CaO in the reducer with and without steam activation	Demonstrated in Phase II
char gasification rates	<ol style="list-style-type: none"> <li>1. 30 years experience in gasification</li> <li>2. Reactivity test data from 5 different working units and test rigs on over 16 different coals</li> <li>3. Literature back up info (ESSO)</li> <li>4. Used reactivity data and current methodology to design previous gasifiers</li> <li>5. Economic impact of reactivity rate sensitivity shows impact to be small</li> <li>6. Unreactive char from Pitts #8 coal successfully gasified in Chem Looping Test Rig in Phase I</li> <li>7. Used previous experience for initial rate calculations. Designed preliminary reactor for GHG study. Checked rates in Phase I and II, rates were conservative.</li> </ol>
<b>Solids Transport issues</b>	
Aggressive coal transport ratios	<ol style="list-style-type: none"> <li>1. Design case can be relaxed if needed</li> <li>2. Reviewed with Dr. Fred Zenz</li> <li>3. PPL test data used in design</li> <li>4. Industry examples of high solids to gas ratios</li> </ol>
Refractory lined transport pipes	<ol style="list-style-type: none"> <li>1. Industry examples of refractory lined transport pipes.</li> <li>2. CFB lower reactor, cyclone ducts, return ducts and control valves are all examples of refractory lined transport vessels at elevated temperatures.</li> <li>3. R&amp;D needed but issue is manageable.</li> <li>4. Design scheduled for Phase III</li> </ol>
Economic impact of changing design to larger transport pipes including impact on \$/kw COE Heat rate	<ol style="list-style-type: none"> <li>1. Reviewed for solids transport issues mentioned. Minimal impact found</li> <li>2. Reviewed for overall impact on plant cost and heat rate. Minimal impact found</li> </ol>

**Table 9-1 – Continued.**

<b>Economic issues</b>	
original plant economics	<ol style="list-style-type: none"> <li>1. Reviewed in GHG Report (CASE 13) on a common basis with 12 other plants economics are favorable</li> <li>2. Reviewed in Phase I relative economics not changed economics are conservative</li> <li>3. Reviewed economics in Phase II report - still favorable</li> <li>4. Scheduled for an update in Phase II and in all succeeding Phases.</li> </ol>
Economics based on peer review	<ol style="list-style-type: none"> <li>1. Reviewed in Phase II relative economics not changed</li> <li>2. Included effects of: solids trans. pipe diameters, transport gas flow, auxiliary power, coal kinetics.</li> <li>3. Showed that effects of issues identified were minimal. They did not effect relative economics in GHG report.</li> </ol>
<b>Sorbent issues</b>	
Sorbent attrition, life expectancy, and long term reactivity	<ol style="list-style-type: none"> <li>1. The process depends on attrition because it needs particles with high specific surface area for absorbing CO<sub>2</sub> with CaO</li> <li>2. Limestone must be continually added to remove sulfur at a Ca/S of ~ 2. The sorbent is replaced as in a CFB.</li> <li>3. Steam reactivation, which maintains reactivity is a part of this process</li> </ol>

**Table 9-1 – Continued.**

<b>Other issues (see Phase I Report)</b>	
Solids flow control with Chiu (SPCV) valve	<ol style="list-style-type: none"> <li>1. Demonstrated in Phase I both in cold flow model and hot test rig.</li> <li>2. Control method developed.</li> <li>3. Operated smoothly at ambient temperature and at 1800 Deg. F. and all temperatures in between and with temperature increasing and decreasing</li> </ol>
Mechanical equipment operating at elevated temperatures	<ol style="list-style-type: none"> <li>1. Demonstrated in Phase I</li> <li>2. All equipment survived. Chiu valve was spotless and undamaged. All pipes, heaters, steam activation boxes, coolers, impactors, controls and instrumentation are fully operational after operation at temperatures up to 2150 Deg F.</li> </ol>
Operation of 2 solids loops in parallel	<ol style="list-style-type: none"> <li>1. Demonstrated in Phase I</li> <li>2. Startup, heatup, and shut down smoothly</li> <li>3. Operation at temperatures to 2150 Deg F. Metal temp.</li> </ol>
Sorbent reactivation	<ol style="list-style-type: none"> <li>1. Demonstrated in Phase I</li> <li>2. Operated sorbent activation solids loop in parallel with combustor solids loop. Operated sorbent reactivation reactor and sorbent impactor.</li> </ol>
CaS to CaSO <sub>4</sub> cycling with no production of SO <sub>2</sub>	<ol style="list-style-type: none"> <li>1. Demonstrated in Phase I</li> <li>2. No SO<sub>2</sub> production seen with the transport reactor at PDU. SO<sub>2</sub> only formed in batch reactor tests.</li> <li>3. Successfully oxidized CaS to CaSO<sub>4</sub> in combustor.</li> </ol>
Sulfur removal under reducing and oxidizing conditions	<ol style="list-style-type: none"> <li>1. Demonstrated in Phase I</li> <li>2. H<sub>2</sub>S removed in reducer, SO<sub>2</sub> in combustor CaO only produced at stoichiometrically neutral conditions.</li> </ol>

3. Limestone transfers more oxygen per pound of sorbent than any of the metal oxide sorbents.
4. Sorbent reactivity is helped by attrition, since the breakup of particles refreshes the surface pore area. In addition, a sorbent re-activation process, which is a commercial Alstom product, can be added at a very small cost
5. Solids do not have to be separated to remove ash. Ash is removed in the solids drain.
6. CO<sub>2</sub> is removed as part of the reducer process.
7. Limestone bed drain material is the same composition as the drain from a CFB. There are no disposal problems.

The UFP process uses low velocity fluid beds, whereas the Alstom process uses transport reactors. This makes the UFP reactors much larger than Alstom's.

#### **9.1.2.4 Review of Kinetic Data**

An issue was raised about whether the main reactants in the Chemical Looping Process had gasification reaction rates, which were fast enough to be commercially useful. A detailed analysis of this subject was done in Alstom's Specification Gate Review documents (**Reference 4**). A copy of the kinetics section is included in **Appendix A5 Chemical Looping Kinetics**.

The main concern centered on the commercial plant economics in the Chemical Looping Phase I report (**Reference 1**). These economics are identical to those developed in the Green House Gas report (Case 13) by Dr. N. Y. Nsakala and G. N. Liljedahl (**Reference 2**). Rates were re-examined along the guidelines suggested by the Peer Review and Specification Review. About 40 sets of coal gasification rate data were examined. Even the slowest rate examined (Pitt 8 DTFS from **Reference 3**) was fast enough to confirm the validity of the reactor size used for cost estimate purposes in the Chemical Looping Phase I report. For example, a carbon gasification rate of about 4%/sec-ata at 1800 degF was used for the commercial plant conceptual design, while the slowest rate examined was about 7%/sec-ata.

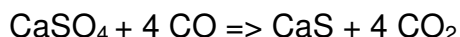
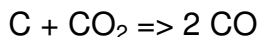
In order to determine the effects of slower kinetics on reactor size, a cost study was done by Alstom personnel not involved in the chemical looping project to determine the cost and performance impacts of low solids-to-gas transport ratios and a larger gasifier reactor.

A reactor that is 10 times the size of the entire gasifier (including the CO<sub>2</sub> removal/H<sub>2</sub> production/water gas shift sections as well as the fixed-carbon gasification sections) was sized and priced. Solids transport lines were priced at a solids-to-gas ratio of 10 which is far lower than that used for the design. Plant efficiency and auxiliary power

were re-estimated in accordance with these very conservative size and performance changes. Both of these more conservative factors combined only increased the cost of the plant by \$64/kW and the cost of electricity by 0.17 cents/kW-hr. With these increases included, the results of this cost study show that the chemical Looping process remains the most competitive economic system even with the very conservative evaluation factors expressed above.

Other conclusions include the following:

- ESSO had tested a process which uses  $\text{CaSO}_4$  to gasify fixed carbon similar in this respect to our proposed Chemical Looping process. Quantitative performance and gasification kinetics are very similar to results achieved by Alstom's Chemical Looping process in both the 4-inch FBC and the Chemical Looping process development unit CL-PDU.
- Alstom's Chemical Looping test data in the 4 inch FBC and in the CL-PDU exhibit strong temperature and particle size dependency.
- As the review team correctly discerned, there are two main solid-gas reactions, which occur during the gasification of fixed carbon by  $\text{CaSO}_4$ . They are as follows:



As the team pointed out, these should be de-coupled in order to better understand the process. This had been done. The 4 Inch FBC tests and previous DTFS tests were specifically intended to determine how these reactions work together to produce CO and  $\text{CO}_2$ .

- The individual reaction rate for each of the test data points was determined. A mathematical process model was developed which uses these rates to predict gas composition. The model was shown to provide predictions with good engineering accuracy (**Reference 1**). This model was extensively used to successfully design the Chemical Looping PDU (CL-PDU).
- As the previous AlstomGasification development program made clear, a suitable unit, capable of simultaneously testing all of the physical and chemical processes that are important to this process, is essential to identifying and solving the development requirements connected with the process. Without such a test facility, little progress can be made because many physical and chemical effects go undetected without such a rig. The prototype planned for Phase IV will be such a rig. Phases 0 through III are specifically intended to develop the data required to ensure a viable prototype in Phase IV.

- From a practical standpoint, what we know about the  $\text{CaSO}_4$  and fixed-carbon reaction rates is more than enough to get us successfully to the prototype phase.

In regards to the issue of  $\text{CaSO}_4$  removal and the production of  $\text{H}_2\text{S}$ , Alstom tested the  $\text{CaS} - \text{CaSO}_4$  loop in Phase I. It was found that the process does not generate  $\text{H}_2\text{S}$  or  $\text{SO}_2$  gas from the  $\text{CaS}-\text{CaSO}_4$  loop since the chemistry of the loop does not allow the reactants to exist in combinations that favor the production of sulfur gas species. A detailed report on the experiment is found in the Phase I Final Report, Section 7.3 (**Reference 1**).

Alstom will be conducting environmental testing at the Prototype Chemical Looping Facility in Phase IV. Alstom submitted a proposal for Phase IV in October 2007.

This will be the first time that a fully integrated Chemical Looping process will be operated. It has always been part of Alstom's plan to characterize environmental performance at the prototype.

In regards to  $\text{CaSO}_4$ , solids will be discharged from the Oxidizer vessel in the Chemical Looping process. The conditions in the Oxidizer are similar to the conditions where ash is discharged from CFB boilers. Therefore, it is expected that the discharge of  $\text{CaSO}_4$  will be no different than from a CFB and that there will be no  $\text{H}_2\text{S}$ .

## 9.2 TCGR

A Technical Concept Gate Review (TCGR) is used by Alstom to review research projects that are ready for scale-up from a small pilot facility to a prototype or demonstration phase. The purpose of the gate review is to make sure that the project is part of the company strategic plan, all of the technical and economic resources needed to successfully complete the project are available and that the concept is in fact ready for the next phase.

The TCGR process requires that the project team answer five basic questions. These questions are answered in a presentation required to last less than 2 hours. In addition, a number of backup documents is also made available before the review meeting.

A team of company experts in various disciplines is assembled to review the backup documents and listen to the presentation. The review team includes a Lead Assessor, a Project Manager representative, a Marketing representative, a Plant Engineering representative, a Construction Services representative, an Engineering representative and an R&D representative. The reviewers make recommendations as to whether the project has passed the review.

In some ways, the TCGR is similar to the ASME third party review. However, the reviewers in the TCGR are experts in the power plant industry, specifically in Alstom key markets.

The TCGR presentation slides are located in **Appendix B**. The five questions that are addressed by the TCGR are:

1. What is Chemical Looping?

This covers material found in Sections 1, 2 and 3 in this report. It also includes a discussion of competing concepts, and how chemical looping meets the original specifications for the chemical looping product.

2. Can we do it?

This section provides a project plan, which for this review covers the prototype phase of the chemical looping project, Phases IV-A and IV-B. It also includes the master project schedule, an estimate of the cost for Phase IV-A, a list of technical issues and a description of the prototype.

3. Is it worth it?

This question discusses the value proposition which indicates that the cost of chemical looping will be favorable against IGCC whether there is a requirement for CO<sub>2</sub> capture or not.

The value proposition also covers the feedback generated from over 18 internal reviews, DOE project reviews, and independent third party reviews as well as our own marketing reviews.

4. How do we prove it?

The ability to prove the concept will require the operation of the prototype. This section goes over performance targets for the prototype and test plans which are designed to address the technical issues raised.

5. What are the risks?

A risk assessment is presented based on the lists of technical issues presented earlier. The risks have been reviewed several times. An assessment of the level of risk and their impact is estimated. Most of the risks have been identified and the work in Phases I, II and III has focused on addressing these risks. The risks are considered manageable and any further development to manage these risks will require the operation of the prototype plant.



## **10. Lessons Learned**

### **10.1 Lessons from Phases I and II**

#### **Operation**

1. The PDU operated at design temperatures that were high enough to perform the required chemistry (about 1100 to 1900 degF).
2. Temperatures were successfully maintained with electric heating elements. The process temperatures could be maintained above 1800°F indicated and probably higher.
3. The PDU can be operated with metal temperatures up to 2150°F and electrical heating element temperatures over 2200°F.
4. Solids recycle feed rates were as high as expected and procedures for recirculation of the solids were developed. Solids were easily recycled at 100 to 200 pounds per hour; occasionally the recycled rate was as high as 400 pounds per hour.
5. Chemical conversion rates were as fast or faster than expected.
6. The PDU achieved 200/1 solids-to-gas ratio routinely and as high as 400/1 on occasion, as measured by combination of heat exchanger and pipe line pressure drop.

#### **Design Information**

7. The mechanical design and the operational characteristics of the SPCV (the medusa), the solids pickup (the sugar scoop), heat exchangers, fluidizing feeders, sorbent activation reactor, high efficiency cyclones, reducer and combustor reactors, impactor, and solid transport lines were determined.
8. Maintenance procedures were developed for inspecting and cleaning out the solids flow paths. A video probe procedure helped find conditions that would not have been found without it.
9. Procedures were developed for removing solids from the SPCV valve, the rotary valve, the sugar scoop and several other locations.
10. Chemical conversion rates were determined for the calcium sulfate/sulfide loop, calcium carbonate loop, char gasification and water gas shift both with and without sorbent and reactivated sorbent.
11. A control system for each of the various loops was operated under cold and hot conditions. Several of the loops were operated in parallel.

12. Solids transport was studied carefully in the cold flow model and the procedures to obtain good solids flow and control were put into practice in the hot PDU.

13. Procedures for handling upsets were developed.

### **Specific Phase I results**

#### **Cold Flow Modeling**

14. Cold flow modeling worked well in visualizing the process operation, solids flow pattern, determining operating procedures and designing test rig components and in trouble shooting operational problems in the PDU.

#### **CaS – CaSO<sub>4</sub> Looping**

15. The calcium sulfide – calcium sulfate reaction works without losing sulfur.

#### **Gasification**

16. Gasification rates are fast even with relatively un-reactive coal chars such as Pittsburgh #8 char.

17. The gasification reactions were started with only solid reactants. Solids were transported with nitrogen. The only carbon was solid carbon from the char. The oxygen was supplied by CaSO<sub>4</sub>.

18. Reaction rates were as fast or faster than the assumptions used to size equipment for the economic analysis.

#### **Solids Transport**

19. Solids recycle at the PDU is limited by the unit's dipleg height (5 feet).

20. Injecting solids in the seal leg feed point needs an automatic feeder at the PDU. Feeding with a manual feeder is not accurate enough for long-term operation.

#### **Knock Out Drums**

21. Knockout drums (called chamber pots) were installed just after the cyclones in the reducer and oxidizer to collect solids after an upset condition. The chamber pots worked well and only the very smallest dust got through to the filters. This procedure allowed the testing to resume almost at once instead of causing the unit to shut down and undergo a cleanout.

#### **Effects of Solids Size Distribution**

22. The size distribution of material in the SPCV was stratified by size distribution. The flow control of solids started to become uneven when the fluidizing requirements changed as the layers of different sized material went through the SPCV. This problem was dealt with by making sure before any testing that the material being loaded into the SPCV was as well mixed as possible.

## **Control Methods**

23. The seal pot control valve (SPCV) worked well and was a good way to control solids flow. The basic operation of the SPCV was developed at the cold flow model.

24. The solids flow rate was controlled by the pressure drop over the risers. Monitoring of the seal leg pressure drop was crucial to operating the PDU.

25. Passive pressure control methods were developed to enable automatically balancing the pressure between the various sections of the PDU such that solids flowed predictably and correctly.

## **Startup**

26. Startup of the PDU for hot operation was tricky at first, but a good procedure was soon developed. Each solids loop was started cold and the solids flow was stabilized. The heaters were then started and the fluidizing and transport air was adjusted as the solids temperature rose to keep the fluidizing velocity within a stable range for solids flow. The heat exchangers in the return legs were kept off-line.

27. During high temperature operation sometimes it became necessary to either physically check the solids level in the seal leg or refill solids in the SPCV and seal leg.

28. A rapid shutdown and restart procedure was developed. The SPCV fluidizing and transport air lines and grease air lines at the dipleg were shut down. Riser transport air was used to blow all of the solids in the piping up into the SPCV. The vacuum pump and transport air were turned off quickly. A similar startup procedure got the system back online quickly. The solids did not have enough time to cool and the flow could be restarted usually in about fifteen minutes.

## **Coal and Sorbent Feeding**

29. Coal was fed into the system with a metering feeder into a pipe that put coal into the PDU at the reducer downcomer leg just above the sugar scoop.

## **Heat Transfer - Heaters**

30. The process temperatures that were measured were lower than the actual temperatures because the thermocouples could not intrude into the process stream in the risers. This was done to avoid disrupting the solids flow in the risers. The actual temperatures were estimated as being 75° higher than the measured temperatures. The 75°F estimate came from a test of the thermocouples that was done at the end of a high temperature run, in which several thermocouples were temporarily inserted directly into the path of the flowing solids.

## **Heat Transfer - Pipes**

31. The PDU process piping is very small. The process solids cooled down about 500°F as they traveled around the loop. Thermocouples and pressure tap probes without insulation in the PDU were found to cool down to below 500°F in nine inches of length.

## **Heat Transfer – Heat Exchangers**

32. Heat exchangers were installed in each of the loops in the return leg. The heat balance around the heat exchangers was used as a solids flow measurement method.

33. Heat transfer coefficients varied widely on the solids side. from 1.5 BTU/hr-F-sq.ft to 80 BTU/hr-F-sq.ft, because of the different solids flow conditions on the inside of the pipe.

## **Solids Flow Measuring in the PDU**

34. Solids flow rate was measured primarily by measuring the pressure drop through the piping system.

35. A second method for calculating solids flow was by determining the heat balance around the heat exchangers as described above. In general, this measurement got the same results as the differential pressure method.

36. A third check was done in the sorbent activation test. The time it took to fill the box was measured and it was found that the resulting flow rate was consistent with the heat exchanger heat balance and the pipe pressure difference methods.

## **Pipe Corrosion in the Reducer**

37. One unexpected result of using electrically heated process reactors was the corrosion that was found in the reducer riser. The scale was formed only in the reducer and only in those areas that were externally heated by the electric heaters. Materials in the PDU are subject to temperatures that are higher than the process temperatures because of the external heating. In the larger plants, there will not be a need for the external heating and material temperatures will be at or below the process temperatures. Therefore, the scaling seen at the PDU is not expected to be a process problem.

### **Inspection Techniques**

38. A video scope was used for internal inspection of the PDU. The video scope significantly reduced the time needed for clean out after a test.

### **Economic Evaluation in Phase I**

39. The reaction rates measured at the PDU were as fast or faster than the assumptions used to size the reactors in the original Greenhouse Gas Report (**Reference 2**). This means that the original cost estimate was still valid and no changes were made to the economic evaluation at this time.

### **CaO – CaCO<sub>3</sub>**

40. Results from the tests clearly show the large effect that CaO has on enhancing the water-gas shift reaction. These effects are described in the Phase II report (**Reference 3**). Of the 60% of the CO that was converted to CO<sub>2</sub> in Test 3, 50 percentage points were captured by the limestone. Additionally, bed samples that were collected for analysis showed about 68% of the CaO was recarbonated to CaCO<sub>3</sub>.

41. No agglomerating tendencies were noticed.

42. Test 6 shows over 95% of the CO fed to the reactor was shifted to form hydrogen.

### **Pyrolysis**

43. In one test, coal was pyrolyzed in the reactor without any fluidizing gas being fed to the bed. In this case, the downstream equipment plugged with tar and the bed formed agglomerated char.

44. In another test, coal was fed into the reactor with nitrogen at 3 feet per second bed velocity. Results relative to tar formation and bed agglomerates were about the same as without bed fluidizing gas.

45. In the next test, the coal was fed into the reactor with a stoichiometric amount of steam in nitrogen and using a small nitrogen purge to prevent steam from entering the coal feed equipment. In this test, coal feed was easily accomplished. Although soot was

present on the reactor outlet filter, no tar was noted. Also, no bed agglomerating tendencies were noted.

### **Heat Tracing System**

46. The initial design of the PDU provided heat tracing for those areas of the PDU where steam could condense out in the pipe. The amount of heat tracing was enough to require that one person was dedicated to continually monitoring the heat tracing system. For Phase II, the additional lines that needed to be heat traced made it impractical to operate without an automatic control system. For Phase II an automatic control system was installed in the PDU and worked well.

### **Solids Transport**

47. Solids transport understanding was extended. The cold flow model was used to investigate solid transport properties and to establish a solids transport map. Two solids pickup devices (sugar scoops) were tested. Three horizontal legs joining the sugar scoops to the riser were also tested.

48. Gas leakage through the dipleg to the cyclone was tested in the PDU by using different gases in the fluidized SPCV and the riser main transport air. No gas leakage was found through the dipleg seal.

49. Static mixing tests were performed to investigate solids mixing in the SPCV at various fluidizing conditions. Solids mixing is fast (on the order of 1 second). Below minimum fluidization, mixing is slow.

### **Practical Solids Velocity Probe**

50. A practical testing and analysis procedure for the solids velocity probe was developed for determining solids mass flows on-line and continuously. It was developed for the cold flow facility. An upgrade of the laser device used to measure the solids velocity in the cold flow models was successfully completed in co-operation with the developer of the device (MSE Meili).

### **High Moisture Gas Sampling Analysis System**

51. The gas sampling and analysis system was developed to work at steam-gas ratios from 0% to 80% steam (by volume). Accordingly, the gas sampling system was equipped with moisture measuring equipment, dryers and automatic heat tracing to allow accurate gas sampling and analysis, even at high moisture content. The tests showed that the new gas sampling and analysis system worked very well.

### **Maintenance**

52. Leak detection and internal inspection methods were improved. Leak detection techniques included CO<sub>2</sub> and natural gas sniffers, which were much better at locating the leaks.

### **Condenser and Water Trap**

53. A condenser was put downstream of all the control valves and just upstream of the vacuum pump. A drain trap was designed to remove the condensate. A reheater was designed to heat the gases into the pump such that the pump outlet was well above the exhaust gas dew point. In operation, the condenser and trap worked reasonably well.

### **Scrubber Water**

54. At the outlet of the vacuum pump a vacuum beaker valve was installed to relieve the vacuum that is caused by water condensing after the test is finished and the piping cools down.

### **Controls**

55. The present pressure control and gas flow control was inadequate for Phase III. The control system needed to be redesigned in Phase III for a more integrated operation of the chemical looping process.

### **Economic Evaluation and Sensitivity in Phase II**

56. The economic evaluation showed that the Chemical Looping equipment is only a small portion of the total plant costs.

57. The original Greenhouse Gas Report estimated a chemical looping plant to have a total plant cost of 1383 \$/kW in 2001 dollars. The worst case impact in the economic update study gave a total plant cost of 1447 \$/kW, for a change of 64 \$/kW. COE changed from 5.22 cents/kW-hr to 5.39 cents/kW-hr. The 'worst case' included lower solids to gas ratios, larger reactors and additional coal and limestone crushing.

## **10.2. Lessons learned in Phase III**

The objective of Phase III was to operate the pilot plant to obtain enough engineering information to design a prototype of the commercial Chemical Looping concept. The activities included:

1. Modifications to the Phase II Chemical Looping process development unit (PDU),
2. Solids transportation studies and additional cold flow modeling,
3. Control and instrumentation studies,
4. Preliminary design guidelines for the prototype plant,
5. Update of the commercial plant economic estimates.

## **Modifications to the PDU**

### **Burner Can Modifications**

At the end of Phase II it was determined that the burner can was leaking from the water jacket. This was determined by a heat balance around the burner. The last test in Phase II was conducted without the burner in operation.

Inspection of the burner found several problems. The observation port which extended through the jacket was welded to the inside wall. There was stress cracking at this weld and a water leak. The weld material was rusty in all welds, which indicated the wrong weld material had used. After the first repair of the leaks, the burner was started up in Phase II, but condensate from the gas burner collected in the bottom of the burner.

The burner was redesigned so that the outlet of the burner was offset to the bottom of the horizontal cylinder and the burner was mounted with a one or two degree tilt toward the outlet so that condensate would run into the outlet pipe toward a drain in the un-cooled section. The new design eliminated the observation port since the flame scanner in the burner tip worked very well. This eliminated the thermal stress at the inner wall where the observation port would have been welded. The weld material was carefully chosen for the application to prevent rusting at the weld seams.

### **Vacuum Pump Installation**

Two vacuum pumps were required for the Phase III control tests. This models the commercial control scheme where the outlets from each loop cannot be mixed.

The installation of the two pumps was designed with a complex set of piping that would allow the use of either pump on each loop (reducer and oxidizer). This flexibility was put in to the PDU in case one pump developed problems. Part of the test program could continue while the pump problem was resolved. The complex pump supply-piping network also allowed for the easier cleanout of the wet gas from the process by allowing the pump to recycle dry atmospheric air after a test.

### **Scrubbers**

Two scrubbers were used because the pumps were designed to work on either the reducer or oxidizer loop.

### **SPCV**

In order to operate the unit with automatic controls, automatic flow control valves were installed in the air supply lines to the fluidizing and transport lines to the SPCV. There are four chambers in the SPVC each with transport and fluidizing air supply. The automatic control valves were placed in series with, and downstream from, the original

manual rotameters. The rotameters were left in the full open condition when the unit was testing automatic control. The rotameters were located upstream of the automatic flow control valves to maintain a constant pressure at the rotometer. In this way, the rotameters provided an independent visual check on the flow readings into the control system.

The second modification was to install manual pressure balancing valves between the crossover lines and the SPCV vent lines. This kept the pressure in the crossover lines from changing too fast for the control system.

### **Control System Hardware.**

The control system was updated to make it easier for the operators to monitor each test. The control system software was upgraded and more instrument channels were added. Two workstations were added, each with a dual monitor setup. In Phases I and II the operators were hampered by the inability to see more than one control screen at a time. The time to change screens on the old control system was sometimes longer than the time required for effective control.

The new system allows four separate control screens to be monitored and each of the two workstations can send a control request into the system. For example, one operator can monitor the system heat up sequence and make adjustments while another can monitor the supply air control. The new automatic control system will require less action from the operator, but the Phase III test required this monitoring capability.

### **Sorbent Activation System Modifications**

System upsets could cause solids in the sorbent activation system to get into the downstream piping and into the condensers. Knockout drums (chamber pots) were successfully used in the main reducer and oxidizer lines to keep solids out of the condenser. For Phase III a chamber pot was put on each of the sorbent activation lines. In Phase I and II testing several upsets caused solids from the activation system to plug up various parts of the PDU. It was felt that chamber pots in the activation system were justified.

### **Feed Systems**

In the previous testing, the coal and limestone feeders were rearranged for the individual test. For Phase III, an additional feeder for the reducer was needed for automatic operation. A coal feeder and bed material feeder were used for the reducer and a bed material feeder was used for the oxidizer.

### **Control System Modifications**

Testing of an automatic control system for the Chemical Looping process required modifications to the control system.

The first vacuum pump was set to control the pressure of the reducer loop at the bottom of the downcomer to a preset value by changing pump speed. The Second vacuum pump was set to maintain the pressure difference from the reducer downcomer to the oxidizer downcomer to within plus or minus 1 in. w. g. by changing pump speed. Flow through the pumps was controlled by setting the main riser flow in each loop.

Recirculation flow in each loop was controlled by setting the transport and fluidizing air to the main SPCV chamber for each loop to maintain a preset delta pressure in the riser for that loop.

The temperature in each loop was used to change the transport flow to the riser required to maintain the correct velocity as temperature changed during heat up or load change. The temperature and flow correlation was programmed into the control system. As the riser flow changed the SPCV fluidizing and transport air were corrected to maintain pressure drop in the riser.

### **PDU Gas Sampling System - Sulfur measurement**

Sulfur in the product gas from the PDU is measured using US EPA Method 16B. In this method, sulfur compounds are oxidized to  $\text{SO}_2$  and the  $\text{SO}_2$  is measured directly. Ordinarily, there are only minute amounts of combustibles in the gas sample and this isn't a problem. In the chemical looping process, the product gas has a lot of  $\text{H}_2$  and CO. This requires a modification to the Method 16B procedure.

The product gas sample needed to be combusted with  $\text{O}_2$ . The total  $\text{SO}_2$  and excess  $\text{O}_2$  was measured and compared with the product gas analysis. The sulfur level was then back calculated.

A series of calibration test cases were run with different bottled gas mixes to show the modified Method 16B was still applicable to the PDU process. The tests were successful.

### **Solids Transport Studies and Cold Flow Modeling**

#### **40-Ft Cold Flow Model Facility**

The 40-ft cold flow model was built to test process scale up issues and to investigate solids flow rates that were much higher than the 15-ft cold flow model.

As reported in the Phase II report, the first pressure test on air resulted in the failure of the primary cyclone. The cyclone exit line to the baghouse was improperly sized and this caused a large increase in pressure in the loop. Also, the cyclone was constructed with thinner plexiglass because of the need to make curved surfaces. After the failure the cyclone was reconstructed with thicker material. The cyclone discharge line to the

baghouse was changed from 2.5 inches to 6 inches to reduce back-pressure. No further pressure related problems were encountered.

It was seen that the 40-ft CFM was easier to operate than the 15-ft CFM. Because of the larger cross-sectional areas, solids flowability was better. The first time the 40-ft CFM operated with solids the unit started right up and the flow stabilized immediately.

Tested data shows consistent agreement in comparing to the 15-ft CFM and other published data for scale up.

### **Original Air Supply System**

The original air tests in the 40-ft showed several problems. There was an instability in the air flow in the riser showing a hysteresis effect from the main pressure control valve. The compressor pressure variance also imposed a velocity variance on the main riser flow. Finally the main flow meter needed to be calibrated.

### **Riser Velocity Changes due to Air Compressor**

The source of the riser flow instability was the compressor pressure cycling even with regulators installed. Compressor pressure was cycling about plus or minus 10 psi between the dryer exit and the test loop. The smoothness of the air supply to the SPCV is critical in controlling solids flow. Part of the problem is that when the air supply system is heavily used, a second compressor is automatically turned on. Without the second compressor the air supply is relatively smooth but the single compressor can only handle about 80% of the tests.

### **Mass Flow Meter Calibration**

The main flow meter deviated from the set point by 264 slpm to 464 slpm over the range of flows, up to 3000 slpm. This was greater than 10% and was not acceptable for control of the CFM.

### **Modified Air System on the 40-Ft**

A modification of the air supply system to the cold flow models was necessary because of the large fluctuation in the main airflow. To fix the problems several modifications were made.

The two compressors operating range was adjusted to smooth the transition from one operating compressor to two operating compressors.

A new pressure regulator was added to the inlet of the air supply system at the cold flow models.

The second pressure regulator in the main air line was resized to minimize the pressure reduction in each step down.

A new pneumatic actuated valve and positioner was added to give better control of the main mass flow control valve.

A new trim valve was added in parallel with the larger flow control valve.

A new PID controller was installed for the main air flow.

An accumulator was installed in the supply header for the grease air and the SPCV fluidizing and transport air supply.

The modified air supply system worked well and improved the solids flow stability in both the 15-ft and 40-ft cold flow models.

### **Riser Flow Stability with New Air Supply System**

The modifications to the air supply system made a big improvement to the flow response. Pressure in the cold flow model supply was below 1% deviation and in the SPCV fluidizing and transport air supply the deviation was down to 0.25%. This was considered acceptable for the chemical looping system.

### **Solids Pick-Up Device**

The SPCV feeds solids into a downward running dipleg. At the bottom of the dipleg is a solids pickup device called a 'sugar scoop'. The sugar scoop injects high velocity air into the stream of solids from the dipleg and transports them up a 20 to 25 degree inclined pipe to the riser. The original design for the sugar scoop included a slight constriction after the solids pickup, which opened up again near the riser. This original design had an orifice effect on the solids and restricted the maximum solids flow.

A new design for the sugar scoop was tested that did not have the restriction in the sloping pipe section. The new straight-sided design showed the capacity to increase solids throughput.

The disadvantage of this design was that the new flow patterns in the sloping pipe section and the inlet to the riser cause a little turbulence. This was seen by wear patterns on the side of the sloping pipe section and at the back of the inlet to the riser. This has implications for the prototype design and will require some design work to deal with the wear potential.

### **Laser Flow Measurement**

A laser velocity meter was developed in Phase II as an alternate way to measure solids flow. Initial calibrations on the 15-ft CFM show the potential for the device to measure flow. In phase III the laser velocity probe was used in both the 15-ft and the 40-ft CFMs.

The laser velocity probe is a non-invasive flow measurement device that requires a line of sight to shine a pair of laser beams into the solids flow. In the cold flow model, it was mounted on the outside of the plexiglass tube of the dipleg. In that location the solids were forming a moving bed. The moving bed solids flow regime has been found to be easier to measure with the laser velocity probe than the other solids transport regimes in the process.

The laser velocity probe was mounted with a slight gap between the tube wall and the probe face. This was to simulate the potential need to apply cooling air in a hot installation. It is anticipated that in the future the probe will be used in the PDU or the prototype by using a quartz window.

### **Calibration of Solids Flow**

The laser velocity probe was calibrated in both the 15-ft CFM and the 40-ft CFM.

In the 15-ft CFM, flow was calculated based on load cell measurements. It was shown that the 15-ft operated in a steady-state mode in both loops and in the crossovers. The laser velocity probe showed a reasonable accuracy in velocity, and by calculation, mass flow measurements. However, background lighting around the CFM affected the detection of solids flow by the laser velocity probe. The low solids flow range needs additional development of the calculation procedure that the laser velocity probe uses.

Calibration of solids flow at the 40-ft CFM required a different procedure. It was not practical to use a batch-type calculation to measure flow because the 40-ft uses a large amount of solids. In this calibration, a butterfly valve was installed in the dipleg and the flow was stopped. The amount of solids in the dipleg and the time to build up was measured. Due to the rapid build-up, a video camera was used to record the build-up and the time was measured by counting video frames. The level of solids was very stable for each test.

### **Dipleg and Sealpot Performance**

The pressure drop along the dipleg was found to be closely related to the amount of grease air injected and the solids downward velocity. The sealing capacity of the dipleg was mainly controlled by the static head of solids and the friction force between the wall and the moving solids in the dipleg. Solids flow circulation was limited by dipleg size and friction.

Noise was induced by the compression of the solids and gas in the dipleg. Grease air allowed the pressure to be spread along the dipleg. With more grease air, noise was reduced and the vibration decreased and eventually disappeared. Grease air acted as

one of the elements to increase solids circulation. As grease air increased, eventually the total pressure drop of the dipleg became equal to the static pressure drop of the solids. At this point the frictional portion of the pressure drop was zero and the solids velocity reached a maximum.

The pressure drop in the fluidized bed and the transfer bed of the SPCV is the key driving force for discharging solids from the SPCV. This is controlled by bed velocity. As fluidizing increases, the bed expands, which increases the solids exit velocity.

### **Sugar Scoop**

Pressure drop across the sugar scoop increased as the velocity of the riser inlet flow increased.

### **Vertical Riser Pressure Drop**

Pressure drop in the vertical section of the riser is a vertical co-current two phase problem. The main focus of the CFM tests was to understand the inter-relationship of the pressure drop, the transport velocity and the solids loading for a given particle size distribution including the choking limit. The choking limit makes the pressure drop of the transport system increase rapidly and causes stoppage of solids transport or causes the failure of the seal in the SPVC.

The operating range can be extended by either reducing the transport velocity until the vertical pipe reaches the choking limit or simply increasing the solids loading by SPCV control until the system pressure cannot support the required pressure drop. These conditions are possible as long as the seal limit in the SPCV can seal against the additional pressure.

In the actual application, an integrated evaluation of the pressure drop along the loop will identify the sensitivity of each segment.

### **Lower-Leg and Elbow Pressure Drop**

Pressure drop in the lower-leg is similar to solids flow transport in a horizontal pipe. Test data showed that as velocity was reduced in the pipe, the pressure drop of the lower-leg segment started to increase due to the saltation of particles. Solids saltation started at the lower elbow turn. The solids built up toward the sugar scoop forming a wedge shape. The lower elbow turn was most critical element in raising the pressure drop

### **Upper Leg and Elbow Pressure Drop**

The pressure drop of the upper elbow was about 30% of the pressure drop of the lower elbow in the 40-ft loop. In the 15-ft loop, the pressure drop of the upper elbow is about 150% of the lower elbow pressure drop. In the 40-ft. the top elbow goes from a round vertical riser shape to a rectangular shape.

## **Cyclone Performance**

The cyclone in the 40-ft has two stages. The cyclone has a very high fractional efficiency for solids separation. When the operating primary dipleg height is above the junction of the secondary cyclone dipleg, the cyclone collected all particles greater than 7 microns. The particles that escaped had a 'd50' of 1.5 microns. Once the operating solids height in the dipleg dropped below the junction with the secondary cyclone dipleg some solids would escape through the secondary cyclone.

## **Slip between Solids and Gas Flows**

The ratio of gas flow to solids flow in the 40-ft tests was typically about 4 to 5 in the vertical riser section for the tested conditions.

## **Flow Stability with the SPCV**

The 15-ft CFM was run continuously for six hours to check the ability of the SPCV to control solids flow. It was seen that the air supply system for the SPCV control had a tendency to drift over time but the overall system stayed stable.

The segregation of large particles in the bottom of the seal pot may contribute to the drift of the air supply. The phenomenon was eliminated in the 40-ft SPCV design by putting in the proper angle in the SPCV wall and by modifying the air control system.

## **Dual Loop Operation**

The 15-ft CFM was modified to simulate the operation of two-loop operation by adding a second identical 15-ft loop and crossover circuits.

The pressure of each loop in the dipleg was kept close to the corresponding pressure in the other loop. This allowed the flow to be relatively steady with crossover flow.

## **Scale Up**

The critical issues for scale up of the chemical looping process are

- Solids saltation in the lower leg sections and elbow turns.
- Solids choking in the vertical section.
- Seal capacity and height of the seal.
- Solids and gas separation.

It was seen that scaling from a ¾" diameter to a 4" diameter riser was successful. The test data also showed good agreement comparing to data from a 12 inch riser in the published data.

## **Automated Control Feasibility**

The information developed in the cold flow modeling was used to help design an automated system for control for the hot PDU. The areas of automated controls investigated in Phase III were: inter-loop pressure control, process temperature trim of injection air control and solids transport rate control.

### **Initial Loop Tuning**

As part of the CL automated control feasibility testing, characterization tests were performed. These tests were conducted in order to develop the loop tuning parameters. Step response testing was performed as the primary system identification tool. PID parameters were selected based on response time and overshoot requirements for each controlled process variable. The following are observations from the loop tuning activities.

Repeatable loop pressure curves were developed at each flow rate. Pump speed was restricted to the pump inlet vacuum manufacturer limit.

The proportional constant of the Reducer loop PID controller was derived from analysis of the pressure response to changes of injection flow rates.

A map of the inter loop differential pressure versus Oxidizer vacuum pump speed was developed.

The initial tuning of the Oxidizer vacuum pump PID loop was performed, to hold loop-to-loop differential pressure at zero. The proportional constant of the PID algorithm was manually derived.

Additional tests indicated that the first Oxidizer controller proportional value produced a response that was too slow. This was corrected.

After setting Oxidizer the PID values, the Reducer tests were repeated to assess loop interactions.

### **Air Only Automated Pressure Control**

Pressure tests were first conducted with air only in the PDU to show the feasibility of controlling pressure in the system using two individual vacuum pumps. The tests also help generate tuning information for the programmable controllers.

### **Automatic Loop Pressure Control Implementation**

The Reducer loop pressure controller maintained a set point pressure using the Reducer loop pressure as the control variable. The reducer vacuum pump speed controller was the manipulated variable

Pressure equalization at the loop cross over elevation was achieved by having a set point of zero for the for the Oxidizer loop PID controller. The differential pressure between loops was the control variable, and the oxidizer loop vacuum pump speed controller was the manipulated variable. Manipulation of the Oxidizer vacuum pump speed moved the Oxidizer loop absolute pressure to track the Reducer loop pressure at the solids crossover elevation. The control objective was to control the differential pressure between loops to within  $\pm 3$  " H<sub>2</sub>O, (0.1 psia).

By measuring the inter loop differential pressure with a narrow range pressure transducer the oxidizer loop differential pressure set point could be set to zero keeping the two loop pressures very closely matched.

### **Load Ramp Rate Test**

The oxidizer and reducer loop vacuum pumps were able to maintain the two loops at the same balanced absolute pressures during the test when the loop injection air (riser air) was changed at 10 SLPM per minute. This injection airflow change would be required in the event of a 10 % load change. Stable pressure control was achieved through a load (injection air) change of 10 %/min.

### **Long Term Stability Tests**

Both of the loops (oxidizer and reducer) were maintained at their set point values for a 2-hour period under automated control. For this air only test the reducer loop pressure and the oxidizer loop pressure controllers both worked correctly to maintain both loops at their set points for the entire test period.

### **Load Following Stability Test**

During this test the process temperature is changed in the range of 80-500°F. This resulted in an injection air trim to for each loop. During both the process temperature increase and decrease, the loop pressure controllers maintained the loop pressures at their set point values.

### **Shut Down Pressure Control Test**

Automatic pressure set point controls were used to successfully shutdown the process without pressure excursions. The shutdown concept was to use the automatic pressure control loop (which controls vacuum pump speed) to bring the vacuum pump to their minimum speed shutoff.

The shutdown test was initiated from the point where there were no crossover or recycle solids flow, main injection airs to both loops were on and both vacuums pumps were in automatic commanding a 14.3 psia solids pressure in both loops. The reducer solids pressure set point was stepped from 14.3 to 16 psia. The automatic pressure controls

held the loop-to-loop differential pressure at the zero set point. At the final 16-psia set point, the vacuum pump speeds were low enough that the pump bypass valves could be opened without pressure excursions. With bypass valves open, the main injection airs remained on for a final loop solids sweep out and then turned off. There was no inter-loop pressure imbalance during the set point changes and the PDU was shutdown without a single significant inter-loop differential pressure event.

### **Process Temperature Trim of Injected Air Control**

The primary control variable of the riser injection air is the load set point. As the reactors heat up, the velocity in the riser changes with temperature. In order to control the solids velocity within each reactor riser the individual loop process temperature further trims the injection air mass flow. Using a control function block the individual loop process temperatures generate the adjustment trim for the injection air mass flow rate.

During this test both the injection air flow trim control and the loop pressure controls must both be in automatic mode. The loop pressure set points must be maintained while the injection air flow rate is modified by the process temperature changes.

### **Solids Transfer Rate Control**

The controls method implemented for this feasibility study used the experimentally developed relationships between the loop riser differential pressures and solids flow rate. Similarly, the SPCV used an experimentally derived relationship between crossover transport airflow rate and crossover solids mass flow rate.

The Phase III solids transfer rate control testing utilized the individual loop vertical riser differential pressures to act as the control variable for the loop solids recycle rate. The manipulated variables were the SPCV recycle transport air mass flow controllers to establish a stable solids recycle rate (lb/hr) in both loops. The loop pressure controllers were in automatic mode to maintain the individual loop pressures at their set point values.

Once the two chemical looping reactor circuits were in recycle mode with both loop pressure controllers in automatic the crossover rate from the Reducer to Oxidizer was set.

Lastly, the oxidizer crossover controller using the DP ratio set point, was placed into automatic mode.

The PDU was operated with both loop pressure controllers and the oxidizer solids crossover controller in automatic mode. Recycle and crossover solids were being transported while the automatic pressure controllers maintained both loops at their set point values.

This finding is significant because it mitigates a concern about the results of the automated pressure testing on air only. In this test solids transport was occurring. This solids flow rate test shows that automated pressure controllers work correctly with solids transport active.

### **Overall Automatic Control Feasibility**

The testing of the automatic pressure control strategy proved encouraging.

Pressure controllers were able to maintain their respective process pressures at the desired set points even while recycle solids and crossover solids were being transported.

The Phase III testing is viewed as a positive indicator of automated control feasibility during a CL startup, load change and shutdown.

The second area of automated controls testing established the feasibility of providing a CL process temperature trim on the loop injection airflow rate.

The implemented control strategy for inter-loop solids transfer was logical, both from the Chemical Looping process and a regulatory controller standpoint. The control methodology, appears to have good promise for providing loop solids inventory control but will likely require modification to accommodate reducer and oxidizer loop injection air differences.

The success of the testing conducted during this phase provides the promise that automated solids transport control can be achieved.

### **Performance Estimate**

The prototype facility will be designed based on chemical looping option three described above. In this option, the plant will produce hydrogen as a synfuel and will remove CO<sub>2</sub> as a separate stream. This is the option described by Case 13 in the Greenhouse gas report. Designing the prototype for this option gives the most flexibility. All of the equipment used in all three options will be installed and therefore the prototype can be operated to characterize any of the three options.

The nominal size for the MTF is used because that size is large enough to operate all of the plant equipment at commercially significant sizes. It is also large enough to operate the process with heat generated from the process fuel. It will not have the external heating required at the PDU. The size is small enough to make a relatively cost effective fully operation chemical looping system.

The MTF is sized for about 1000 pounds per hour of coal feed. The prototype will be sized for a nominal coal feed of 2000 pounds per hour. This will give the prototype the

ability to operate in the hydrogen producing mode and produce enough product gas to characterize performance. When operating in the other modes, coal flow will be lower.

## Heat Exchangers

An engineering study was done to investigate the feasibility of using high temperature heat exchangers to preheat the air to the process, and to identify the issues that need to be resolved in the Phase IV heat exchanger design effort. Gas-to-gas heat exchangers in power plants are usually not designed to operate with gas temperatures as high as 2000 degrees. The problems anticipated include differential expansion of the tubes in the heat exchangers.

A specification was created for two heat exchangers. One was sized for the anticipated CO<sub>2</sub> stream in the Case 13 size plant. The other was sized for the N<sub>2</sub> rich stream in the prototype plant.

The rough cost estimates that came back were very high. The commercial sized air heater was \$5.4 million and the prototype was \$1.2 million. The physical size of the equipment was also very large. However, this exercise showed that commercial equipment exists that can be used for this application.

The prototype has special needs for flexibility that the commercial design doesn't have. Also the prototype will not have to operate at 90%+ reliability for 20 years. This means that Alstom Power Plant Labs will internally design the heat exchangers for this application and either fabricate them on site or have them custom built .

## Calcination Tests

In the chemical looping process, CO<sub>2</sub> is absorbed from the process gas. The solids containing the formed CaCO<sub>3</sub> are separated from the process gas and fed to a calcination reactor. In this process step, the reaction conditions (CO<sub>2</sub> partial pressure and/or temperature) are changed to favor the release of CO<sub>2</sub>.

Depending on the design of this process step, the reaction can be rather instantaneous and sometimes referred to as "flash calcination". The gas evolution could potentially create very high linear gas velocities in the reactor and as a result uncontrolled particle entrainment.

It was deemed necessary to study the process difficulties caused by this gas evolution. CaCO<sub>3</sub>-chemistry requires the reactor temperature to be above 1700-1800 °F. To simplify the experimental set up, a new approach was developed using NaHCO<sub>3</sub> at roughly 520 °F.

Al<sub>2</sub>O<sub>3</sub> was used in the experiments together with the NaHCO<sub>3</sub>. It had a dual function: a) it acted as a heat carrier for the calcination reaction and b) it simulated inert ash.

The experiment showed it was obvious that very rapid calcination took place in the reactor within less than a second. Generated gas blew out some of the solids, both through the funnel and the side tube at the top.

It is clear from both visual observations and video documentation that material blew out of the reactor due to the gas generated by the calcination. The chemical analysis shows that about half of the  $\text{NaHCO}_3$  was calcined and responsible for the generated gas. These factors will be considered when designing the calciner for the prototype.

## **Materials**

The Chemical Looping Concept uses many components that are used in the power industry and a few that are new designs. Most of the components in the chemical looping gasifier island have specifications that are different from conventional applications.

The main areas of concern were;

1. High temperature refractory lined vessels without water walls. These are used in CFB boilers. However, CFB boilers operate at temperatures up to about 1700 °F in the reactor, with possibly higher local temperatures. The three reactors in the Chemical Looping concept will operate at temperatures between 1800 °F and 2000 °F.
2. High Temperature refractory lined transfer lines. The issue of thermal expansion is a concern.
3. The reducer will have high concentrations of Hydrogen at elevated temperatures. Both refractory materials and vessel wall materials need to be selected to account for the Hydrogen.

## **Refractory Requirements**

### **Chemical Issues**

Hydrogen, steam and carbon monoxide are three that will have detrimental effects on the refractory linings.

The hydrogen rich atmospheres within the Reducer represent challenges for the refractory lining as well as the steel shell.

Hydrogen is a much more highly conductive gas than air, so the thermal conductivity of the refractory materials is adversely affected. As a result, thicker refractory linings are required in order to achieve the same thermal performance and steel shell temperatures when hydrogen is present. The higher the concentration of hydrogen, the worse the effect will be on the insulating ability of the refractory.

The hydrogen can be very chemically reactive with refractory materials, particularly constituents, such as iron and silica. The refractory products selected for use in the

applications areas with hydrogen atmospheres must be low iron regardless of the operating temperature.

In hydrogen atmospheres, at temperatures greater than 2000°F and with increasing hydrogen atmosphere dew points, silica will be extracted from the refractory matrix, weakening the refractory and leading to failure. In addition, the leached silica is likely to be deposited downstream in the process. It is important in these conditions to use high alumina, low silica refractory products.

Hydrogen will penetrate to the outer steel casing at refractory expansion joints, construction joints as well as through the porosity of the refractory materials themselves.

High pressure steam is also capable of extracting silica from refractory materials at temperatures above 1600°F, so again, high alumina, low silica refractory products should be used in these areas to form the hot face refractory layer.

In reducing conditions, concentrations of carbon monoxide will react with iron oxide present within the refractory lining to form iron carbide deposits. These deposits will grow within the refractory matrix causing cracking and failure. Only refractory materials containing low iron should be used in these conditions. Fortunately, in our chemical looping process, it should also be noted the presence of hydrogen has been shown to inhibit the carbon dioxide disintegration process.

### **Refractory Lining Constructability**

The refractory linings inside larger vessels within the Chemical Looping process may be cast, gunited or bricked.

In the smaller components and the transfer lines, the refractory linings will need to be constructed by forming and casting from the outside. The transfer lines will need to be segmented into manageable pieces, ie. approximately 8 to 10 foot lengths. This approach would also offer easier maintenance of these components in the future. This also would allow for the transfer lines and smaller components to have the refractory lining shop installed and then shipped to the plant site for final assembly.

The refractory lining will grow due to thermal expansion and allowance for this must be made in the lining design. The thermal expansion is typically taken into account by creating an expansion joint at regular intervals and packing with ceramic fiber blanket. Unfortunately, this also provides more opportunity for hydrogen to reach the steel shell and the more porous backup refractory layers. In CFB Boiler experience, in order to minimize “pinch-spalling” caused by bed material infiltrating the expansion joint, the joints are kept smaller than 0.5 inches.

Once the construction is complete, the refractory linings will need to be initially heated at a carefully controlled rate in order to dry-out the materials without damaging the

lining. The actual dry-out rate will be determined by the type and thickness of the refractory materials selected. Typically, the dry-out rate will be at temperature ramp rates no greater than 50 to 75°F per hour to approximately 1500°F.

## **Refractory Heat Up**

A study was done to determine if a prototype chemical looping plant can be constructed and operated without using external heating of the process equipment as was done in the pilot plant. Heat up rates were determined to verify that a refractory-lined design could be heated up in a reasonable time, and that the steady state heat loss would not cool the process to the point where the process could not maintain temperature.

The study concluded that the prototype can be heated up and operated within a reasonable time. The warm up will require up to 8.4 hours. The steady state heat loss is low enough to allow the process to maintain process temperature. The steady state heat loss from the major components is estimated to be about 3.6%

## **Commercial Plant Economic Studies**

The Phase III work develop no major changes to the process flow sheet or the design of any equipment for the chemical looping commercial plant design. Therefore, no changes to the relative economic rankings in the Greenhouse Gas report conclusions were warranted.

A separate independent CO<sub>2</sub> Technology assessment was made in 2006 and updated in 2007 and 2008. The purpose of this assessment was to rank the various CO<sub>2</sub> technologies according to a set of criteria to determine the most promising methods to deal with CO<sub>2</sub> capture.

The assessment was done by assembling a list of CO<sub>2</sub> technologies. Of these, 19 were selected. An initial assessment was made and it was determined that an in depth analysis was needed. The technologies were analyzed for technical and economic issues. Product summaries and development plans were considered. Financial analyses were done including a consideration of customer needs. The analysis resulted in a list of product rankings.

The results of the CO<sub>2</sub> technology assessment show that the cost of electricity for all of the technologies with CO<sub>2</sub> capture is lowest for the Chemical Looping case with calcium. The cost of electricity for chemical looping is also lowest as the CO<sub>2</sub> allowance price increases and becomes lower than the reference plant at about \$11.00 per ton of CO<sub>2</sub> emitted.

The conclusions from this newer CO<sub>2</sub> Technologies assessment are consistent with the conclusions from the original Greenhouse Gas Report (**Reference 2**). Chemical looping using calcium has the potential for large-scale capture of CO<sub>2</sub> at a reasonable cost.

Chemical looping is the most promising of the emerging CO<sub>2</sub> technologies for new plants and retrofit of existing units.

### **Design of a Chemical Looping System for PC Retrofit**

A brief study was done to examine the impact of firing a synthetic-gas fuel, produced by the Alstom's Chemical Looping gasifier, on boiler performance in a PC designed boiler. In addition, the study assessed boiler island equipment modification requirements and any potential barriers to boiler conversion and integration with the chemical looping system.

Since the main driver for boiler conversion is CO<sub>2</sub> emission reduction, economic comparison with other potentially competing technologies, such as O<sub>2</sub> firing with a CO<sub>2</sub> (flue gas) recycle system and ammonia-scrubbing system was made. To this end, approximate investment costs and performance were estimated for the three retrofit technologies; economic analysis was carried out.

The boiler performance was achieved with minimum boiler island modifications and no barriers were found to boiler repowering or integration with the gasifier system. The economic comparison with other potentially competing technologies such as the ammonia scrubbing system and O<sub>2</sub>/recycle flue gas system illustrated that the Chemical Looping technology is more cost effective than the O<sub>2</sub>/recycle flue gas system and is similar in cost to the ammonia scrubbing system. The small differences in cost are believed to be well within the accuracy range of the analysis. As these technologies mature, the analysis should be revisited for a more thorough examination.

## 11. Economics Update

This section provides a brief description of the applications of Alstom's chemical looping technology for CO<sub>2</sub> capture to both new and retrofit power generation and to industrial usage. It also provides an economic comparison of Alstom's chemical looping technology with other CO<sub>2</sub> capture technologies. As further described in this section, all of the economic comparisons are on a common basis, with costs as of mid-2006. Since that time, commodity prices for steel and energy, as well as for construction labor have caused significant increases and fluctuations in the cost of power plants and electricity. Accordingly, no claim is made for the absolute accuracy of the costs provided in this section. However, all of these economic results are on the same economic basis, so the comparisons presented should provide a reasonable relative comparison of economics.

This mid-2006 time period represents the most recent time that Alstom compared all of these technologies on a common basis. Since that time technical progress is being made with respect to all of these technologies. At some point in the future, another comparative examination should be made. Until such a re-examination becomes available and with the above limitations firmly in mind, the relative comparisons provided below provide our best current assessment of the relative merits of Alstom's chemical looping technology.

### 11.1 Chemical Looping Retrofit for PC or CFB

The objectives of this brief study was to examine the impact of firing a synthetic-gas fuel, produced by the ALSTOM's Chemical Looping gasifier, on boiler performance in a PC designed boiler. In addition, the study assessed boiler island equipment modification requirements and any potential barriers to boiler conversion and integration with the chemical looping system.

Since the main driver for boiler conversion is CO<sub>2</sub> emission reduction, economic comparison with other potentially competing technologies, such as O<sub>2</sub> firing with a CO<sub>2</sub> (flue gas) recycle system and advance-scrubbing system was made. To this end, approximate investment costs and performance were estimated for the three retrofit technologies; economic analysis was carried out. Since detail analyses were beyond scope of this study, much of the technical and cost information was prorated from previous reports (**Reference2** and **Reference19**).

#### Investment Cost and Economic Analyses

Investment cost was estimated for the retrofit Case 2 only, applying cost factors used in **Reference 2** and **Reference 19**. Since good technical and economic information was available for the **Reference 19** study, the PC-4 plant from that study was selected as the Base case. All costs and performance results from this study were prorated for the PC-4 plant conversion. To assess commercial potential of the chemical looping conversion case, an economic comparison was made with two other competing technologies: the O<sub>2</sub> (cryogenically produced) gas recirculation and advanced scrubbing

systems. The costs are expressed in 2003 dollars. In estimating the cost the following assumptions were made:

1. The following systems are existing and do not require any modifications:
  - a. Feedwater and miscellaneous BOP systems
  - b. Seam turbine generator c) cooling water system d) accessory electric plant
2. The following systems are added:
  - a. Sorbent handling
  - b. Sorbent preparation and feed
  - c. Chemical looping system
  - d. CO<sub>2</sub> capture system
3. The following systems are modified:
  - a. Boiler island
  - b. Ash/spent sorbent handling systems
  - c. Instrumentation and controls
4. Terminal points of the analyzed system are the same as in **Reference 2** and consistent with the other two technologies used in comparison

The conversion of the 753 MW PC-4 steam plant to fire the synthetic fuel resulted in the net plant efficiency decreasing by 5.3% percentage point to 34.44%. Compared to the advanced scrubbing system and O<sub>2</sub>/recycle flue gas system, the respective net plant efficiencies were 35.58% and 30.66%.

The investment cost for the chemical looping system conversion case was approximately \$359.7Million, which included \$24.5Million for the boiler island modification. Boiler island cost allocations were made for the installation of new coal piping; pulverizer modifications, to produce coarser coal size particles; windbox modifications, to fire the synthetic fuel; primary air ductwork from the chemical looping system; booster primary air fan and motors and the additional heat transfer surface for the air heaters. Comparable investment cost for the advanced scrubbing system and O<sub>2</sub>/recycle flue gas system was \$346.18Million and \$334.9 Million respectively. Based on the \$/kW basis, the investment cost for these three retrofit technologies was: \$571/kW, \$571/kW and \$658/kW respectively.

The cost of electricity was calculated also. For the chemical looping, the advanced scrubbing and O<sub>2</sub>/recycle flue gas repowering systems the respective incremental cost of electricity was 1.86 cents/kWhr, 1.76 cents/kWhr and 2.37 cents/kWhr. **Figure 11-1** shows the economic results of the analyses.

## Conclusion

This brief study examined boiler performance and key barriers to re-powering PC fired boilers to fire the synthetic fuel produced by the Chemical Looping System gasifier. The boiler performance was achieved with minimum boiler island modifications and no barriers were found to boiler re-powering or integration with the gasifier system. The

economic comparison with other potentially competing technologies such as the advanced scrubbing system and O<sub>2</sub>/recycle flue gas system illustrated that the Chemical Looping technology is more cost effective than the O<sub>2</sub>/recycle flue gas system and is similar in cost to the advanced scrubbing system. The small differences in cost are believed to be well within the accuracy range of the analysis. As both technologies mature, the analysis should be revisited for a more thorough examination.

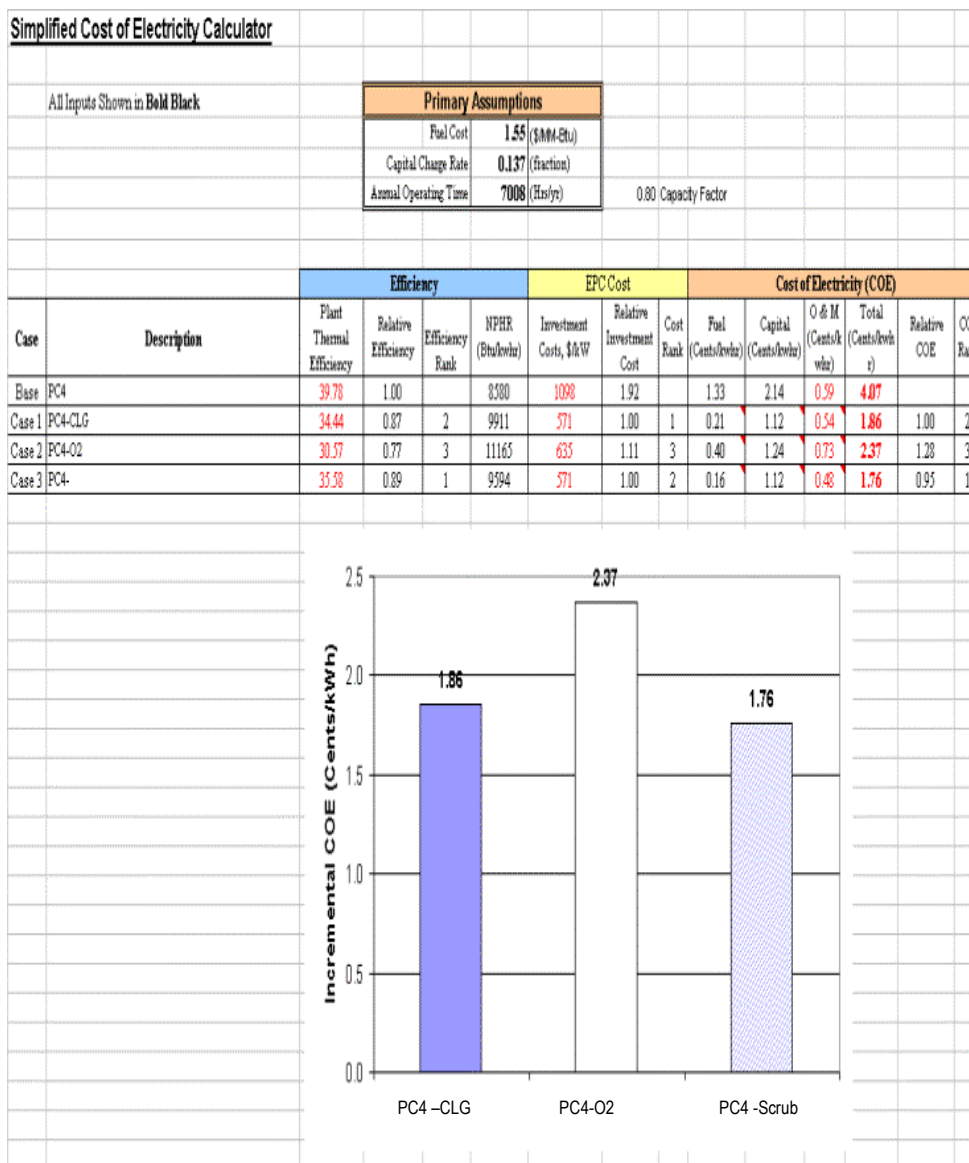


Figure 11-1 - Incremental Cost of Electricity for Chemical Looping Gasifier (PC4-CLG), O<sub>2</sub>/Flue Gas Recirculation System (PC4-O2) and Advanced Scrubbing System (PC4-scrub)

## 11.2 Economics Update

The Phase III work develop no major changes to the process flow sheet or the design of any equipment for the chemical looping commercial plant design. Therefore, no changes to the relative economic rankings in the Greenhouse Gas report conclusions were warranted.

A separate independent CO<sub>2</sub> Technology assessment was made in 2006 and updated in 2007 and 2008. The purpose of this assessment was to rank the various CO<sub>2</sub> technologies according to a set of criteria to determine the most promising methods to deal with CO<sub>2</sub> capture.

The assessment was done by assembling a list of CO<sub>2</sub> technologies. Of these, 19 were selected. An initial assessment was made and it was determined that an in depth analysis was needed. The technologies were analyzed for technical and economic issues. Product summaries and development plans were considered. Financial analyses were done including a consideration of customer needs. The analysis resulted in a list of product rankings.

The types of products considered were:

1. High efficiency plants.
2. Biomass plants, both co-firing and 100% biomass.
3. CO<sub>2</sub> ready conventional plants.
4. Oxy-fired plants, pulverized fuel and CFB.
5. CO<sub>2</sub> scrubbing.
6. Chemical Looping, Metal oxides and Calcium.

The areas of consideration were:

1. Net plant thermal efficiency on a % HHV basis.
2. CO<sub>2</sub> emissions in lbm/kw-hr.
3. EPC investment cost in \$/kw
4. Levelized cost of Electricity (COE) in cents/kw-hr.
5. Variable cost of generation in cents/kw-hr.
6. CO<sub>2</sub> mitigation costs in \$/ton of CO<sub>2</sub> captured.

The assessment considered 'greenfield' plants only. The plant size was a nominal 400 MWe net. The steam cycle was supercritical (3915 psia, 1085F, 1148F, 2.5 in Hga and 7339 BTU/Kw-hr). Plant auxiliary power was estimated. The EPC investment costs were based on April 2006 US dollars. O&M costs were done using the Greenhouse Gas Report project calculation basis. Fuel costs were \$1.50 per million BTU for coal, and \$3.00 per million BTU for biomass. The capital charge rate was 13.5%. The capacity factor was 80%. The CO<sub>2</sub> allowance price varied from 0 to \$50.00 per ton of CO<sub>2</sub>.

The results of the CO<sub>2</sub> technology assessment show the cost of electricity for all of the technologies with CO<sub>2</sub> capture is lowest for the Chemical Looping case with calcium (Figure 11-2). This is consistent with the Greenhouse gas report (Reference 2). The cost of electricity for chemical looping is also lowest as the CO<sub>2</sub> allowance price increases and becomes lower than the reference plant at about \$11.00 per ton of CO<sub>2</sub> emitted (Figure 11-3).

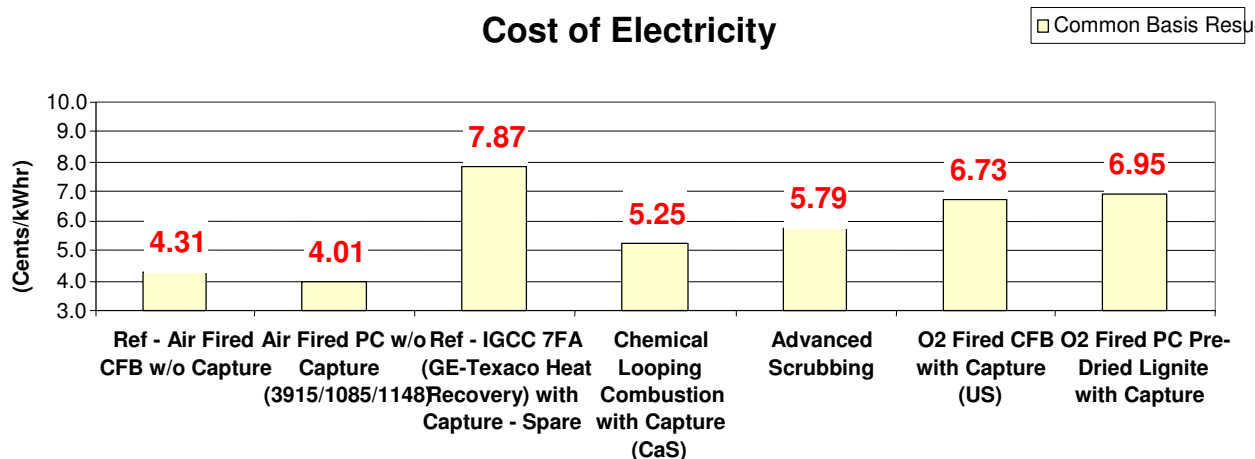


Figure 11-2 – Cost of Electricity for Different CO<sub>2</sub> Technologies

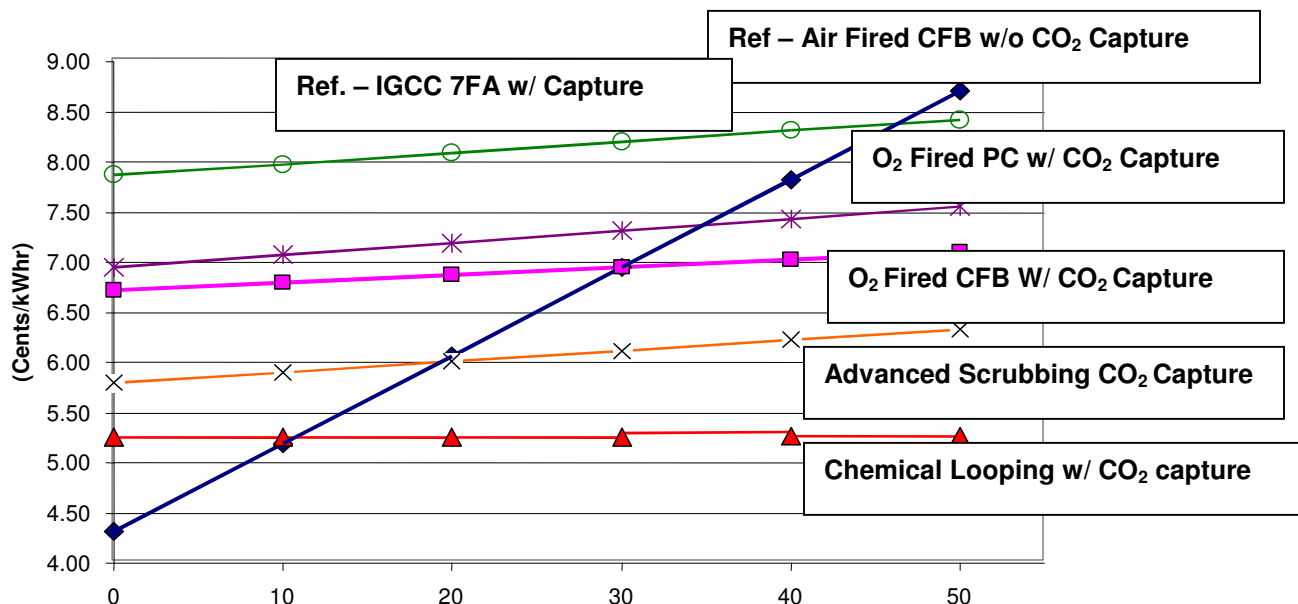
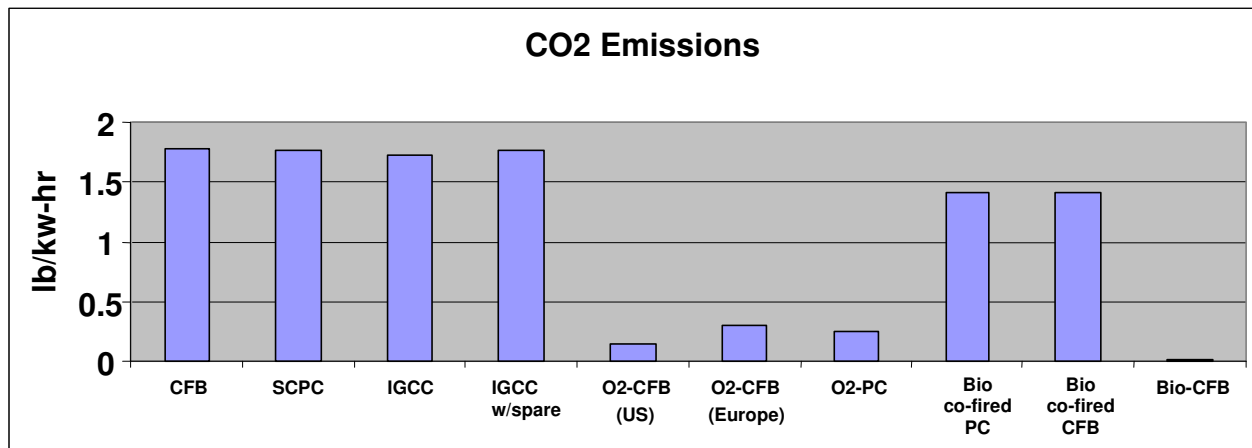


Figure 11-3 - CO<sub>2</sub> Allowance Price (\$/Ton CO<sub>2</sub> Emitted)

The products that were reviewed were categorized as either short-term products or long-term products.

For the short-term products such as oxy-firing and biomass, CO<sub>2</sub> emissions are compared in **Figure 11-4**. As expected, the full biomass fired CFB has the lowest CO<sub>2</sub> emissions followed by the oxy-fired CFB and oxy-fired PC. The biomass co-firing CO<sub>2</sub> emissions depend on the amount of biomass co-fired. In this study, the amount of biomass co-fired is only 20%, which is reflected in the relatively high CO<sub>2</sub> emissions.



**Figure 11-4 – CO<sub>2</sub> Emissions for Short-Term CO<sub>2</sub> Technologies**

The specific investment costs for short-term CO<sub>2</sub> technologies are shown in **Figure 11-5**. The oxy-firing cases are predicted to cost about the same as IGCC and a little more than the Biomass Cases.

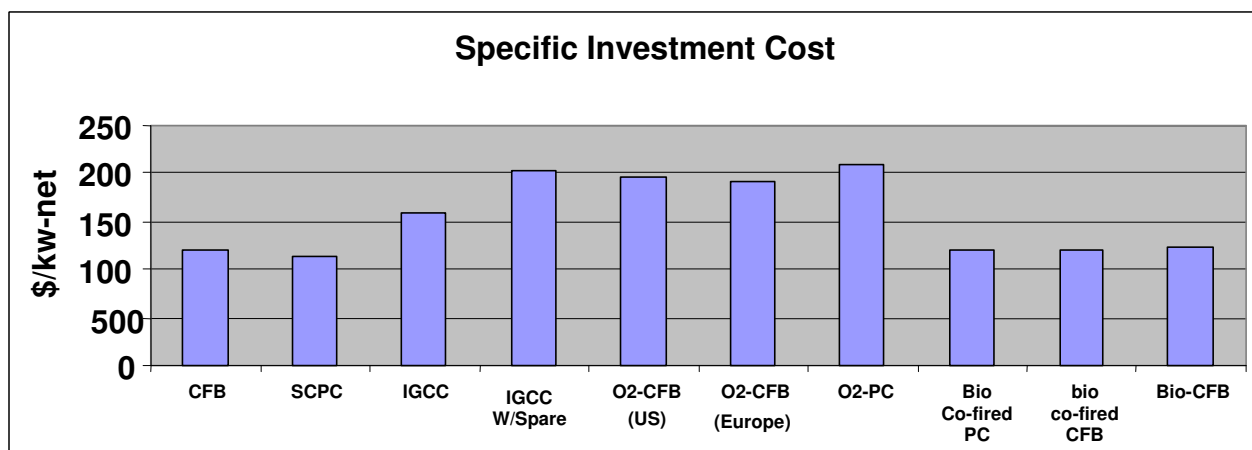


**Figure 11-5 – Investment Costs for Short-Term CO<sub>2</sub> Technologies**

CO<sub>2</sub> mitigation costs for the short-term CO<sub>2</sub> technologies are shown in **Figure 11-6**. The oxy-firing cases are slightly above \$20.00 per ton of CO<sub>2</sub> captured. The biomass cases are slightly below \$20.00 per ton of CO<sub>2</sub> captured.

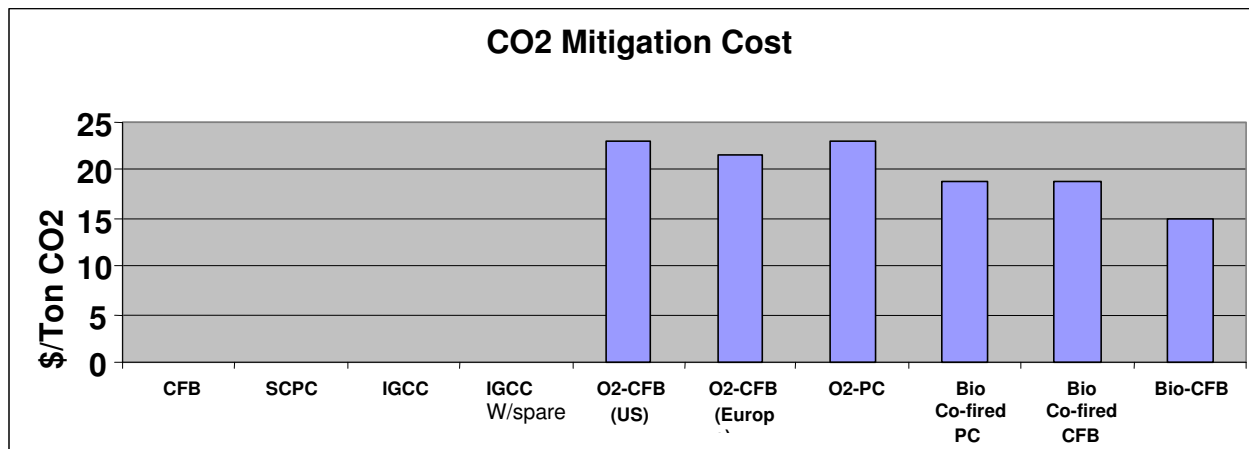


**Figure 11-6 – CO<sub>2</sub> Mitigation Costs for Short-Term CO<sub>2</sub> Technologies**

The long-term CO<sub>2</sub> Technologies are chemical Looping and advanced scrubbing. As shown in **Figure 11-7**, CO<sub>2</sub> emissions from both of these are much lower than the reference cases.

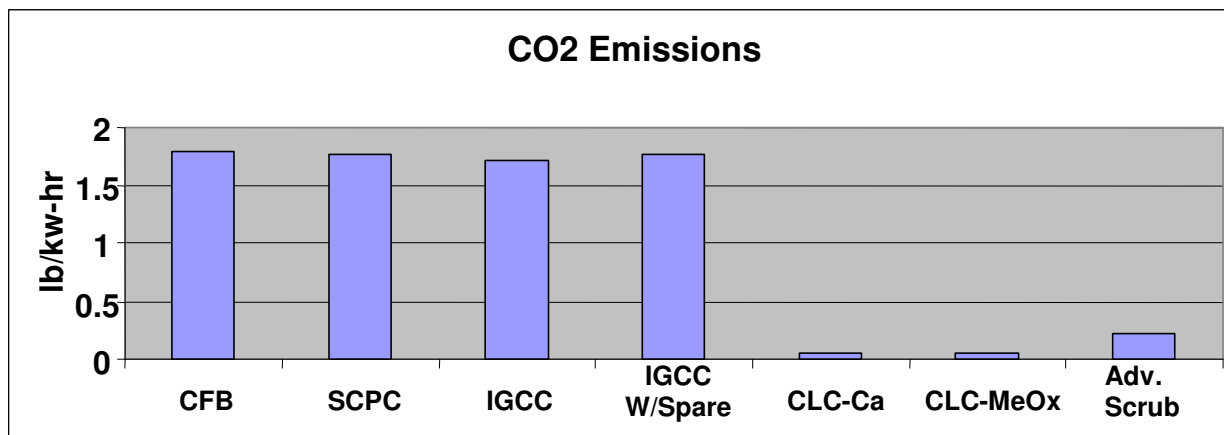


**Figure 11-7 – CO<sub>2</sub> Emissions from Long-Term CO<sub>2</sub> Technologies**

The specific investment costs are shown for the long-term CO<sub>2</sub> Technologies in **Figure 11-8**. Chemical Looping combustion using calcium is less than or about the same as the reference IGCC plants and only a little higher than the reference CFB or PC plants without capture.

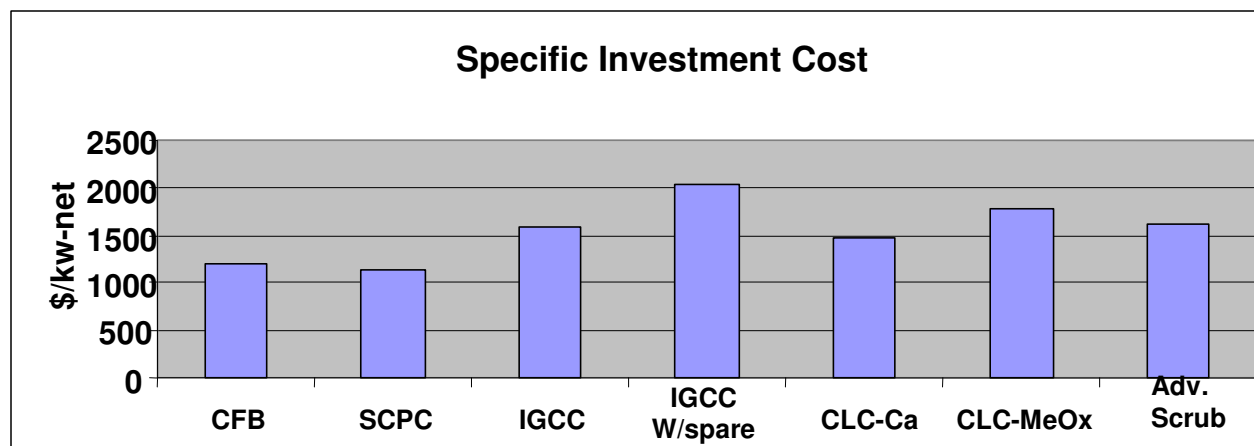


**Figure 11-8 – Specific Investment Cost for Long-Term CO<sub>2</sub> Technologies**

The CO<sub>2</sub> mitigation costs for the long-term CO<sub>2</sub> technologies are shown in **Figure 11-9**. The CO<sub>2</sub> mitigation costs for Chemical looping combustion using calcium is the lowest of the long-term CO<sub>2</sub> technologies and also of the short-term CO<sub>2</sub> technologies (**Figure 11-9**).

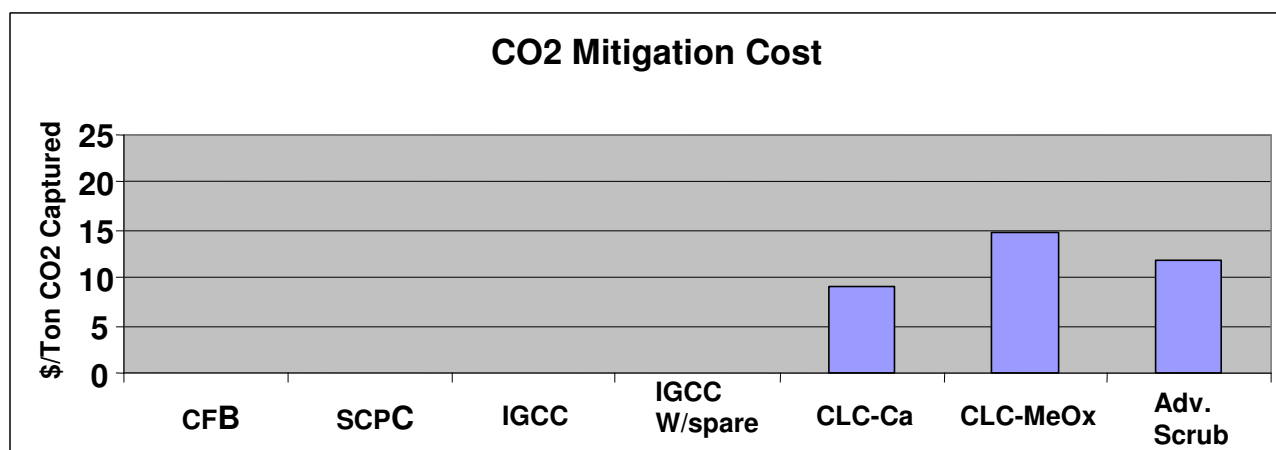


**Figure 11-9 – CO<sub>2</sub> Mitigation Costs for Long-Term CO<sub>2</sub> Technologies**

The conclusions from this newer CO<sub>2</sub> Technologies assessment are consistent with the conclusions from the original Greenhouse Gas Report (**Reference 2**). Chemical looping using calcium has the potential for large-scale capture of CO<sub>2</sub> at a reasonable cost. Chemical looping is the most promising of the emerging CO<sub>2</sub> technologies.

### 11.3 COE for H<sub>2</sub> production

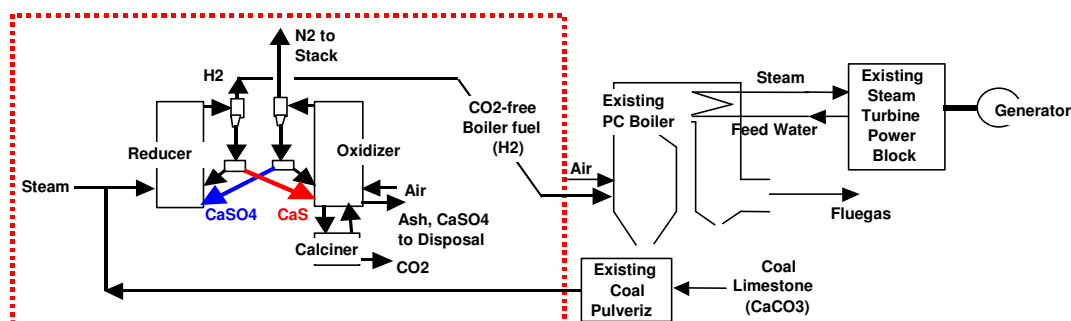
#### Retrofit to Existing Pulverized Coal-Fired Power Plants

**Figure 11-10** shows a few of the potential retrofit concepts. In Retrofit Concept 1, Alstom's Chemical Looping system is configured to produce CO<sub>2</sub>-free hydrogen while capturing nearly pure CO<sub>2</sub> as a separate stream from the Calcliner for use or sequestration. The hydrogen from the chemical looping system is used as a CO<sub>2</sub>-free fuel for the existing boiler. The existing coal pulverizers are used to co-pulverize coal and limestone for the chemical looping system. Alstom has studied this concept during the US DOE sponsored Chemical Looping Pilot Plant work (Phase III). The results have shown that very little modification is required for the existing boiler and full generator output power can be achieved. Previous co-grinding tests of coal and limestone at Alstom have shown that the full coal throughput can be achieved with little reduction in fineness for all types of coal and limestone. The fineness thus produced is finer than required for effective use in the Chemical Looping process.

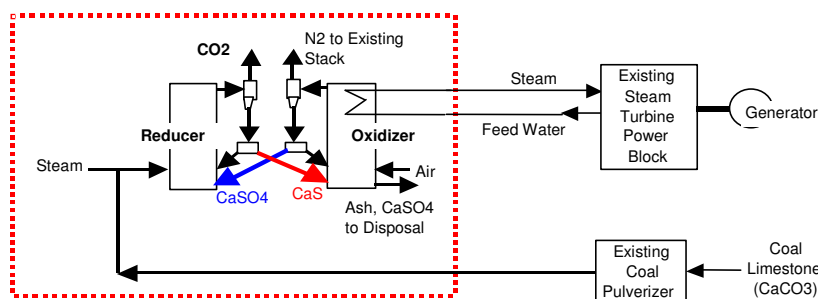
Retrofit Concept 2 of **Figure 11-10** shows another way to use Alstom's Chemical Looping process to capture CO<sub>2</sub> from an existing PC power plant. As with the previous concept, the existing coal pulverizers are used to co-pulverize coal and limestone for the chemical looping system. The Chemical Looping process is configured to produce high pressure, superheated steam for power generation and CO<sub>2</sub> for use or sequestration. The steam is sent to the existing steam turbine and the original PC boiler is not used. The full generator power output can be achieved. The cost and performance of this configuration were studied by Alstom and reported in **Reference 2** (GHG Report).

Retrofit Concept 3 of **Figure 11-10** is similar in concept to Retrofit Concept 1, except that the existing boiler is modified to serve the function of the Oxidizer. This use of the existing boiler in this fashion avoids the requirement for including the Oxidizer and high pressure, superheat steam production equipment (i.e. boiler pressure parts) in the Chemical Looping system. This Concept has not yet been studied by Alstom in any detail. However, if it proves practical, this approach could reduce retrofit cost.

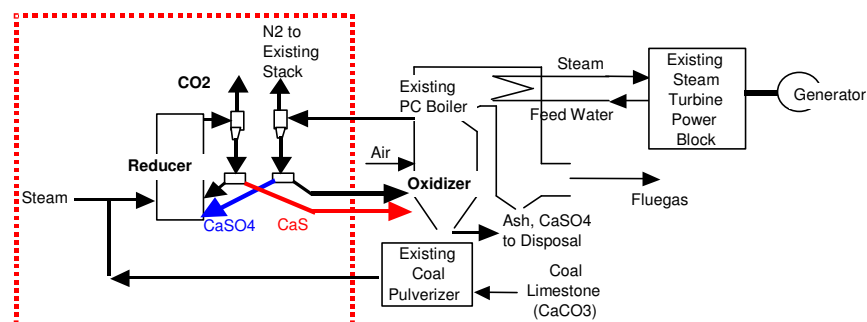
There are other Retrofit Concepts as well. For example, Retrofit Concept 1B (a variation of Retrofit Concept 1) could include a larger Chemical Looping system in which the extra Product Gas (hydrogen) could be fired in a combustion turbine to replace the power required to compress and liquefy the CO<sub>2</sub> that is required for use or sequestration of the CO<sub>2</sub>; or to provide extra station capacity. The hot gas turbine exhaust could be directed to the existing boiler, which could serve the function of a combined cycle heat recovery steam generator. The cost of electricity (COE) of this approach would be somewhat lower than for Concept 1 because combustion turbo-generators are lower in cost than steam turbine island costs for a given electrical output.



**Concept 1 – Chemical Looping CO2-Free Fuel; Minimum Boiler Modification**



**Concept 2 – Chemical Looping Oxidizer Replaces Boiler**



**Concept 3 – Chemical Looping uses the Boiler as the Oxidizer**

**Figure 11-10 – PC Retrofit Concepts using Alstom’s Chemical looping Process**

In summary, work to-date at Alstom has shown that Alstom’s Chemical Looping process has wide applicability to the electric power industry for both new capacity and retrofit applications and for both pulverized coal (PC) and circulating fluidized bed (CFB) power plants. Laboratory testing (bench and pilot scale) has shown that the process can use virtually any coal, biomass, opportunity fuel (e.g. coal waste, oil resid, petcoke) or carbon-based fuel as the fuel source. Virtually any limestone, dolomite or even CFB spent sorbent can be used as the oxygen carrier.

## Retrofit Cost of Electricity

The cost of retrofitting Alstom's Chemical Looping to the fleet of US (or world-wide) PC power plants is equally promising. **Table 11-1** provides preliminary performance and cost information for Retrofit Concepts 1 (CO<sub>2</sub>-free hydrogen) and Retrofit Concept 2 (steam turbine re-powering).

The performance and cost information for the Base Case (PC supercritical without CO<sub>2</sub>) capture is based on one of Alstom's recent commercial projects. Performance for Retrofit Concept 1 (CO<sub>2</sub>-free hydrogen) was developed by Alstom during the on-going US DOE sponsored Chemical Looping development project (Phase III). Performance for Retrofit Concept 2 (steam turbine re-powering) was developed by Alstom with the help of WorleyParsons as reported in **Reference 2**. Preliminary capital costs for the two retrofit concepts were developed based on US DOE cost factors taken from **Reference 22** and adjusted to match the Base Case. Performance for CO<sub>2</sub> compression is based on US DOE program goals. Economic factors used for constructing **Table 11-1** are typical of today's electric power industry.

**Table 11-1 – PC Power Plant Chemical Looping Retrofit Economics**

Case	Description	Plant Thermal Efficiency (%)	CO <sub>2</sub> Capture (%)	Investment Costs, \$/kW	Fuel (Cents/kwhr)	Capital (Cents/kwhr)	O & M (Cents/kwhr)	Total (Cents/kwhr)	COE Increase for CO <sub>2</sub> Capture (%)	COE Increase for CO <sub>2</sub> Transportation & Sequestration (%)	Total COE Increase (%)
Base	Base Case: Supercritical PC	39.78	0%	1098	1.33	2.14	0.59	4.07			
Case 1	PC Retrofit Concept 1	37.02	95%	1440	1.43	2.81	0.48	4.72	16.0%	4.0%	20.0%
Case 2	PC Retrofit Concept 2	37.22	95%	1499	1.42	2.93	0.48	4.83	18.6%	4.0%	22.6%

The investment costs shown for PC Retrofit Concepts 1 and 2 include the cost of the original plant (Base Case: Supercritical PC). The efficiency includes all plant auxiliary power and the power required to compress and liquefy the captured CO<sub>2</sub> to 2000 psig.

These preliminary results show that using Alstom's Chemical Looping process for capturing CO<sub>2</sub> from existing PC power plants has the potential to keep power costs to within 20% of the original (Base Case) cost of electricity. Efficiency penalties costs for Alstom's Chemical Looping process are low compared to other CO<sub>2</sub> capture alternatives because the process captures CO<sub>2</sub> at temperatures higher than the power cycle temperatures, thus eliminating the thermodynamic penalty normally associated with CO<sub>2</sub> capture. Incremental costs for Alstom's Chemical Looping process are low compared to other CO<sub>2</sub> capture alternatives because the chemical reactions are fast which allows for small equipment and low capital cost.

To illustrate this point, **Figure 11-11** compares the size of Retrofit Option 1 equipment with that of a conventional coal-fired power plant.

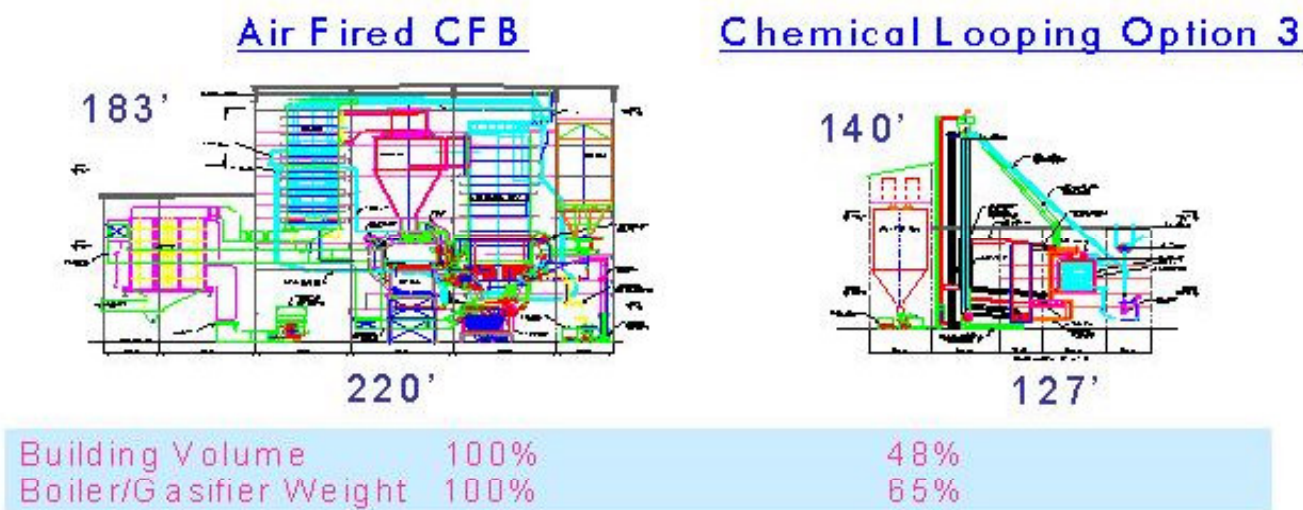
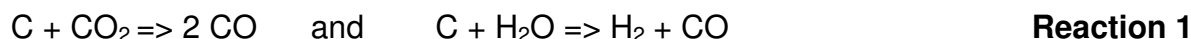


**Figure 11-11 – Comparison with a Conventional Power Plant**

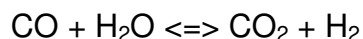
**Figure 11-11** shows that Chemical Looping Option 3 (see **Section 2**), which is the configuration used for Retrofit Concept 1, requires only 65% of the materials that are needed for a modern Alstom Circulating Fluidized Bed (CFB) boiler. Retrofit Concept 2 (which employs Option 1, **Section 2**) is somewhat more costly because the equipment is larger due to the usage of more air (0.3 air-to-coal for Option 3 vs. 1.2 for Option 1).

### CO<sub>2</sub> Capture Efficiency

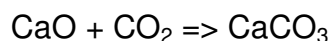
As reported in References 1 and 3, Alstom's Chemical Looping system can easily meet the requirement to capture over 90% of the carbon in the coal as CO<sub>2</sub>. In Retrofit Concept 1, CO<sub>2</sub> is captured in the Reducer by first producing syngas (CO and H<sub>2</sub>) via the following carbon gasification reactions:



These reactions consume the coal's carbon and hydrogen, producing CO and H<sub>2</sub> when the ratio of coal-to-hot-CaSO<sub>4</sub> is correctly chosen. Bench tests have shown that virtually all carbon in the coal can be converted to CO<sub>2</sub> and CO by these reactions. Next, the water-gas shift reaction converts the CO to H<sub>2</sub> and CO<sub>2</sub> via the following reaction:



Next, the CO<sub>2</sub> is captured by CaO via the following carbonation reaction:



Bench test results have produced over 98% pure hydrogen from these reactions. The  $\text{CO}_2$  is released from the  $\text{CaCO}_3$  in the Calciner as described in connection with **Figure 11-10**.

In Retrofit Concept 2 and 3, the  $\text{CO}_2$  is captured in the Reducer via Reactions 1 and 2, above. When the ratio of coal-to-hot- $\text{CaSO}_4$  is correctly chosen (i.e. a higher  $\text{CaSO}_4$ -to-Coal ratio is used than in Retrofit Concept 1), nearly all of the Product Gas formed in the Reducer is  $\text{CO}_2$  with some  $\text{H}_2\text{O}$  formed from the hydrogen in the coal. Condensing the  $\text{H}_2\text{O}$  leaves the  $\text{CO}_2$  for compression and sequestration. Bench tests have shown that virtually all of the carbon in the coal can be consumed in this manner.

## 11.4 Prototype Cost

The cost for the prototype equipment was originally estimated by using material costs from the MTF and updating these costs. In Phase III a preliminary prototype design study was done. A heat and mass balance was done and a simplified process flow diagram was made. Using this information, sizes for each of the major pieces of equipment and major lines was estimated and a preliminary layout was made. This is described in **Section 8.7 Prototype Preliminary Design**.

The preliminary prototype design was used to estimate material types and weights. Weights for the prototype equipment is shown in **Table 11-2**.

An updated cost estimate was made from the weight estimate. It was found to be consistent with the original cost estimate.

**Table 11-2 – Prototype Equipment Weights.**

PROTOTYPE Equipment weights							
Equipment:	Length - ft	Refractory			Steel		
		density=	125.00	#/ft3	density=	495.000	#/ft3
		Xsect ft2	volume-ft3	weight #	Xsect ft2	volume ft3	weight #
1 Reducer	60	3.142	188.50	23,562	0.249	14.910	7,381
2 Combustor	60	3.142	188.50	23,562	0.249	14.910	7,381
3 Calciner	20	3.142	62.83	7,854	0.249	4.970	2,460
4 R -Pri-cycl -barrel	17	7.277	123.70	15,463	0.507	8.618	4,266
5 O -Pri-cycl -barrel	17	7.277	123.70	15,463	0.507	8.618	4,266
6 R -Pri-cycl -exp	2	4.680	9.36	1,170	0.345	0.689	341
7 O -Pri-cycl -exp	2	4.680	9.36	1,170	0.345	0.689	341
8 R -SEC-cycl -barrel	10	6.021	60.21	7,527	0.428	4.285	2,121
9 O -SEC-cycl -barrel	10	6.021	60.21	7,527	0.428	4.285	2,121
10 R -Pri-cycl -Disch	2	2.526	5.05	632	0.210	0.420	208
11 O -Pri-cycl - Disch	2	2.526	5.05	632	0.210	0.420	208
12 R -Sec-cycl - Disch	30	2.304	69.12	8,639	0.196	5.884	2,913
13 O -Sec-cycl - Disch	30	2.304	69.12	8,639	0.196	5.884	2,913
14 R -Pri-cycl -inlet duct	10	1.680	16.80	2,100	0.477	4.767	2,360
15 O -Pri-cycl -inlet-duct	10	1.680	16.80	2,100	0.477	4.767	2,360
16 R -Sec-cycl -inlet duct	6	1.390	8.34	1,042	0.380	2.279	1,128
17 O -Sec-cycl - inlet duct	6	1.390	8.34	1,042	0.380	2.279	1,128
18 Red Feed Tube	50	1.571	78.54	9,817	0.150	7.517	3,721
19 Red Xover Let down	50	1.571	78.54	9,817	0.150	7.517	3,721
20 Red Calc let down	40	1.571	62.83	7,854	0.150	6.013	2,977
21 Calc lift tube	40	1.571	62.83	7,854	0.150	6.013	2,977
22 Oxi feed tube	40	1.571	62.83	7,854	0.150	6.013	2,977
23 Oxi Xover lift tube	40	1.571	62.83	7,854	0.150	6.013	2,977
24 Solids Supply	100	1.571	157.08	19,635	0.150	15.033	7,441
25 MBHE 1 vessel	10	10.250	102.50	12,813	3.333	33.333	16,500
26 MBHE 2 vessel	10	10.250	102.50	12,813	3.333	33.333	16,500
27 R SPCV 1	6	5.458	32.75	4,094	1.736	10.417	5,156
28 R SPCV 2	6	5.458	32.75	4,094	1.736	10.417	5,156
29 O SPCV 1	10	5.458	54.58	6,823	1.736	17.361	8,594
30 AH 1	10	10.250	102.50	12,813	3.333	33.333	16,500
31 AH 2	10	10.250	102.50	12,813	3.333	33.333	16,500
32 AH 3	10	10.250	102.50	12,813	3.333	33.333	16,500
33 MBHE 1 Tubes	4000				0.044	175.896	87,069
34 MBHE 1 Tubes	4000				0.044	175.896	87,069
35 AH 1 tubes	4000				0.044	175.896	87,069
36 AH 2 tubes	4000				0.044	175.896	87,069
37 AH 3 tubes	4000				0.044	175.896	87,069
38 Lift Tube 1-cycl -barrel	10	6.021	60.21	7,527	0.428	4.285	2,121
39 Lift Tube 2-cycl -barrel	10	6.021	60.21	7,527	0.428	4.285	2,121
40 Lift Tube-3-cycl -barrel	10	6.021	60.21	7,527	0.428	4.285	2,121
Sub Totals				300,462			613,797
add for fittings, nipples and flanges							153,449
TOTALS				300,462			767,246
Grand Total =							1,067,708

## 12. Future Developments

The overall objective of the Chemical Looping Project is to develop and verify the high temperature chemical and thermal looping process concept and to design, construct and demonstrate a pre-commercial, demonstration version of this advanced system. After successful completion of Phase III, two additional phases are envisioned to bring the Chemical Looping concept to commercial status.

Based on Phase I and II work, all of the necessary chemistry has been verified in the PDU. All rates are significantly faster than those used to design the GHG study Chemical Looping commercial plant concept.

Phase III of the development program concentrated on the remaining solid transport work. These items include the following:

- solids feed-and-bleed for operation of the Reducer,
- higher solid-to-gas ratios in the 40 foot cold flow model,
- calciner design
- conversion of the PDU for two-stack operation (Oxidizer and Reducer);
- more operational practice with the PDU
- work on the PDU to work out control strategies and automatic controls.

The objective of Phase III was to operate the pilot plant to obtain the remaining engineering information necessary to design a prototype of the commercial Chemical Looping concept. The activities included modifications to the Phase II Chemical Looping PDU, solids transportation studies, and additional cold flow modeling. The deliverable was recommendations for preliminary design guidelines for the prototype plant, results from the pilot plant testing, and an update of the commercial plant economic estimates.

Successful completion of the Phase III provided sufficient information to engineer, procure, construct and test the Chemical Looping Prototype (MTF size coal flow, about 1000 lb/hr coal) in Phase IV, which will subsequently lead to demonstration. The objective of Phase IV is to design, build and operate a prototype unit in the size range of 5 to 10 million BTU's per hour of heat input (i.e. 500 to 1000 lb/hr of coal). This work will include prototype testing and development. A commercial plant re-design along with an economic re-check will be done. Cold flow tests will be done. Engineering studies and commercial planning will also be done. Plans for the demonstration plant will also be done including arranging funding, selecting demonstration sites, finding sponsors, contacting A&E's, and other demonstration plant requirements. A final report will be written describing the results of the prototype construction and testing and will include the updated demonstration and commercialization plans.

The objective of Phase V is to design, build and operate a demonstration plant. This will include developing project management plans, lining up participants, signing agreements, securing funding, doing environmental impact studies, permitting, EPC, startup and commissioning, operations, testing, modifying the unit as required and

standards development. A commercial planning update will also be done. A final report will be written documenting all the Phase V activities.

These two phases constitute the remaining work required to bring Alstom's Chemical Looping process to commercial status. There will be a decision point at the end of each phase, during which Alstom and the DOE will review of the results of the phase and then separately decide whether or not to proceed with the next phase. As part of these decision points, the work scope, cost and schedule of the following phases will be re-examined by Alstom and changed as required.

The Chemical Looping Process has considerable flexibility. It can be deployed in at least three (3) configurations. In the simplest configuration, or Option 1, it will operate to separate CO<sub>2</sub> from the remaining flue gases in two (2) reactors (oxidizer and reducer). Such a plant would be capture ready since the CO<sub>2</sub> is already separated.

With a change in the operation to reduce the amount of CaSO<sub>4</sub> in contact with the coal, Option 2 can be realized, which can provide a syngas to boilers, gas turbines, industrial processes, and combined cycles. The addition of steam and a lime/carbonate loop provides for the capture and independent release of CO<sub>2</sub> along with the production of hydrogen (Option 3). This option will have the best performance and lowest cost of electricity. It is also the most complex. It is anticipated that the like order of commercialization will be from Option 1 to Option 3. Thus, more emphasis will be given to Option 1 in the future phases.

## References

1. Andrus, H. E., Jr., et. al., Hybrid Combustion-Gasification Chemical Looping Coal Power Technology Development – Phase 1 Final Report, U.S. DOE, December, 29, 2004
2. Nsakala, N. Y. and Liljedahl, G. N., Greenhouse Gas Emissions Control by Oxygen Firing in Circulating Fluidized Bed Boilers, Alstom Power – U.S. DOE Report, PPL Report No, PPL-03-CT-09, 15 May 2003.
- 3 Andrus, H. E., Jr., et. al., Hybrid Combustion-Gasification Chemical Looping Coal Power Technology Development – Phase II Final Report, U.S. DOE, June, 9, 2006.
4. Andrus, H.E., Thibeault, P. R., Chemical Looping Spec Gate review and Peer Review Report, 22 August, 2005.
5. Johnson, K, et. al., Sorption-Enhanced Steam Reforming of Methane in a Fluidized Bed Reactor.
6. Zenz, F. A., and Othmer, D. F., Fluidization and Fluid-Particle Systems, Reinhold Publishing Corp., NY, 1960 pp 326-332.
7. Zenz, F. A., letter “Dense Phase Vertical Conveying Lines” 5/10/05.
8. Wirth, K. E., Zirkulierende Wirbelschichten Strömungsmechanische Grundlagen, Anwendung in der Feuerungstechnik, Springer-Verlag, 1990.
9. Mei, J. S., Hydrodynamics of a Transport Reactor Operating in Dense Suspension Up Flow Conditions for Coal Combustion Applications, 18<sup>th</sup> International Conference of FBC, 2005
10. Shadle, L. J., Slip Velocities in the Homogeneous Flow Regime in an Industrial Scale Cold Flow CFB
11. Wolk, R., et. al., Evaluation of Innovative Fossil Fuel Power Plants with CO2 Removal, Interim Report, Parsons Energy and Chemicals Group, Inc, December, 2000.
12. Zenz, F. A., Pneumatic Conveying in Vertical Upflow, Research Report, 2005.
13. Zenz, F. A., et. al., Particle Conveying in Mainly Horizontal Extrusion Flow, Research Report.
14. Kulkarni, P. P., et. al. Advanced Unmixed Combustion/Gasification: Potential Long Term Technology for Production of H2 and Electricity from Coal with CO2 Capture, presented at the Pittsburgh Coal Conference, September 2006

15. Kulkarni, P. P., et. al. Fuel-Flexible Gasification-Combustion Technology for Production of H<sub>2</sub> and Sequestration-Ready CO<sub>2</sub> Phase II, Quarterly Technical Progress Report No. 26, Reporting Period: July 01, 2007 – September 30, 2007.
16. Kulkarni, P. P., et. al. Fuel-Flexible Gasification-Combustion Technology for Production of H<sub>2</sub> and Sequestration-Ready CO<sub>2</sub>, Quarterly Technical Progress Report No. 13, Reporting Period: October 01, 2007 – December 31, 2007.
17. Rizeq, G., et. al. Advanced Gasification-Combustion Technology for Production of Hydrogen, Power and Sequestration-Ready CO<sub>2</sub>, presented at the Gasification Technologies 2003 conference, October, 2003.
18. Rizeq, G., et. al. Fuel-Flexible Gasification-Combustion Technology for Production of Hydrogen and Sequestration-Ready Carbon Dioxide, US DOE Project Fact Sheet, July, 2005.+
19. M.Palkes, G. Liljedahl, R. Waryasz, Economics and Feasibility of Rankine Cycle Improvements for Coal Fired Power Plants, February 28, 2004
20. “Fluid Meters Their Theory and Application”, report of the ASME Committee on Fluid Meters, Sixth Edition, 1971, edited by Howard S. Beam
21. Strakey, Joseph P., “The Future of Gas Turbine Technology”, presented at the 3<sup>rd</sup> International Conference, European Network, October 11, 2006, Brussels Belgium.
22. Klara, J., et al., “Cost and Performance Baseline for Fossil Energy Plants”, DOE/NETL –2007/1281, Revision, August 2007.
23. Merrow, Edward W., et. al., “Understanding Cost Growth and Performance Shortfalls in Pioneer Process Plants”, R-2569-DOE, Prepared for the U.S. Department of Energy, Rand Corporation, September 1981.